

UNIVERSITÀ
DEGLI STUDI
DI PADOVA

Sede Amministrativa: Università degli Studi di Padova

Dipartimento di Scienze Chimiche

SCUOLA DI DOTTORATO DI RICERCA IN: Scienze Molecolari

INDIRIZZO: Scienze Chimiche

CICLO XXVII

**Novel Cp^{*}-iridium(III) complexes with di(N-heterocyclic carbene) ligands:
synthesis, characterization and catalytic activity**

Direttore della Scuola: Ch.mo Prof. Antonino Polimeno

Supervisore: Dr. Cristina Tubaro

Dottorando: Andrea Volpe

INDEX

| | |
|---|------------|
| ABSTRACT | 1 |
| SOMMARIO | 7 |
| Chapter 1: INTRODUCTION | |
| N-HETEROCYCLIC CARBENE LIGANDS | 13 |
| 1.1 Properties of N-heterocyclic carbene ligands | 13 |
| 1.2 Synthesis of NHC-metal complexes | 24 |
| 1.3 Applications of NHC-metal complexes..... | 26 |
| 1.4 Iridium(III) complexes with N-heterocyclic ligands: synthesis and applications . | 30 |
| 1.4.1 Synthesis of Ir(III)-NHC complexes..... | 30 |
| 1.4.2 Applications of Ir(III)-NHC complexes..... | 32 |
| 1.5 Water oxidation reaction | 40 |
| 1.5.1 Water oxidation reaction catalyzed by iridium(III) complexes..... | 45 |
| 1.6 Aim of the research..... | 50 |
| Chapter 2: RESULTS AND DISCUSSION | |
| SYNTHESIS AND CHARACTERIZATION OF THE IRIDIUM(III) di-NHC COMPLEXES 1-3, 5-10 AND 2a | 53 |
| Chapter 3: RESULTS AND DISCUSSION | |
| WATER OXIDATION WITH IRIDIUM(III) COMPLEXES BEARING DI(N-HETEROCYCLIC CARBENE) LIGANDS | 75 |
| 3.1 Water oxidation in presence of a sacrificial oxidant..... | 75 |
| 3.2 Water oxidation with iridium(III) complexes bearing di(N-heterocyclic carbene) ligands in a photo-induced process | 97 |
| Chapter 4: RESULTS AND DISCUSSION | |
| SYNTHESIS, CHARACTERIZATION AND CATALYTIC ACTIVITY IN TRANSFER HYDROGENATION OF DINUCLEAR DI(N-HETEROCYCLIC) CARBENE IRIDIUM(III) COMPLEXES..... | 105 |
| 4.1 Synthesis of the dinuclear Ir(III) complexes | 105 |

| | |
|---|-----|
| 4.2 Transfer hydrogenation of ketones catalyzed by the dinuclear di-NHC complexes of iridium(III) 15 and 16 | 111 |
|---|-----|

Chapter 5: RESULTS AND DISCUSSION

REACTIVITY AND COORDINATION PROPERTIES OF NON-CLASSICAL CARBENES ..119

| | |
|---|-----|
| 5.1 Studies on the synthesis and reactivity of expanded ring carbenes..... | 119 |
| 5.2 Studies on the synthesis and reactivity of asymmetric mixed di(N-heterocyclic) carbenes | 125 |

Chapter 6: CONCLUSIONS.....133

Chapter 7: EXPERIMENTAL SECTION137

| | |
|--|-----|
| 7.1 Materials and methods | 137 |
| 7.2 Synthesis of the dimeric iridium(III) precursor $[\text{IrCl}_2\text{Cp}^*]_2$ | 138 |
| 7.3 Synthesis of the diimidazolium salts L¹·2HBr – L⁷·2HBr | 139 |
| 7.3.1 Synthesis of the diimidazolium salt 1,1'-di-tert-butyl-3,3'-methylenediimidazolium dibromide L⁵·2HBr | 140 |
| 7.3.2 Synthesis of the diimidazolium salt 1,1'-di- <i>n</i> -octyl-3,3'-methylenediimidazolium dibromide L⁶·2HBr | 140 |
| 7.4 Synthesis of the dibenzimidazolium salts L⁸·2HPF₆ and L⁹·2HBr | 141 |
| 7.4.1 Synthesis of the dibenzimidazolium salt 1,1'-dimethyl-3,3'-methylenedibenzimidazolium bis(hexafluorophosphate) L⁸·2HPF₆ | 141 |
| 7.4.2 Synthesis of the dibenzimidazolium salt 1,1'-dimethyl-3,3'-ethylenedibenzimidazolium dibromide L⁹·2HBr | 142 |
| 7.5 Synthesis of the diimidazolium salt 1,1'-dimethyl-3,3'-ethylene-5,5'-dibromodiimidazolium dibromide L¹⁰·2HBr | 142 |
| 7.6 Synthesis of the diimidazolium salts L¹¹·2HPF₆ and L¹²·2HPF₆ | 143 |
| 7.6.1 Synthesis of the diimidazolium salt 1,1'-dimethyl-3,3'-methylenediimidazolium bis(hexafluorophosphate) L¹¹·2HPF₆ | 143 |
| 7.6.2 Synthesis of the diimidazolium salt 1,1'-dimethyl-3,3'-ethylenediimidazolium bis(hexafluorophosphate) L¹²·2HPF₆ | 144 |
| 7.7 Synthesis of the diimidazolium salts L¹³·2HBr - L¹⁵·2HBr | 144 |

| | | |
|--------|---|-----|
| 7.7.1 | Synthesis of the diimidazolium salt 1,1'-dimethyl-3,3'-(<i>o</i> -xylylene)diimidazolium bis(hexafluorophosphate) $L^{13} \cdot 2PF_6$ | 145 |
| 7.8 | Synthesis of the diimidazolium salt 1,1'-di(2-pyridine)-3,3'-methylenediimidazolium bis(hexafluorophosphate) $L^{16} \cdot 2HPF_6$ | 145 |
| 7.9 | General procedure for the synthesis of the silver(I) complexes $[Ag_2(L^1)_2](PF_6)_2$ - $[Ag_2(L^4)_2](PF_6)_2$, $[Ag_2(L^6)_2](PF_6)_2$, $[Ag_2(L^7)_2](PF_6)_2$, $[Ag_2(L^9)_2](PF_6)_2$, $[Ag_2(L^{10})_2](PF_6)_2$, $[Ag_2(L^{14})_2](PF_6)_2$, $[Ag_2(L^{15})_2](PF_6)_2$ | 146 |
| 7.10 | Synthesis of the silver(I) complex bis(1,1'- <i>tert</i> -butyl-3,3'-methylen-2,2'-diylidene)disilver(I) bis(hexafluorophosphate) $[Ag_2(L^5)_2](PF_6)_2$ | 150 |
| 7.11 | General procedure for the synthesis of the silver(I) complexes $[Ag_2(L^8)_2](PF_6)_2$, $[Ag_2(L^{12})_2](PF_6)_2$, $[Ag_2(L^{13})_2](PF_6)_2$ and $[Ag_3(L^{16})_2(CH_3CN)_2](PF_6)_3 \cdot 2H_2O \cdot 0.5HPF_6$ | 151 |
| 7.12 | Synthesis of the iridium(III) complexes of general formula $[IrClCp^*(L^n)](PF_6)$ | 154 |
| 7.13 | Synthesis of the iridium(III) complexes $[IrCp^*(L^2)(CH_3CN)](PF_6)_2$ (2a) | 159 |
| 7.14 | Synthesis of the dinuclear iridium(III) complexes $[Ir_2Cl_2Cp^*_2(L^{15})] - [Ir_2Cl_2Cp^*_2(L^{16})](PF_6)_2$ | 160 |
| 7.15 | Water oxidation | 162 |
| 7.15.1 | Water oxidation reaction with Ce(IV) as sacrificial oxidant: procedure using the pressure/voltage transducer | 162 |
| 7.15.2 | Water oxidation reaction with $NaIO_4$ as sacrificial oxidant: procedure using the pressure/voltage transducer | 162 |
| 7.15.3 | Water oxidation reaction with Ce(IV) as sacrificial oxidant: procedure using the GC-MS | 163 |
| 7.15.4 | Water oxidation reaction with $NaIO_4$ as sacrificial oxidant: procedure using the GC-MS | 163 |
| 7.15.5 | Light driven oxidation of water | 164 |
| 7.15.6 | Dynamic light-scattering experiments | 165 |
| 7.15.7 | UV-Vis experiments | 165 |
| 7.16 | Transfer hydrogenation of ketones | 165 |
| 7.17 | Synthesis of the salts I-VII | 166 |
| 7.17.1 | Synthesis of I | 166 |

| | |
|---|------------|
| 7.17.2 Synthesis of II | 167 |
| 7.17.3 Synthesis of III | 167 |
| 7.17.4 Synthesis of V | 167 |
| 7.18 Reactions with the expanded rings salts I-VII | 168 |
| 7.19 Synthesis of azides | 170 |
| 7.20 General procedure for the synthesis of the coupled imidazole-triazole | 171 |
| 7.21 Synthesis of [3-(2,6-diisopropylphenyl)-1-methyl-5-((3-mesitylimidazolium) methyl)-1,2,3-triazolium] trifluoromethanesulfonate/bromide L¹⁷·(HOTf/HBr) | 172 |
| 7.22 Synthesis of [3-(2,6-diisopropylphenyl)-1-methyl-5-((3-mesitylimidazolium) methyl)-1,2,3-triazolium] bis(hexafluorophosphate) L¹⁷·2HPF₆ | 173 |
| 7.23 General procedure for the synthesis of the ligand precursors L¹⁸·(HBF₄/HBr) and L¹⁹·(HBF₄/HBr) | 174 |
| 7.24 Synthesis of [3-(2,6-diisopropylphenyl)-1-benzyl-5-((3-mesitylimidazolium) methyl)-1,2,3-triazolium] bis(hexafluorophosphate) L²⁰·2HBr | 175 |
| 7.25 Attempt to coordinate ligand L¹⁷ to iridium, via deprotonation with Cs ₂ CO ₃ . | 175 |
| 7.26 General procedure for the synthesis of silver(I) NHC-MIC complexes [Ag₂(L¹⁷)₂](OTf/Br) , [Ag₂(L¹⁷)₂](PF₆)₂ , [Ag₂(L¹⁸)₂](BF₄/Br) , [Ag₂(L¹⁹)₂](BF₄/Br) , [Ag₂(L²⁰)₂](Br)₂ | 176 |
| 7.27 Attempt to coordinate ligand L¹⁷ to iridium, via transmetalation from the corresponding silver complex | 179 |
| 7.28 X-ray crystal structure determination | 180 |
| Publications | 183 |
| Communications to congresses | 183 |
| Chapter 8: REFERENCES | 185 |

ABSTRACT

Initially, N-heterocyclic carbene ligands (NHCs) were considered ancillary ligands alternative to more classical two-electron donor ligands, phosphorous- (phosphines, phosphites, etc) and nitrogen-based (amines, imines, etc). Nowadays their role in organometallic chemistry is pivotal, and they found application in many different fields.

The Cp*Ir(III)-based complexes gained interest during the past years because they may be employed as catalysts in many organic transformations, and the inclusion of a NHC ligand in the coordination sphere of the complex generally enhanced both its robustness and catalytic activity. An appealing catalytic application of Cp*Ir(III)-NHC complexes is the water oxidation reaction, that is the oxidative half-reaction of an overall process called “artificial photosynthesis”. This is a promising route to provide, in the future, the production of green and sustainable energy alternative to the consumption of fossil fuels, and to convert solar energy into chemical one.

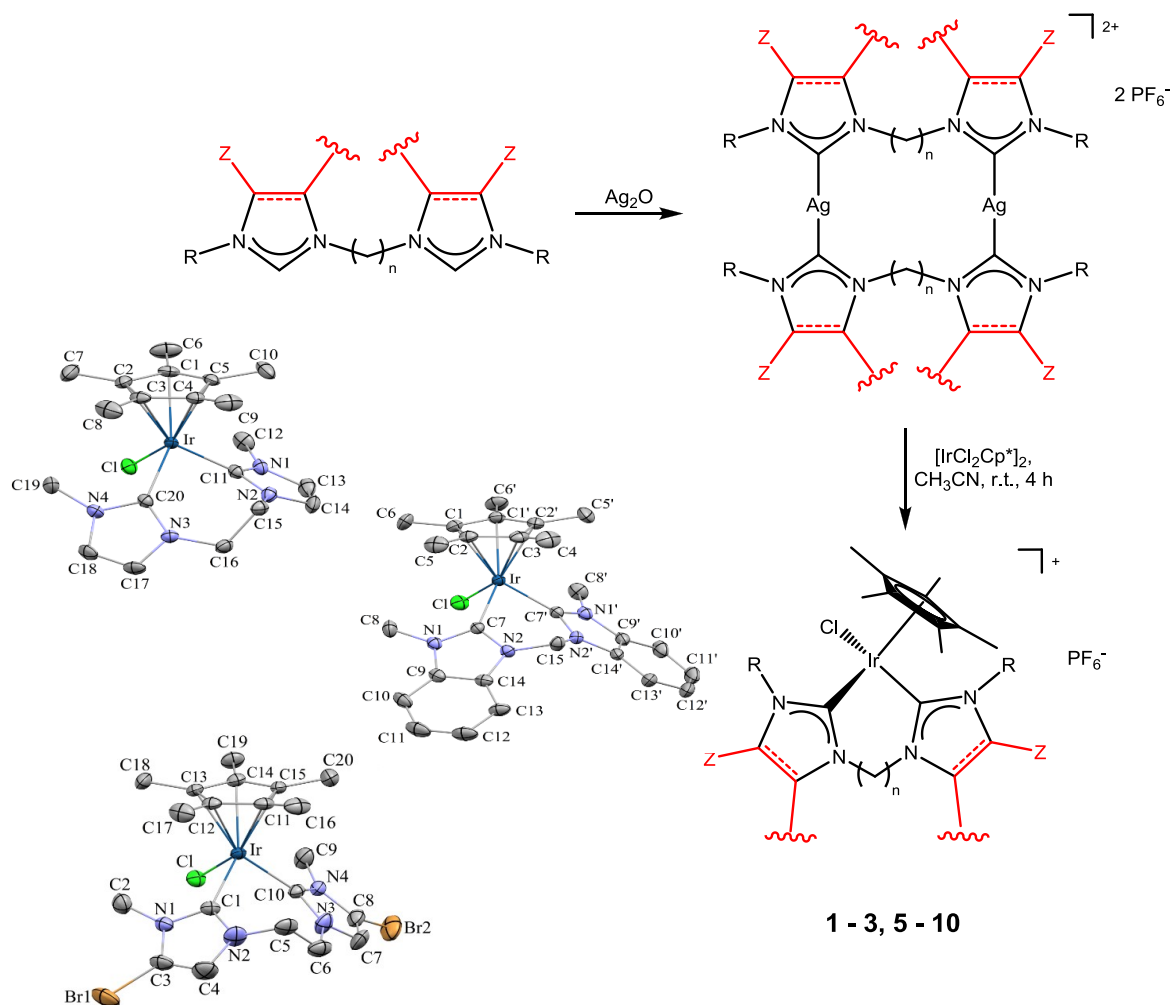
This PhD thesis is aimed to the study of iridium(III) complexes bearing di-(N-heterocyclic carbene) ligands (di-NHC), focusing either on the synthetic aspects and on the catalytic activity. Furthermore, the evaluation of the final steric and electronic properties of the complexes deriving by changes in the structure of the di-NHC ligand, will be addressed; the final aim is to find a relationship between the structure of the ligand and the properties and catalytic behavior of the complexes. In this regard, the catalytic activity will be evaluated mainly in water oxidation reaction, but also other organic transformations will be considered (transfer hydrogenation of ketones).

The obtained results will be divided in four main chapters: i] Synthesis and characterization of a series of mononuclear Ir(III) di-NHC complexes (**Chapter 2**); ii] Water oxidation reaction catalyzed by the mononuclear Ir(III) di-NHC complexes synthesized in the frame of the present PhD project (**Chapter 3**); iii] Synthesis, characterization and catalytic activity of novel dinuclear di-NHC Ir(III) complexes

(Chapter 4); iv] Reactivity and coordination properties of mono- and di-NHC ligands deriving from non-classical carbene units (Chapter 5).

i] Synthesis and characterization of a series of mononuclear Ir(III) di-NHC complexes.

A series of novel di-NHC iridium(III) complexes, having general formula $[\text{IrClCp}^*(\text{di-NHC})](\text{PF}_6)$, have been synthesized through the transmetalation of the di-NHC moiety from pre-formed, isolated and characterized dinuclear di-NHC silver(I) complexes. In the obtained Ir(III) complexes, the di-NHC ligand is coordinated to the metal centre in chelating fashion; this has been confirmed by the determination of the X-ray crystal structure of some complexes. The optimized synthetic protocol has been extended to several di-NHC ligands having different substituents at the nitrogen atoms and length of the alkyl bridging group. The effect of the substituents on the electron density, both on the metal and the carbene carbon, has been evaluated.



ii] Water oxidation reaction catalyzed by the mononuclear Ir(III) di-NHC complexes.

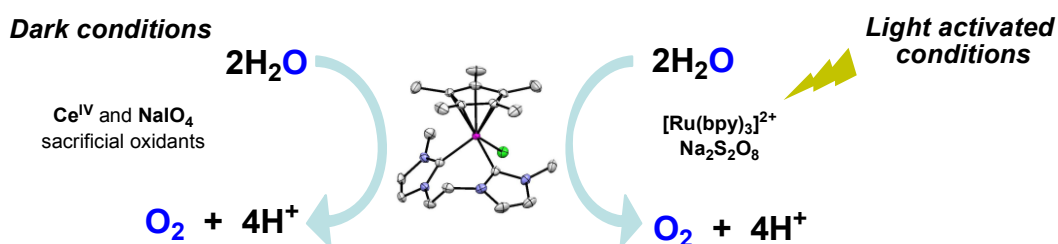
Some of the synthesized mononuclear di-NHC complexes have been successfully employed as catalysts for the water oxidation reaction in presence of Ce(IV) (as $(\text{NH}_4)_2[\text{Ce}(\text{NO}_3)_6]$, referred also as CAN) as sacrificial oxidant. One of the most active complexes (complex **2**) has been tested also in presence of NaIO_4 , showing activity comparable to that reported in literature for other Ir(III)-NHC complexes.

The catalyst fate under turnover conditions has been investigated by detecting the evolving gas *via* GC-MS measurements, and a small amount of CO_2 was observed concomitantly to the O_2 evolution. The amount of CO_2 derives probably from the oxidative degradation of the ligand set.

Complex **2** has been also employed in a photo-induced process, coupled with a photosensitizer ($[\text{Ru}(\text{bpy})_3]^{2+}$) and a sacrificial acceptor of electrons ($\text{S}_2\text{O}_8^{2-}$),

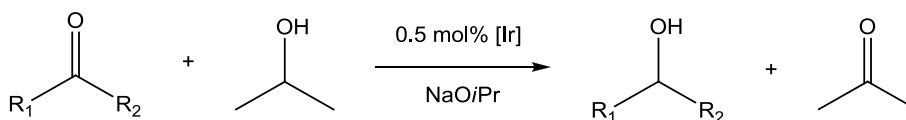
Abstract

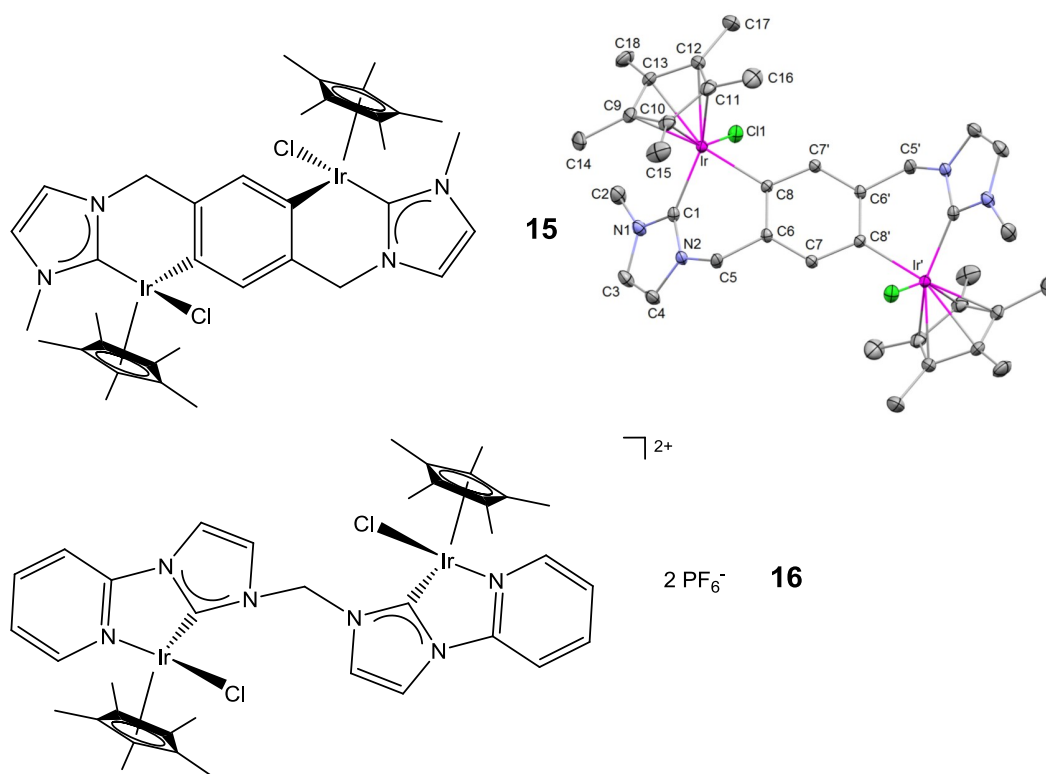
exhibiting activity remarkably different than that observed employing IrCl_3 under the same experimental conditions. IrCl_3 is a well-known precursor of IrO_x nanoparticles, so the observed difference may be considered a proof of the molecular nature of the catalyst. Further investigations allowed to detect, through EPR measurements, the formation of an Ir(IV) species, which is a plausible intermediate in the catalytic cycle, confirming the molecular nature of the employed catalyst.



iii] Synthesis, characterization and catalytic activity of novel dinuclear di-NHC Ir(III) complexes.

Novel dinuclear di-NHC Ir(III) complexes have been synthesized employing ligand precursors having a flexible and long bridging group between the carbene units or wingtip substituents with donor functionalities. Such complexes have been fully characterized, and in the case of complex **15** the crystal structure was also obtained. Such complexes have been successfully employed as catalysts in transfer hydrogenation of ketones: a scope of substrates has been spanned, and the tested complexes, especially complex **16**, showed moderate to good activity.





iv] Reactivity and coordination properties of mono- and di-NHC ligands derived from non-classical carbene units.

In the frame of a collaboration with the group of Prof. C. J. (Kees) Elsevier (University of Amsterdam), the possibility to obtain Ir(III) complexes with six-membered saturated NHCs was investigated. Unfortunately, the results obtained in this regard are not satisfactory, probably for the intrinsic instability of the ligand precursors and/or of the corresponding free carbenes.

Furthermore, the synthesis and the reactivity of mixed NHC-MIC ligands has been successfully carried out. The synthesis of the corresponding silver(I) complexes was performed and a preliminary optimization of the transmetalation reaction conditions has been accomplished, leading to the obtainment of a novel Ir(III) complex bearing a NHC-MIC ligand.



SOMMARIO

Inizialmente, i leganti carbenici N-eterociclici erano considerati leganti ancillari alternativi ai più classici leganti donatori bieletronici al fosforo (fosfine, fosfiti, etc) e all'azoto (ammine, immine, etc). Al giorno d'oggi il loro ruolo nella chimica organometallica è invece più centrale, e complessi con leganti carbenici trovano applicazione in diversi campi.

Negli ultimi anni è aumentato l'interesse verso complessi basati sul frammento $Cp^*Ir(III)$, perché possono essere utilizzati come catalizzatori in numerose trasformazioni organiche; inoltre, l'introduzione di un legante NHC nella sfera di coordinazione del complesso dovrebbe aumentare sia la sua stabilità che la sua attività catalitica. Un'interessante applicazione catalitica dei complessi $Cp^*Ir(III)$ -NHC è la reazione di ossidazione dell'acqua, che è la semi-reazione di un processo più complesso chiamato "fotosintesi artificiale". Nell'ambito del problema globale legato alla produzione e al consumo di energia, questo processo rappresenta una possibile alternativa all'utilizzo dei combustibili fossili e in futuro potrebbe permettere la produzione di energia in modo *green* e sostenibile per conversione dell'energia solare in energia chimica.

Questa Tesi di Dottorato ha come scopo lo studio di complessi di iridio(III) aventi nella sfera di coordinazione leganti dicarbenici N-eterociclici (di-NHC) e sarà focalizzata sia sugli aspetti sintetici che sull'attività catalitica dei complessi ottenuti. Inoltre, verranno discusse le proprietà steriche ed elettroniche dei complessi in funzione dei cambiamenti apportati alla struttura dei leganti di-NHC utilizzati; lo scopo ultimo sarà quello di trovare una relazione tra la struttura del legante, le proprietà stereo-elettroniche del complesso e la sua attività catalitica.

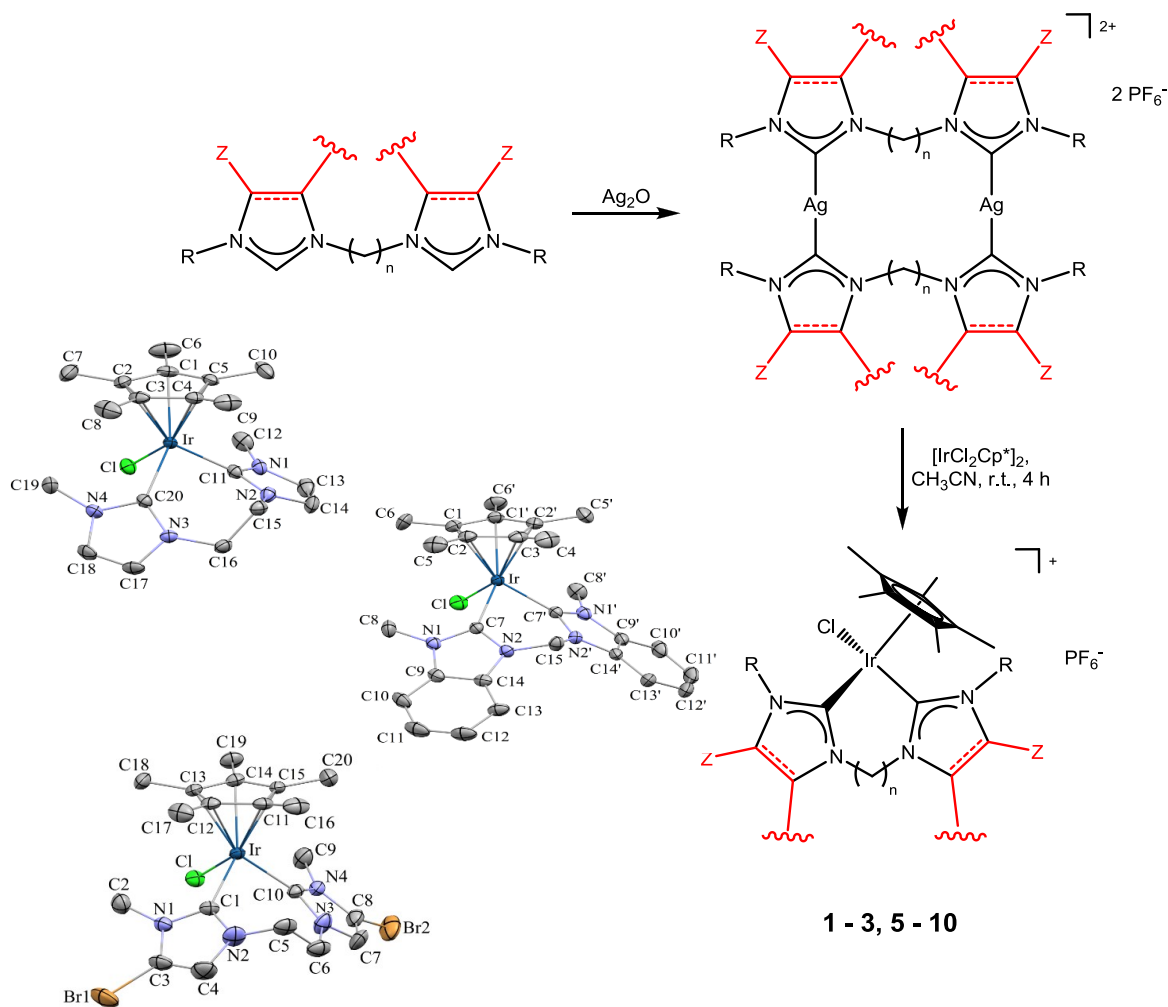
A questo proposito, l'attività catalitica sarà principalmente valutata nella reazione di ossidazione dell'acqua, ma verranno prese in esame anche altre trasformazioni organiche (*transfer hydrogenation* di chetoni).

I risultati ottenuti verranno divisi in quattro capitoli principali: i) Sintesi e caratterizzazione di una serie di complessi mononucleari di Ir(III) aventi un legante

di-NHC nella sfera di coordinazione (**Capitolo 2**); ii] Reazione di ossidazione di acqua catalizzata dai complessi mononucleari di-NHC di Ir(III) sintetizzati nell'ambito di questo progetto di Dottorato (**Capitolo 3**); iii] Sintesi, caratterizzazione e attività catalitica di nuovi complessi dinucleari di Ir(III) con leganti di-NHC (**Capitolo 4**); iv] Reattività e proprietà coordinanti di leganti mono- e dicarbenici derivanti da unità carbeniche non-classiche (**Capitolo 5**).

i] Sintesi e caratterizzazione di una serie di complessi mononucleari di Ir(III) aventi un legante di-NHC nella sfera di coordinazione.

Una serie di nuovi complessi mononucleari di iridio(III), aventi un legante di-NHC coordinato è stata sintetizzata mediante reazione di transmetallazione del legante di-NHC dai corrispondenti complessi di argento(I) pre-formati, isolati e caratterizzati. Nei complessi di Ir(III) ottenuti, il legante di-NHC è coordinato al centro metallico in modo chelato; ciò è stato confermato da tecniche di caratterizzazione in soluzione e, per alcuni complessi, dalla risoluzione ai raggi X della struttura. Il protocollo sintetico ottimizzato è stato esteso a leganti di-NHC caratterizzati da diversi sostituenti agli atomi di azoto e da gruppi alchilici a ponte tra le unità carbeniche di diversa lunghezza. E' stato valutato inoltre l'effetto dei sostituenti sulla densità elettronica presente sul metallo e sul carbonio carbenico.



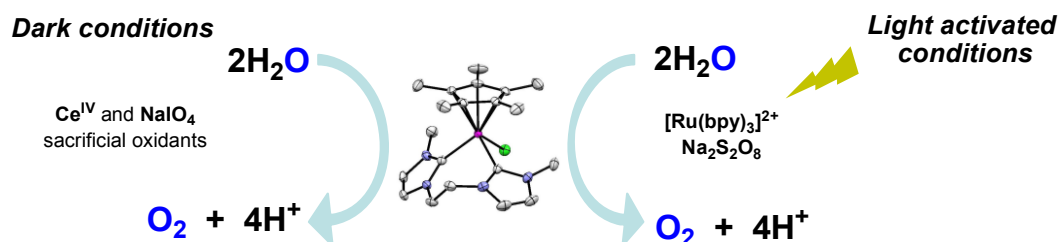
ii] Reazione di ossidazione di acqua catalizzata dai complessi mononucleari di-NHC di Ir(III) sintetizzati nell'ambito di questo progetto di Dottorato

Alcuni dei complessi mononucleari di Ir(III) sintetizzati sono stato impiegati con successo come catalizzatori nella reazione di ossidazione di acqua in presenza di Ce(IV) (come $(\text{NH}_4)_2[\text{Ce}(\text{NO}_3)_6]$, abbreviato con CAN) come ossidante sacrificale. Uno dei complessi più attivi (complesso **2**) è stato testato anche in presenza di NaIO_4 , esibendo un'attività catalitica comparabile con quella riportata in letteratura per complessi Ir(III)-NHC.

L'evoluzione del catalizzatore durante la catalisi è stata valutata determinando i gas prodotti utilizzando un GC-MS ed è stata osservata la formazione di una piccola quantità di CO_2 , il cui sviluppo è concomitante all'evoluzione di O_2 . La quantità di

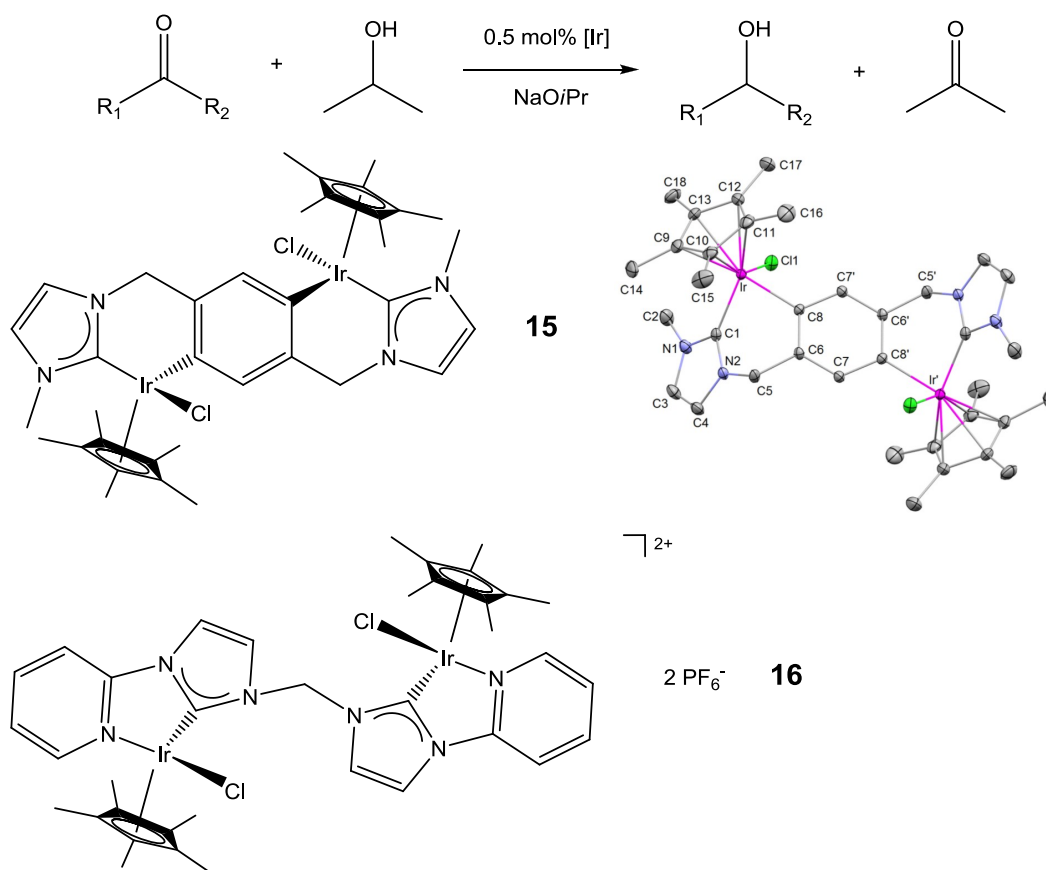
CO₂ osservata deriva probabilmente dalla degradazione ossidativa dei leganti nella sfera di coordinazione del complesso.

Il complesso **2** è stato inoltre utilizzato in un processo foto-indotto, accoppiato a un fotosensibilizzatore ([Ru(bpy)₃]²⁺) ed a un accettore sacrificale di elettroni (S₂O₈²⁻), mostrando una buona attività catalitica. Il comportamento del complesso **2** (in termini ad esempio di curva di evoluzione dell'ossigeno, tempo di vita del catalizzatore, resa quantica,...) è inoltre diverso da quanto osservato utilizzando IrCl₃ nelle stesse condizioni sperimentali. E' ben noto che IrCl₃ è un precursore di IrO_x nanoparticellare, perciò la differenza osservata può essere considerata una prova circa la natura molecolare del catalizzatore. Ulteriori investigazioni hanno permesso di identificare, attraverso misure EPR, la formazione di specie di Ir(IV), che è un intermedio probabile del ciclo catalitico; l'insieme di questi dati sembra confermare la natura molecolare del catalizzatore utilizzato.



iii] Sintesi, caratterizzazione e attività catalitica di nuovi complessi dinucleari di Ir(III) con leganti di-NHC

Utilizzando precursori dei leganti con gruppi lunghi e flessibili a ponte tra le unità carbeniche o aventi sostituenti con una funzionalità donatrice, sono stati sintetizzati nuovi complessi dinucleari di-NHC di iridio(III). Tali complessi sono stati completamente caratterizzati e, nel caso del complesso **15**, è stata inoltre risolta la struttura ai raggi X. Questi complessi sono stati impiegati con successo come catalizzatori nella reazione di *transfer hydrogenation* di chetoni: è stato eseguito uno screening di substrati e i complessi, soprattutto **16**, hanno mostrato una buona attività catalitica.



iv] Reattività e proprietà coordinanti di leganti mono- e di-NHC derivanti da unità carbeniche non-classiche

Nell'ambito di una collaborazione con il gruppo del Prof. C. J. (Kees) Elsevier (Università di Amsterdam), è stata valutata la possibilità di ottenere complessi di Ir(III) con leganti NHC saturi a sei membri. Sfortunatamente, i risultati ottenuti non sono stati soddisfacenti, probabilmente a causa della instabilità intrinseca dei precursori del leganti e/o dei corrispondenti carbeni liberi.

Invece, risultati migliori sono stati ottenuti nella sintesi e nello studio della reattività di leganti misti NHC-MIC, infatti sono stati sintetizzati i corrispondenti complessi di argento(I) ed è stata eseguita una preliminare ottimizzazione delle condizioni di reazione per la transmetallazione Ag(I)/Ir(III) del legante; in questo modo è stato ottenuto un nuovo complesso di Ir(III) avente un legante NHC-MIC nella sfera di coordinazione.



Chapter 1: INTRODUCTION

N-HETEROCYCLIC CARBENE LIGANDS

1.1 Properties of N-heterocyclic carbene ligands

N-heterocyclic carbenes (NHCs) (**Figure 1.1**) were firstly reported by the pioneering works of Öfele and Wanzlick in 1968.^[1] Later, Lappert and co-workers investigated the synthesis of NHC-metal complexes treating electron-rich olefins (ene-tetramines) with transition metal complexes.^[2] However, the interest for this class of ligands largely increased when Arduengo *et al.* finally achieved to isolate and crystallize the first free carbene in 1988, by quantitative deprotonation of the salt 1,3-diadamantylimidazolium iodide.^[3]

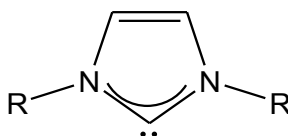


Figure 1.1: Generic N-heterocyclic carbene (imidazol-2-ylidene derived).

After the cited works, a huge number of studies on the synthesis of NHC-metal complexes and their use in catalysis has been done.^[4] Probably the most noteworthy application in this field involves ruthenium(II)-NHC complexes for the olefin metathesis, the so-called “second generation Grubbs’s catalysts” (**Figure 1.2**), for which prof. R. H. Grubbs was awarded with the Nobel Prize in 2005.^[5]

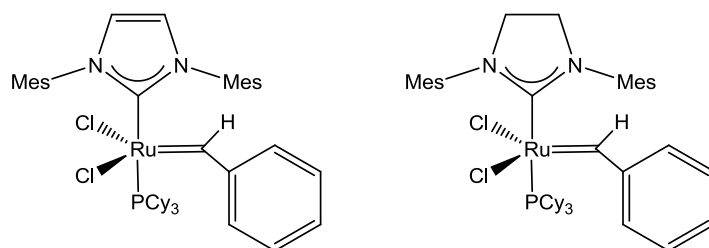


Figure 1.2: “Second generation Grubbs’s catalysts” for olefin metathesis.

Metal-carbene complexes were originally classified in two categories, Schrock- or Fischer-type carbenes, depending on the nature of the bonding between the carbene ligand and the metal centre (**Figure 1.3**). The Schrock-type coordinated carbenes are considered nucleophiles, the coordination to a metal centre leads to the formation of a covalent $M-C_{\text{carbene}}$ bond; this type of carbene ligands usually binds to early transition metals in high oxidation state, like Ti(IV), Ta(V), W(VI). The coordinated Fischer-type carbenes have instead an electrophilic nature, they are formally considered to be in a singlet ground state electronic configuration, so they can form a σ bond with the metal; this type of carbenes has an empty p_{π} orbital, which can be stabilized by the π -backdonation from the d_{π} orbitals of the metal and for this reason, these ligands strongly bind to late transition metals in low-medium oxidation state.^[6,7,8]

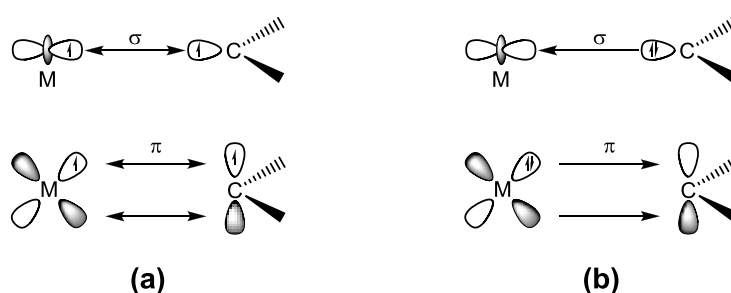


Figure 1.3: Metal-carbene interaction in Schrock-type (a) and Fischer-type (b) carbene complexes.

The NHC ligands may be considered Fischer-type carbenes for the nature of their metal-carbon bond: in fact, they bind primarily through σ -donation of the carbene lone pair to the metal. The main difference with Fischer-type carbenes is the extent

of the π -backdonation from the metal, which is believed to be negligible in N-heterocyclic carbene ligands. This can be explained with the high energy of the vacant p_π of the carbene centre (see below, **Figure 1.4**), as a consequence of the donation from the α -nitrogen atoms. Nevertheless, recently it has been demonstrated that, depending on the metal and the substituents on the carbene, a certain grade of backdonation from the metal may occur.^[9]

NHCs are very versatile two electrons donor ligands, often compared to phosphine ligands, able to coordinate a wide variety of late transition metals, both in high and low oxidation state, as well as several main group elements.^[7]

As pointed out by Nolan *et al.*, these ligands are recognized to be stronger σ -donors than other two electron donor ligands, such as amines, ethers and phosphines.^[10]

In particular with respect to the phosphine complexes, the NHC complexes are considered to be more stable. The M-C bond is in fact stronger than M-P bond (44-54 Kcal/mol vs. 25-37 Kcal/mol)^[11] and this allows to work without any excess of ligand, when using for example the related complexes as catalysts. The stronger bond might significantly reduce the degradation of the complexes when subjected to harsh conditions, like high temperatures, oxidative and acid environments.^[7,12,13]

To explain the exceptional stability of the N-heterocyclic carbene ligands, two electronic effects, induced by the presence of two nitrogen atoms in α -positions of the carbene carbon, need to be considered (**Figure 1.4**):

- the inductive effect led by the higher electronegativity of the nitrogen atoms, so that they act as σ -withdrawing substituents;
- the π -backdonation from the filled p_π orbitals of the nitrogen atoms to the empty p_π orbital of the carbene carbon (mesomeric effect).

As a consequence of these electronic effects, the σ orbital of the carbene carbon is lowered in terms of energy, while the π -donation destabilizes the p_π orbital, enhancing its energy. The increased gap between the σ and the p_π orbitals of the carbene favours the singlet ground state electronic configuration.

As mentioned before, the higher energy of the p_π orbital of the carbene carbon, caused by the π -donation from the nitrogen atoms, is the main reason why the π -backbonding from the metal to the NHC ligand is considered negligible and inferior to that verified in Fischer-type carbenes.

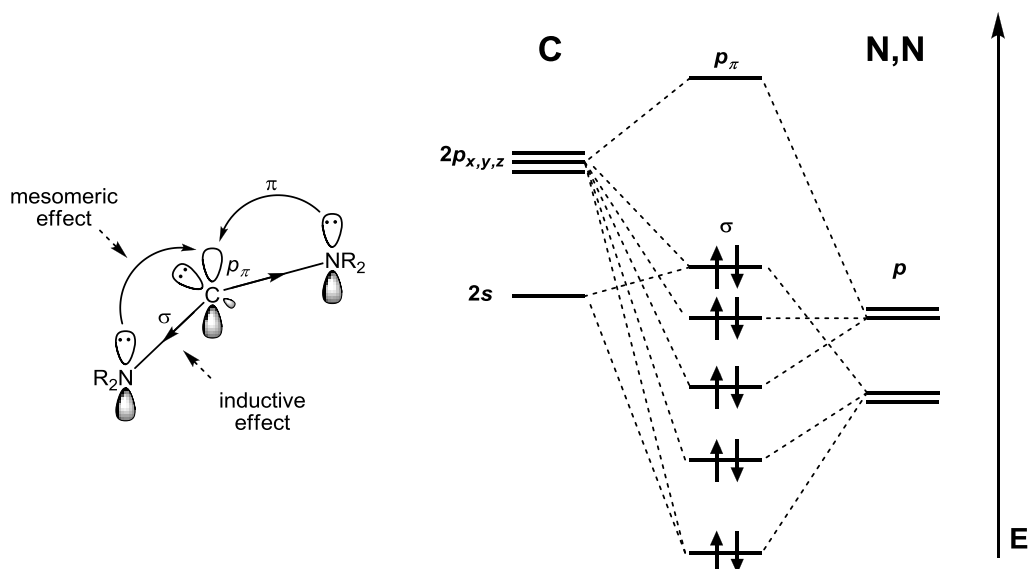


Figure 1.4: Inductive and mesomeric effect stabilizing the N-heterocyclic carbene (left); qualitative molecular orbital diagram of the N-C-N fragment (right).

A further stabilization is provided by the inclusion of the carbene R_2NCNR_2 fragment into a cyclic structure, thus moving from an acyclic diaminocarbene to a N-heterocyclic carbene. The introduction of an unsaturated bond between the carbon atoms in 4 and 5 positions of the ring ensures an electron delocalization; although this aromatic effect is less pronounced than in the imidazolium salt, the imidazol-2-ylidene is ca. 25 Kcal/mol more stable than the imidazolin-2-ylidene (**Figure 1.5**).^[14]

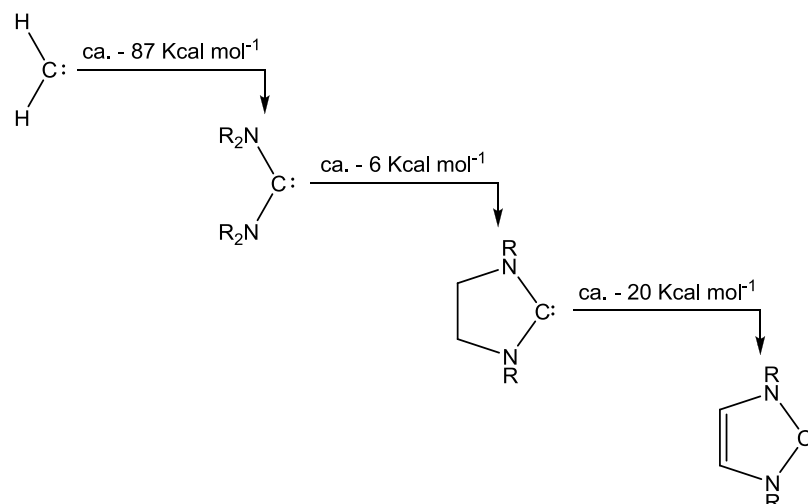


Figure 1.5: Stabilization in carbene moieties moving from :CH_2 to NHC ligand.

During the last two decades, the stereoelectronic properties of the N-heterocyclic carbenes have been intensively studied.

In order to determine the electronic effects of the NHC ligands on the resulting complexes, several approaches have been reported so far, both empirical and theoretical, and probably for a rigorous classification of the properties of the ligands a combination of the different methods is required.^[15,16]

One of the most commonly employed methods is the evaluation of the Tolman electronic parameter, also known as TEP. This method was developed by Tolman in the 70's and the original aim was to describe the electronic properties of phosphine ligands, through the measurement of the IR carbonyl stretching frequencies in phosphine-containing carbonyl complexes.^[17] Since CO is a π -acceptor ligand, it is clear that in such complexes the value of the stretching frequency of the C-O bond strongly depends on the electron density on the metal centre: higher is the electron density on the metal, stronger will be the M-C_{CO} bond (major back-donation from the metal to the π^*_{CO}), causing a weakening of the C-O triple bond and a consequent red-shift (bathochromic) of its stretching frequency (**Figure 1.6**).

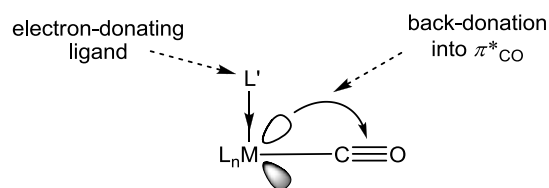


Figure 1.6: Weakening of the C-O bond due to the back-donation from the metal to the π^*_{CO} induced by the electron-donation from the ligand L.

By far, this method has been extended to a large number of ligands other than phosphines, and the TEP evaluation for NHC ligands clearly pointed out their stronger donor ability compared to that shown by phosphine ligands, even the most basic ones (e.g. P^tBu_3).^[10,15]

The first complexes used for the comparison of TEP values were nickel-based, with general formula $[\text{Ni}(\text{CO})_3(\text{L})]$; in this case, the C-O stretching frequency depends only on the ligand L, and it decreases (so the TEP value) with increasing donor ability of the considered L ligand. By now, the nickel-based complexes are being replaced by rhodium- and iridium-based complexes with general formula $[\text{MCl}(\text{CO})_2(\text{L})]$, because of the high toxicity (and the related problems) of the carbonyl complex $[\text{Ni}(\text{CO})_4]$, typically used as precursor. The synthesis of the complexes $[\text{IrCl}(\text{CO})_2(\text{NHC})]$ and $[\text{RhCl}(\text{CO})_2(\text{NHC})]$ is most often performed via substitution of a COD (1,5-cyclooctadiene) ligand with two molecules of CO from the complex $[\text{MCl}(\text{COD})(\text{NHC})]$, and thus leading to a *cis*-arrangement; in these cases, the TEP values are calculated as the average of the two carbonyl stretching vibrations.^[15]

The TEP determination has though some drawbacks: the IR spectrum strongly depends on the solvent, so some comparisons are not suitable due to the impossibility of dissolving all complexes in the same solvent; moreover, in some cases the differences between the registered frequencies are very small, especially dealing with NHCs, so that the use of a high resolution IR spectrophotometer is necessary.

The steric effects of a ligand can be evaluated in several ways; the ligand cone angle (θ), used generally to determine the steric hindrance of phosphine ligands, could not be extended straightforwardly to NHC ligands; in this case the commonly used

parameter is the $\%V_{\text{bur}}$ (buried volume), which is the measure of the ligand overall bulkiness (**Figure 1.7**).^[17,18]

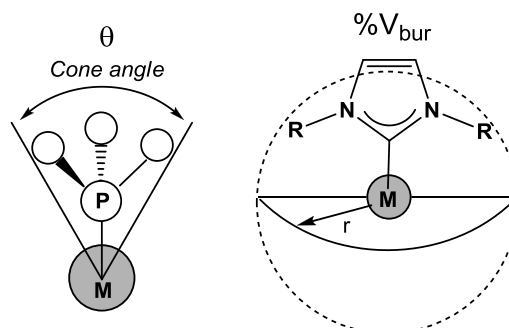


Figure 1.7: Schematic representation for Tolman cone angle θ (left) and $\%V_{\text{bur}}$ (right).

Recently, Gusev proposed the *repulsiveness* r as alternative method for the determination of the steric properties of an N-heterocyclic carbene. This parameter takes account of the repulsive energy between CO and the NHC ligands in complexes with general formula $[\text{Ni}(\text{CO})_3(\text{NHC})]$ and is directly connected to the reaction enthalpy of the decarbonylation reaction of the complex to form $[\text{Ni}(\text{CO})_2(\text{NHC})]$; since the most stable $[\text{Ni}(\text{CO})_3(\text{NHC})]$ complex is the one with the least bulky carbene unit, 1,3-*H*-imidazol-2-ylidene, the loss of a CO ligand from the coordination sphere appears to be under steric control.^[19] The evaluation of r parameter was useful to point out that changing the N,N'-groups has a small impact on the steric properties of the carbene ligand, while increasing the ring size (for example, moving from a five- to a six-membered N-heterocycle) can dramatically change its bulkiness.

An enormous advantage derived from the use of NHC ligands in place of phosphines is the greater possibility to modulate their stereo-electronic properties by varying the substituents at the nitrogen atoms and at the carbon atoms of the carbenic units. For example, the studies reported so far pointed out that NHC ligands with N-alkyl substituents are generally more electron donating than NHC ligands with N-aryl substituents.^[16]

An even larger effect on the stereo-electronic properties of the NHCs is provided by the structure of the N-heterocycle employed and by the position of the carbene carbon in the ring. A wide range of complexes with different N-heterocyclic rings have been reported so far (**Figure 1.8**), most of them derived from a five-membered ring, like imidazole, imidazoline or 1,2,4-triazole, but also from six-, seven- and eight-membered rings. For example it is generally accepted that the saturated carbene unit imidazolin-2-ylidene is slightly more electron donor than the unsaturated one imidazol-2-ylidene.^[16] Crabtree and co-workers demonstrated that the *abnormal* imidazol-5-ylidenes are exceptionally more donating than the more classical imidazol-2-ylidenes, with TEP values significantly lower.^[20] Free C₄-NHCs are generally less stable than C₂-NHCs; considering the higher acidity of the C₂-proton, in order to obtain the activation of the C₄-H bond, the most convenient way is given by protecting the C₂ position, substituting the proton with an alkyl or an aryl group prior the metalation. In some particular cases, the metalation to C₄ position may occur also when dealing with C₂ free carbenes with bulky substituents at the nitrogen atoms (e.g. ^tBu groups).^[21]

A rising class of five-membered ring NHCs is represented by 1,3,4-trisubstituted-1,2,3-triazol-5-ylidenes. The triazolium salts can be easily synthesized *via* Cu-catalyzed alkyne azide cycloaddition (CuAAC), followed by an alkylation or an arylation of the nitrogen atom in 3 position.^[22] The electronic properties of the carbene ligands derived from such precursors have been evaluated with orthogonal techniques, and all data show their strong σ -donor nature, with an electron-donor ability that lies in between that shown by imidazol-2-ylidenes and imidazol-4-ylidenes. A big difference of this type of carbene ligands with respect to the more classical imidazol-2-ylidenes needs to be underlined: when considering the possible resonance structures of the free carbene 1,2,3-triazol-5-ylidene, a neutral structure cannot exist.^[22] Although this charge separation is actually scarcely pronounced because of the aromatic delocalization of the electron density, these carbenes are also commonly called “mesoionic carbenes” (or MICs) because of their formal persistent zwitterionic nature.^[22,23,24]

When the carbene unit is formed by a ring with more than five atoms (six-, seven- and eight-membered rings), it is also called “expanded ring carbene” and a limited number of complexes with such ligands has been reported so far.^[25] It turned out that this class of NHCs is the most basic and their steric properties are also interesting: the large N-heterocycle leads in fact to an extremely large N-C_{carb}-N angle (in some case higher than 120 °); this results in a twisting of the N-substituents toward the metal centre, thus providing steric protection, but also strongly influencing the interaction between the metal and the incoming substrate when the complex is employed in catalysis, with consequences on the activity and the regioselectivity of the organic transformation.^[25a]

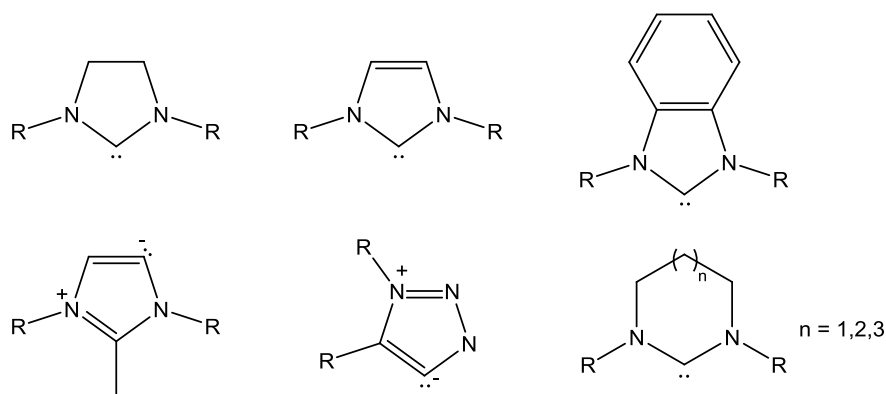


Figure 1.8: Example of NHC ligands based on different carbene units.

The nature of the substituents on the NHC ligand may also influence the coordination motif to the metal centre; a particular example involves the NHC ligands with a lateral group able to coordinate the metal centre (like an alkoxy, a phosphine or an amine group, a pyridine, for example) or an aryl group that can undergo metalation. The employment of such ligands can lead to both chelate mononuclear or bridged dinuclear structures (**Figure 1.9**).^[26]

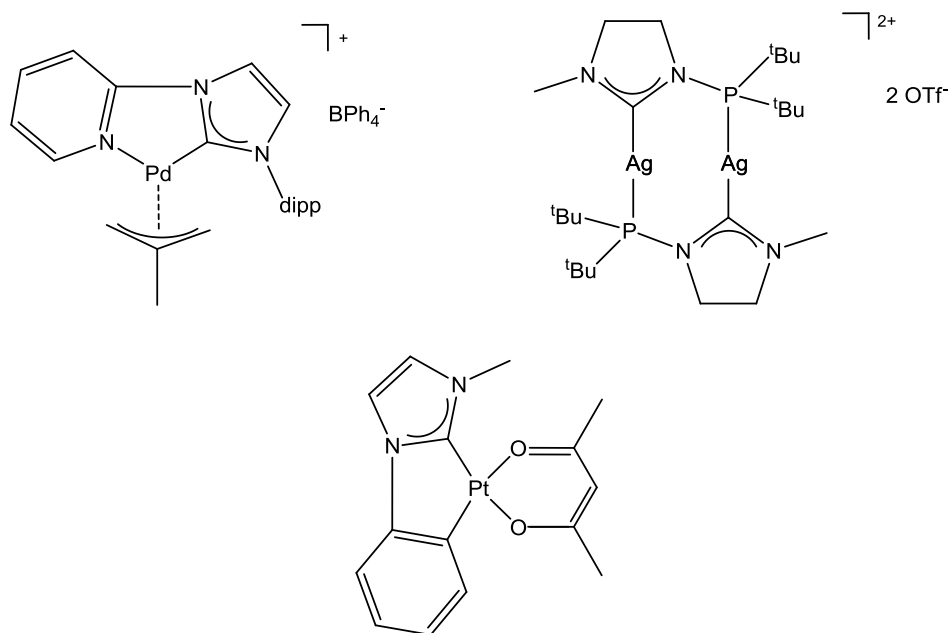


Figure 1.9: Examples of metal-NHC complexes bearing NHC ligands functionalized with a coordinating group such as pyridine (top left), a phosphine (top right) or an orthometallated phenyl ring (bottom).

Another step forward in the field of NHC ligand is related to the possibility of obtaining poly-NHC ligands, deriving from the connection of two or more carbene units with appropriate linkers. The use of a dicarbene ligand in place of two monocarbene ligands may lead, for instance, to the synthesis of a chelate complex, which should be more stable via chelate effect.^[27] This is a clear advantage if the complex is employed as catalyst; furthermore, the different steric hindrance of the chelate ligand with respect to the monodentate ligands may also influence the selectivity of the reaction.

The structure of the resulting complexes bearing poly-NHC ligands is strongly influenced by the metal centre employed. Focusing the attention on dicarbene ligands, the chelate coordination is not the only one possible: especially when dealing with group 11 metals, a bridged coordination is preferred, with the ligand simultaneously coordinated to two metal centres, resulting in a di-NHC dinuclear complex (**Figure 1.10**).^[28] For transition metals of other groups, this coordinating fashion is more rare, although possible when the bridging group between the carbene units is sufficiently longer or rigid.^[29]

This peculiarity is very interesting from many points of view: for example, when the dicarbene dinuclear complexes are employed as catalysts, a cooperative effect between the two metal centres may occur, resulting in an enhancement of the catalytic activity with respect to the mononuclear analogues.^[30] Another important effect was reported for group 11 metals, especially when dealing with gold(I)-diNHC complexes: an electronic communication between the two metals may provide a metallophilic interaction, obtaining complexes interesting in the field of the photoluminescence.^[28c]

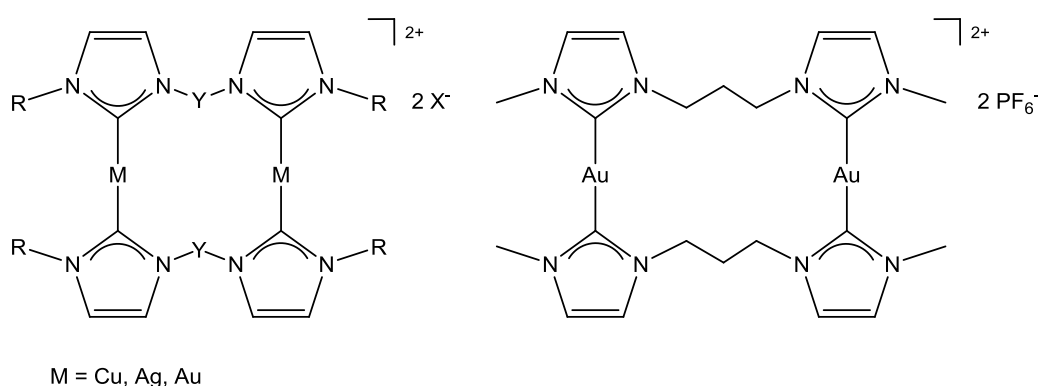


Figure 1.10: Examples of typical structures obtained for di-NHC complexes with group 11 metals (left) and a luminescent di-NHC dinuclear complex of gold(I).

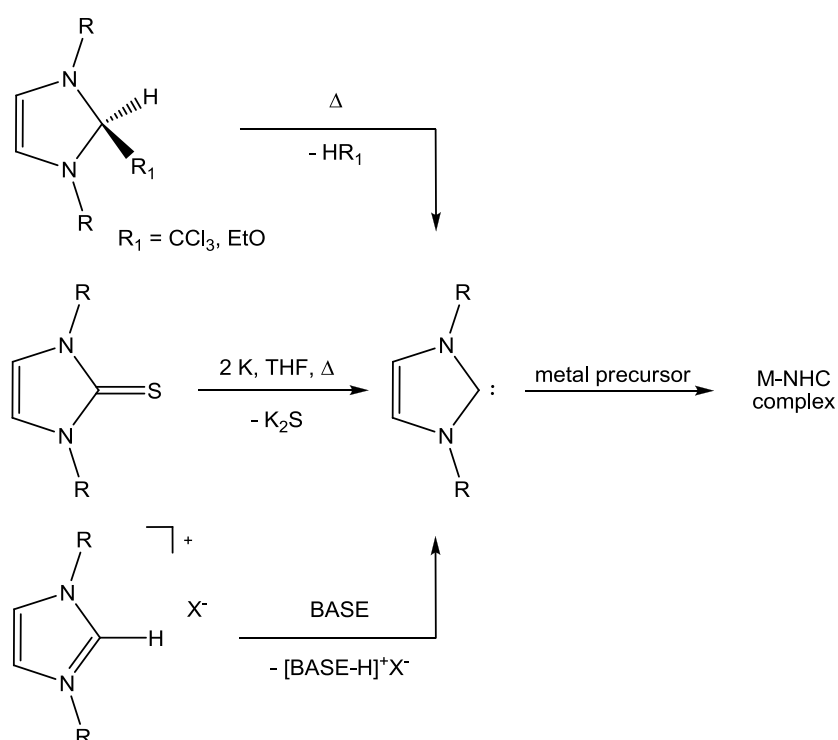
The coordination to a metal centre of a di-NHC ligand can change also by introducing a donor-functionalized bridge, like a pyridine, obtaining a CNC pincer ligand. This class of tridentate ligands is known to provide a further stabilization to the complexes; furthermore, the bridge can behave as hemilabile ligand, thus favouring, during the catalytic cycle, the generation of a free coordination site for the substrate coordination.^[31]

The works regarding di-NHCs are more abundant than those on tris-NHCs. Meyer and co-workers reported one of the first examples of tripodal NHC ligands, with the carbene units connected by (CH₃)C- or N-bridge (1,1,1-[tris-(3-alkylimidazol-2-ylidene)R]-ethane or tris[2-(3-alkylimidazol-2-ylidene)ethyl]amine, respectively), able to bridging coordinate three metal centres.^[32] Tetra-NHCs are even less

common, especially because of the complicated synthesis of the precursor salts and of their low solubility due to the tetra-cationic nature.^[33]

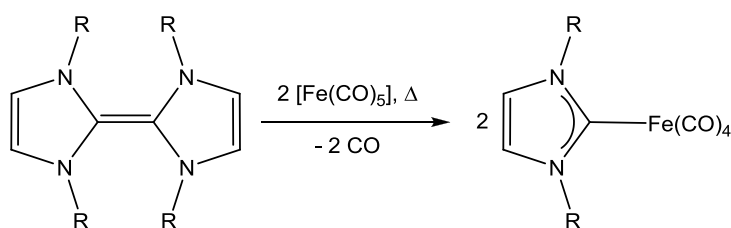
1.2 Synthesis of NHC-metal complexes

Several procedures have been explored so far for the synthesis of metal-NHC complexes. The first method consists in the direct reaction between the metal precursor and the pre-formed free carbene, which could be generated following different methodologies depending on the carbene precursor (**Scheme 1.1**): i] the thermal treatment of a 1,3-disubstituted imidazole bearing a good leaving group in 2 position (thermolysis of chloroform or alcohol); ii] the treatment of a imidazole-2-thione with potassium; iii] the deprotonation of the azolium salt with an external base.^[13] The last way is widely used and many bases have been proposed during the last decades, depending on the ligand precursor, like KO^tBu , Li^nBu , NaOAc , NaH , Cs_2CO_3 and others.



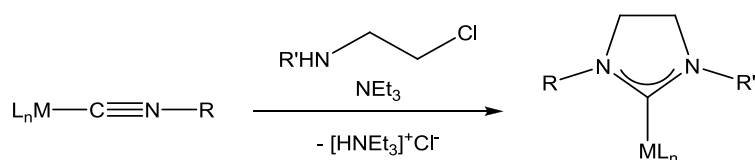
Scheme 1.1: Methods to synthesize free carbenes and NHC-metal complexes.

One of the main drawbacks in the generation of a free carbene is its tendency to dimerize, giving the corresponding olefin (enetetramine); to overcome this problem, the free carbene can be stabilized by introducing bulky substituents at the nitrogen atoms or can be generated *in situ* in presence of the metal precursor.^[13] The electron-rich olefins may be also considered as carbene precursors: in fact, when treated at high temperatures, their nucleophilic nature may favour the thermal cleavage in the presence of an electrophilic metal precursor,^[2,34,35] leading to the synthesis of the NHC-complex (**Scheme 1.2**).^[2]

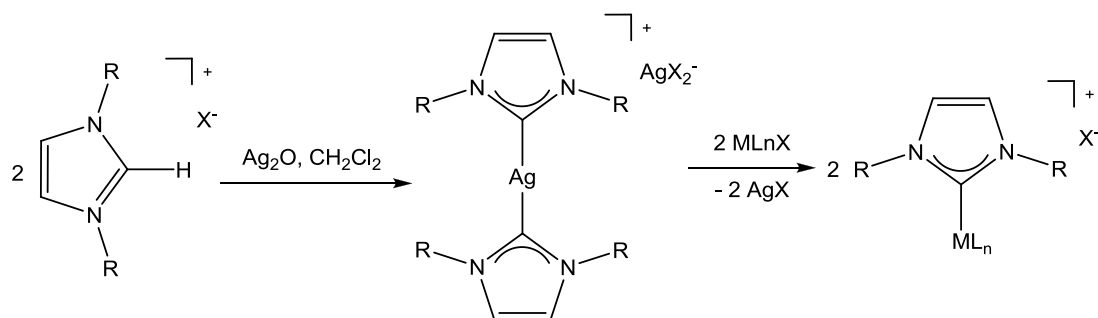


Scheme 1.2. Synthesis of a Fe(0)-NHC complex from thermal cleavage of an electron rich olefin.

Finally, two strategies to synthesize N-heterocyclic carbene complexes without the formation in solution of the free carbene are also possible: i] the nucleophilic attack of an amine to a functionalized isonitrile coordinated to the metal centre, followed by intramolecular cyclization and consequent NHC formation (**Scheme 1.3**);^[13,36] ii] the transmetalation of the carbene moiety from a silver(I)-NHC complex to another metal centre (**Scheme 1.4**).^[37,38,39]



Scheme 1.3: General synthesis of metal-NHC complexes from metal-isonitrile complexes *via* nucleophilic attack of an amine.



Scheme 1.4: General synthesis of metal-NHC complex via transmetalation of the carbene ligand from silver(I)-NHC complexes.

The latter method is one of the most applied and was firstly proposed by Lin *et al.* in 1998.^[38] Silver(I)-complexes can be easily synthesized, even in air, by reaction between an azolium salt and a silver(I) source, like a Ag_2O , AgNO_3 or AgOAc , which may act both as a base and metal precursor. The NHC-silver complex showed to be an excellent transfer agent for the carbene fragment to a large number of transition-metal centres. A commonly used strategy aimed to facilitate the process is the employment of halide metal precursor: the formation of the insoluble Ag-halide salt provides the driving-force of the transmetalation reaction.

1.3 Applications of NHC-metal complexes

The main application of NHC complexes regards their use as catalysts in organic transformations. Initially considered as phosphine-mimics for their coordination properties, NHC complexes showed during the past years a superior impact in catalysis as regards both the activity and the scope of the reactions.

The first related publication was reported by Herrmann *et al.* in 1995, when NHC-complexes of palladium(II) (**Figure 1.11**) were successfully employed as catalysts for the Heck reaction.^[40]

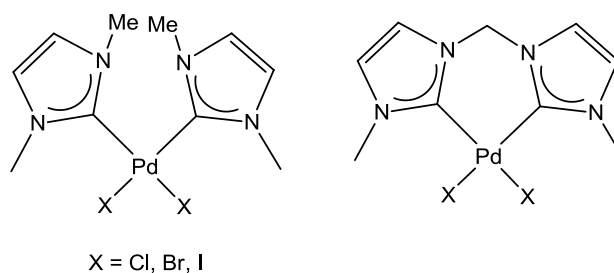


Figure 1.11: Complexes proposed by Herrmann *et al.* as catalysts for the Heck reaction.

A number of articles followed this first work and the applications in catalysis are virtually extended through all the organic reactions, like the already cited olefin metathesis with the Grubbs's catalysts, the C-C coupling reactions (Heck, Suzuki-Miyaura, Kumada-Corriu, Stille, Sonogashira reactions), the C-N or C-O coupling reactions (like the Ullmann-Goldberg reaction), the C-H activations, and many other more.^[4,41]

The application of N-heterocyclic carbene ligands is not limited merely to act as ancillary ligands for the synthesis of stable metal catalysts.^[22,42]

A number of NHC-metal complexes are now studied for biomedical application, especially because the strong metal-carbon bond should ensure the stability of the complex under physiological conditions. In particular, complexes of palladium(II) and group 11 metals bearing NHC ligands have shown promising properties in the field of anticancer research (**Figure 1.12**, top).^[43,44,45] Moreover, highly stable antimicrobials NHC-complexes of silver(I) are now studied for the replacement of conventional silver antibiotics (**Figure 1.12**, bottom).^[46]

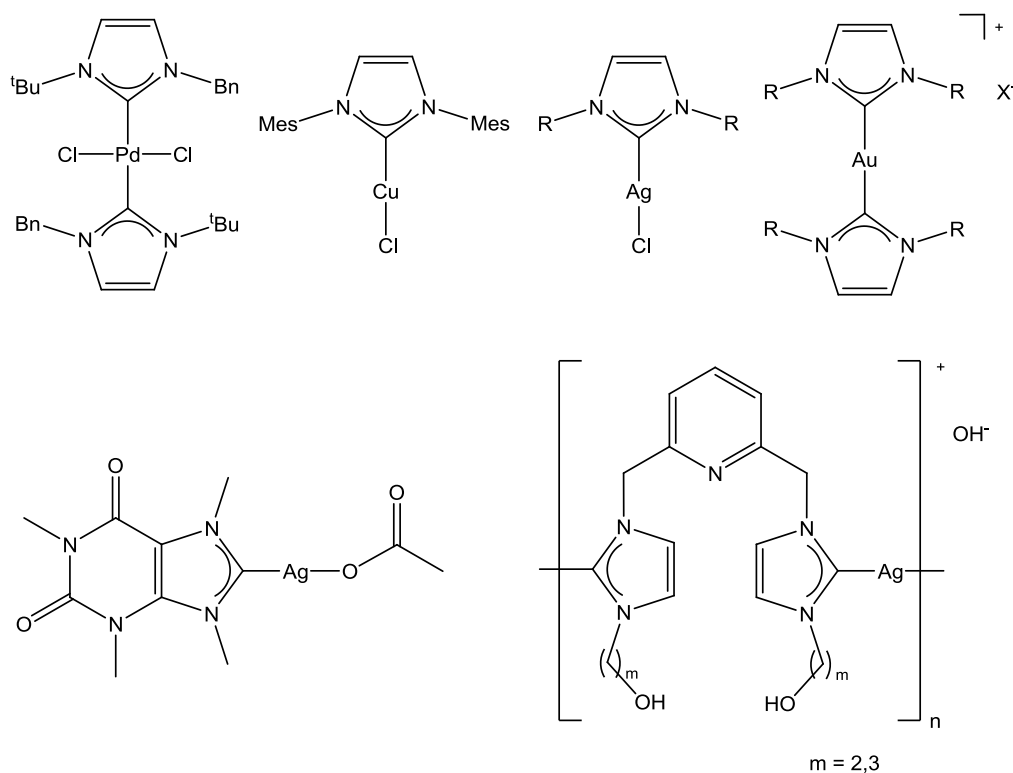


Figure 1.12: Examples of metal-NHC complexes of Pd(II), Cu(I), Ag(I) and Au(I) with cytotoxic activity (top) and Ag(I) complexes with antimicrobial activity (bottom).

The strength of the metal-carbon bond could be fundamental also for the application of the NHC metal complexes in material science. Palladium(II) and gold(I) complexes bearing NHC ligands have been successfully used as liquid crystals (**Figure 1.13**, top): the synthesized NHC-containing metallomesogens resulted to be very resistant and robust toward decomposition of the material at the so called “clarity point” (when the phase transition from the mesophase to the liquid phase occurs).^[42,47]

Even more interesting appears the possibility of tuning the electronic properties of the ligand by a proper choice of the substituents, which obviously has a great influence on the overall properties of the resulting complex. Complexes of iridium(III), platinum(II) and gold(I) (**Figure 1.13**, bottom) are well known to possess luminescence properties and can be used for the production of luminescent devices, like light-emitting electrochemical cells or as dopants for Organic Light-

Emitting Diodes (OLEDs). The lifetime of the emission state, as well as the wavelength of the emission, can be finely modulated by changing the wingtip groups or the carbenic unit.^[48]

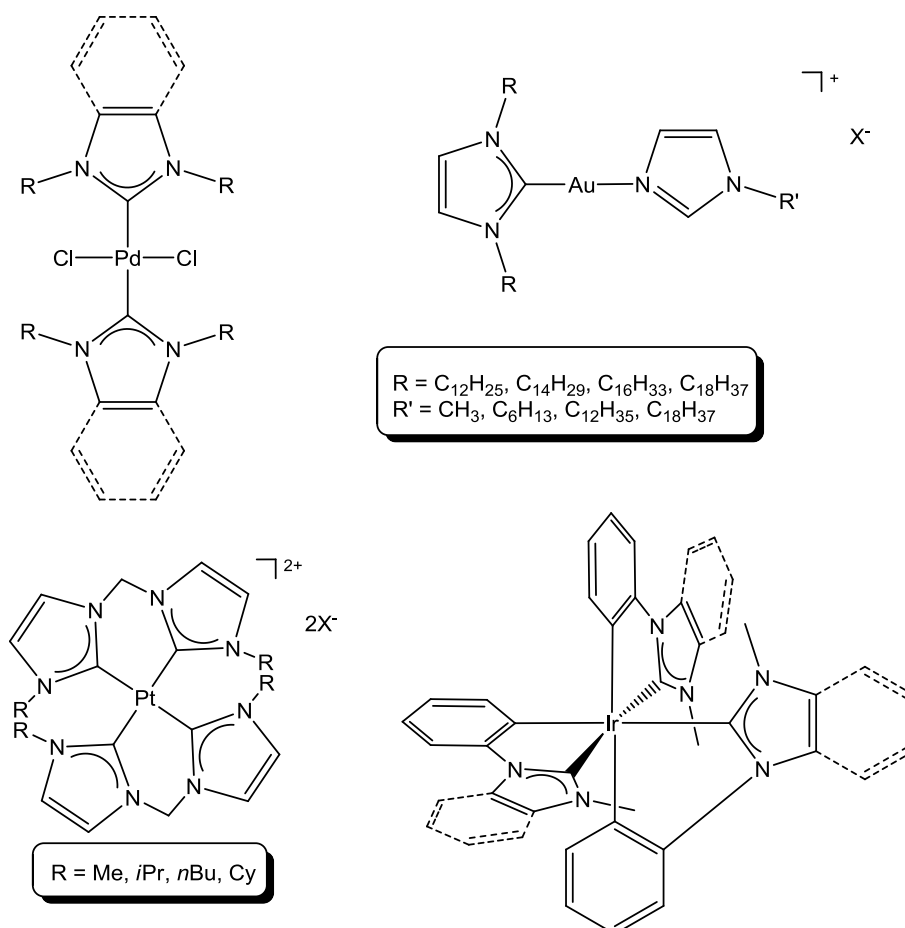


Figure 1.13: Examples of Pd(II) and Au(I) complexes bearing a NHC ligand with long alkyl wingtip groups with liquid crystalline behaviour (top); examples of Pt(II)- and Ir(III)-NHC complexes having photoluminescent properties (bottom).

1.4 Iridium(III) complexes with N-heterocyclic ligands: synthesis and applications

1.4.1 Synthesis of Ir(III)-NHC complexes

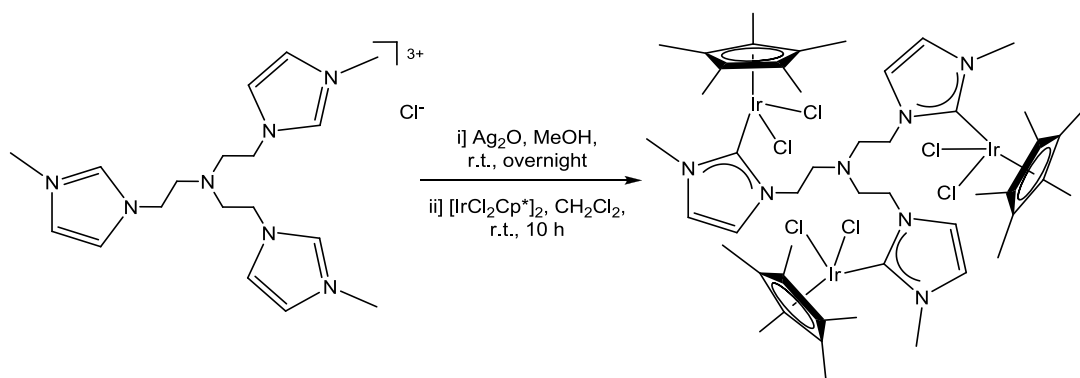
Focusing the attention on the synthesis of iridium(III)-NHC complexes, a number of approaches was proposed so far. The majority of the reported Ir(III)-NHC complexes has in the coordination sphere a Cp* ligand (Cp* = 1,2,3,4,5-pentamethylcyclopentadienyl group), because the precursor, i.e. the complex $[\text{IrCl}_2\text{Cp}^*]_2$, is easy to synthesize and the ancillary Cp* ligand is an anionic ligand strongly bonded to the iridium centre, thus leading to stable complexes. Another precursor often used is the cyclometallated complex $[\text{Ir}(\text{Arpy})_2\text{Cl}]_2$ (with Arpy = ortho-metalated arylpyridine), especially when the purpose is the study of the photoelectronic properties of the finally obtained complexes.

Ir(III)-NHC complexes are mainly synthesized following two procedures:

- I. Transmetalation of the carbene ligand from a silver(I)-NHC complex.
- II. Deprotonation of an azolium salt with a base, followed by reaction of the so-formed carbene with the iridium(III) precursor.

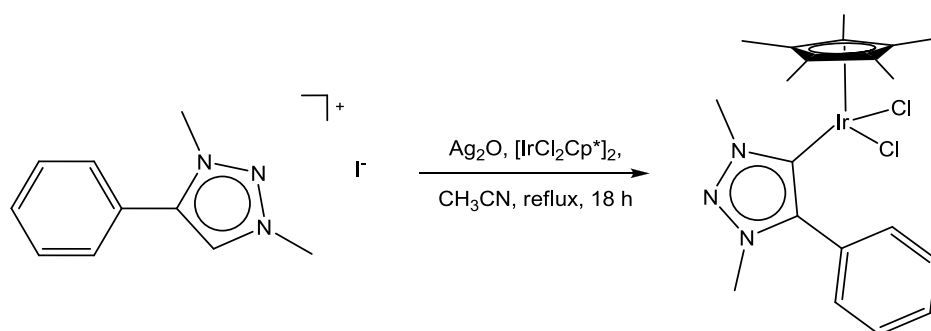
I. Transmetalation of the carbene ligand from a silver(I)-NHC complex

This is the most widely used approach, especially when dealing with poly-NHC ligands.^[39,49] As described in **Section 1.2**, this is a two-step synthetic procedure (**Schemes 1.4** and **1.5**): the first step is the synthesis of the Ag(I)-NHC complex through the reaction of the ligand precursor with an excess of Ag₂O (but also AgNO₃ or Ag₂CO₃). The second step is the transmetalation reaction of the carbene moiety to the iridium(III) centre. This last step can be performed either isolating the silver(I) complex or treating directly the solution containing the silver complex (obtained after removal of Ag₂O in excess) with the Ir(III) source. When using $[\text{IrCl}_2\text{Cp}^*]_2$ as precursor, the transmetalation could be favoured by the precipitation of AgCl as by-product, that can be easily removed by filtration.



Scheme 1.5: Synthesis of an Ir(III)-NHC via transmetalation of the carbene moiety from a Ag(I)-NHC complex.

Recently, it has been proved that the reaction between silver(I) oxide, iridium(III) precursor and azolium salt can occur also in one pot, without isolation or pre-formation of the silver(I) complex (**Scheme 1.6**).^[50]

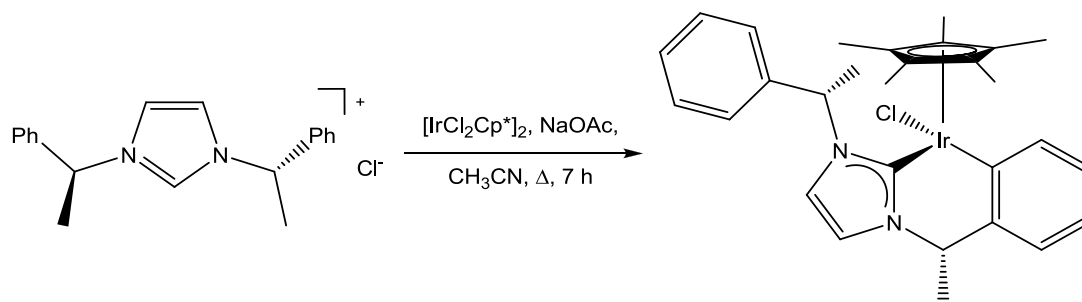


Scheme 1.6: Synthesis of an Ir(III) complex bearing a MIC ligand *via* one pot reaction of a triazolium salt, Ag₂O and [IrCl₂Cp*]₂.

II. Deprotonation of an azolium salt with a base, followed by reaction of the so-formed carbene with the iridium(III) precursor.

This is a widely used approach, especially for the synthesis of Ir(III)-NHC complexes bearing monocarbene ligands.^[51]

The carbene could be generated *in situ* by deprotonating the azolium precursor with an external base, typically NaH, KHDMS or KO^tBu; the reaction can occur either in the presence of the Ir(III) precursor or the latter can be added successively to the solution of the pre-formed carbene (**Scheme 1.7**).^[51c]



Scheme 1.7: Synthesis of an ortho-metalated Ir(III)-NHC complex *via* deprotonation *in situ* of the imidazolium salt with sodium acetate.

1.4.2 Applications of Ir(III)-NHC complexes

Iridium(III) complexes bearing N-heterocyclic carbenes are applied in a number of different catalytic reactions, both involving the reduction or the oxidation of a substrate, like transfer hydrogenation reaction, including Oppenauer-type oxidation of alcohols, and more recently, also for the water oxidation reaction.^[4]

Iridium(III)-NHC complexes are intensively employed in the transfer hydrogenation (TH) reactions, which consist in the reduction of unsaturated substrates like carbonyl compounds, alkenes, imines and nitrocompounds (**Figure 1.14**). Such category of reactions is very interesting because usually the unsaturated functional groups are reduced under mild conditions, using a sacrificial hydrogen-donor, instead of the potentially dangerous H₂ gas, that usually requires to carry out the reaction at high pressures.

The hydrogen-donors are typically cheap and commercially available substrates, like organic molecules such as alcohols (methanol, ethanol, benzyl alcohol, *i*-propanol) or formic acid and derivatives; in most of the cases, the sacrificial hydrogen-donor is used also as solvent.^[52,53,54,55,56,57]

The transfer hydrogenation reaction has been extensively studied and mechanistic insights suggested that generally the activation of the substrate is provided by metal-hydrides (both monohydrides and dihydrides);^[55] the formation of such intermediates in the catalytic cycle is promoted by an external base, so such reactions are typically carried out under basic conditions.

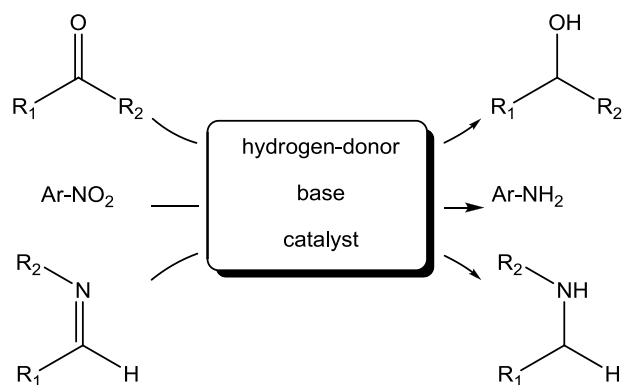
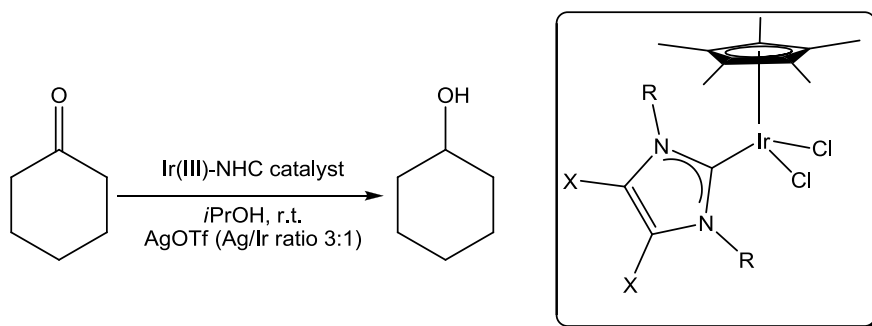


Figure 1.14: General scheme of transfer hydrogenation reaction of ketones, nitroarenes and imines.

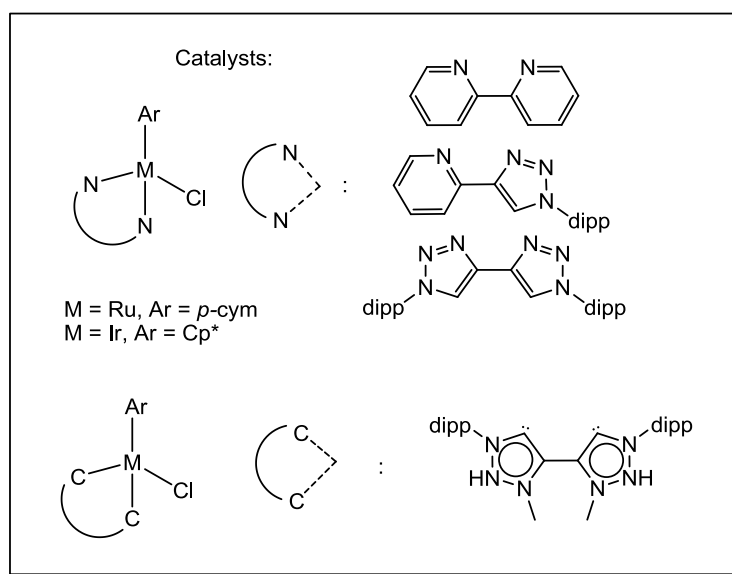
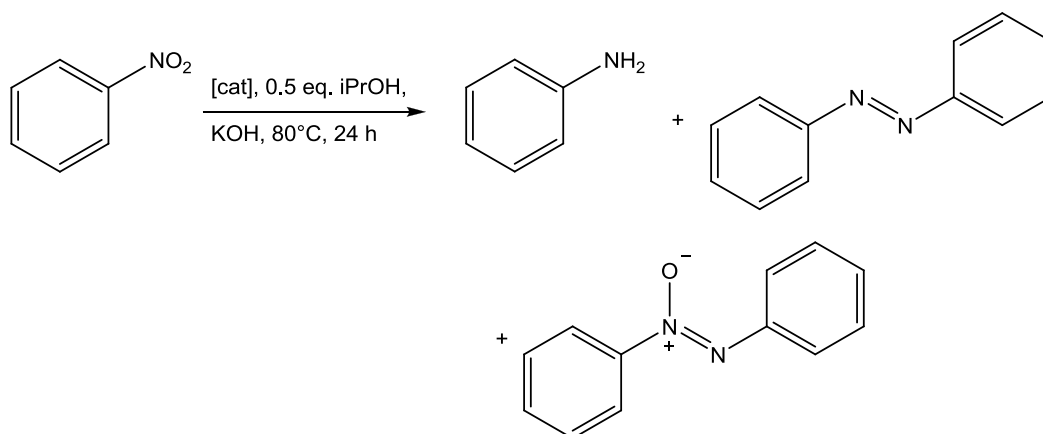
During past years the scope of this class of reactions has been further extended and employing Ir(III)-NHC complexes, both with classical imidazol-2-ylidene and with mesoionic carbenes, a wide range of highly functionalized substrates was successfully reduced, with high efficiency (up to quantitative conversion of the substrates) and selectivity in the distribution of the products.

In a representative work by Peris *et al.*, a series of Ir(III)-NHC of general formula $[\text{IrCl}_2\text{Cp}^*(\text{NHC})]$ (**Scheme 1.8**) was tested for the reduction of C=O and C=N bonds of several substrates, in the absence of a base.^[55] The tested catalysts are highly active for the transfer hydrogenation of cyclohexanone, and quantitative conversions within 15 minutes were observed using 2 mol% of catalyst. Lowering the catalyst loading to 0.1 mol%, quantitative conversions were indeed achieved, although in longer periods (8-12 h). Moderate conversion (29 %, in 17 h) was observed also when the complex with R = *n*Bu and X=H was used at 0.01 mol%. It is worth to underline that the presence of the NHC ligands surely improves the catalytic activity of the system and clearly has some effects on the mechanism of the reaction, because under the same conditions the complexes $[\text{IrCl}_2\text{Cp}^*]_2$ and $[\text{IrCl}_2\text{Cp}^*(\text{PMe}_3)]$ are completely ineffective. The scope of the catalytic activities of this type of complexes was explored and they have shown high activity for a number of substrates, such as aliphatic and aromatic ketones, aldehydes and *N*-benzylideneaniline.



Scheme 1.8: Transfer hydrogenation of cyclohexene reaction and iridium(III)-NHC complexes proposed by Peris *et al.*

Another representative example that highlights the influence of the carbene ligand on the selectivity of the transfer hydrogenation reaction was reported by Sarkar and co-workers: they synthesized and tested a series of Ru(II) and Ir(III) complexes bearing different chelating ligands, like bipyridine, pyridyl-triazole, bis-triazole and bis-(1,3,4-trisubstituted-1,2,3-triazol-5-ylidene) in the nitrobenzene reduction (**Scheme 1.9**).^[57]



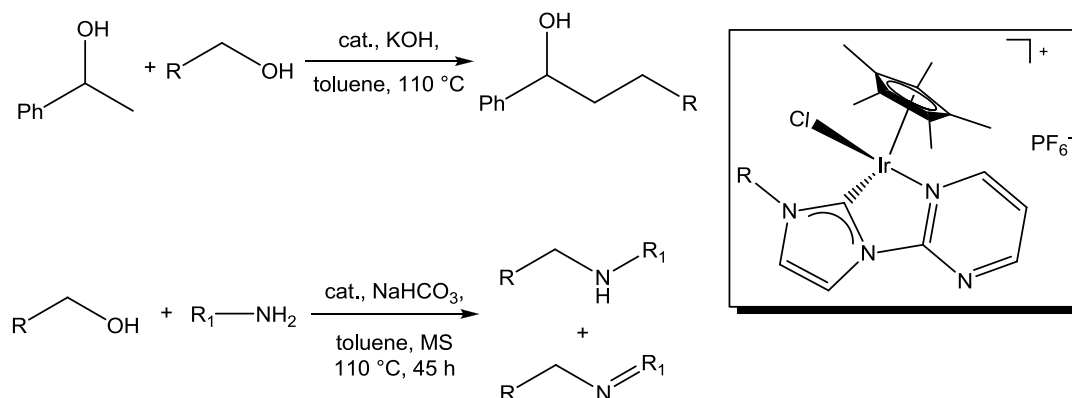
Scheme 1.9: Transfer hydrogenation of nitrobenzene catalyzed by Ru(II) or Ir(III) catalysts.

Firstly, the distribution of the products is strongly influenced by the metal centre employed: after 24 hours of reaction, with Ru(II) the main product is aniline, while with Ir(III) the aniline amount is less than 10 %. Interestingly, also the ligand has a role: focussing the attention on the Ir(III) catalysts, when the complex bearing a N,N'-chelate ligand was employed, the reaction is selective for the azobenzene production, while employing the Ir(III)-MIC catalyst the main product was azoxybenzene.

Ir(III)-NHC complexes were also employed in C-C and C-N coupling reactions *via* alcohol activation, which represents an environmental friendly way to synthesize functionalized alcohols and amines, because it overcomes the employment of toxic

Introduction

halides as alkylating agents, usually adopted in the more conventional synthetic processes. Crabtree and co-workers reported two complexes of iridium(III) bearing chelating NHC-pyrimidine ligands which are not only active in transfer hydrogenation of ketones reaction with good results, but also in β -alkylation of secondary alcohols and N-alkylation of amines (**Scheme 1.10**).^[56]



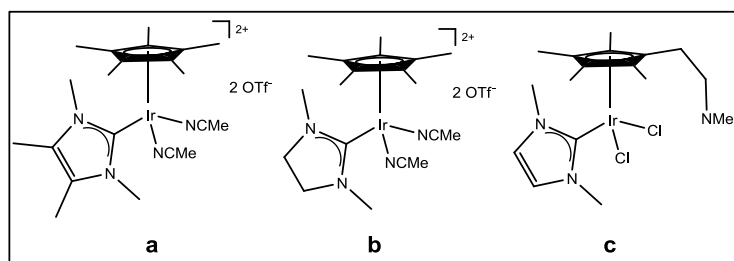
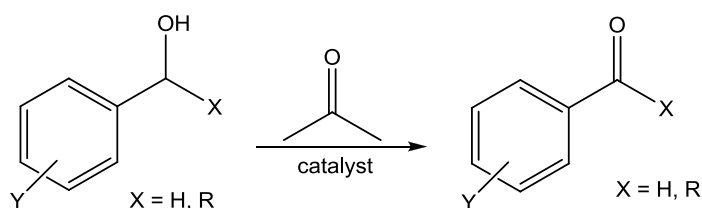
Scheme 1.10: β -alkylation of secondary alcohols (top) and N-alkylation of amines (bottom).

In the β -alkylation of secondary alcohols reaction, this type of complexes have shown good activity for the conversions of several substrates within 3 hours, with a high selectivity toward the formation of the corresponding alcohol with respect to the ketone.

The catalytic tests performed for the N-alkylation of amines reaction gave also good results, comparable to the best catalysts reported for this class of reactions: high conversion were observed for a series of substrates, with moderate to good selectivities for the amines with respect to the imines. These reactions are usually performed using strong bases, like KOH, but employing such catalytic systems it is possible to use a weaker base, like NaHCO₃; this peculiarity is important because the reaction can be performed in milder conditions, and also more sensitive substrates can be converted.

An interesting catalytic application was proposed by Yamaguchi *et al.* in the first half of the last decade employing Ir(III)-NHC complexes in the Oppenauer-type oxidation

reaction (**Scheme 1.11**).^[51a,58] This reaction is a promising way to obtain aldehydes and ketones from primary and secondary alcohols, respectively, because a non-toxic and cheap agent can be used as oxidant, typically acetone; this reaction belongs indeed to the class of hydrogen transfer reactions and is often referred as hydrogen transfer oxidation of alcohols.



Scheme 1.11: Oppenauer-type oxidation of primary and secondary alcohols (top); examples of the catalysts employed by Yamaguchi *et al.*

In this reaction, the dinuclear complex $[\text{IrCl}_2\text{Cp}^*]_2$ is only moderately active, but the introduction of a N-heterocyclic carbene in the coordination sphere resulted in a significant enhancement of the catalytic activity. Yamaguchi and co-workers proposed a series of monocarbene mononuclear $\text{Cp}^*\text{Ir(III)}$ -based complexes and the most active in the model reaction (complex **a**), i.e. the oxidation of 1-phenylethanol to acetophenone, was tested with good results for the transformation of a wide scope of substrates, both primary and secondary alcohols, under basic conditions. The lowest yields were obtained with acid-sensitive alcohols, probably due to the dicationic nature of the pre-catalyst. Lately, the performances were improved by functionalizing the Cp^* ligand with a 2-(dimethylamino)ethyl group (complex **c**), which not only makes unnecessary the employment of an external base, but also

leads to an intramolecular deprotonation, allowing the successful oxidation also of acid-sensitive substrates.

As mentioned previously, Ir(III) complexes are able to activate C-H bond and this peculiarity was explored for the catalytic H/D exchange.^[59] In this regard, a wide range of organic molecules can be activated successfully, with several deuterium sources. For this aim, the first employed catalysts were Cp*Ir-phosphino complexes, but replacing the phosphine ligands with NHCs both the activity and the stability of the catalytic system were improved. This represents another example in which the strong electron-donor ability of NHCs combined with their tunability provided to obtain more active catalyst; for this topic, the best results were obtained employing the strongest donor NHC ligands.

Iridium(III)-NHC complexes have found also application beyond catalysis.

Recently, a number of heavy transition metals, like Re(I), Ru(II), Pt(II), Ag(I) and Au(I) have been employed to obtain complexes characterised by photoelectronic properties potentially interesting to produce light-emitting materials.^[48] The appeals of using luminescent devices based on organometallic complexes is due to the higher control on the final properties provided, the enhanced stability of the resulting material and the easier synthesis with respect to OLEDs. Also Ir(III) complexes bearing cyclometallated ligands were investigated for this purpose, and a number of examples of light-emitting electrochemical cells (LEECs) have been reported, mostly emitting in the green or red region. In order to modulate the energy of the emission a wide range of ancillary ligands has been screened, especially with nitrogen as donor atom. In this field, a great interest is gained by N-heterocyclic carbene ligands, because of the previously described properties: they provide high stability, strong electron-donor ability and tunability of the properties by changing the substituents, both on the carbene unit and the nitrogen atoms. The NHCs are strong field ligands, and their application led to the obtainment of several complexes with high ligand-field splitting effects; the gap energy between HOMO

and LUMO orbitals can be finely modulated by slightly changing the ligand structure, thus leading to a change in the absorption and emission energy. In 2005, Thompson *et al.* reported the first examples of Ir(III)-NHC complexes emitting in blue or near-UV regions, both at low (77 K) and room temperature (**Figure 1.15**); the quantum yields showed by the proposed complexes were also considerably promising.^[60] Lately, the same authors implemented their work by the inclusion of the described complexes as dopants in polystyrene films, obtaining an emitting material in which the complexes keep the long lifetimes showed previously.^[61] Also chelating dicarbene ligands can be used to this aim: De Cola and co-workers proposed a series of (di-NHC)-Ir(III) complexes (**Figure 1.15**) displaying a deep-blue emission, with high quantum yields; moreover, the proposed complexes showed good solubility in a wide range of solvents, so they were applied successfully as blue phosphors for the production of blue-emitting electrochemical cells.^[62]

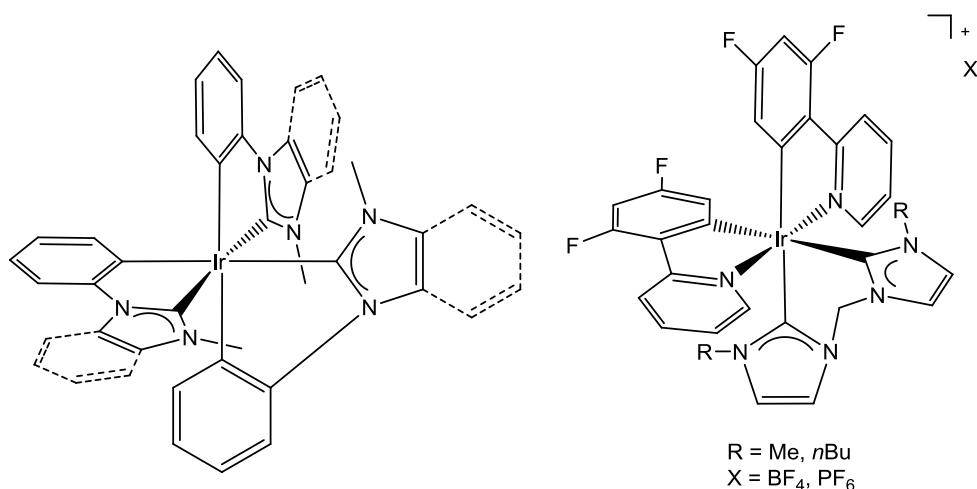
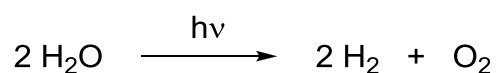


Figure 1.15: Examples of luminescent iridium(III) complexes.

Another interesting example of the potential application of iridium(III) bearing N-heterocyclic carbene was the water oxidation reaction, which will be discussed in more detail in the following section.

1.5 Water oxidation reaction

The fast growth of the world population has rapidly increased the global consumption of energy, and in few decades the use of the classical sources of energy will not be sustainable anymore. Nowadays, probably the most important and challenging aim of research is the development of systems able to produce renewable energies alternative to the combustion of fossil fuels. In this regard, probably the most promising way is to use sunlight as energy vector to promote the production of molecular hydrogen from water. The overall process has been renamed solar-driven water splitting, but it is also referred as artificial photosynthesis.^[63]



The appeal of such process is given by many factors: the consumed substrate is the cheapest, renewable and most abundant available, as well as the energy source; notably, the by-product of the reaction is molecular oxygen, so also the CO₂ emissions will decrease.

As suggested by the name, the water splitting process is inspired by the natural photosynthesis, accomplished by plants, algae and cyanobacteria. In the natural systems, the water is oxidised to generate protons and electrons, that are necessary to provide the sustainment of life processes and to produce carbohydrates used as feedstock, by reducing carbon dioxide. The artificial photosynthesis is based on the same principles: in the overall process, water is oxidized to O₂, producing 4 electrons that can reduce H⁺ to H₂.

A synthetic device able to perform the overall process of solar-driven water splitting should be composed by some fundamental components (**Figure 1.16**): i] a system (photosensitizer) that can harvest the sunlight; ii] a charge separator that provides the transfer of the excited electron from the photosensitizer to the reductive catalyst; iii] a reductive catalyst for the production of hydrogen from protons; iv] an

oxidative catalyst that can oxidize water producing 4 electrons for the regeneration of the photosensitizer and four protons for the reductive reaction.^[64,65,66,67]

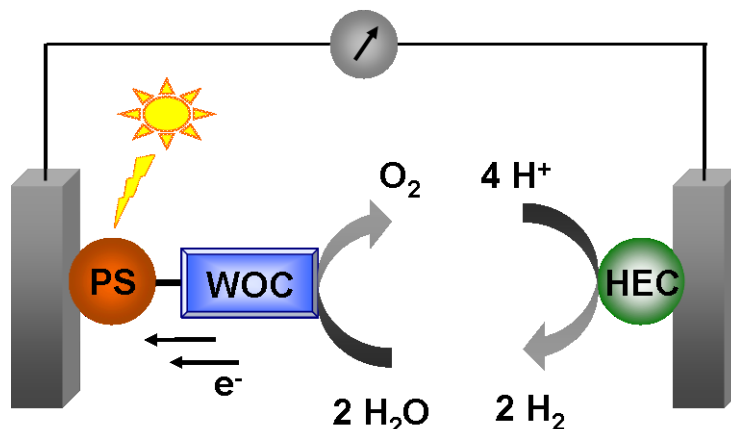
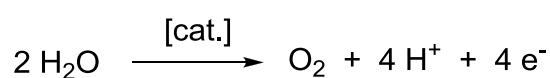


Figure 1.16: Schematic example of a photochemical cell for the water splitting process; PS = photosensitizer, WOC = water oxidation catalyst, HEC = hydrogen evolving complex. Figure adapted from reference [64].

While a large number of efficient catalytic systems have been reported so far for the reductive half-reaction, the development of effective catalysts for the oxidation of water still represents the bottleneck for the satisfactory accomplishment of the overall process.



Actually, such reaction is thermodynamically unfavourable, since it is characterized by a Gibbs free energy (ΔG) value of ca. 237 kJ mol^{-1} . As can be clearly noted from the equation, the reaction is rather complicated from a mechanistic point of view, since the loss of 4 protons and 4 electrons, and the formation of a new O-O double bond are involved. As a consequence to such considerations, an effective catalyst is needed in order to overcome the high activation barrier of the reaction.

In natural processes, the oxidative half-reaction of water splitting is performed by enzyme-cofactor complex Photosystem II (PSII), a bulky and large metalloprotein, in

which the real active site is composed by a core called Oxygen-Evolving Complex (OEC).^[68] Recently, Kamiya and co-workers reported the crystal structure of the OEC, pointing out the presence of four manganese atoms and one calcium ion, connected by oxo-bridges; such structure can be considered as a cuban-like Mn_4CaO_5 cluster.^[69] Reasonably, the mechanism for the water oxidation provided by OEC is complicated, but the multimetallic structure suggests a cooperative effect between the metal centres.

Considering the structure of OEC and the complicated mechanism of the water oxidation reaction, at first glance it appears necessary the employment of a multimetallic OEC-mimicking catalyst;^[70] actually, during the last decades a number active complexes, both with poly- and mononuclear structure, were reported.^[64-67,71,72]

The first notable work was reported by Meyer *et al.* in 1982, with the so-called “blue dimer”; this complex is a dinuclear oxo-bridged ruthenium complex (*cis,cis*- $[(bpy)_2(H_2O)Ru(\mu-O)Ru(H_2O)(bpy)_2]^{4+}$, with bpy = bipyridine), able to catalyze the reaction in presence of Ce(IV) as sacrificial oxidant (as $(NH_4)_2[Ce(NO_3)_6]$, abbreviated as CAN).^[73]

Although the final aim is to develop a system able to catalyse the overall photo-assisted process, once combined with the other cell components described previously (**Figure 1.16**), the first evaluation of the catalytic behaviour of a metal complex is more conveniently performed in the presence of a sacrificial oxidant in a homogeneous reaction. Despite such “dark conditions” are different from the light-driven ones, the use of a sacrificial oxidant presents some advantages.^[65,67,74] i] the catalysts, the conditions and the sacrificial oxidant themselves can be rapidly screened; ii] the amount of evolved oxygen is usually high, so the detection of gas and the comparison between the different catalytic systems is straightforward.

The most used and the best characterized sacrificial oxidant reported is surely the cerium(IV) complex $(NH_4)_2[Ce(NO_3)_6]$ (CAN). The CAN is stable, commercially available, water-soluble and has the unique advantage to be a one-electron oxidant,

so it can only drive the water oxidation catalysis by monoelectronic steps. Moreover, it possesses a strong absorption band in the UV spectrum at 340 nm, so that the water oxidation reaction can be monitored following the decrease of such band. The use of CAN as sacrificial oxidant has however some drawbacks: i] it affords a very low pH (*ca.* 0.7-0.9) in solution, but the advisable pH in a photosynthetic cells is neutral or basic; ii] the reduction potential is very high (1.75 V vs. NHE at pH = 0.9), which represents an advantage when dealing with catalysts with high potential barrier but can also lead to the presence of side reactions, such as the oxidative degradation of the organic ligands in the coordination sphere of the complex. Moreover, the nitrate ions of the complex may interfere with the catalytic process, complicating the study of the mechanism. Since CAN has both advantages and drawbacks, during last years few other sacrificial oxidants were considered, like for example $\text{Ce}(\text{OTf})_4$,^[75] or the two-electron sacrificial oxidants potassium peroxymonosulfate (Oxone®), sodium hypochlorite and sodium periodate.^[74] The advantage of employing a bielectronic oxidant is that in some cases the one-electron oxidation steps may lead to the formation of unstable intermediates of the the water oxidation catalyst. The employment of Oxone® was successful with complexes based on first-row transition metals, especially manganese, but its capability to drive the reaction with second- and third-row transition metals is poor. Moreover, Oxone® itself could act as an oxo-transfer agent, so that the formed oxygen could not come entirely from the catalytic routine.

Sodium periodate, NaIO_4 , was instead successfully employed to drive the water oxidation with metals belonging of all the three rows. This sacrificial oxidant has a reduction potential of 1.6 V vs. NHE, a bit lower than CAN: this may represent an advantage because it should limit the occurrence of side oxidation reactions. Despite also NaIO_4 may be an oxo-transfer itself, like Oxone®, it presents the advantage with respect to CAN to be stable in a wider range of pH (*ca.* from 2 to 7.5, as demonstrated by its Pourbaix diagram), and this provides experimental conditions that mime better the operating conditions necessary for the implementation of a device for the artificial photosynthetic process. Despite the

mentioned drawbacks related to the use of NaIO_4 , a number of catalysts sensitive to the acidic and oxidative conditions led by CAN, were characterized using this sacrificial oxidant.

Taking inspiration from Meyer's pioneering work, a number of Ru-based catalysts have been employed. Earlier works were aimed to increase the stability of the dinuclear complex, introducing a bridging group stronger than the oxo-bridges,^[72,76] but lately Thummel *et al.* reported the first series of mononuclear Ru-complexes bearing chelating ligands, demonstrating that also monomeric catalysts can be used.^[77]

Often the harsh conditions exploited by the use of a sacrificial oxidant, especially when dealing with CAN, may lead to an oxidative degradation of the coordinating ligand set of the complex; in order to produce a more robust system, also fully inorganic structures were reported: for example, a polyoxometallate tetra-ruthenium complex showed good activity and robustness in presence of Ce(IV) as sacrificial oxidant.^[78]

The ruthenium is not the only metal centre employed in the catalytic water oxidation reaction: during last 15 years several transition-metal complexes were indeed investigated. In order to mime the OEC-structure, a large number of works regarding Mn-based catalysts have been reported, but only few resulted actually promising, mostly because in general the Mn-complexes are characterized by low stability.^[79,64]

Notably, also other first-row transition metals were employed, such as iron,^[80] cobalt, copper.^[64] The use of such metals is preferable because of their abundance and the lower costs with respect to second- and third-row transition metals.

Also iridium(III) complexes were reported to catalyze the oxidation of water and the most important and promising results are reported in the next section.

1.5.1 Water oxidation reaction catalyzed by iridium(III) complexes

Grätzel and Kiwi firstly described the activity in the water oxidation reaction of IrO_2 nanoparticles, more than 30 years ago. More recently, $\text{IrO}_2 \cdot n\text{H}_2\text{O}$ nanoparticles were also employed in a photoelectrical cell able to perform the overall water splitting process; in such device, the $\text{IrO}_2 \cdot n\text{H}_2\text{O}$ nanoparticles served as photocatalyst for the oxidative half-reaction and were coordinated to a photosensitizer anchored to a working electrode covered with a semi-conductive TiO_2 film.^[81]

However, the employment of nanoparticles as catalytic system has some drawbacks: the control of their properties is not straightforward and the mechanism of the catalytic cycle is complicated to be rationalized. Molecular catalysts are therefore preferable, because their stereo-electronic properties can be easily tuned by a proper choice of the ligands in their coordination sphere, strongly influencing their catalytic behaviour. Moreover, the mechanism of the reaction could be easily investigated by mean of the most common spectroscopic techniques.

The breakthrough on employing iridium(III) complexes reaction was in 2008, when Bernhard and co-workers reported the first of Ir(III)-based catalysts active in presence of CAN as sacrificial oxidant (**Figure 1.17**).^[75]

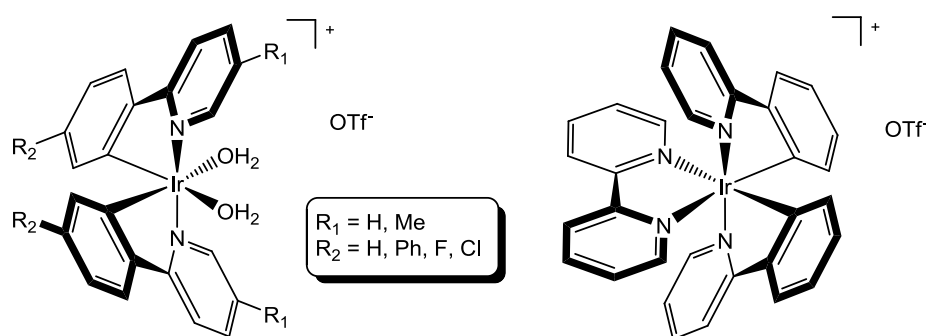


Figure 1.17: Complexes of Ir(III) active as catalyst for water oxidation reaction reported by Bernhard (left); $[\text{Ir}(\text{ppy})_2(\text{bpy})](\text{OTf})$ (with ppy = phenylpyridine and bpy = bipyridine) (right).

These complexes are relatively simple, characterized by a good robustness, provided by the strong metal-carbon bond of the ortho-metallated phenylpyridine

ligands, and they display catalytic activity also for several days. Further experiments have confirmed that O_2 is generated from water and not from the nitrate ion of CAN; moreover, it was demonstrated that a small amount of CO_2 is produced together with the O_2 evolution, deriving probably from the partial degradation of the coordinated ligands. Notably, no activity was observed when the complex $[Ir(ppy)_2(bpy)]^+$ (**Figure 1.17**, right) was employed, clearly indicating that a free coordination site is necessary for the catalysis.

The described work was then followed by the publications of Crabtree *et al.* who developed Cp^*Ir -based complexes (**Figure 1.18**).^[82,83] As mentioned previously, the Cp^* is an anionic ligand that strongly binds the iridium centre, providing further stability to the complex. The proposed Cp^* half-sandwich complexes are very active in water oxidation, reaching a production of oxygen one order of magnitude faster than the cyclometallated complexes proposed by Bernhard.

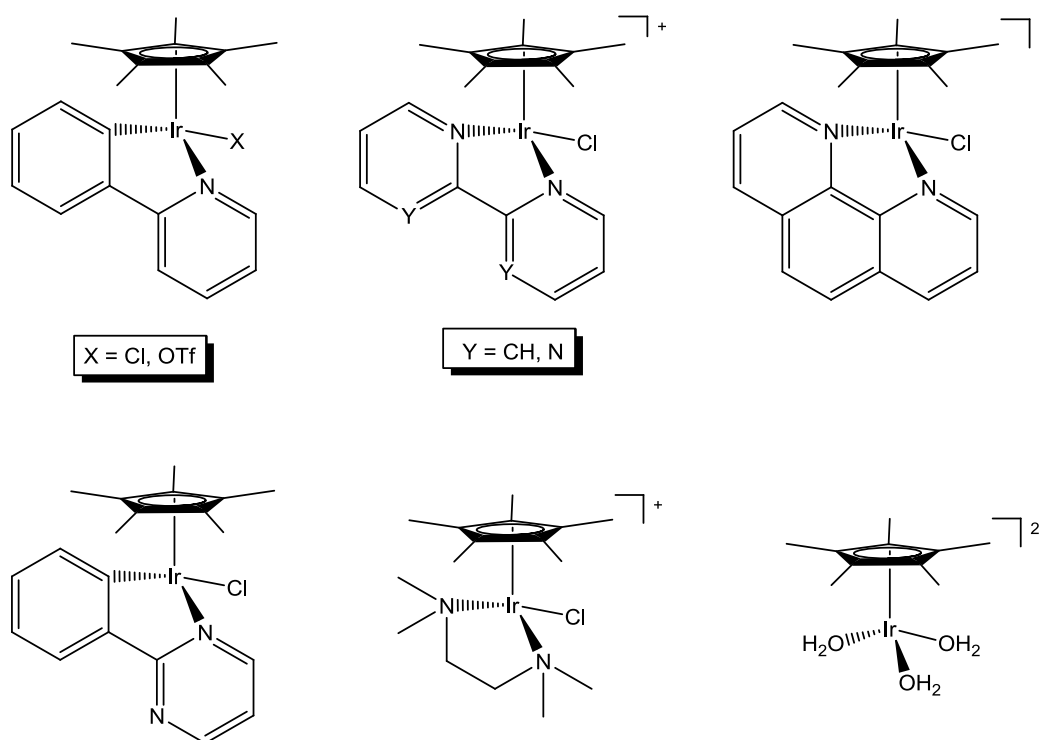


Figure 1.18: $IrCp^*$ complexes used by Crabtree *et al.* in the water oxidation reaction.

On the basis of these first works, extensive studies have been carried out by several research groups on the catalytic activity of $IrCp^*$ -complexes and on the evolution of

the catalysts, in order to discriminate the actual nature of the catalytic active species.^[84,85,86,87,88,89,90,91,92,93,94,95] For example, the complex $[\text{IrCp}^*(\text{H}_2\text{O})_3](\text{SO}_4)$ is by now considered only a precursor of heterogeneous iridium oxides.^[84,85,86,87]

Other works demonstrated that also Cp^*Ir -based complexes bearing chelating bipyridine ligands (general formula $[\text{IrCp}^*(4,4'\text{-di-R-2,2'-bpy})(\text{H}_2\text{O})](\text{X})_2$) may form colloids, after complete removal of the Cp^* moiety: in particular, Fukuzumi *et al.* observed that the substituents on the bpy ligand play a decisive role on the final stability of the resulting complex: with $\text{R} = \text{OH}$ a clear transformation of the starting complex to $\text{Ir}(\text{OH})_3$ was observed, while with the other substituents ($\text{R} = \text{OMe}$, Me , COOH) the bpy ligand is retained.^[96]

Lin and co-workers performed a study about the fate of an IrCp^* -catalyst anchored to a Zr-based metal-organic framework: the loss of the Cp^* ligand led to the formation of the real active species, and formation of acetates and formates species deriving from the ligand was detected.^[97]

Finally, Macchioni *et al.* studied the catalyst degradation under oxidative environment by means of NMR techniques. They observed the decomposition of the Cp^* ancillary ligand to form acetic acid and formic acid; it is reasonable to believe that such species may be further oxidized producing carbon dioxide, which could not be however detected via NMR spectroscopy.^[90,91,93] A similar decomposition was observed firstly by Maitlis *et al.* more than thirty years ago for the rhodium dimer complex $[\text{Rh}_2\text{Cp}^*_2(\text{OH})_3]\text{Cl}\cdot 4\text{H}_2\text{O}$, which in water in the presence of an oxidant forms acetic acid, CO_2 , rhodium(III) acetate and metallic rhodium.^[98] In their work, Macchioni *et al.* proposed, for the water oxidation reaction, the catalytic cycle reported in **Figure 1.19**; several intermediates of high-valence iridium are invoked and the authors suggest that the oxidative degradation occurs when the intermediate $[\text{IrCp}^*\text{L}_n(\eta^2\text{-O}_2)]^{m+}$ is in equilibrium with the superoxide species $[\text{IrCp}^*\text{L}_n(\eta^1\text{-O}_2)]^{m+}$. This latter species should start the Cp^* decomposition by an intramolecular attack to either the quaternary carbon or the methyl group of the Cp^* moiety. Such intramolecular reaction can lead to the oxidation of the methyl

group to a CH_2OR group and of the quaternary carbon to a $\text{C}(\text{OR})$ group ($\text{R} = \text{H}, \text{OH}$); such groups can be further oxidized as depicted in **Figure 1.20**.

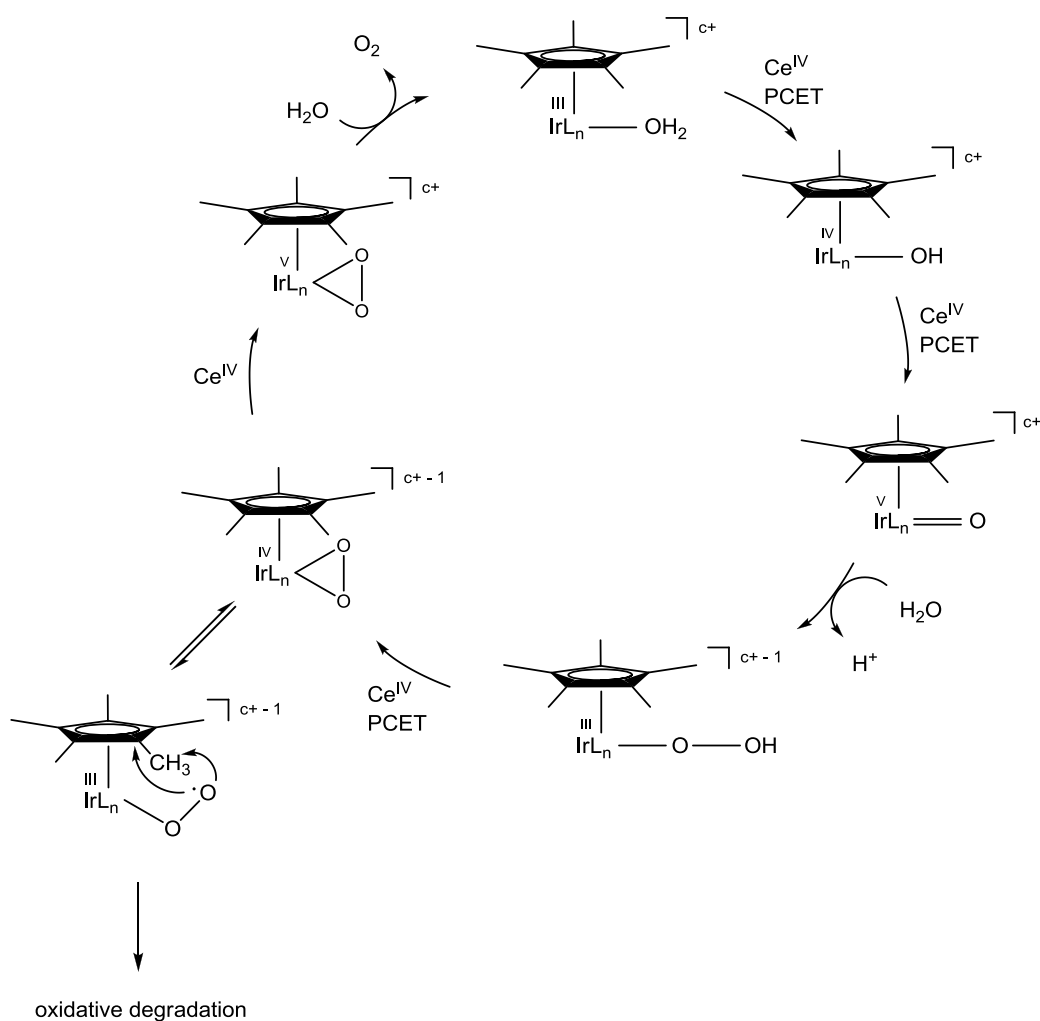


Figure 1.19: Mechanism proposed by Macchioni *et al.* for the water oxidation and the degradation of the Cp* moiety.

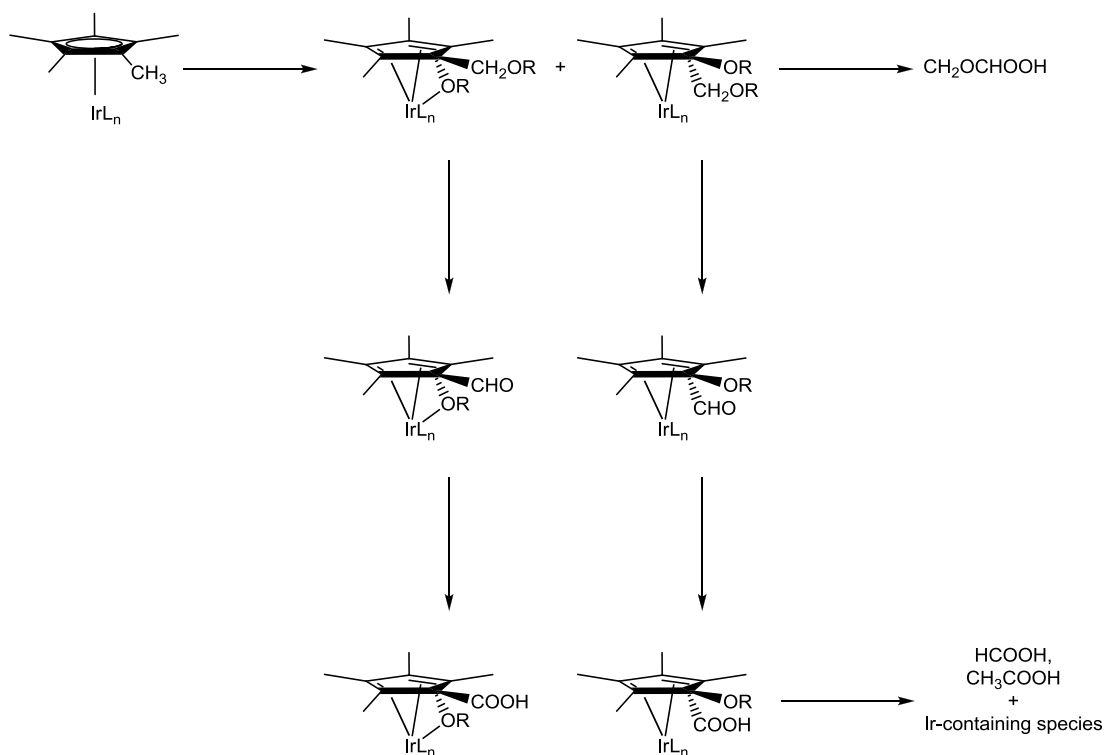


Figure 1.20. Decomposition pathway proposed by Macchioni *et al.*.

The same research group performed another elegant work related to the previously described: they managed to intercept and characterize (through *in situ* NMR spectroscopy, ESI-MS measurements and X-ray crystal structure) some intermediate species, deriving from the oxidative degradation of the Cp*Ir-based complexes driven by different sacrificial oxidant (H₂O₂, NaIO₄ and CAN).^[93] The oxidative transformation involves the three species reported in **Figure 1.21**; interestingly, the evolution species formed are active in the water oxidation reaction, showing an activity comparable to that observed with the starting complex; this strongly suggests a multisite mechanism involving all these single molecular species, active since the occurrence of the complete degradation of the Cp* ligand.

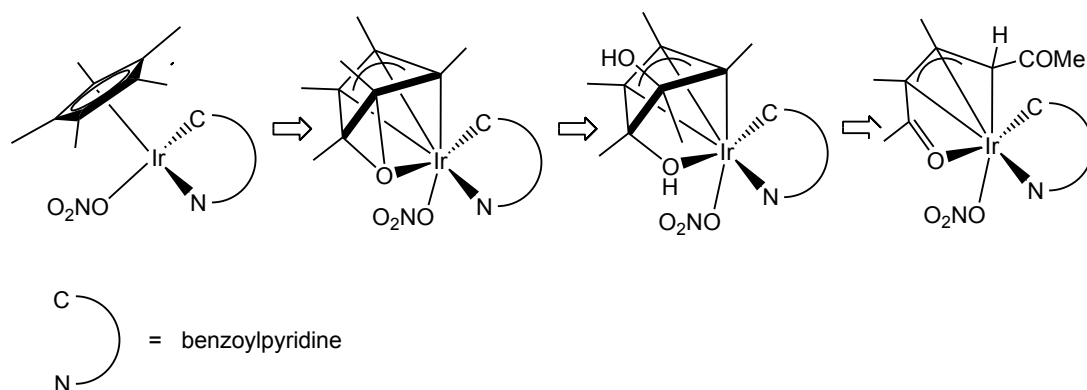


Figure 1.21. Decomposition pathway proposed by Macchioni *et al.*

The higher activity provided by the coordination of the strong electron-donor Cp* ligand, as well as all the studies reported above, suggested that the key-steps of the catalytic cycle may involve intermediates in which the iridium has high-oxidation states. Since the oxidation of the metal centre is easier when bearing strong donor ligands, NHCs are surely good candidates as ancillary ligands; furthermore, because of their good donor ability, they could also stabilize species in high oxidation state. In fact, Cp*Ir(III) complexes bearing N-heterocyclic carbenes were also successfully employed, both as classical imidazole-2-ylidenes and as 1,2,3-triazol-5-ylidenes.^[64] Their catalytic behaviour will be further discussed in **Chapter 3**.

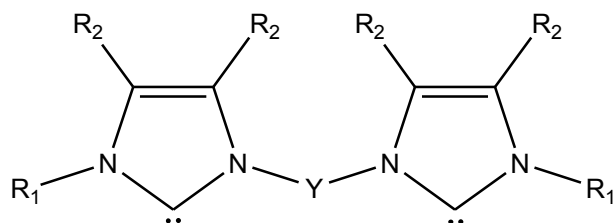
1.6 Aim of the research

The present research is focused on the study of one of the most important class of ligands in organometallic chemistry: the N-heterocyclic carbene ligands.

Nowadays such ligands are widely used as ancillary ligands in complexes applied in several different fields, because of their unique properties described in the previous sections:

- i. they are σ -donors stronger than other two electron-donor ligands;
- ii. they tightly bind the metal, forming stable complexes due to the strong metal-carbon bond;
- iii. their properties, both steric and electronic, can be readily tuned by changing the substituents on the nitrogen atoms and on the backbone on the azole ring, and the carbene unit itself.

Our interest in di-NHC ligands derived from several factors, like the possibility to obtain more stable complexes due to the chelate effect, and the enhanced modulability provided by the higher number of substituents with respect to the mono-NHCs.



Most of the Cp*Ir(III)-NHC reported in literature have mono-NHC ligands and only a limited number of Ir(III) complexes bearing di-NHC ligands are reported; furthermore, the majority of them presents the ligand coordinated in a bridged fashion between two metal centres.

For the mentioned reasons, one of the aims of this PhD project was the optimization of a synthetic procedure for the synthesis of iridium(III) complexes bearing di-NHC ligands coordinated in chelate fashion; the synthesized complexes will be characterized through several convergent techniques (^1H and ^{13}C NMR spectroscopy, mass measurements, cyclic voltammetry, etc).

The influence of small modifications of the ligands on the overall properties of the resulting complexes will be accomplished; in particular the changes that will be evaluated are: 1) the bridging group between the carbene units; 2) the wingtip substituents; 3) the backbone substituents; 4) theazole ring employed.

As regards this last point, the reactivity and the coordination properties of less conventional N-heterocyclic carbene units, in particular derived from six-membered saturatedazole ring and triazol-5-ylidenes, will be evaluated. This part of the project will be carried out in the frame of a collaboration with the group of Prof. Cornelis J. (Kees) Elsevier (Van't Hoff Institute of University of Amsterdam).

As described in **Section 1.4**, the iridium(III)-NHC complexes are applied as catalysts in several transformations, and recently have been successfully employed also in water oxidation reaction. This reaction is considered the bottleneck for the development of a system able to perform the overall process of water splitting, also named “artificial photosynthesis”, which represent a sustainable way to produce energy alternative to the consumption of fossil fuels, by harvesting the sunlight energy and transforming it in chemical energy (stocked as H₂ and O₂ molecules).

In the frame of the present PhD project, some of the synthesized di-NHC Ir(III) complexes will be tested as catalysts in the water oxidation reaction, in order to evaluate if a di-NHC ligand coordinated in chelate fashion may provide beneficial effects, both in the activity and in the robustness of the active species.

The catalytic activity of the complexes will be tested in presence of a sacrificial oxidant, mostly using the cerium(IV) complex (NH₄)₂[Ce(NO₃)₆], but also the use of NaIO₄ will be considered.

One of the major issue related to the employment of an Ir(III) catalyst is the identification of the real nature of the active species and, for this reason, also some mechanistic insight will be investigated.

A preliminary evaluation on the employment of the synthesized complexes in a photo-assisted process, by coupling the catalyst with a photosensitizer and a sacrificial acceptor of electrons, will be also addressed.

Finally, in the frame of a collaboration with the group of Prof. W. Baratta (University of Udine), the catalytic activity of some of the synthesized di-NHC Ir(III) complexes will be evaluated also in other organic reactions, like the transfer hydrogenation of ketones.

Chapter 2: RESULTS AND DISCUSSION

SYNTHESIS AND CHARACTERIZATION OF THE IRIDIUM(III) di-NHC COMPLEXES 1-3, 5-10 AND 2a

The iridium(III) complexes **1-3** and **5-10** were synthesized *via* transmetalation of the di-NHC moieties from the corresponding silver(I) di-NHC complexes, following a method described in **Section 1.2**.

The diazoliun dibromides salts, precursors of the carbene ligands, were easily synthesized by coupling of two azole units and the alkyl dibromide. The salts $L^n \cdot 2HBr$ ($n = 8, 11, 12$) were obtained from the $L^n \cdot 2HBr$ salts, carrying out a quantitative metathesis of the bromide ions with hexafluorophosphate ones, by treatment with a slight excess of NH_4PF_6 .

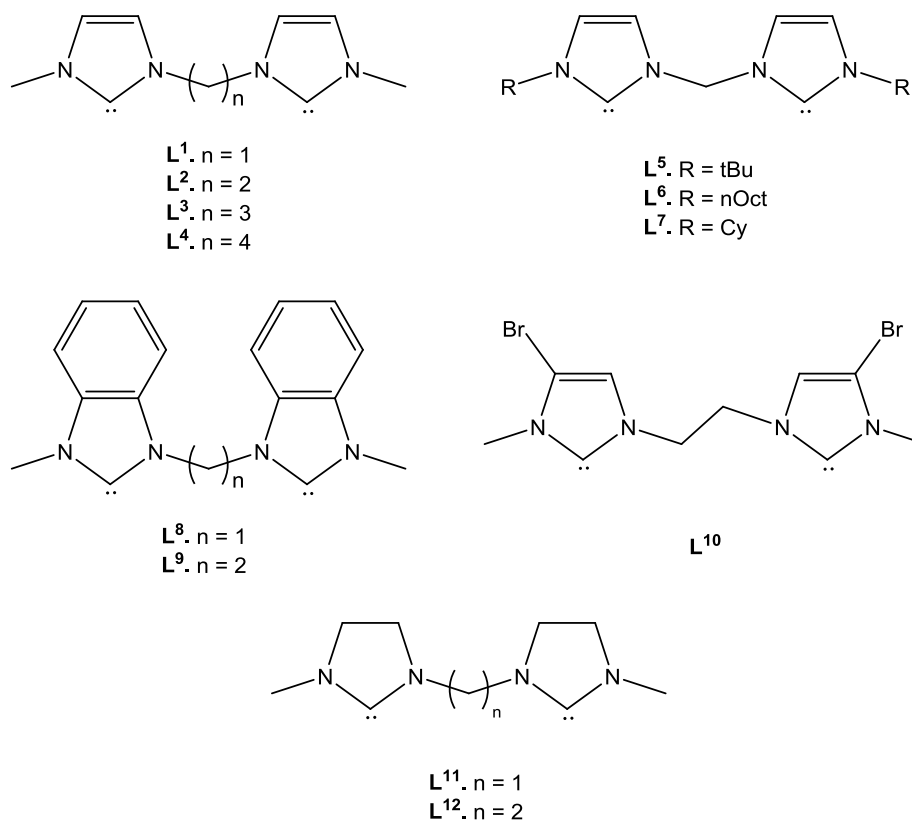


Figure 2.1: di-NHC ligands derived from the diimidazolium salts employed.

The silver(I) complexes bearing the di(N-heterocyclic carbene) ligands L^1 – L^4 , L^6 , L^7 , L^9 and L^{10} were synthesized following a two-step procedure (procedure **a**, **Scheme 2.1**):

- i] reaction between the diimidazolium dibromide and silver(I) oxide (excess) in water, at room temperature for 24 hours, under inert atmosphere and exclusion of light; the unreacted Ag_2O was then removed by filtration of the reaction mixture through Celite™.
- ii] anion metathesis with NH_4PF_6 in water, to give precipitation of the silver(I) di-NHC complex having PF_6^- as counterions.

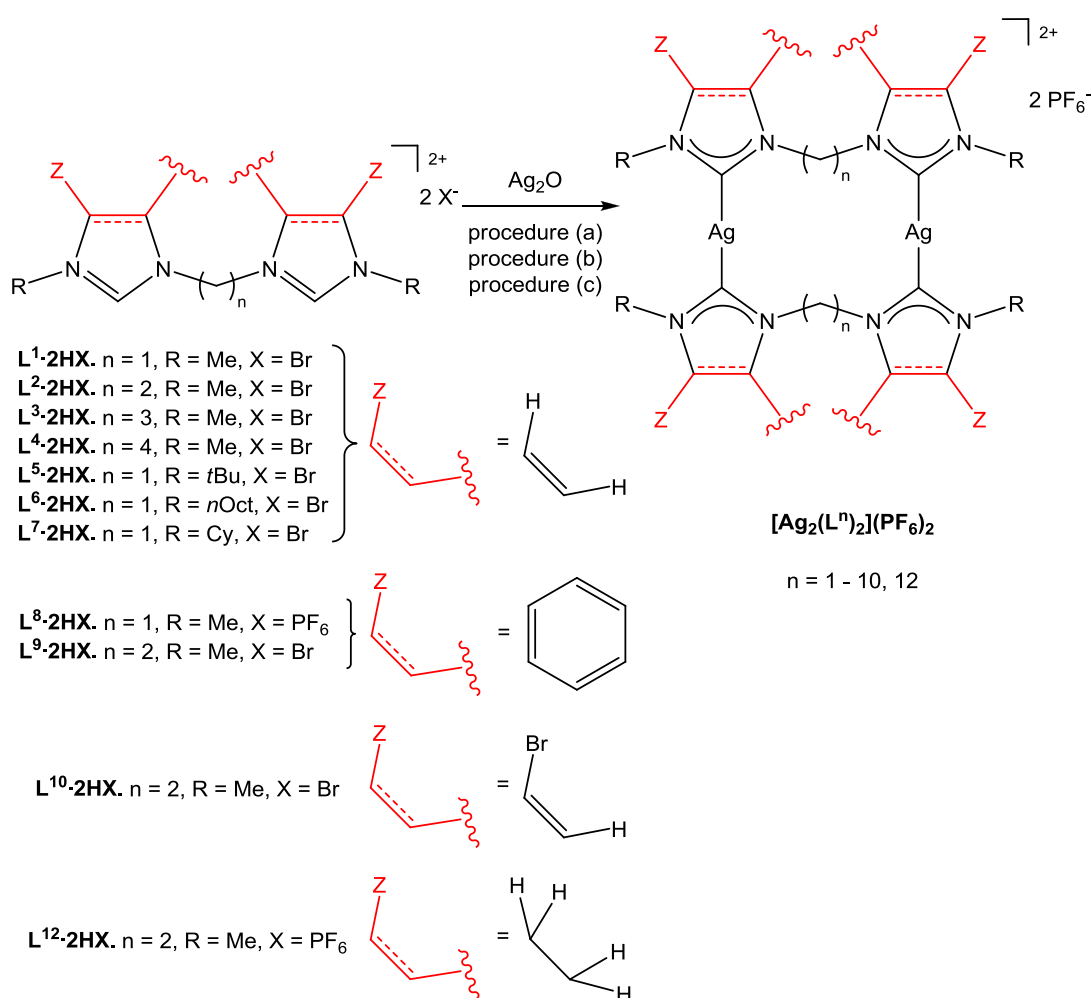
As reported in the previous chapter (**Section 1.2**), the silver(I) oxide Ag_2O acts both as base, necessary for the deprotonation of the diimidazolium salt to give H_2O as by-product, and as metal source.

The silver(I) complex $[Ag_2(L^5)_2](PF_6)_2$ was synthesized following the same procedure, but performing the reaction at 0 °C for 30 minutes, and using KPF_6 for the Br^-/PF_6^- metathesis (procedure **b**, **Scheme 2.1**).

The described synthetic procedure (rt for 24 h) does not afford complex $[Ag_2(L^8)_2](PF_6)_2$ in pure form: the expected silver(I) complex was formed together with a decomposition product deriving probably from the coupling of the benzimidazole rings. Such decomposition pathway was observed also by Lin *et al.* in a synthesis of di(N-heterocyclic carbene) complexes of copper(I).^[99] In order to overcome the described decomposition, another synthetic procedure was adopted, reported by Wang and co-workers for the synthesis of trinuclear di(N-heterocyclic carbene) silver(I) complex (procedure **c**, **Scheme 2.1**).^[100] The complex $[Ag_2(L^8)_2](PF_6)_2$ was synthesized by reaction of the salt $L^8 \cdot 2HPF_6$ with an excess of Ag_2O in acetonitrile, at 60 °C for 24 hours, under inert atmosphere and exclusion of light, followed by removal of unreacted Ag_2O by filtrating the mixture. The same

procedure allows also to synthesize the silver complex $[\text{Ag}_2(\text{L}^{12})_2](\text{PF}_6)_2$, starting from the diimidazolium salt $\text{L}^{12} \cdot 2\text{HPF}_6$.

Several unsuccessfully attempts to synthesize the complex bearing the ligand L^{11} (1,1'-dimethyl-3,3'-methylene-diimidazolin-2,2'-diylidene) were performed, but it was impossible to isolate the desired product. The most probable reason is the intrinsic instability of the ligand, mainly related to the presence of two saturated azole rings connected by a methylene bridge; notably, in some ^1H NMR spectra of the isolated dark brown solid, the signal of the methylene protons was absent.



Scheme 2.1: Synthesis of the dinuclear di(N-heterocyclic carbene) silver(I) complexes bearing the ligands L^1 - L^{10} and L^{12} . **Procedure a:** i] 1 eq. of salt precursor, 2.5 eq. of Ag_2O , H_2O , r.t., 24 h; ii] 2.1 eq. of NH_4PF_6 . **Procedure b:** i] 1 eq. of salt precursor, 4 eq. of Ag_2O , H_2O , 0 °C, 30'; ii] 2.1 eq. of NH_4PF_6 ; **Procedure c:** 1 eq. of salt precursor, 4 eq. of Ag_2O , CH_3CN , 60 °C, 24 h.

The silver(I)-NHC complexes $[\text{Ag}_2(\text{L}^1)_2](\text{PF}_6)_2$, $[\text{Ag}_2(\text{L}^3)_2](\text{PF}_6)_2$, $[\text{Ag}_2(\text{L}^5)_2](\text{PF}_6)_2$ and $[\text{Ag}_2(\text{L}^7)_2](\text{PF}_6)_2$ were already reported in a previous work.^[28a, 101] The spectroscopic data are consistent with literature and, accordingly to what reported, they have dinuclear structures, in which the two silver(I) centres are connected by two di-NHC bridging ligands. The complexes $[\text{Ag}_2(\text{L}^4)_2](\text{PF}_6)_2$, $[\text{Ag}_2(\text{L}^6)_2](\text{PF}_6)_2$, $[\text{Ag}_2(\text{L}^8)_2](\text{PF}_6)_2$, $[\text{Ag}_2(\text{L}^{10})_2](\text{PF}_6)_2$ and $[\text{Ag}_2(\text{L}^{12})_2](\text{PF}_6)_2$ have been synthesized for the first time during this PhD project and their spectroscopic analyses suggest, for these species, structures similar to those already known.

The synthesized novel di-NHC silver(I) complexes have been isolated and characterized through the classical techniques, such as ^1H NMR, ^{13}C NMR and mass measurements. The ^1H and ^{13}C NMR spectra of these complexes present a low number of signals, indicating a highly symmetric structure. Their formation is confirmed by the lack of the signal in their ^1H NMR spectra at high ppm (higher than 7.5-8 ppm) attributable to the protons in 2,2' position of the imidazole rings, suggesting the deprotonation of the diimidazolium salt (**Figure 2.2**).

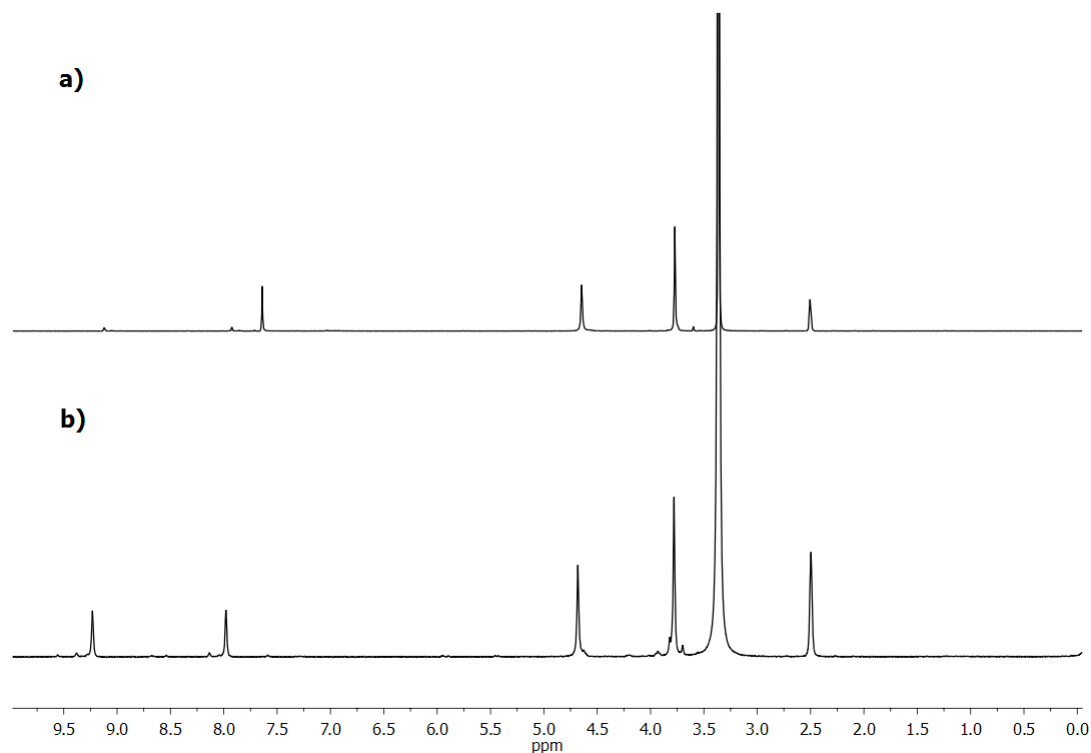


Figure 2.2: Comparisons of the ^1H NMR spectra of the ligand precursor $\text{L}^{10}\cdot 2\text{HBr}$ (bottom) and the dinuclear dicarbene silver(I) complex $[\text{Ag}_2(\text{L}^{10})_2](\text{PF}_6)_2$ (top).

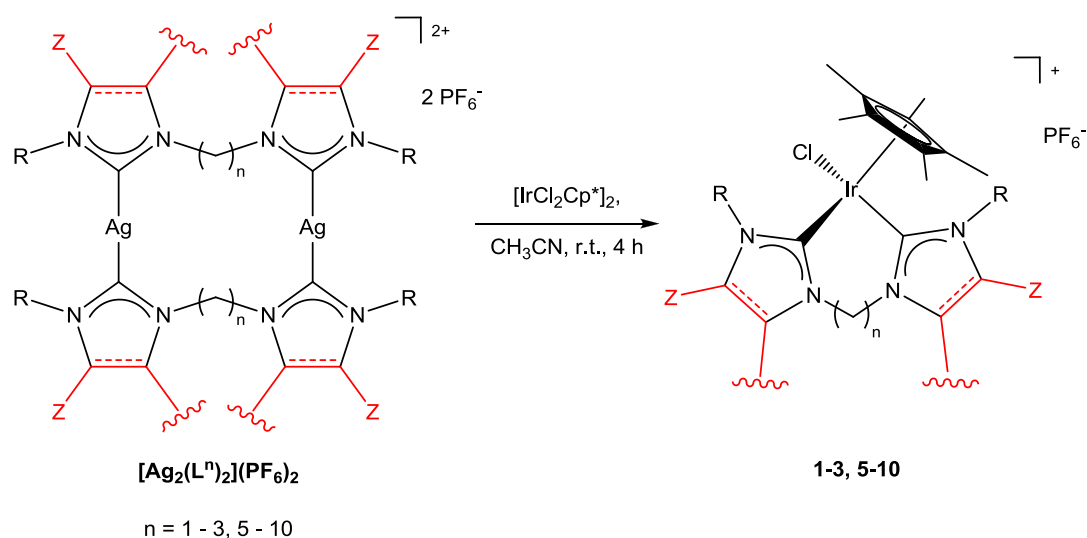
In the heteronuclear multiple-bond correlation spectroscopy (HMBC) spectra of the complexes, the signal of the carbene carbon is present as two doublets, due to the coordination of the carbon to the silver centre, which has two spin $\frac{1}{2}$ isotopes with comparable natural isotopic distribution (^{107}Ag 52 %, ^{109}Ag 48 %). All the silver(I) complexes show the signal of the carbene carbon around 180-190 ppm, except for the complex bearing the ligand L^{12} , in which the signal is at 204 ppm, indicating a stronger electron-donor ability of the saturated carbene unit, as mentioned in the **Section 1.1**.

The mass measurements (ESI-MS, positive mode) for the novel silver(I) complexes showed as main peak the fragment $[\text{Ag}_2(\text{L}^n)_2(\text{PF}_6)]^+$; the peak of the fragment $[\text{Ag}_2(\text{L}^n)_2]^{2+}$ is also present, although with a lower intensity. The simulated isotopic distribution patterns of the proposed fragments correspond to those obtained experimentally.

Results and Discussion

The iridium(III) di-NHC complexes **1-3** and **5-10** were synthesized by Ag(I)/Ir(III) transmetalation of the di-NHC moiety, by reaction of the corresponding di(N-heterocyclic carbene) dinuclear silver(I) complex and the iridium(III) precursor $[\text{IrCl}_2\text{Cp}^*]_2$ (Ag:Ir ratio 1:1) in acetonitrile, at room temperature for 4 hours.

In this synthetic procedure the Ag(I)-NHC complexes served as carbene transfer agent and, using the complex $[\text{IrCl}_2\text{Cp}^*]_2$ as Ir(III) precursor, AgCl is the only by-product of the reaction. Silver(I) halides are insoluble in organic solvents, so that their precipitation provides the driving force of the transmetalation reaction; moreover, the silver chloride can be easily separated from the product by filtrating the mixture.



Scheme 2.2: Synthesis of the iridium(III) complexes **1-3** and **5-10**.

As shown in **Scheme 2.2**, the obtained iridium(III) di-NHC complexes present a mononuclear structure with the di(N-heterocyclic carbene) ligand coordinated in a chelating fashion to the metal centre. The complexes were characterized by ^1H NMR, ^{13}C NMR, mass spectrometry and elemental analysis. The ^1H NMR spectra show the presence of an AB system (for the complexes **1, 5-8**) or AA'BB' system (for complexes **2, 9, 10**), ascribed to the diastereotopic nature of the protons of the bridge; this suggests a chelated coordination mode of the dicarbene ligand and a slow six- or seven-membered metallacycle boat-to-boat interconversion.^[102]

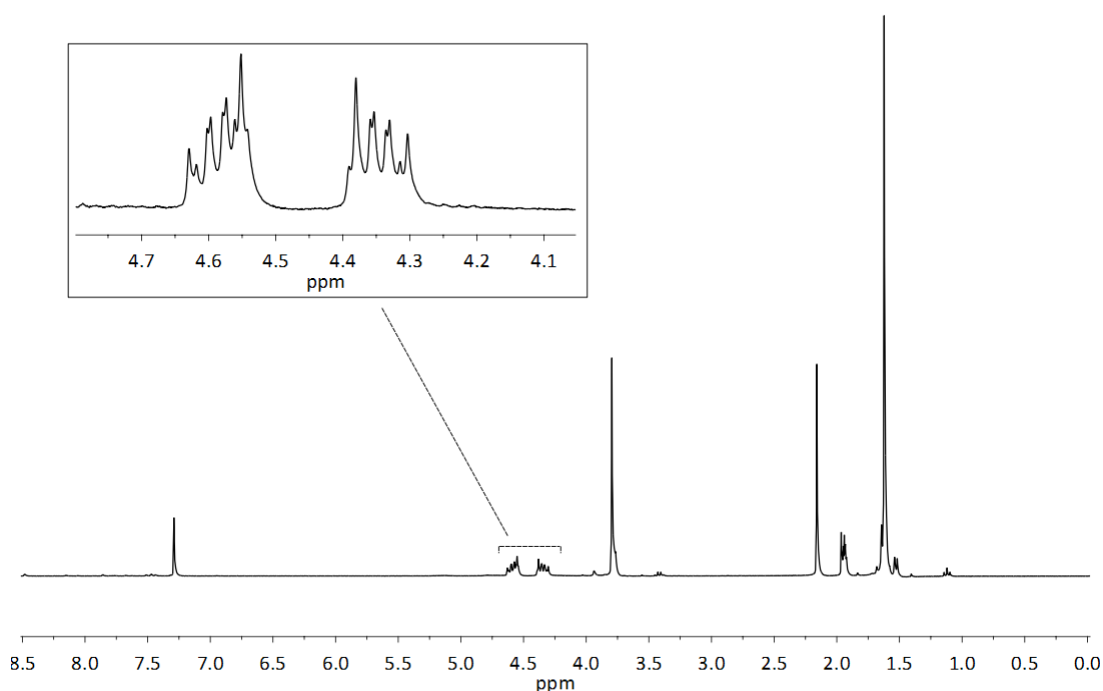


Figure 2.3: ^1H NMR spectrum of complex **10** (CD_3CN , 25 °C). In the inset, particular of the AA'BB' system ascribable to the protons of the bridge CH_2CH_2 between the carbene units.

The ^{13}C NMR spectra show the expected coordinated carbene resonance at around 145-163 ppm, in line with those reported in literature for carbene carbons coordinated to Ir(III) centres.^[54,58,59,103,104] A more detailed discussion on the position of the carbene carbon signal depending on the type of N-heterocyclic ring will be reported later in this Section.

The mass measurements (ESI-MS or MALDI-TOF, positive mode) show for all complexes the presence of a main peak with m/z values corresponding to the $[\text{IrClCp}^*(\text{di-NHC})]^+$ fragment; moreover, the observed isotopic distribution patterns correspond to the simulated ones.

In some cases (complexes **5**, **7** and **8**), the obtained solids were however contaminated by variable percentage of the precursor $[\text{IrCl}_2\text{Cp}^*_2]_2$, as indicated by EA and ^1H NMR spectra.

The results obtained in the attempts to synthesize the iridium complex **3** (with the ligand having a propylene bridging group), *via* this same synthetic procedure, were

somewhat unsatisfactory. In fact, although the immediate precipitation of the silver halide suggests that the reaction proceeds, a clean and univocally characterized product has not been isolated. The ^1H NMR spectrum of the obtained solid present in fact the coexistence of broad and large signals together with sharp and defined ones; this could be tentatively explained with the presence of two forms of similar Ir(III) complexes. VT NMR experiments have been performed in the range $-40 - 70$ °C, in order to define if the two species are in equilibrium to each other. The NMR spectra of the species with sharp signals resulted to be unaffected by the temperature. On the other hand, the broad signals at room temperature became sharper both lowering and enhancing the temperature; the only difference in these two cases is the number of the signals, for example the methyl protons give two singlets at -40 °C at 3.90 and 3.75 ppm, while a singlet appears at 70 °C at 3.86 ppm. This indicates dynamic processes like for example slow boat-to-boat interconversion, which do not allow the free rotation of the Cp* ligand thus rendering the two imidazol-2-ylidene rings non-equivalent in the temperature range between -40 °C and room temperature. At the moment it is not possible to define precisely the nature of the two species. The ESI-MS spectra of the solid present indeed a unique signal at 567 m/z , assignable to the fragment $[\text{IrClCp}^*(\text{di-NHC})]^+$. Also the elemental analyses are consistent with the formulation of the product as **3** $[\text{IrClCp}^*(\text{di-NHC})](\text{PF}_6)$. To further support this hypothesis, crystals of complex **3** have been obtained by layering hexane over a dichlorometane solution of the crude product and will be discussed further in the text.

The described transmetalation procedure was also performed unsuccessfully employing the silver(I) complex $[\text{Ag}_2(\text{L}^4)_2](\text{PF}_6)_2$, in which the ligand L^4 has two methylimidazol-2-ylidene units connected by a butylene bridge. The ^1H NMR spectrum of the isolated solid presents several signals in the range of ppm, relative to the resonance of the methyl groups, thus suggesting the presence of at least two species; moreover, the product is contaminated by the ligand precursor, so during the synthesis also carbene re-protonation probably occurs. This result can be

explained considering the high flexibility of the long alkyl bridge, which may decrease the stability of the silver(I) complex.

Also the synthesis of the iridium(III) complex bearing the ligand **L**¹² (1,1'-dimethyl-3,3'-ethylenediimidazolidin-2-ylidene) led to an impure product, in fact, although a partial transmetalation of the di-NHC ligand occurred, in the isolated solid there is still present a high percentage of the dimer precursor [IrCl₂Cp*]₂, as confirmed by the ¹H NMR spectrum of the mixture. The contamination with the Ir(III) precursor was further confirmed by ESI-MS experiments: the signal of the desired product at 570 *m/z*, ascribable to the [IrClCp*(di-NHC)]⁺ fragment is present, but the main signal in the mass spectrum is the fragment [IrCl₃Cp*₂]⁺, resulting from the dimer precursor after loss of a chloride ligand; all the attributions were confirmed by comparing the experimental isotopic distribution pattern with the calculated one. The unsuccessful synthesis of this iridium(III) complex in pure form can be a consequence of the instability of the silver(I) related precursor, which could undergo decomposition during the reaction, as demonstrated in a previous work employing a similar di-NHC ligand, in which the imidazolin-2-ylidene units were connected by a propylene bridge.^[105] In order to overcome this problem, the synthesis was performed also without pre-isolating the silver(I) complex, but by treating directly the filtrate solution containing [Ag₂(**L**¹²)₂](PF₆)₂ with [IrCl₂Cp*]₂, although with scarce results. Because of these preliminary results, no further investigations aimed to the synthesis of the iridium(III) complex with ligand **L**¹² were performed.

The crystal structure of the iridium(III) complexes **1–3**, **7–10** have been fully elucidated by X-ray diffraction analysis. The ORTEP views of the complexes are reported in **Figures 2.4–2.10** together with the atomic labeling scheme. A list of the most important bond distances and angles is reported in **Table 2.1**.

The synthesis and full characterization of complex **1** has already been reported by Heinekey and co-workers in 2005: the synthetic procedure was different, that is, by

reaction of the diimidazolium dichloride salt with $[\text{IrCp}^*(\text{CH}_3\text{CN})_3](\text{PF}_6)_2$ in acetonitrile and in the presence of triethylamine as base.^[106] In our case we have solved the already published crystal structure of complex **1** in order to confirm the nature of the obtained product; for this reason the crystal data are reported in this thesis and the structure details will be discussed in cumulative way together with the similar dicarbene iridium complexes.

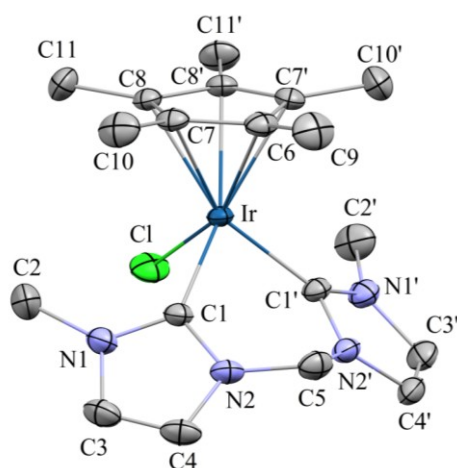


Figure 2.4: ORTEP view of the cationic part of complex **1**. Symmetry code used for generate atoms ' = $x, \frac{1}{2}-y, z$. Ellipsoids are drawn at their 30 % probability level. Hydrogen atoms and PF_6^- anion have been omitted for clarity.

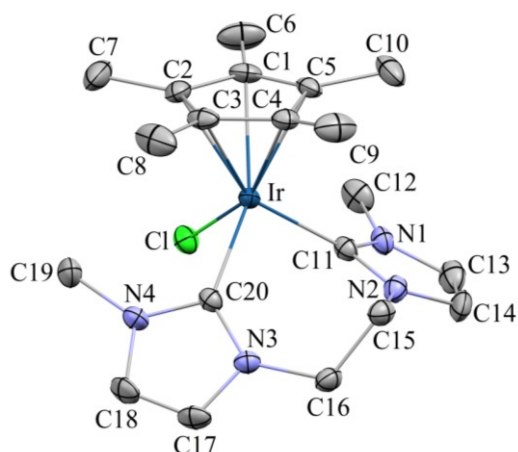


Figure 2.5: ORTEP view of the cationic part of complex **2**. Ellipsoids are drawn at their 30 % probability level. Hydrogen atoms and PF_6^- anion have been omitted for clarity.

In the case of compound **3** the low quality of the crystals prevented to refine accurately all structural parameters, nevertheless the connectivity of the atoms and bond distances and angles have been determined and reported therein.

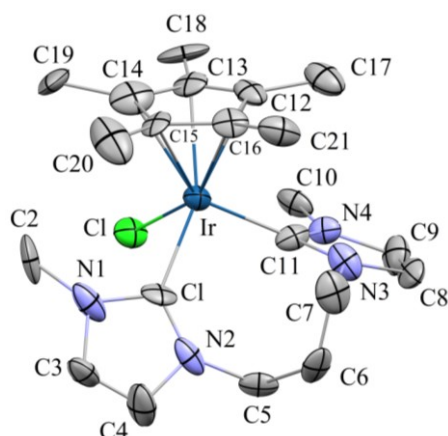


Figure 2.6: ORTEP view of the cationic part of complex **3**. Ellipsoids are drawn at their 30 % probability level. Hydrogen atoms and PF_6^- anion have been omitted for clarity.

In the unit cell of complex **7**, two crystallographically independent cationic complexes of the type $[\text{IrClCp}^*(\text{Cylm-CH}_2\text{-ImCy})]^+$ and two PF_6^- anions are present. **Figure 2.7** reports only the view of one of the two cationic complexes, together with the atomic labeling scheme.

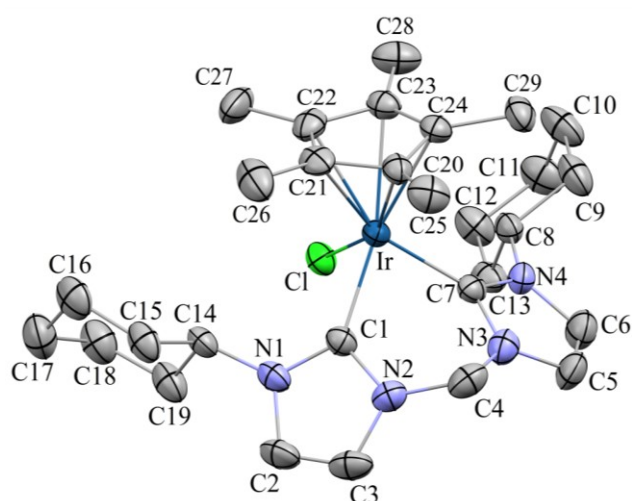


Figure 2.7: ORTEP view of the cationic part of complex **7**. Ellipsoids are drawn at their 30 % probability level. Hydrogen atoms and PF_6^- anion have been omitted for clarity.

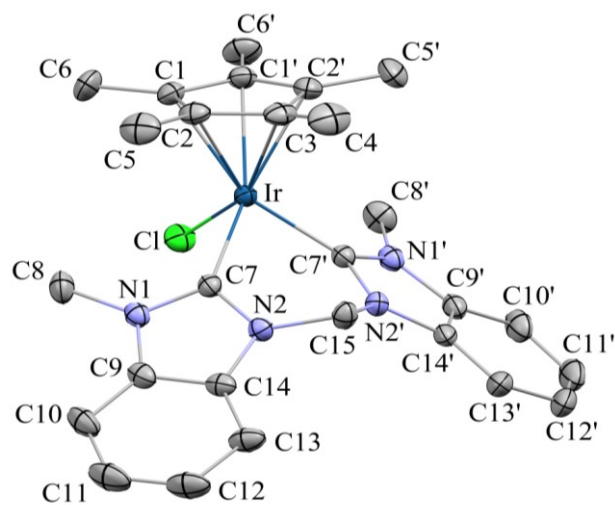


Figure 2.8: ORTEP view of the cationic part of complex **8**. Symmetry code used for generate atoms ' = $x, \frac{1}{2}-y, z$. Ellipsoids are drawn at their 30 % probability level. Hydrogen atoms and PF_6^- anion have been omitted for clarity.

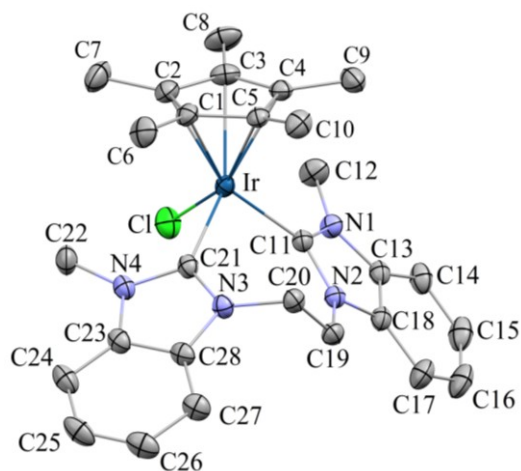


Figure 2.9: ORTEP view of the cationic part of complex **9**. Ellipsoids are drawn at their 30 % probability level. Hydrogen atoms and PF_6^- anion have been omitted for clarity.

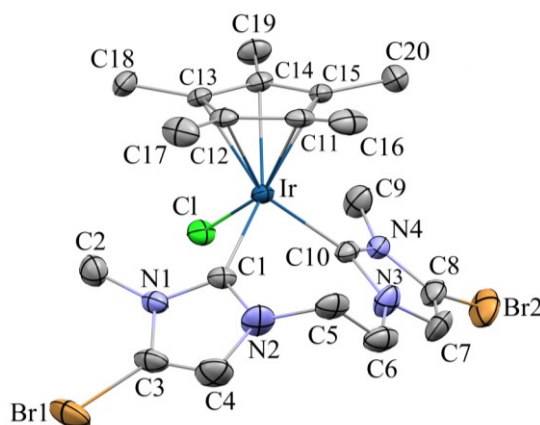


Figure 2.10: ORTEP view of the cationic part of complex **10**. Ellipsoids are drawn at their 30 % probability level. Hydrogen atoms and PF_6^- anion have been omitted for clarity.

Considering the centroid of the Cp* ring (CT), the iridium atom shows in all cases a distorted tetrahedral environment. The three bond angles at the iridium atom involving the centroid of the Cp* ring ($\text{CT-Ir-C}_{\text{carbene}}$ and CT-Ir-Cl) are wider than the other three ($\text{C}_{\text{carbene-Ir-C}_{\text{carbene}}}$ and $\text{C}_{\text{carbene-Ir-Cl}}$), probably as a consequence of the steric hindrance exerted by the Cp* ring.

The complex assumes a three-legged piano-stool structure with the dicarbene ligand engaged in two positions and the chloride Cl^- in the remaining one. The structure of the complexes resembles that of a closely related dicarbene complex reported by Jin and co-workers.^[104] The $\text{Ir-C}_{\text{carbene}}$ bond lengths [in the range 2.018 – 2.088 Å] are in agreement with reported Ir-NHC bond lengths.^[54,58,59,103,104,106,107]

The $\text{C}_{\text{carbene-Ir-C}_{\text{carbene}}}$ angle depends mainly on the bridge between the two carbene units and becomes wider with the lengthening of the aliphatic chain: 85 ° for CH_2 , 92 ° for CH_2CH_2 and 96 ° for $\text{CH}_2\text{CH}_2\text{CH}_2$. The same trend is observed in the values of the dihedral angle formed between the mean planes of the substituted imidazole moieties in the di(N-heterocyclic carbene) chelating ligand. A progressive increase of the value is observed by passing from the ligand with a CH_2 bridge to the one containing a $\text{CH}_2\text{CH}_2\text{CH}_2$ bridge. These values are reported in **Table 2.1**.

Results and Discussion

Table 2.1: More significant distances (Å) and angles (°) in the iridium(III) complexes **1-3**, **7-10**.^a

| | 1 ^b | 2 | 3 | 7 | 8 | 9 | 10 |
|-----------------------------|-----------------------|-----------|-----------|------------|----------|-----------|-----------|
| Ir-Cl | 2.4071(13) | 2.420(1) | 2.423(7) | 2.4133(18) | 2.414(1) | 2.421(1) | 2.429(1) |
| Ir-C _{carbene} | 2.024(3) | 2.019(5) | 2.0882(-) | 2.018(7) | 2.020(4) | 2.021(3)- | 2.066(5)- |
| | | 2.063(6) | 2.02(3) | 2.025(6) | | 2.059(4) | 2.044(5) |
| Ir-CT | 1.925 | 1.855(5) | 1.941 | 1.922 | 1.905 | 1.948 | 1.940 |
| C _{carbene} -Ir- | 85.2(2) | 92.0(2) | 96(1) | 84.7(3) | 85.1(1) | 92.8(1) | 91.5(2) |
| C _{carbene} | | | | | | | |
| CT-Ir-Cl | 121.44 | 123.21(2) | 120.5 | 122.81 | 119.64 | 123.90 | 121.46 |
| C _{carbene} -Ir-Cl | 89.04(10) | 89.0(2) | 96.7(8) | 90.8(2) | 92.0(1) | 89.5(1) | 88.6(1) |
| | | 85.9(2) | 83.7(8) | 90.20(19) | | 84.35(9) | 87.2(1) |
| CT-Ir-C _{carbene} | 129.56 | 130.33(2) | 131.10 | 127.22 | 128.48 | 129.36 | 128.37 |
| | | 124.08(2) | 119.69 | 128.84 | | 124.81 | 127.39 |
| γ ^c | 46.32 | 50.86 | 57.04 | 48.53 | 45.57 | 53.45 | 57.09 |
| | | | | (53.23) | | | |

^a CT = centroid of the pentamethylcyclopentadienyl ligand.

^b The structure of complex **1b** was already solved and reported; the parameters and distances found in this thesis matched those already published.^[106]

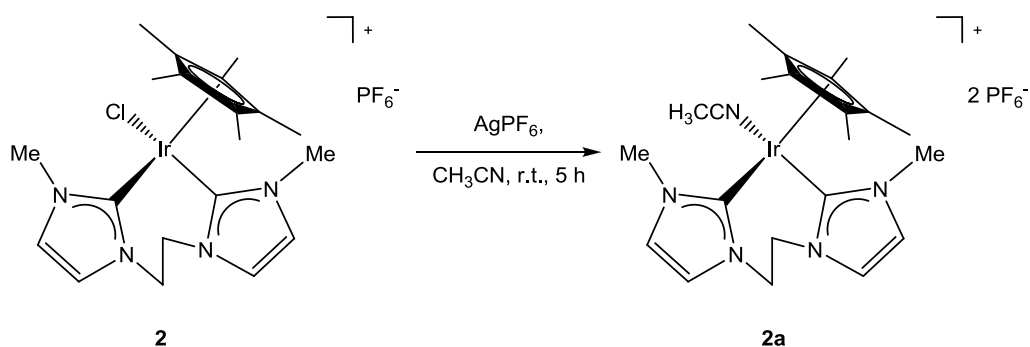
^c Dihedral angle between the mean planes of the NHC moieties.

Considering the crystal packing of the complexes in the case of compound **9** a weak π π stacking is observed between the six member aromatic rings of two adjacent molecules. The CT...CT distance between the centroids of the rings is of 3.625 Å.

On the other hand in compound **1** contacts between chlorine atom and the pentamethylcyclopentadienyl ligand of two adjacent molecules are present. The five C...Cl contact distances span from 3.387 to 3.471 Å. Also in the case of compound **2** an analogous type of contact is present but in this case the C...Cl distances span from 3.319 to 4.124 Å.

Lastly, in the case of compound **10** contacts between a fluorine atom of the PF_6^- anion and the bromine atoms of the ligand are present. The distances are of 3.236 and 3.246 Å.

Complex **2a** was obtained by treating complex **2** with one equivalent of AgPF_6 in acetonitrile solution, allowing the replacement of the chloride ligand with a solvent molecule.



Scheme 2.3: Synthesis of the iridium(III) complex **2a**.

The resulting product displays ^1H and ^{13}C spectra comparable, in terms of position and pattern, to those obtained for complex **2**, indicating that the geometry of the complex is maintained after the treatment with the silver salt. In particular, the AA'BB' system of the ethylene bridging group between the carbene units is present also in the ^1H NMR spectrum of **2a**. In general the signals in the ^1H NMR spectrum are slightly downfielded (ca. 0.1 ppm) with respect to those of complex **2**. The slight

deshielding of the proton signals maybe a consequence of the increased global charge of the complex. The effect of the ligand substitution is also verified by ^{13}C NMR spectroscopy: in particular, all the signals, except the carbene carbon are slightly downfielded, for the same reason cited above. The carbene carbon signal of **2a** falls instead at 141.3 ppm vs. 146.8 ppm in **2**. Such shift on going from halide complexes to solvent species has been already observed in previous works concerning palladium di-NHC neutral and dicationic complexes.^[108] The removal of the chloride anion was confirmed by ESI-MS (positive mode) analysis, which showed the main peak at $m/z = 259$, associated to the $[\text{IrCp}^*(\text{di-NHC})]^{2+}$ fragment.

As described in the previous chapter (**Section 1.1**), the most used experimental method for the determination of the electron-donor ability of a ligand is the determination of the Tolman's electron parameter (TEP).^[17] This approach has though some drawbacks: $[\text{Ni}(\text{CO})_3(\text{L})]$ or $[\text{MCl}(\text{CO})_2(\text{L})]$ complexes need to be prepared (starting from the highly toxic $[\text{Ni}(\text{CO})_4]$ or from expensive Rh or Ir precursors $[\text{MCl}(\text{COD})(\text{L})]$) or simulated via DFT calculations.

Despite the available data are far less than those reported for the TEP values, recently also the ^{13}C NMR spectroscopy was used as a method to evaluate the donor strength of a ligand, because the chemical shift of the carbene carbon strongly depends on the electron-density localized on the carbon atom. Huynh and co-workers have evaluated the donor ability of a series of NHC ligands by measuring the changing of the chemical shift of the carbene carbon in the 1,3-diisopropylbenzimidazol-2-ylidene ($i\text{Pr}_2\text{-bimy}$) ligand upon coordination of different NHC ligands in *trans* position in palladium(II) complexes (generic formula $[\text{PdBr}_2(i\text{Pr}_2\text{-bimy})(\text{NHC})]$).^[109] The chemical shift of the carbene carbon in a the $i\text{Pr}_2\text{-bimy}$ ligand depends on the Lewis acidity of the metal centre, which is clearly influenced by the donor ability of the ancillary ligands. In particular, more electron donor NHC ligands cause a downfield shift of the *trans* carbene carbon.

Another factor that should be considered in the prediction of the ^{13}C carbene chemical shift is the type of the substituents on the carbene unit. Donor

substituents should increase the electron density on the carbene carbon atom, resulting in a upfield shift.

All the synthesized iridium(III) di-NHC complexes have the general formula $[\text{IrClCp}^*(\text{di-NHC})](\text{PF}_6)$; they differ only for the di(N-heterocyclic carbene) ligand, so the electron density on the carbene carbons is influenced only by the wingtip substituents, the bridging group and theazole ring employed; since that, it might be possible to find a correlation between the electron density at the carbene carbon and at the iridium(III) centre. The values of the carbene carbons chemical shift obtained from ^{13}C NMR spectra for the complexes **1**, **2**, **5–10** are reported in **Table 2.2**.

Table 2.2: Resonance of the carbene carbon atoms in the ^{13}C NMR spectra of the complexes **1**, **2**, **5–10** (CD_3CN , 25 °C)

| Complex | 1 | 2 | 5 | 6 | 7 | 8 | 9 | 10 |
|----------------------|----------|----------|----------|----------|----------|----------|----------|-----------|
| NCN (ppm) | 151.4 | 146.8 | 145.6 | 151.5 | 151.0 | 163.0 | 160.7 | 149.4 |

The obtained chemical shifts for the complexes **1** and **2** differ by 4.6 ppm (151.4 and 146.8 ppm, respectively): the two complexes have both methylimidazol-2-ylidene as carbene units, but bridges of different lengths. It is reasonable to suppose that the CH_2 group of the bridge can donate electron-density to the carbene carbon: in the case of complex **1**, only a methylene group donates to two carbene units, with a diluted effect compared to complex **2**, in which two methylene groups are present, thus causing a higher electron density on the carbene carbon which is therefore more shielded.

Analogue considerations can be done for the chemical shifts of the complexes **8** and **9** (163.0 and 160.7 ppm, respectively).

It is interesting to compare the chemical shift of the carbene carbon signals obtained for the complexes **1**, **5**, **6** and **7** (151.4, 145.6, 151.5 and 151.0, respectively), which differ only for the wingtip substituents; when the substituents are methyl (complex **1**), *n*-octyl (complex **6**) or cyclohexyl (complex **7**) the electron-density on the carbene carbon appears to be very similar, while with a *tert*-butyl group, a clear shielding is observed, leading to a difference of *ca.* 5 ppm. This result seems to indicate a more electron-donor ability by the *tert*-butyl with respect to the other N-substituents employed. The same effect is not observed for complex **7** with the cyclohexyl substituents; this is in contrast to what reported by Buscemi *et al.* for [PdBr₂(di-NHC)] complexes, in which the substitution of methyl with cyclohexyl as wingtip substituents led to an upfield of the carbene carbon signal around *ca.* 10 ppm.^[108] The same effect in the substitution has however been observed with phosphine ligands; for example the pK_a of PR₃ (R = Me, *t*-Bu, Cy) varies in the order PtBu₃ > PCy₃ > PMe₃.^[110]

Comparing the chemical shift of the carbene carbon signals for the complexes **2**, **9** and **10**, which have differentazole rings (methylimidazol-2-ylidene, methylbenzimidazol-2-ylidene and 5-bromo-methylimidazol-2-ylidene, respectively), the value of δ_c is **9** > **10** > **2**; this indicates that in complex **9** the carbene carbon is less shielded, as a consequence of a more extensive electron delocalisation in the condensed aromatic ring.^[105,108] The carbene carbon signal of complex **10** is downfielded of only 2.6 ppm with respect to the value obtained for complex **2**; this suggests that introduction of a bromide substituent in position 5 has a negligible effect on the electron density of the carbene carbon. This evidence can be explained considering the double effect of an halide substituent: since Br is more electronegative, an electron-withdrawing effect occurs, but is partially balanced by the mesomeric effect of back-donation of electron-density from the occupied *p* orbitals.

Since the early work of Lever in 1990, it is well known that the ligands may have a huge impact on the electrochemical behaviour of a complex, and the

electrochemistry can be a powerful tool in order to quantify the extension by which a given ligand can change the redox potential of a generic couple $M(n)/M(n-1)$.^[105,108,111]

The redox potential of a metal centre is closely related to its effective electron-density, which depends on the ability to donate electrons by the coordinated ligands. The reduction potentials of the couple Ir(IV)/Ir(III) were measured for the complexes **1**, **2**, **5**, **7**, **8**, **9** and **10**, through cyclic voltammetry experiments. All the data were collected in the same conditions, at room temperature and in acetonitrile, employing NMe_4PF_6 as supporting electrolyte; the obtained values (**Table 2.3**) should only depend on the effects of the dicarbene ligand on the electronic properties of the iridium centre. Moreover, the use of the non-coordinating anion PF_6^- should leave the coordination sphere intact, because no replacement of the ligands can occur.

Table 2.3: $E_{1/2}$ values obtained for the complexes **1**, **2**, **5–10**^a

| <i>complex</i> | 1 | 2 | 5 | 6 | 7 | 8 | 9 | 10 |
|----------------|----------|----------|----------|----------|----------|----------|----------|-----------|
| $E_{1/2}$ | 1.38 | 1.40 | 1.38 | 1.37 | 1.39 | 1.48 | 1.53 | 1.50 |

^a Conditions: $[Ir] = 0.5$ mM, 0.1 M Me_4NPF_6 , CH_3CN (vs. Ag/AgCl, scan rate = 100 mV s⁻¹)

As reported in **Figure 2.11**, at scan rate higher than 100 mVs⁻¹, all the complexes show a quasi-reversible peak at $E_{1/2}$ values that lie in the range 1.37 - 1.53 V (vs. Ag/AgCl), relative to the couple Ir(III)/Ir(IV).

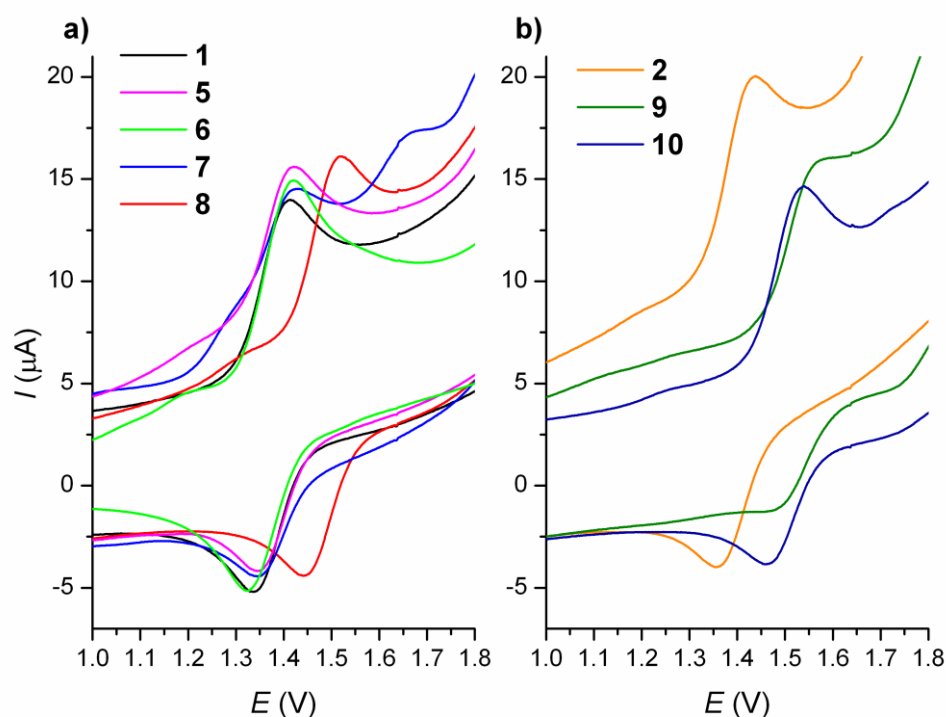


Figure 2.11: Cyclic voltammetry of complexes with methylene as bridging group between the carbene units **1**, **5**, **6**, **7** and **8** (left), and of complexes **2**, **9** and **10** (right). Conditions: $[\text{Ir}] = 0.5 \text{ mM}$, $0.1 \text{ M Me}_4\text{NPF}_6$, CH_3CN (vs. Ag/AgCl , scan rate = 100 mV s^{-1})

Comparing the results obtained for the complexes **1**, **5**, **6** and **7**, which all have a methylene bridge, it seems clear that the wingtip substituents (methyl, *tert*-butyl, *n*-octyl and cyclohexyl, respectively) do not affect the electron-density on the metal, since the reduction potentials are very similar. This is in contrast with the results reported for the $\text{Au}(\text{I})/\text{Au}(\text{0})$ reduction in dinuclear complexes bearing similar di(*N*-heterocyclic carbene) ligands, in which the wingtip cyclohexyl substituents increase the electron-density on the metal.^[105]

On the other hand, when changing the heterocyclic ring, a great effect is observed: moving from the imidazol-2-ylidene ring to the benzimidazol-2-ylidene one, the difference in $E_{1/2}$ is around $+0.1 \text{ V}$; the greater reduction potential observed for complex **8** can be explained considering the enhanced electron delocalisation due to the condensed aromatic ring, which makes the metal more electron-poor. This result is in accordance with that reported for gold(I) complexes bearing analogue di-

NHC ligands.^[105] The same effect is observed also for the complexes having an ethylene bridge between the carbene units: the $E_{1/2}$ of complex **2** is lower than the values obtained for complexes **9** and **10**, demonstrating once again that the nature of the N-heterocyclic ring has a great influence on the redox properties of the resulting complexes. In particular the electron density on the metal centre decreases in the order **2** > **9** \approx **10**, so that the electron donor ability of the different carbene units follows the order imidazol-2-ylidene > 5-bromo-imidazol-2-ylidene \approx benzimidazol-2-ylidene.

Finally, the bridge between the heterocyclic rings has only a negligible influence on the $E_{1/2}$ potential (**Figure 2.12**), and therefore on the electron-density on the metal centre: the $\Delta E_{1/2}$ in the couple **1** and **2**, as well as **8** and **9**, is in fact limited to -0.03 V.

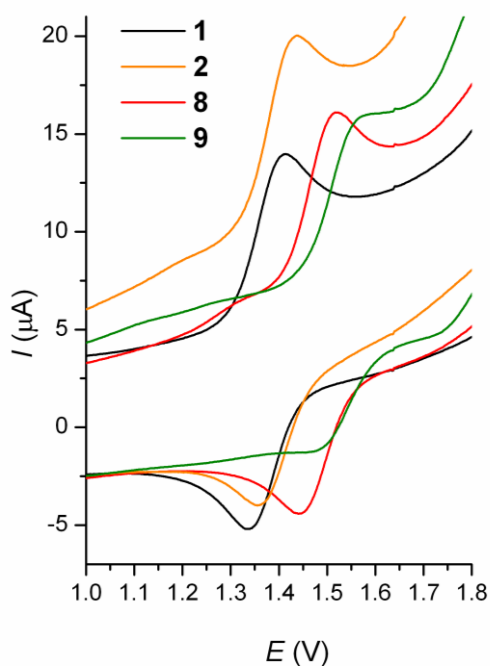


Figure 2.12: Cyclic voltammetry of complexes **1**, **2**, **8** and **9**. Conditions: [Ir] = 0.5 mM, 0.1 M Me_4NPF_6 , CH_3CN (vs. Ag/AgCl, scan rate = 100 mV s^{-1})

Results and Discussion

The results obtained from ^{13}C NMR spectroscopy and from cyclic voltammetry are related to different parameters: the electron-density on the carbene carbon and the overall electron-density on the metal centre.

Typically, the first may be related to the σ -donating ability of a given ligand and in the CH_2 or CH_2CH_2 series of ligands, the scale of electron donor capability obtained via NMR spectroscopy is: $5 > 1 \approx 6 \approx 7 > 8$ and $2 > 10 > 9$ respectively.

A similar trend can be obtained also for the electron density on the metal centre, via CV measurements; in this case the electron density on the metal increases in the order $1 \approx 5 \approx 6 \approx 7 > 8$ and $2 > 9 \approx 10$.

For the CH_2 series, the two scales compare well as it is clearly apparent from **Figure 2.13** (a trend line has been drawn), nonetheless complex **5** falls off-correlation; this should not surprise because different factors need to be consider in each metric.

The same considerations could be extended also to CH_2CH_2 series, however due to the limited number of complexes, the correlation could not be significant.

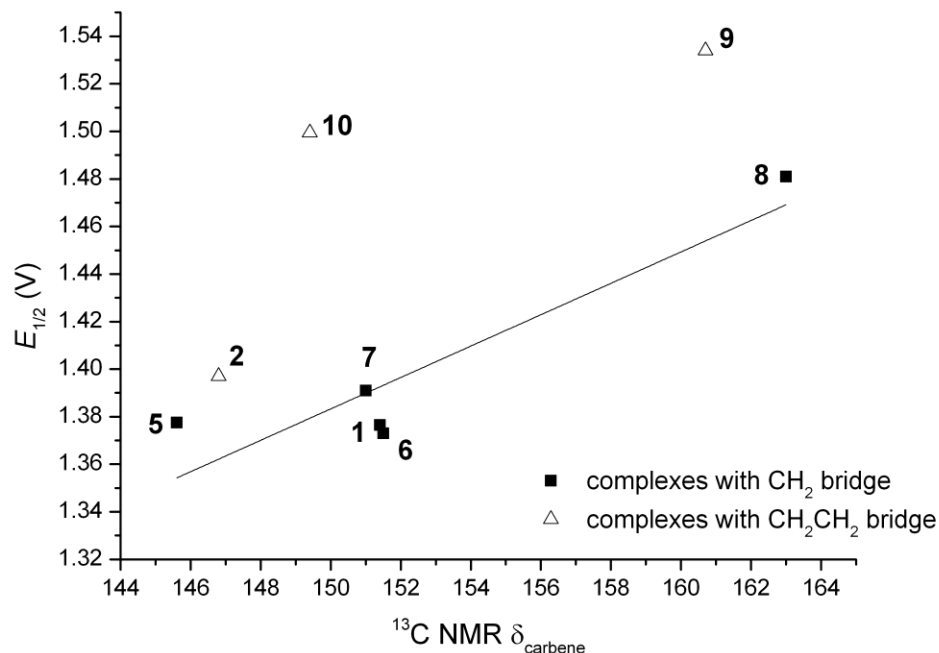


Figure 2.13: Correlation of the $E_{1/2}$ of the complexes **1**, **2**, **5**, **6**, **7**, **8**, **9** and **10** measured at rate scan of 100 mV s^{-1} , $[\text{Ir}] = 0.5 \text{ mM}$, $\text{Me}_4\text{NPF}_6 = 0.1 \text{ M}$, CH_3CN , with their ^{13}C chemical shift of the carbene carbon.

Chapter 3: RESULTS AND DISCUSSION

WATER OXIDATION WITH IRIDIUM(III) COMPLEXES BEARING DI(N-HETEROCYCLIC CARBENE) LIGANDS

3.1 Water oxidation in presence of a sacrificial oxidant

As described in **Section 1.5.1**, the catalytic activity in the water oxidation reaction of iridium(III) was firstly demonstrated by Bernhard and co-worker in their pioneering work published in 2008 and then further exploited by the group of R. H. Crabtree.

Following these works, during the very last years a number of active iridium(III) molecular complexes have been proposed for the water oxidation reaction,^[64] and also the NHC ligands (normal and abnormal ones) were successfully employed, showing results in line, if not better, with the best catalytic systems based on such metal. The introduction of a NHC ligand in the coordination sphere should indeed provide an enhanced stability to the complexes; moreover, the great electron-donor strength of such ligands may favor the formation of the Ir(IV) and Ir(V) hypothesized intermediates. In particular, a very high activity was observed by Reek and co-workers employing neutral Ir(III)-NHC complexes with general formula [IrCp*X₂(NHC)] (with: X = Cl or OH, NHC = 1,3-dimethylimidazol-2-ylidene), especially in terms of initial rate of oxygen evolution (TOF at = 0.5 s⁻¹ when X = Cl, 1.5 s⁻¹ when X = OH, complexes **B** and **C** in **Figure 3.1**).^[112] Furthermore, all the Ir(III) complexes bearing N-heterocyclic carbene ligands showed a good robustness toward the presence of a strong oxidant like CAN.^[113]

Albrecht *et al.* described a number of complexes bearing mesoionic carbene ligands derived from 1,2,3-triazol-5-ylidene with outstanding stability, as clearly demonstrated by the high turnover number obtained: the best results were obtained with the neutral Ir(III)-NHC complex **F** (**Figure 3.1**), which exhibited the best TON ever obtained to date (TON = 22800).^[50,114,115]

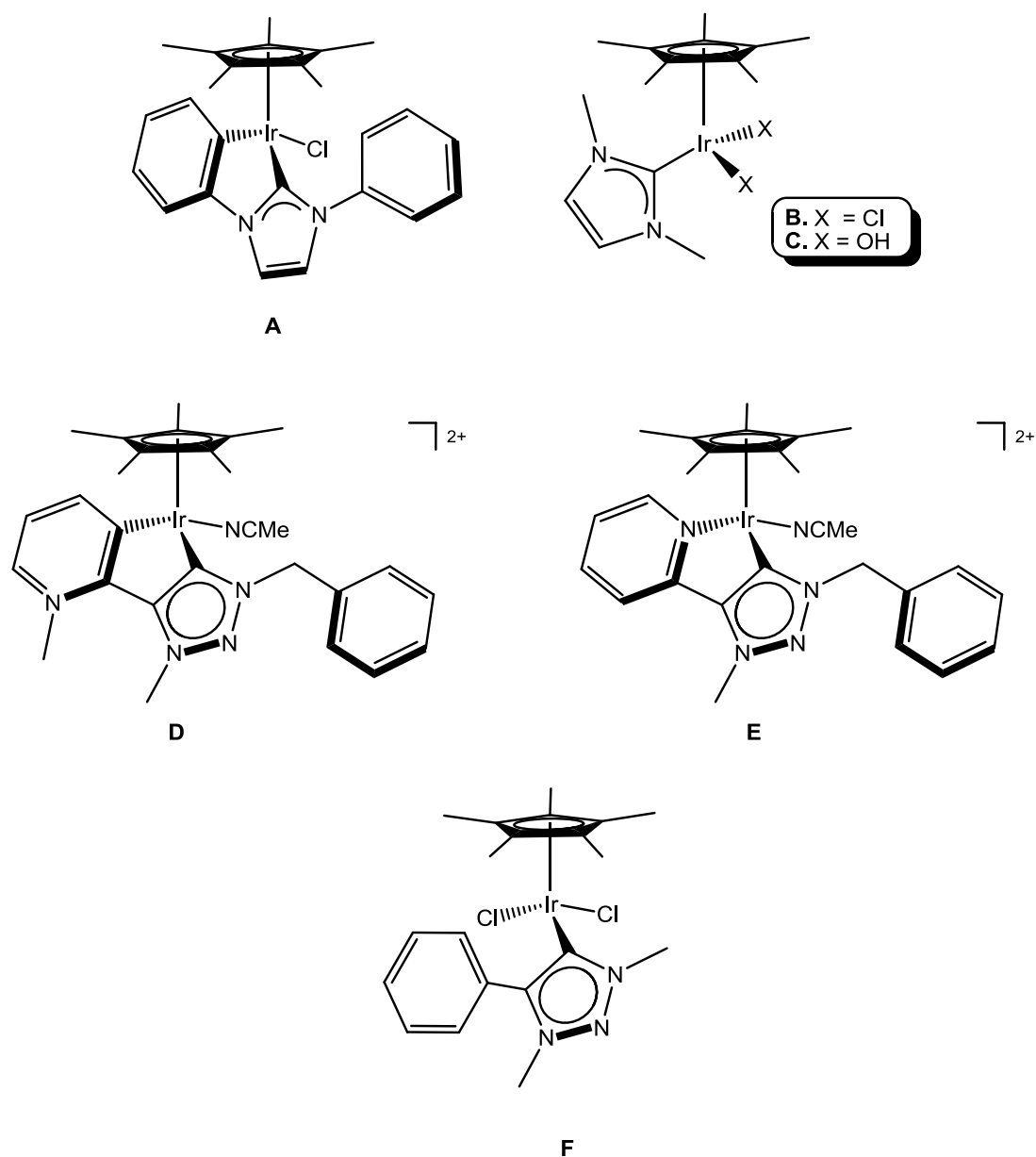
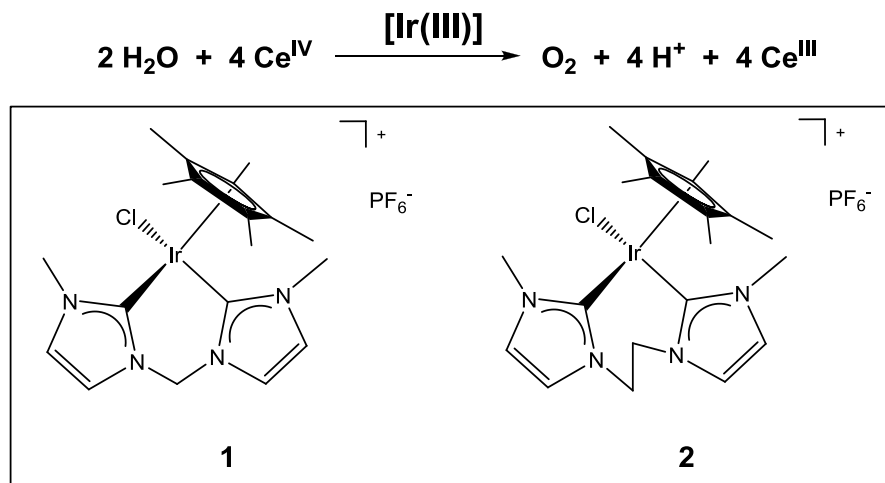


Figure 3.1: Iridium(III) complexes bearing NHC ligands active as catalysts for water oxidation reaction.

Considering the great potentialities of NHC complexes as catalysts for water oxidation, the synthesized iridium(III) di(N-heterocyclic carbene) complexes, described in **Chapter 2**, were employed in this reaction. This part of the work was carried out within a collaboration in our Department with the group of Prof. Marcella Bonchio and Dr. Andrea Sartorel.

The catalytic behaviour of Ir(III)-dicarbene complexes **1** and **2** has been preliminary evaluated in presence of CAN as sacrificial oxidant.



Scheme 3.1: Water oxidation reaction in presence of Ce(IV) as sacrificial oxidant and the complexes **1** and **2**.

The obtained results were compared with those obtained, in the same experimental conditions, with the dinuclear precursor $[\text{IrCp}^*\text{Cl}_2]_2$. The catalytic activity of this last complex was already reported by Crabtree *et al.* in an evaluation of the efficiency of a series of Cp^*Ir -based complexes, and despite of a good activity, the real nature of the active species was still unclear, since a loss of a well-defined kinetic order is observed; this complex may indeed form colloidal nanoparticles or some sort of multimetallic aggregates.^[83]

In a typical experiment, an aqueous solution of CAN (0.38 M, 10 mL) was stirred at 25 °C and allowed to equilibrate in a reactor connected to a pressure-voltage transducer mounted into the headspace. The catalyst was then injected as an acetonitrile solution (small volume, 25-400 μL , in order to keep almost constant the concentration of the reagents). In all cases, the oxygen evolution started immediately and the pressure change in the reactor headspace was monitored using a home-made interface designed in LabView. Under such conditions, the pH of the solution is around 0.9 and was considered not to change significantly during the catalytic reaction, despite the expected formation of H^+ ions during oxygen

Results and Discussion

evolution; this is reasonable if one considers that CAN in aqueous media forms aquo/hydroxo species and the reduction of Ce(IV) to Ce(III) provides a release of OH⁻ ions, as suggested by Bernhard *et al.*^[75]

The two di-NHC complexes and the [IrCp*Cl₂]₂ were tested at different iridium(III) concentrations, spanning from 31 to 500 μM. The obtained results are summarized in **Table 3.1**.

Table 3.1: Catalytic performance of complexes **1**, **2** and [IrCl₂Cp*]₂ as water oxidation catalysts in the presence of Ce(IV) as terminal oxidant (dark conditions).

| [Ir] μM | 1 | | | 2 | | | [IrCl ₂ Cp*] ₂ | | |
|------------|--|---------------------------|--|--|---------------------------|--|--|---------------------------|--|
| | O ₂ [μmol] (TON) ^b | Yield [%] ^a | TOF [s ⁻¹] ^c | O ₂ [μmol] (TON) ^b | Yield [%] ^a | TOF [s ⁻¹] ^c | O ₂ [μmol] (TON) ^b | Yield [%] ^a | TOF [s ⁻¹] ^c |
| 500 | 908 (181) | 98 | 0.07 | 908 (181) | 98 | 0.07 | 612 (122) | 65 | 0.22 |
| 250 | 908 (373) | 98 | 0.11 | 908 (373) | 98 | 0.15 | 786 (323) | 85 | 0.45 |
| 125 | 908 (726) | 98 | 0.12 | 908 (726) | 98 | 0.20 | 901 (721) | 95 | 0.61 |
| 62 | 880 (1419) | 95 | 0.10 | 889 (1434) | 96 | 0.20 | 869 (1402) | 92 | 0.46 |
| 31 | - | - | - | 861 (2779) | 93 | 0.20 | 896 (2895) | 95 | 0.23 |

Reaction conditions: 10 mL Milli-Q H₂O, [CAN]=0.38 M, 25°C, catalyst introduced from a 5 mM solution in acetonitrile.

a Determined after 8 h. *b* Calculated as μmol O₂/μmol Ir. *c* Calculated as μmol O₂/μmol Ir per second. Determined in the initial 5 minutes of O₂ production, at conversion <10 %.

The long-term activity of the complexes has been expressed as turnover number (TON) calculated as the total amount of evolved O₂ over the amount of iridium, while the initial performance of the catalysts has been evaluated with the turnover frequency (TOF, s⁻¹), defined as the TON per unit of time and usually measured from the initial rate of O₂ evolution.

In all cases the amount of total oxygen produced and, as a consequence, the TON values are limited by the consumption of the sacrificial oxidant (93-98 % of Ce(IV) conversion); therefore, the TON values are very similar for both complexes and depend only on the catalyst concentration, reaching a maximum value of 2800 for complex **2** at 31 μM concentration of Ir(III). The results obtained by employing [IrCp*Cl₂]₂ are consistent with those reported by Crabtree^[83] and, both TOF and TON values, for this catalytic system are slightly superior to those obtained with **1** and **2**; nonetheless, it is worth to note that the reaction order is not an integer number, suggesting that probably the mechanism with this complex involves the formation of undefined multimetallic cluster or IrO₂ nanoparticles.

Considering that complexes **1** and **2** provided a quasi-quantitative conversion of the Ce(IV) present in solution and that they are active for long periods (up to 5 hours) it is possible to assume a good robustness of the catalysts under acidic conditions.

In terms of initial rate of oxygen production, catalyst **2** appears to be more active than complex **1**, especially when lowering the iridium(III) concentration (TOF=0.20 s⁻¹ at 62 μM of [**2**] and TOF=0.10 s⁻¹ at the same concentration for **1**). The obtained TOF value for **2** of 0.20 s⁻¹ compares well with the most active iridium based catalysts reported so far.^[75, 83]

The kinetic profiles obtained for the three catalysts (**1**, **2** and [IrCl₂Cp*]₂) at 62.5 μM of Ir(III) are reported in **Figure 3.2**; in addition, also the curves obtained with **2** 31 and 125 μM are reported.

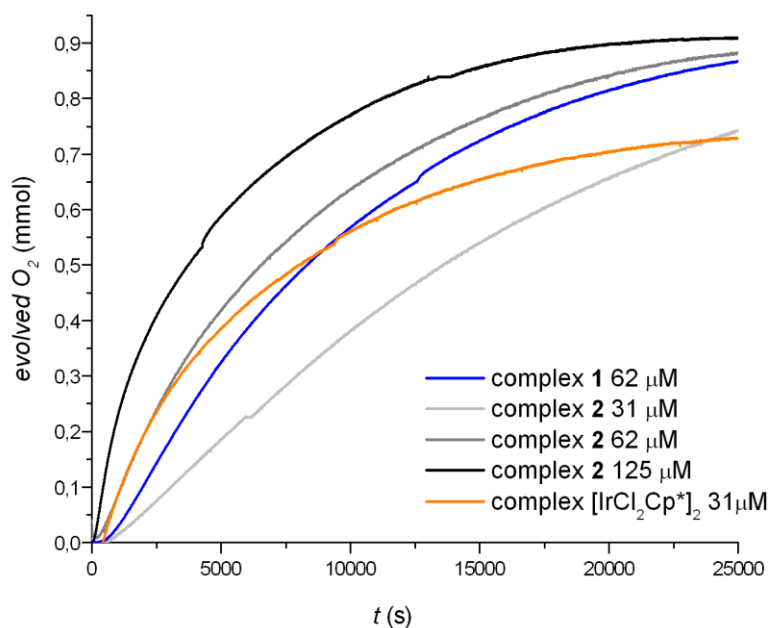


Figure 3.2: Oxygen evolution (mmol) vs. time (s) for complexes **1**, **2** and $[\text{IrCl}_2\text{Cp}^*]_2$. Experimental conditions: $(\text{NH}_4)_2[\text{Ce}(\text{NO}_3)_6]$ (0.38 M), $[\text{Ir}] = 31\text{-}125 \mu\text{M}$, MilliQ water (10 ml).

Generally, a well-defined kinetic order of the catalytic reaction might support the hypothesis of a “molecular” catalysis; in fact, if the catalyst evolves to more complex systems, such as nanoparticles, the rate dependence on catalyst concentration takes more complex forms.

For instance, the kinetic profiles observed with cyclometalated complexes proposed by Bernhard *et al.* are quite irregular and that could be associated either to an incubation time of the pre-catalyst and to a change of the mechanism during the reaction; especially at high concentration of catalyst, the oxygen evolution rate decreases, suggesting the presence of a competitive side reaction or a change (decomposition) in the catalyst structure.^[75] Also Brudvig and co-workers suggested that oligomerization of the pre-catalyst may occur, observing a non-first-order kinetic.^[83] For example, the deposition of iridium oxide on the electrode surface was observed when the tris-aquo complex $[\text{IrCp}^*(\text{OH}_2)_3](\text{SO}_4)$ was employed as water oxidation electrocatalyst; such complex evolves in solution during the reaction and it is only the precursor of the deposited layer (the so-called “blue layer”) which is

now considered the actual catalyst: in fact, recovering and rinsing the electrode covered by such blue layer, high activity was observed for several catalytic cycle.^[84,85,86,88]

In order to obtain some insight on the real nature of the catalytically active species of the employed complexes, an evaluation of the initial rate of oxygen production versus catalyst concentration was performed. Focusing on the most active complex **2**, a linear relation was observed at low concentration (31-125 μM of $[\text{Ir(III)}]$) plotting $\log(k_{\text{in}})$ (k_{in} initial rate) versus $\log[2]$ (with slope 1) (**Figure 3.3**).

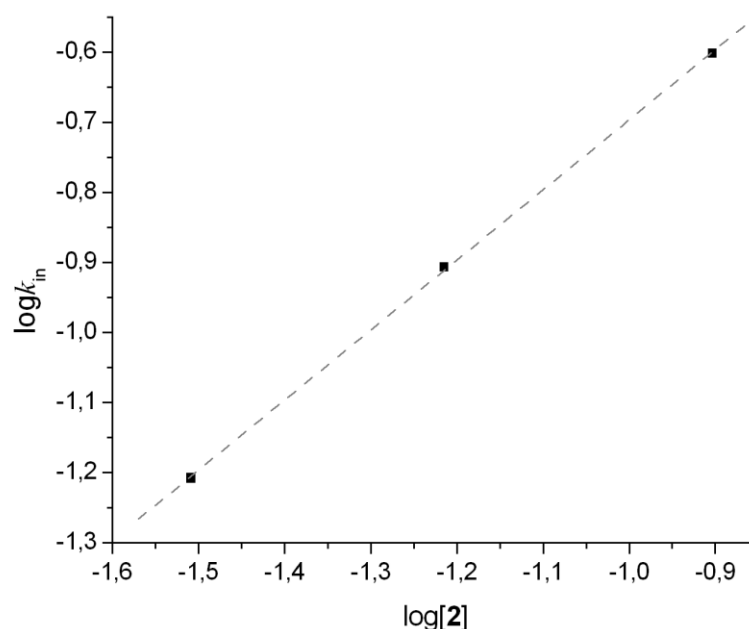


Figure 3.3: Plot of $\log(k_{\text{in}})$ vs $\log([\text{Ir}])$ for catalyst **2** in the concentration range 31-125 μM .

This result strongly suggests that complex **2** behaves a molecular catalyst; a slight deviation from linearity of the plot was verified at higher concentrations, probably due to the formation of undesired aggregates or to the occurrence of a dinuclear catalytic route. Having a molecular catalyst and not a mere precursor of IrO_2 nanoparticles allows to tune the stereo-electronic properties of the complex by a rational design of its coordination sphere; moreover, a molecular catalyst can be

easily functionalized with pendant groups able, for example, to interact with a surface in order to obtain an artificial photosynthetic cell.

It is worth to underline that in several experiments, an aliquot of the resulting mixture at the end of the reaction was analyzed by dynamic light scattering technique (DLS); such experiments have been demonstrated to be useful for discriminating the evolution of the pre-catalyst from homogeneous to heterogeneous forms. In all the measurements, no nanoparticles were detected; this can be consider a further support to the molecular nature of our catalyst, although these results should be carefully consider because the detection of nanoparticles via DLS requires generally high concentration of colloids, probably higher than those that can be possibly formed with our system.

As mentioned in **Section 1.5**, the employment of a sacrificial oxidant for driving the water oxidation catalyst provides some benefits: i] the study in bulk solution of the catalytic behavior; ii] the amount of produced oxygen is large and so easy to evaluate in terms of TOF and TON values; iii] the experiments can be carried out rapidly, so also the screening of the reaction conditions and the catalysts can be easily performed. The main characteristic of a sacrificial oxidant is a reduction potential high enough to oxidize the catalyst under examination. The results obtained with the catalysts in the presence a sacrificial oxidant should be considered as an indication of robustness and as a preliminary evaluation of their suitability in a system able to carry out the light-driven process.

Complex **2** was tested as catalyst also in the presence of sodium periodate (50 mM) as sacrificial oxidant, following the same procedure and apparatus described for the catalytic tests employing CAN. Recently sodium periodate NaIO_4 was successfully employed to drive the water oxidation with Cp^* -iridium(III) metal complexes.^[116] This sacrificial oxidant has a reduction potential of 1.6 V vs. NHE, lower than CAN (which is 1.7 V vs. NHE): this may represents an advantage, because it should limit

side-oxidative reactions. Although NaIO_4 may be an oxo-transfer itself, it presents the advantage, with respect to CAN, of being stable over a wide range of pH (*ca.* 2-7.5, as demonstrated by its Pourbaix diagram), thus providing experimental conditions more similar to those used in the artificial photosynthetic device. Since the most interesting results were obtained at iridium(III) concentrations between 31 and 125 μM , we decided to test complex **2** under similar conditions, as summarized in **Table 3.2**.

Table 3.2: Catalytic performance of complex **2** in the presence of NaIO_4 as sacrificial oxidant.

| $[\text{Ir}] [\mu\text{M}]$ | O_2 [μmol] (TON) ^a | Yield [%] ^b | TOF [s^{-1}] ^c |
|-----------------------------|---|---------------------------|---|
| 130 | 190 (146) | 76 | 0.04 |
| 65 | 220 (338) | 88 | 0.07 |
| 32 | 221 (691) | 88 | 0.12 |

Reaction conditions: 10 mL Milli-Q H_2O , $[\text{NaIO}_4]=50$ mM, 25°C, catalyst introduced from a 5 mM solution in acetonitrile.

a Calculated as $\mu\text{mol O}_2/\mu\text{mol Ir}$. b Determined after 4 h. c Calculated as $\mu\text{mol O}_2/\mu\text{mol Ir}$ per second; determined in the initial 5 minutes of O_2 production.

It results from **Table 3.2** that in all cases the evolved oxygen corresponds to a sodium periodate conversion in the range 76-88 %. Such values correspond to TONs up to 690 with complex **2** at concentration of 32 μM . The TOF values depend on the catalyst concentration and reach the highest value of 0.12 s^{-1} , which can be

considered satisfactory since it is comparable with the most active Ir-based catalytic systems.

As reported in **Section 1.5.1**, several groups demonstrated the necessity of a free coordination site at the metal catalyst, to allow the interaction with a water molecule and the oxidation process. In the complexes synthesized in the frame of this PhD project, the chloride ligand may be reasonably considered as the most labile, so under turnover conditions such ligand may be reasonably replaced via mass effect by water. We decided therefore to remove the chloride ligand before the catalytic tests, by treating complex **2** with one equivalent of AgPF_6 in acetonitrile; this allowed to isolate complex **2a** in which the chloride ligand has been replaced by a more labile acetonitrile solvent molecule.

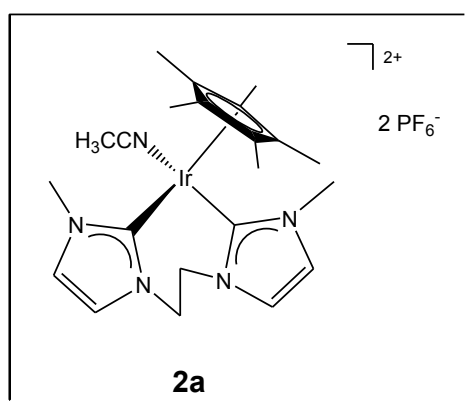


Figure 3.4: Iridium(III) di-NHC complex **2a**.

Higher TOF values, up to 0.50 s^{-1} at $[\text{Ir}] = 31 \text{ }\mu\text{M}$, have been obtained, confirming the higher reactivity of this solvento complex. The obtained results are summarized in **Table 3.3**; in **Figure 3.5** a comparison of the kinetic profiles obtained with complexes **2** and **2a** at $62.5 \text{ }\mu\text{M}$ of $[\text{Ir}]$ is also reported.

Table 3.3: Catalytic performance of complex **2a** as water oxidation catalysts in the presence of Ce(IV) as terminal oxidant (dark conditions).

| <i>[Ir]</i> [μM] | O_2 [μmol] (TON) ^b | Yield [%] ^a | TOF [s ⁻¹] ^c |
|-------------------------------|---|---------------------------|--|
| 500 | 923 (184) | > 99 | 0.15 |
| 250 | 925 (370) | > 99 | 0.24 |
| 125 | 924 (739) | > 99 | 0.42 |
| 62 | 926 (1494) | > 99 | 0.37 |
| 31 | 904 (2919) | 98 | 0.50 |

Reaction conditions: 10 mL Milli-Q H₂O, [CAN]=0.38 M, 25°C, catalyst introduced from a 5 mM solution in acetonitrile.

^a Determined after 8 h. ^b Calculated as $\mu\text{mol O}_2/\mu\text{mol Ir}$. ^c Calculated as $\mu\text{mol O}_2/\mu\text{mol Ir}$ per second. Determined in the initial 5 minutes of O₂ production, at conversion <10 %.

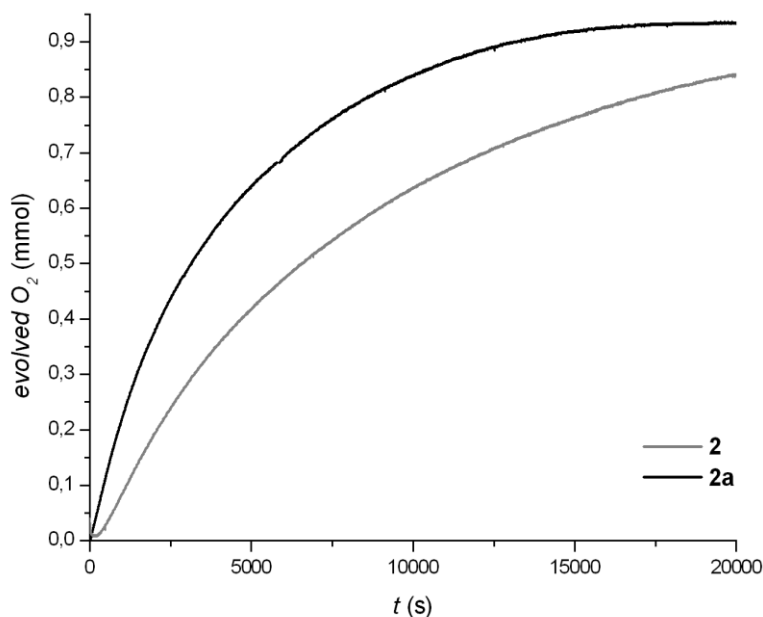


Figure 3.5: Oxygen evolution (mmol) vs. time (s) for complexes **2** and **2a**. Experimental conditions: $(\text{NH}_4)_2[\text{Ce}(\text{NO}_3)_6]$ (0.38 M), $[\text{Ir}] = 62 \mu\text{M}$, MilliQ water (10 ml).

Such overall results seem to support the hypothesis of chloride removal as activation step of the pre-catalyst.

Aimed to further explore the potentiality of the catalytic system in our hands, several attempts to synthesize a complex with an aquo ligand in place of the chloride were carried out. Taking inspiration from the synthetic procedure reported by Bernhard *et al.*,^[75] we tried to synthesize such complex by treating complex **2** with AgPF_6 in a mixed solvent ethanol/water 9:1 or CH_2Cl_2 /water (r.t. and 50 °C), however the isolated solid presents an ^1H NMR spectrum with at least three similar species, including the starting complex **2**. This could be a consequence of the scarce solubility of complex **2** in the two chosen reaction mixtures, and therefore, we decided for the moment to not further proceed with the synthesis of the aquo-complex analogue to **2** and **2a**. Probably a mixture acetonitrile/water might have been the best choice, and in future we further plan to run some experiments in this regard.

As mentioned previously, many aspects need to be taken into account to get more insight on the mechanism of the water oxidation catalyzed by Ir(III)-based catalysts. The described results suggest a molecular nature of the catalyst and the necessity of a free coordination site in order to activate the substrate. Finding further evidences of the mechanism and of the intermediates involved in a catalytic cycle may be quite challenging, mainly related to their intrinsic instability that leads to short-time dynamic transformation.

As proposed by Crabtree's and Lin's research groups, the mechanism should involve iridium species in high oxidation states. In particular, Crabtree and co-workers demonstrated the possible formation of iridium(IV) species through EPR measurements on a sample obtained by treating the Ir-NHC complex **A** (**Figure 3.1**) with $[\text{Ru}(\text{bpy})_3]^{3+}$.^[113]

Crabtree *et al.* reported also a study on the activation modes of the Cp*Ir-based complexes when the catalysis is driven by NaIO_4 , by employing high resolution mass measurement techniques.^[117] Some evidences suggest that the first changes on the pre-catalyst structure occur on the Cp* moiety, which may be partially oxidized by the sacrificial oxidant, leading to the formation of the actual active species.

This hypothesis was also asserted by Lin *et al.*, who used Ir(III)-catalyst in metal-organic frameworks (MOF) and evidenced the formation of a Ir(IV)=O species during the catalytic cycle.

The mechanism widely proposed for the catalytic cycle of water oxidation reaction catalyzed by iridium(III) complexes in presence of CAN involves both the formation of Ir(IV) and Ir(V) intermediates, as reported in **Figure 1.19**.

Aimed to probe the fate of complex **2** under catalytic conditions, we carried out a series of convergent experiments; in particular some interesting results were obtained by ^1H NMR spectroscopy, GC-MS analysis and UV-Vis spectroscopy.

Through ^1H NMR spectroscopy it was possible to demonstrate that the structure of complex **2** is retained in aqueous media, and spanning a pH range 0.6 – 7 (acidic pH imposed by adding D_2SO_4), no changes in the ^1H NMR spectra were observed for

period times over 24 hours. Interestingly, by adding either CAN or NaIO₄ a second set of signals forms after a short period of time, and finally, this second species became the major one in solution. The signals pattern of this latter species is similar to that shown by **2**, thus it seems reasonable to state that the di-NHC ligand remains coordinated to the complex and that the changes involve the other ancillary ligands (either by substitution of the chloride with a solvent molecule or by partial decomposition of the Cp* ligand).

The catalytic tests described previously were conducted by following the oxygen evolution, converting the change of the pressure in the headspace of the reactor into moles of produced oxygen. This detection technique may lead to an inaccurate evaluation of the catalytic behavior, because of the possible formation of other gases, in particular CO₂. In order to better understand the fate of complex **2** under turnover conditions and high concentration, catalytic tests in a reactor directly connected to a GC-MS were performed. With this apparatus, all the developed gases can be detected and quantified by referring to a previous calibration. Complex **2** was tested in the presence of either CAN or NaIO₄, so also the effect of the employed sacrificial oxidant may be evaluated. Indeed, a small quantity of CO₂ was detected in both cases, concomitant to the oxygen evolution; such results are comparable with those reported by Bernhard *et al.*^[75] The formation of carbon dioxide is probably due to a partial oxidation of the iridium ligand set, overlapped to the main catalytic cycle of water oxidation reaction. The kinetic profiles of CO₂ evolution paralleling oxygen evolution are reported in **Figure 3.6**.

It can be noted that the formation of O₂ and CO₂ occurs simultaneously and both processes start immediately after addition of **2** to the reaction mixture, without appreciable lag time. The molar ratio between the CO₂ produced and catalyst **2** turns out to be approximately 3.4 and 4.0 respectively in the Ce^{IV} and NaIO₄ protocols. These values correspond to ca. 20 % degradation of the organic ligand set of **2** and might account for the partial oxidation of the Cp* ligand, as recently observed in the presence of Ce^{IV}. However, CO₂ production employing NaIO₄ as the

oxidant could be underestimated, due to bicarbonate ion HCO_3^- presence in solution at neutral pH. Interestingly, CO_2 formation (and therefore catalyst decomposition) is not significantly affecting the TOF performance of the oxygenic route, that maintains a constant value for times longer than 2000 seconds, when the competitive evolution of CO_2 has already slowed down (**Figure 3.6**). This observation explains the well-behaved linear dependence on catalyst concentration, despite its concomitant degradation (**Figure 3.3**).

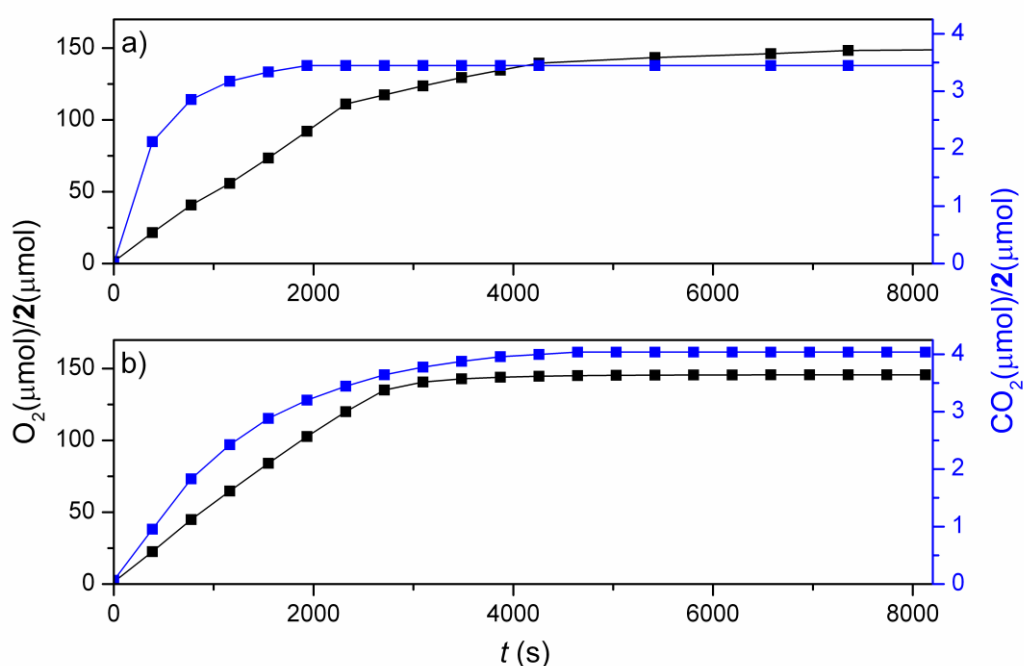


Figure 3.6: GC-MS monitoring of CO_2 formation over the course of water oxidation experiments, with CAN (a), and with NaIO_4 (b). Reaction conditions: (a) 10 mL Milli-Q H_2O , $[\text{CAN}] = 0.38 \text{ M}$, 25°C , $[\mathbf{2}] = 500 \mu\text{M}$; (b) 10 mL Milli-Q H_2O , $[\text{NaIO}_4] = 50 \text{ mM}$, 25°C , $[\mathbf{2}] = 130 \mu\text{M}$.

The same experiment was performed with complex **1** in the presence of CAN as sacrificial oxidant, and the amount of CO_2 detected resulted very similar to that obtained with **2**; the profiles of the evolution of the two gases (O_2 and CO_2) are also similar, thus allowing to extend the consideration just made for complex **2** also to complex **1**.

Several research groups studied the evolution of Ir(III)-based water oxidation catalysts in order to discriminate the real nature of the catalytic active species; for example complex $[\text{IrCp}^*(\text{H}_2\text{O})_3](\text{SO}_4)$ is by now considered only a precursor of heterogeneous iridium oxides.^[84-87] Fukuzumi *et al.* demonstrated that also Cp^*Ir -based complexes bearing chelating ligands like bipyridines may form colloids following the complete removal of the Cp^* moiety.^[96] Finally, Macchioni has studied via NMR the catalyst degradation under oxidative environments and observed the decomposition of the Cp^* ancillary ligand to form acetic acid and formic acid (see **Section 1.5**). It is reasonable to believe that such species may be further oxidized to carbon dioxide, and this should account for the CO_2 formation observed, in our case, through the GC-MS measurements with complex **2**.^[90,91,93]

The whole of these studies clearly pointed out that the Cp^* moiety is sensitive to the oxidative environment required for the catalytic tests. In the case of complex **2**, the oxidative degradation of the ligand set was less than 20 %; this result is much lower than that obtained for the complex $[\text{IrCp}^*(\text{H}_2\text{O})_3](\text{SO}_4)$ (80 % of formed acetic acid deriving from the Cp^* moiety) and evidences the stabilizing effect of the chelating di-NHC in terms of robustness of the overall catalytic system.

In order to get more insights into the catalyst transformation under turnover regime, a UV-Vis spectroscopic analysis was carried out during the catalytic reaction (**Figure 3.7**). In such experiments, the absorption spectra of the reaction mixture were registered in the range 450 – 800 nm for a period of time longer than the one associated with slowing down of the rate usually observed both with CAN and NaIO_4 (*ca.* 1 hour) For both sacrificial oxidant the same procedure was followed: the sacrificial oxidant was added to a solution of complex **2** and in both cases a vigorous bubbling, due to the oxygen evolution, was observed; this provides a sudden rising of the spectra baseline, but no other major modifications were observed. After *ca.* one hour, new absorption bands were detected at 606 and 593 nm with CAN and

NaIO_4 , respectively (**Figure 3.7**); notably, such absorption bands appeared when the oxygen evolution has already depleted.

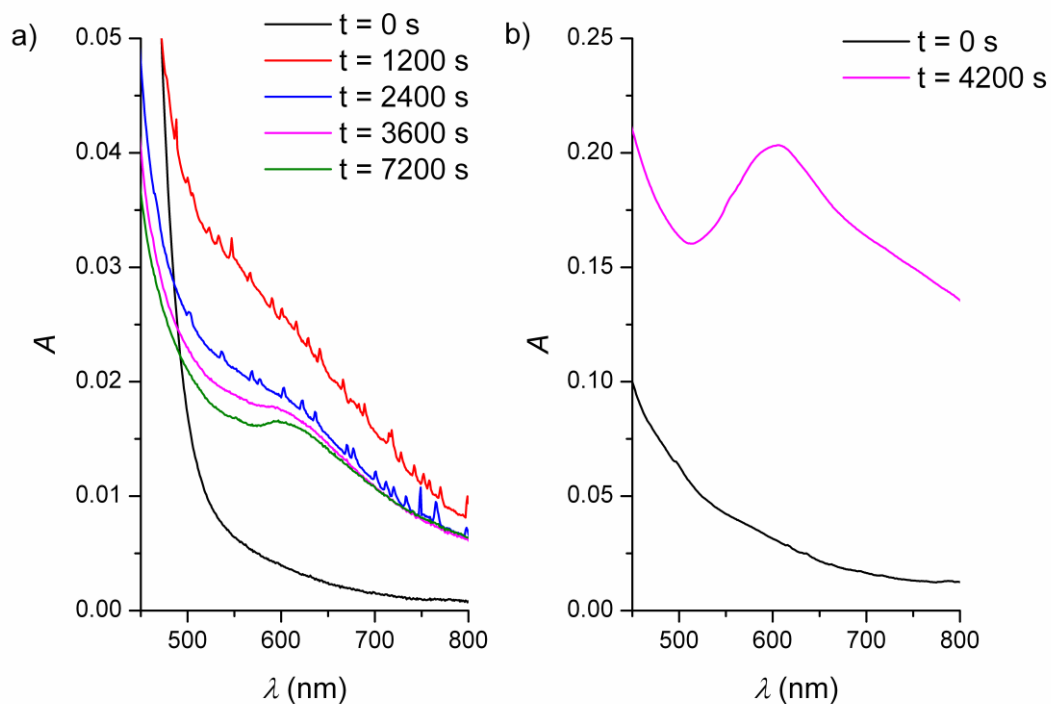


Figure 3.7: UV-Vis spectra of **2** treated with CAN (a) and with NaIO_4 (b). Conditions: (a) $[\text{CAN}] = 0.1 \text{ M}$, 25°C , $[\mathbf{2}] = 500 \mu\text{M}$; (b) $[\text{NaIO}_4] = 50 \text{ mM}$, 25°C , $[\mathbf{2}] = 130 \mu\text{M}$. The raising of the baseline is due to oxygen bubble formation during the course of the experiments.^[84]

Light absorption in the range 550 – 650 nm have been associated both to IrO_2 nanoparticles formation or to Ir(IV) molecular species (d-d or MLCT transitions); this may not be considered a conclusive evidence, but, since these bands appear after the majority of oxygen production, it is indicative of a post-cycle catalyst transformation and adds no information on the competent WOC species. In order to better clarify these results, a series of experiments were performed by mixing different ratios of catalyst/sacrificial oxidant, sampling an aliquot of the mixture and freezing it immediately to intercept some Ir intermediates in high oxidation states through both NMR and EPR spectroscopies; unfortunately, neither broadening of proton NMR signal (indicating the formation of paramagnetic species) nor EPR signals relative to Ir(IV) species were observed.

As stated previously, one of the main advantages of using a molecular catalyst is the possibility of finely tuning the stereo-electronic properties of the complex catalyst by a proper choice of the ligand set. As described in **Chapter 2**, during this PhD project several Ir(III) complexes bearing chelating N-heterocyclic carbene ligands have been synthesized. Since complexes **1** and **2** have shown promising efficiency in the catalysis of water oxidation reaction, either in terms of short- and long-time activity (expressed as TOF and TON values), all the other complexes were tested in the same catalytic conditions.

As demonstrated in **Chapter 2** by mean of convergent techniques, like ^{13}C NMR spectroscopy and cyclic voltammetry, the electronic properties of the complexes appear to be strongly influenced by the nature of the carbene unit. In particular, complexes **8**, **9** and **10** (**Figure 3.8**) are characterized by a clearly different electron-density on the iridium(III) centre, while the other complexes bear ligands that seem to not have a great difference in the electron-donor ability when compared with **1** and **2**.

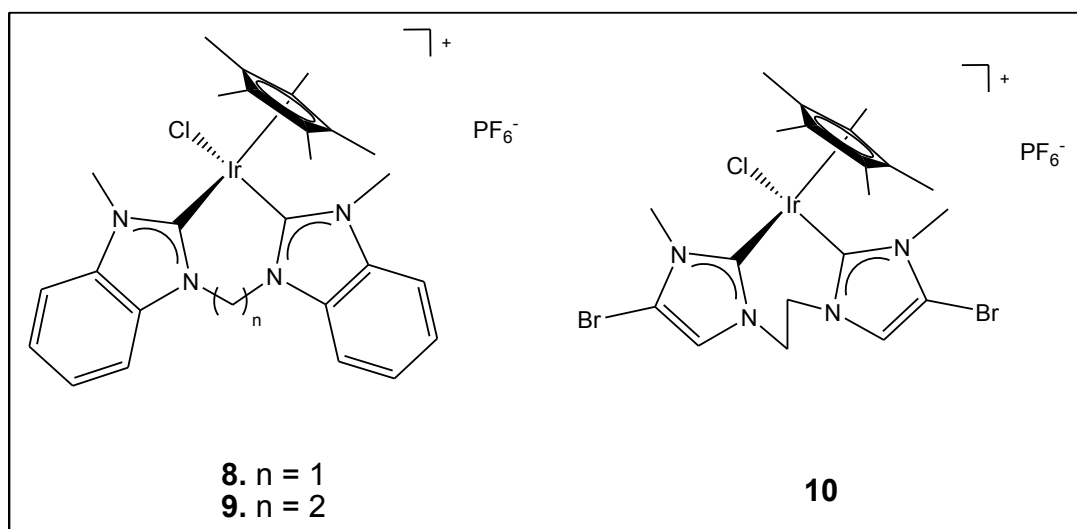


Figure 3.8: Iridium di-NHC complexes **8**, **9** and **10**.

As reported in **Chapter 2**, the complexes **8**, **9** and **10** present different stereoelectronic properties, based on the cyclic voltammetry measurements; for

this reason they were tested as catalysts in the water oxidation reaction in presence of CAN, under the same condition employed for the complexes **1**, **2** and **2a**; the obtained results are summarized in the **Table 3.4** and **Figure 3.9**.

Table 3.4: Catalytic performance of complexes **8**, **9** and **10** as water oxidation catalysts in the presence of Ce(IV) as terminal oxidant (dark conditions).

| <i>[Ir]</i> μM | 8 | | | 9 | | | 10 | | |
|------------------------------|-------------------------------------|------------------------|-------------------------------------|-------------------------------------|------------------------|-------------------------------------|-------------------------------------|------------------------|-------------------------------------|
| | O₂ | Yield | TOF | O₂ | Yield | TOF | O₂ | Yield | TOF |
| | [μmol] | [%]^a | [s⁻¹]^c | [μmol] | [%]^a | [s⁻¹]^c | [μmol] | [%]^a | [s⁻¹]^c |
| | (TON)^b | | | (TON)^b | | | (TON)^b | | |
| 500 | 908 (180) | 98 | 0.07 | n.d. ^d | n.d. ^d | 0.02 | 356 (71) | 37 | 0.04 |
| 125 | 1013 (810) | 98 | 0.12 | 1008 (810) | 99 | 0.09 | 497 (398) | 52 | 0.12 |
| 62 | 1017 (1630) | 99 | 0.20 | 939 (1500) | 99 | 0.11 | 483 (773) | 51 | 0.65 |
| 31 | 1033 (3304) | 99 | 0.20 | 1111 (3300) | 99 | 0.09 | - | - | - |

Reaction conditions: 10 mL Milli-Q H₂O, [CAN]=0.38 M, 25°C, catalyst introduced from a 5 mM solution in acetonitrile.

a Determined after 8 h. *b* Calculated as $\mu\text{mol O}_2/\mu\text{mol Ir}$. *c* Calculated as $\mu\text{mol O}_2/\mu\text{mol Ir}$ per second. Determined in the initial 5 minutes of O₂ production, at conversion <10 %. *d* It was not possible to determine the yield and the TON values, because the kinetic experiment was stopped before the plateau.

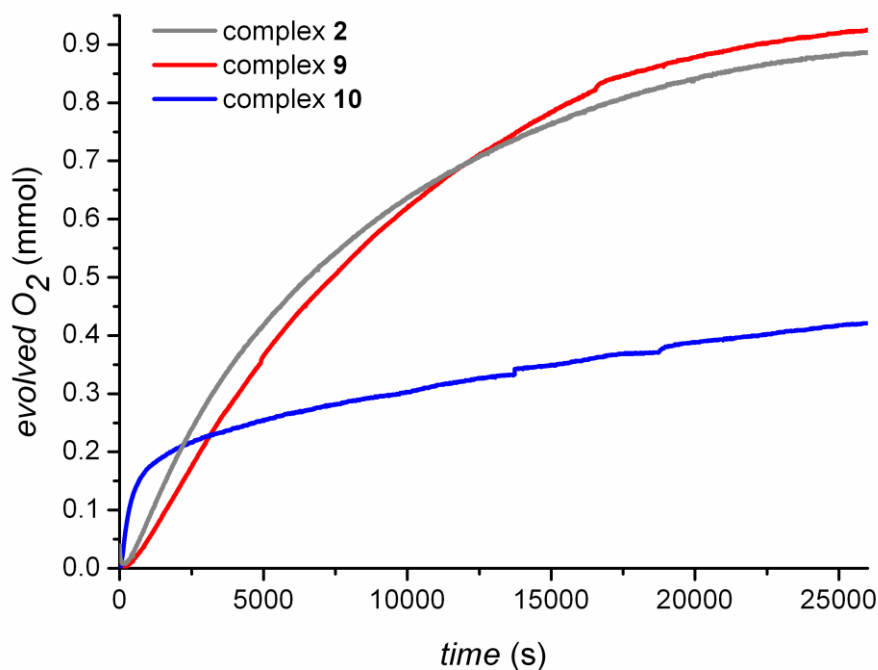


Figure 3.9: Oxygen evolution (mmol) vs. time (s) for complexes **2**, **9** and **10**. Experimental conditions: $(\text{NH}_4)_2[\text{Ce}(\text{NO}_3)_6]$ (0.38 M), $[\text{Ir}] = 31\text{-}125 \mu\text{M}$, MilliQ water (10 ml).

Complexes **8** and **9** provided both the quasi-quantitative conversion of the sacrificial oxidant CAN, with TON values comparable to those obtained with the complexes **1** and **2**; the initial oxygen production rates depend on the catalyst concentration in linear manner, so that also in these cases the nature of the active species should be molecular. In particular, complex **8** provides a catalytic activity in terms of TOF values very similar to that obtained with **2**, while complex **9** seems to be less active. These two complexes were also tested monitoring the nature of the evolved gases by GC-MS measurements: also in these cases, an initial amount of CO_2 was detected, but in quantities superior to those obtained with complexes **1** and **2**. Quantifying the ratio $\text{CO}_2/\text{catalyst}$, an oxidative degradation in between 30 – 45 % of the carbon content in the coordination sphere was calculated. Such results could be explained by considering the higher number of carbon atoms that can be oxidatively decomposed under acidic conditions; moreover, the different electron-

density on the metal due to the presence of a weaker-electron donor ligand may favor the Cp* decomposition described previously.

Complex **10** showed a very high initial catalytic activity when employed at low concentration (62.5 μM of [Ir]), with a TOF value of 0.65 s^{-1} . Nevertheless, the overall conversion of the sacrificial oxidant was only moderate (around 50 %), TON of 770 at concentration of 62.5 μM , thus indicating that some inactivation pathways occur after a short time. In order to better clarify such results, the evolution of complex **10** in presence of CAN was followed by ^1H NMR spectroscopy: treating the complex with a slight excess of CAN (5 equivalents) a rapid transformation occurs as indicated by the appearance of several new signals in the NMR spectrum. For instance, in the region relative to the methyl protons of the Cp* ligand (1.5 - 1.7 ppm, typically a singlet) were present at least five singlets, suggesting a fast degradation of this ligand. Moreover, the intensity of all the signals (signal/noise ratio in the spectrum) was significantly decreased suggesting that, not only decomposition occurs in solution, but also either volatile or insoluble species were formed. At the moment, it is not clear why complex **10** is more unstable in solution with respect to the other similar complexes.

Finally, in order to evaluate the influence of the substituents at the nitrogen atoms, we decided to test complex **6** in the water oxidation reaction driven by Ce(IV). Such di-NHC complex presents a ligand in which the two imidazol-2-ylidene units are connected by a methylene bridge as in complex **1**, but with a *n*-octyl group instead of a methyl group as wingtip substituents.

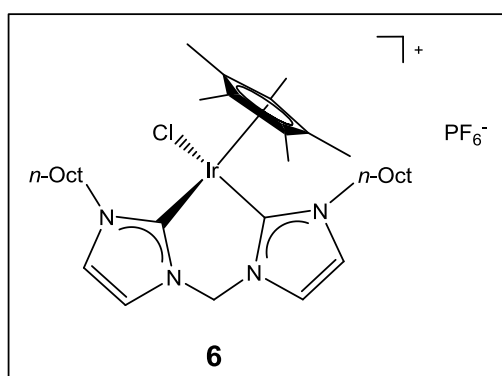


Figure 3.10: Iridium(III) di-NHC complex **6**.

A long alkyl group should be more hydrophobic than a methyl substituent and may impose very different structural behavior in aqueous media, both for the mentioned lipophilic nature and for its steric hindrance.

This particular complex was synthesized and used as catalyst taking inspiration from a recent work by Macchioni and Albrecht: they use in fact an iridium(III) complex with a mesoionic carbene ligand, derived from a triazol-5-ylidene, with alkyl chains of different length as wingtip substituents (**Figure 3.11**). In particular, with a long alkyl chain the observed catalytic activity is much higher than that of the complex with the simple methyl substituent (for example, with R = *n*-Oct the TOF is 2.87 s^{-1} ; with R = Me the TOF is 0.26 s^{-1}).^[118]

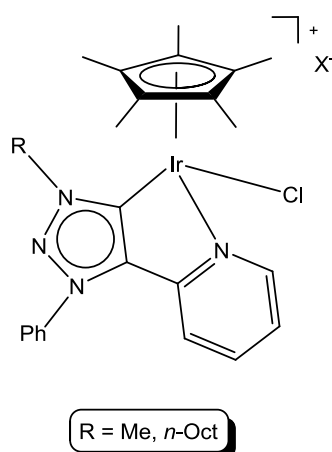


Figure 3.11: Iridium(III) complexes bearing a mesoionic carbene ligand differently substituted at nitrogen, described by Albrecht and Macchioni.

In order to verify if such process could happen also with our di-NHC ligand, complex **6** was tested under the same conditions described previously. Unfortunately, the catalytic activity exhibited by **6** is poorer with respect to the analogue **1**: at [Ir] concentration of $125 \mu\text{M}$, the final conversion of CAN is around 20 % (TON = 175), while with **1** the full conversion was obtained (TON = 730). Moreover, also the initial rate of oxygen evolution is slower than that observed with **1**: with the latter complex, the TOF value was 0.12 s^{-1} , while with **6** is one order of magnitude lower (0.011 s^{-1}).

Such preliminary results suggest that, in our case, there is no beneficial effects on substituting a short alkylic group like a methyl with a more sterically hindered and hydrophobic alkylic group like a *n*-octyl.

3.2 Water oxidation with iridium(III) complexes bearing di(N-heterocyclic carbene) ligands in a photo-induced process

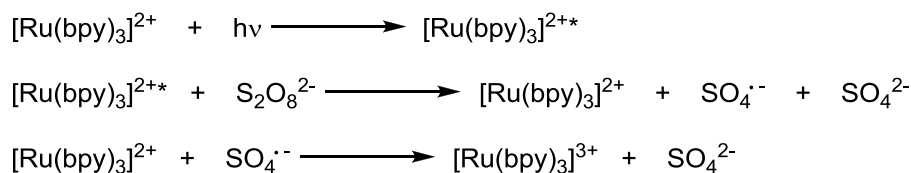
As mentioned previously, the employment of a sacrificial oxidant provides a rapid screening of the catalytic behavior of a complex, both in terms of activity and robustness in harsh conditions. However, the main drawback in the use of CAN as sacrificial oxidant is related to the experimental conditions, which are very different from those eventually required for the implementation of an effective catalytic system into a device, able to perform the overall water splitting process, like an artificial photosynthetic cell (an example of such device is reported in **Figure 1.16**).

For this reason, the photo-driven water splitting is a challenge and several groups are working to reach this goal, which should enable the conversion of solar energy into chemical bonds via artificial photosynthetic processes. This reaction is typically performed by combining the catalyst with a photosensitizer (PS) and a sacrificial acceptor of electrons (SA): the three component system should provide, upon visible-light irradiation and consequent excitation of the PS, a cascade of electron transfer events in the chain $WOC \rightarrow PS \rightarrow SA$, until the loss of the four electrons necessary to the transformation of two molecules of H_2O to O_2 and four H^+ .

The PS/SA couple ($[Ru(bpy)_3]^{2+}$ and sodium persulfate) has a well-established chemistry, which has been already combined with IrO_2 nanoparticles and ruthenium(II) complexes.^[70,81b] The role of the photosensitizer is to efficiently absorb the light and reach an excited state with a life-time sufficiently long to transfer an electron to a second species, thus creating a charge separation. Surely, the most studied photosensitizer is the cation $[Ru(bpy)_3]^{2+}$ (bpy = bipyridine), (reduction potential 1.26 vs. NHE). This complex has a characteristic absorption band in the visible region (maximum ≈ 450 nm) derived from a metal-to-ligand charge transfer (MLCT); the excited short-lived singlet state is transformed rapidly

by intersystem crossing in a long-lived triplet state $^3[\text{Ru}(\text{bpy})_3]^{2+*}$, the actual species that will transfer the electron to the sacrificial acceptor of electrons. The thermodynamic of this process has been studied in depth and it turned out that for the reduction potentials of the couples $[\text{Ru}(\text{bpy})_3]^{3+}/[\text{Ru}(\text{bpy})_3]^{2+*}$ and $[\text{Ru}(\text{bpy})_3]^{3+}/[\text{Ru}(\text{bpy})_3]^{2+}$ are -0.86 and 1.26 V vs. NHE, respectively; consequently, it is thermodynamically easier for a SA to accept the electron when the PS is at an excited state rather than in the ground state. The role of the sacrificial acceptor of electrons is therefore the quenching of the photoexcited state of the photosensitizer, and the most commonly used is sodium persulfate; $\text{Na}_2\text{S}_2\text{O}_8$ is characterized by a high oxidation potential (2.05 V vs. NHE for the couple $\text{S}_2\text{O}_8^{2-}/2\text{SO}_4^{2-}$) and it might be itself an oxidant, either for the ligand and the catalyst. The advantage of using such SA is that, once it has accepted the electron from the PS*, a bond cleavage rapidly occurs to form SO_4^{2-} and the radical $\text{SO}_4^{\cdot-}$. The reaction scheme occurring with a photo-driven $[\text{Ru}(\text{bpy})_3]^{2+}/\text{S}_2\text{O}_8^{2-}$ system is summarized in

Scheme 3.2.



if a WOC is present in the system, the following reactions can occur:



Scheme 3.2: Sequence of reactions usually accepted for the photo-driven water oxidation in the presence of $[\text{Ru}(\text{bpy})_3]^{2+}/\text{S}_2\text{O}_8^{2-}/\text{WOC}$.

The di-NHC Ir(III) complex **2** was preliminary tested in a photo-driven catalytic water oxidation process. Complex **2** was chosen because it has been demonstrated to be the most active catalyst; furthermore its behavior under turnover conditions has been deeply investigated in dark conditions.

In the performed catalytic tests, the reactions were conducted in a buffer solution of 50 mM NaHCO₃/Na₂SiF₆ at pH = 5.2, employing [Ru(bpy)₃]Cl₂ and Na₂S₂O₈ at concentration 1 mM and 5 mM, respectively. The irradiation of the solution was performed by a monochromatic LED emitting at 450 nm, which corresponds to the absorption maxima of the photosensitizer. The results are summarized in **Table 3.5** and TOF (calculated in the initial 3 minutes of oxygen evolution), TON and quantum efficiency (QE) are reported. The QE is defined as the amount of absorbed photons that are actually exploited to produce oxygen and is a parameter that can be used to compare the activity of the catalyst with the benchmark reported in literature.

Table 3.5: Catalytic Performance of **2** and IrCl₃ in the photoactivated ($\lambda=450$ nm) cycle with [Ru(bpy)₃]Cl₂ (bpy=2,2'-bipyridine) and Na₂S₂O₈.

| [Ir] μM | 2 | | | IrCl ₃ | | |
|-----------------------|--|--|---------|--|--|---------|
| | O ₂ , μmol (TON) ^b | R ₀ , ^a $\mu\text{molO}_2\text{s}^{-1}$ (TOF, s ⁻¹) ^c | QE % | O ₂ , μmol (TON) ^b | R ₀ , ^a $\mu\text{molO}_2\text{s}^{-1}$ (TOF, s ⁻¹) ^c | QE % |
| 100 | 14.0 (9.3) | 2.93×10 ⁻³ (1.99×10 ⁻³) | 3.8 | 6.4 (4.2) | 1.84×10 ⁻³ (1.25×10 ⁻³) | 2.3 |
| 50 | 5.72 (7.6) | 2.35×10 ⁻³ (3.13×10 ⁻³) | 3.1 | - | - | - |
| 25 | 2.93 (7.8) | 1.82×10 ⁻³ (4.85×10 ⁻³) | 2.3 | - | - | - |

Reaction conditions: 15 mL of 50 mM Na₂SiF₆/NaHCO₃ buffer, pH = 5.2; [Ru(bpy)₃]²⁺=1 mM, [Na₂S₂O₈]=5 mM, catalyst introduced from a 5 mM solution in acetonitrile. Irradiation performed with monochromatic LED emitting at 450 nm.

[a] Determined in the initial 3 minutes of O₂ production. [b] Calculated as $\mu\text{mol O}_2/\mu\text{mol Ir}$.

[c] Calculated as $\mu\text{mol O}_2/\mu\text{mol Ir}$ per second.

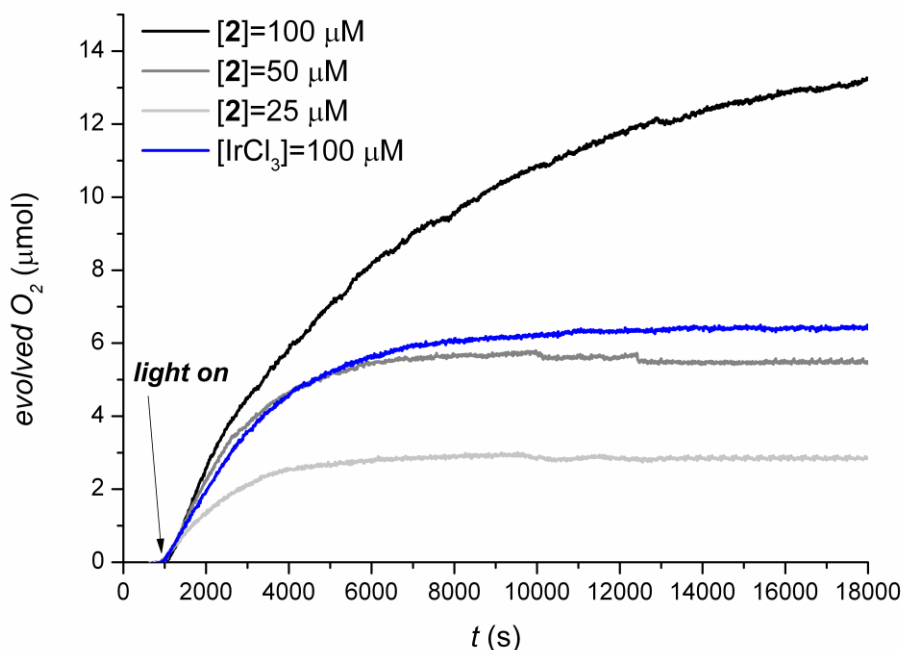


Figure 3.12: Oxygen evolution kinetic for **2** and IrCl₃. Reaction conditions: 15 mL of 50 mM Na₂SiF₆/NaHCO₃ buffer, pH = 5.2; [Ru(bpy)₃]²⁺=1 mM, [Na₂S₂O₈]=5 mM. Irradiation performed with monochromatic LED emitting at 450 nm.

As reported in **Table 3.5**, IrCl₃ has been tested under the same conditions, in order to compare its activity with complex **2**. In fact, it is well known that such salt under the same conditions acts as precursor for IrO_x nanoparticles. The remarkably different behaviour between the two catalytic systems, both considering the initial rate of oxygen evolution and the final amount of oxygen produced, might represent a good indication that complex **2** acts as a molecular catalyst and do not evolve in colloidal species.

At the same concentration ([Ir] = 100 μM), the two catalytic systems deactivate at very different times: IrCl₃ reaches the plateau after *ca.* 1 hour of irradiation, while **2** is active for more than 5 hours. Significantly, also the QE are different: with IrCl₃ is 2.3 %, remarkably lower than that observed with **2** (3.8 %).

With complex **2** the oxygen evolution occurs concomitantly to the solution irradiation, and the yield based on the persulfate content reaches 37 % (with [Ir] =100 μM) after 5 hours of irradiation. The observed TONs fall in the range 7.6 – 9.3,

while the TOFs slightly increase with the catalyst concentration and lie between $1.99 \cdot 10^{-3}$ and $4.85 \cdot 10^{-3} \text{ s}^{-1}$.

Finally, it should be considered that oxygen production in such photoactivated cycles is often limited by degradation of the photosensitizer, which becomes more relevant when the electron transfer from the catalyst to the photosensitizer is slow.

As in dark conditions, also in a light-driven process a big challenge is represented by the discrimination of the real nature of the active species; in particular, if it is a molecular catalyst or a precursor of IrO_2 colloids. Since the use of a hydrogen carbonate buffer hampers the identification and quantification of CO_2 as a possible degradation product of the organic ligand set, and the strong absorption of the sensitizer makes it impossible to monitor the build-up of any reaction intermediates by UV/Vis spectroscopy, we decided to gain some insight about this issue investigating the evolution of the complex **2** in the photo-activated cycle by EPR spectroscopy. In such experiments, a 1:1 solution of acetonitrile/50 mM $\text{NaHCO}_3/\text{Na}_2\text{SiF}_6$ buffer containing **2** (0.5 mM), $[\text{Ru}(\text{bpy})_3]^{2+}$ (0.5 mM) and $\text{Na}_2\text{S}_2\text{O}_8$ (10 mM) was irradiated by a monochromatic LED at 450 nm and then the solution was immediately frozen.

Interestingly, in the resulting EPR spectrum the X-band continuous-wave (CW) is characterized by the presence of an Ir-centered rhombic signal superimposed on a second signal attributed to the Ru(III) oxidized form of the photosensitizer ($g_{\perp} = 2.65$; **Figure 3.13**). The same rhombic signal was observed also by irradiation for 1 minutes a solution containing only the complex **2** and $[\text{Ru}(\text{bpy})_3]^{2+}$, but without the $\text{Na}_2\text{S}_2\text{O}_8$; in this latter case, the formation of $[\text{Ru}(\text{bpy})_3]^{3+}$ is ruled out and this fact allows the spectral simulation of the Ir-based signal, which provides three g values ($g = 2.4, 2.2$ and 1.85), consistent with a low-spin d^5 iridium(IV) complex with $S = 1/2$. This Ir(IV) species might be considered as a plausible intermediate of the catalytic cycle, as suggested also by Crabtree *et al.* basing their proposal by similar observations.^[113]

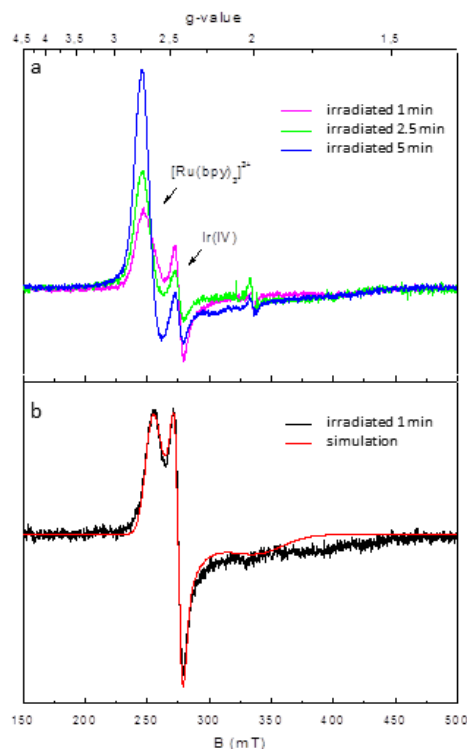


Figure 3.13: X-band CW-EPR spectra registered for **2** at 10 K under photoirradiation conditions; [**2**] = 0.5 mM in 50:50 acetonitrile: 50 mM Na₂SiF₆/NaHCO₃ buffer, pH = 5.2 (illumination with monochromatic LED emitting at 450 nm). (a) [Ru(bpy)₃]²⁺ = 0.5 mM, [Na₂S₂O₈] = 10 mM (b) [Ru(bpy)₃]²⁺ = 0.5 mM.

The described EPR experiments suggest that photoinduced electron transfer can occur from the di-NHC Ir(III) catalyst towards both the photogenerated oxidant [Ru(bpy)₃]³⁺ and the excited state of the photosensitizer (reductive quenching of [Ru(bpy)₃]^{2+*}).

Aimed to support these observations, an electrochemical study on the properties of **2** in NaHCO₃/Na₂SiF₆ buffer solution was performed: in the cyclic voltammogram of **2**, an irreversible wave with an anodic peak potential of $E_{pa} = 0.96$ V versus Ag/AgCl is observed, likely ascribable to the Ir^{IV}/Ir^{III} couple (**Figure 3.14**). This wave is followed by a more intense one starting at $E = 1.05$ V and likely ascribable to water oxidation. The catalytic nature of this wave is confirmed by the increase of the normalized current at 1.4 V versus the scan rate (inset in **Figure 3.14**), compatible with a rate-determining chemical step prior to electron transfer to the electrode.

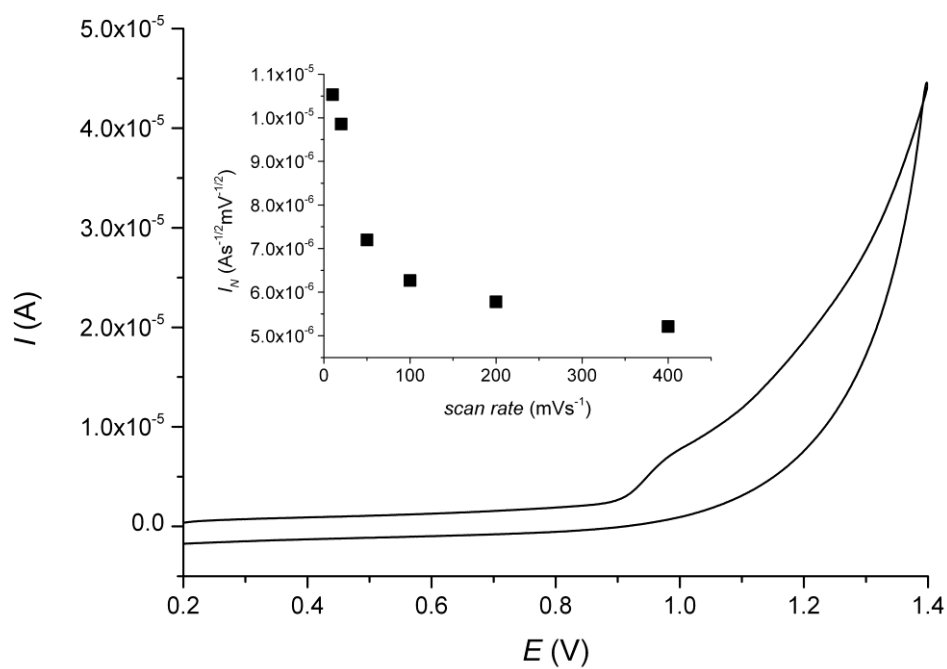


Figure 3.14: Cyclic voltammetry of $0.5 \text{ mM } \mathbf{2}$ in $50 \text{ mM Na}_2\text{SiF}_6/\text{NaHCO}_3$ buffer, $\text{pH} = 5.2$ and 0.5 M LiClO_4 (reference $\text{Ag}/\text{AgCl}/3 \text{ M NaCl}$, scan rate 20 mVs^{-1}). Inset: plot of the normalized current at 1.4 V versus the scan rate.



Chapter 4: RESULTS AND DISCUSSION

SYNTHESIS, CHARACTERIZATION AND CATALYTIC ACTIVITY IN TRANSFER HYDROGENATION OF DINUCLEAR DI(N-HETEROCYCLIC) CARBENE IRIDIUM(III) COMPLEXES

4.1 Synthesis of the dinuclear Ir(III) complexes

The dinuclear iridium(III) complexes **15** and **16** were synthesized *via* transmetalation of the di-NHC moieties from the corresponding silver(I) di-NHC complexes, following a similar procedure described previously for the synthesis of the monuclear complexes **1-3** and **5-10** (Chapter 2).

The azolium salts $L^n \cdot 2HBr$ ($n = 14, 15$) and $L^n \cdot 2HPF_6$ ($n = 13, 15$) were synthesized according to literature procedures. The synthesis was straightforwardly carried out by coupling the N-methylimidazole with α, α' -dibromo-*o*-xylene ($L^{13} \cdot 2HBr$), α, α' -dibromo-*m*-xylene ($L^{14} \cdot 2HBr$) or α, α' -dibromo-*p*-xylene ($L^{16} \cdot 2HBr$). The salt $L^{13} \cdot 2HPF_6$ was isolated from $L^{13} \cdot 2HBr$ by simple Br^-/PF_6^- anion metathesis. A similar synthetic procedure was performed also for the synthesis of $L^{16} \cdot 2HPF_6$: the coupling between the N-(2pyridin)-imidazole ring and the CH_2Br_2 , followed by the metathesis of the bromide ions with hexafluorophosphate, by treatment with a slight excess of NH_4PF_6 .

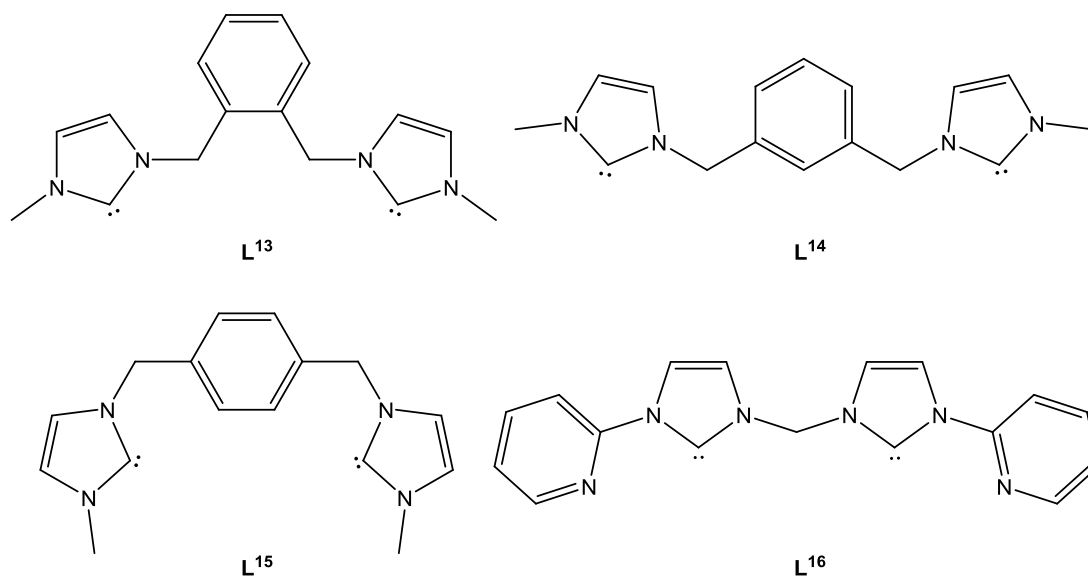
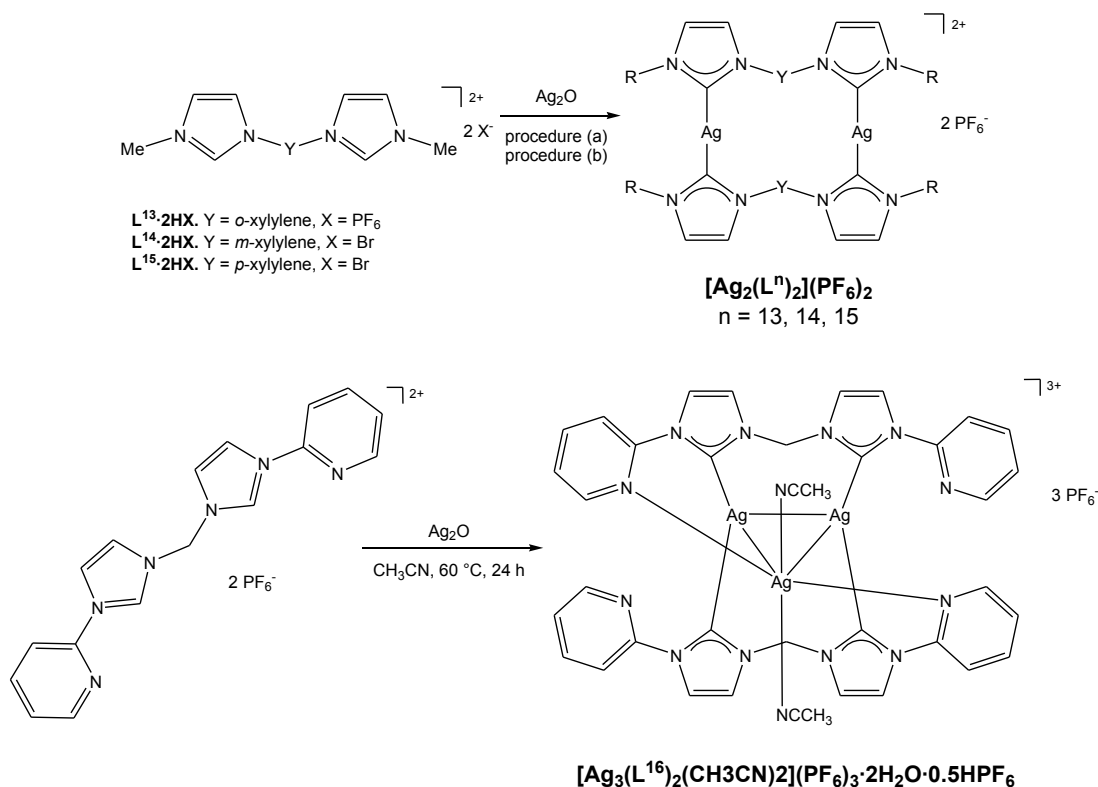


Figure 4.1: NHC ligands derived from the diimidazolium salts employed.

The silver(I) complexes bearing the dicarbene ligands L^{14} and L^{15} were successfully synthesized in two step, following the same procedure performed for the synthesis of the silver(I) complexes bearing the ligands L^1 - L^4 , L^6 , L^7 , L^9 and L^{10} , described in **Chapter 2**. In such synthetic procedure the first step is the reaction between the diimidazolium salt and an excess of Ag_2O in water, for 24 hours at room temperature; then, after the separation of the unreacted Ag_2O by filtration, a treatment of the filtrate solution with a slight excess of NH_4PF_6 provides the precipitation of the desired dicarbene dinuclear silver(I) complex, which can be easily collected by filtration (procedure **a**, **Scheme 4.1**).

The silver(I) complexes bearing the ligands L^{13} and L^{16} were synthesized by reacting the diimidazolium salt $L^n \cdot 2HPF_6$ ($n = 13, 16$) with an excess of Ag_2O in acetonitrile at $60\text{ }^\circ\text{C}$, for 24 hours, as described for the synthesis of the complexes $[Ag_2(L^8)_2](PF_6)_2$ and $[Ag_2(L^{12})_2](PF_6)_2$ (procedure **b**, **Scheme 4.1**). Following such synthetic procedure, no anion metathesis is necessary, so the filtrate solution was concentrated under reduced pressure and diethyl ether was added, providing the precipitation of the solid product, collected then by filtration.



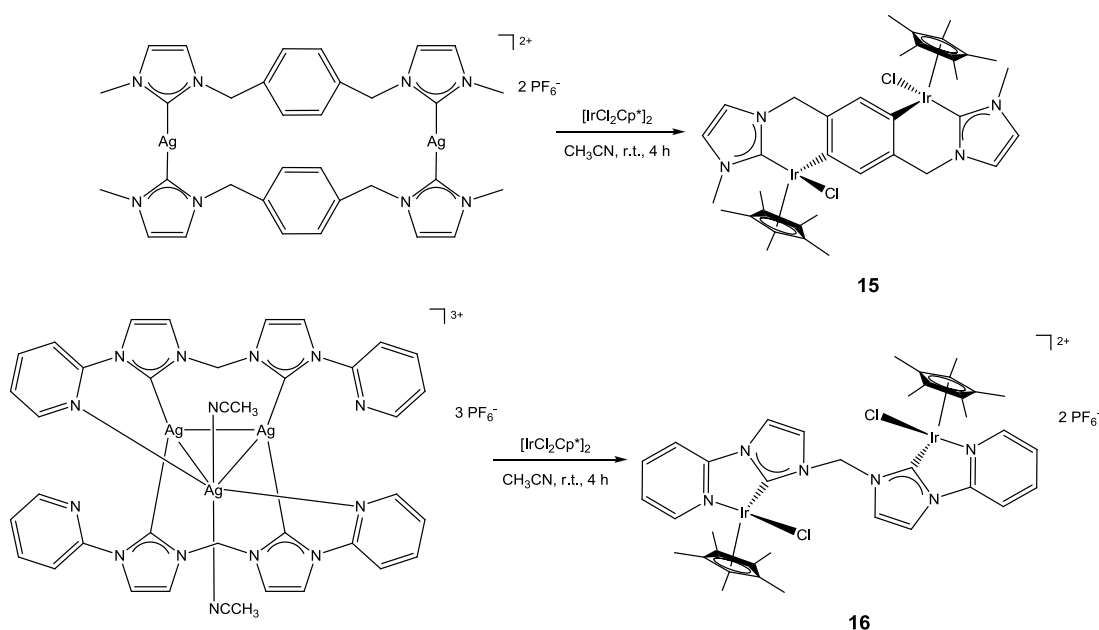
Scheme 4.1: Synthesis of the silver(I) complexes $[Ag_2(L^n)_2](PF_6)_2$ (n = 13, 14, 15) (top); synthesis of the silver(I) complex $[Ag_3(L^{16})_2(CH_3CN)_2](PF_6)_3 \cdot 2H_2O \cdot 0.5HPF_6$ (bottom).
Procedure a: i) 1 eq. of salt precursor, 2.5 eq. of Ag_2O , H_2O , r.t., 24 h; ii) 2.1 eq. of NH_4PF_6 .
Procedure b: 1 eq. of salt precursor, 4 eq. of Ag_2O , CH_3CN , r.t., 24 h.

As reported in **Chapter 2**, the formation of the desired complexes was confirmed by the lack of the protons in 2 position of the azole rings in the 1H NMR spectra of the products; moreover, all the spectroscopic data are consistent with those reported in literature for this complexes, so it can be reasonably assumed that the obtained products have the same structures.

The complexes $[Ag_2(L^n)_2](PF_6)_2$ (n = 13, 14, 15) all present a dinuclear structure, in which the two dicarbene ligands bridged the two silver(I) atoms, in a similar fashion to what described for the complexes bearing ligands $L^1 - L^{10}$ and L^{12} .^[28a,119] The methylene protons of the xylylene bridges between the carbene units present a singlet signal in the 1H NMR spectra of the silver(I) complexes: since this magnetic equivalence, a fluxional behaviour of the complexes in solution is suggested.

According to the literature, the structure proposed for the complex with ligand **L**¹⁶ has the formula $[\text{Ag}_3(\text{L}^{16})_2(\text{CH}_3\text{CN})_2](\text{PF}_6)_3 \cdot 2\text{H}_2\text{O} \cdot 0.5\text{HPPF}_6$, so it is a trimetallic complex with two bridging dicarbene ligands and coordinated acetonitrile molecule.^[100]

The dinuclear iridium(III) di-NHC complexes **15** and **16** were synthesized by transmetalation of the dicarbene moiety from the silver(I) centre to iridium(III) centre, under similar conditions described for the synthesis of the complexes **1-3** and **5-10**, although employing a stoichiometry L:Ir 1:2. It was not possible to obtain in pure form the iridium(III) complexes with the dicarbenes having a ortho- or meta-xylene bridging group.



Scheme 4.2: Synthesis of the dinuclear di-NHC complexes **15** and **16**.

As shown in the **Scheme 4.2**, the obtained iridium(III) di-NHC complexes both present a dinuclear structure with one dicarbene ligand coordinated in a bridging fashion to two metal fragments $\{\text{IrCp}^*\text{Cl}\}$. In both cases, the typical hexacoordination of the Ir(III) centre is provided by the coordination of a donor function of the dicarbene ligand employed. In the case of the cationic complex **16**, the iridium coordination sphere is completed by the nitrogen atom of the imidazol-

2-ylidene pyridine substituent, while complex **15** is neutral on account of the double metalation of the phenylene ring, which acts as a linker between the two NHC moieties.

In the case of complex **15**, such coordination is probably favoured by the rigid structure imposed by the bridging group between the carbene units, encumbering the formation of a chelate structure. The ^1H NMR spectrum of complex **15** presents an AB system for the signals of the methylene protons of the bridge, suggesting an enhanced tension with respect to what verified for the corresponding silver(I) complex $[\text{Ag}_2(\text{L}^{15})_2](\text{PF}_6)_2$, in which the methylene hydrogens give indeed rise to a singlet. The mass measurements (MALDI, positive mode) confirmed the dinuclear structure: a peak at 955 m/z is present, corresponding to the fragment $[\text{Ir}_2\text{ClCp}^*_2(\text{di-NHC})]^+$.

The ^{13}C NMR spectra of complex **15** presents a unique signal for the carbene carbons at δ 157.5, in the typical range of carbene carbons coordinated to a iridium(III) center,^[54,58,59,103,104] well upfield with respect to the corresponding silver complex (δ ca. 180 ppm).

The coordinating bridging fashion obtained for complex **15** is not considered very surprising, since a number of iridium(III) complexes bearing cyclometalated ligands are reported, obtained by activation of an aromatic C-H bond in the ligand (for example in the wingtip groups of imidazol-2-ylidene units or 2-phenylpyridine). Such category of complexes are interesting from many point of view: as described in **Chapter 1**, Ir(III) complexes bearing cyclometalated ligands showed peculiar photoluminescent properties, but having a metalated ligand can provide an additional reactivity also in catalysis, provided by a reversible cleavage of the coordinated moiety.

The molecular structure of compound **15** was definitely established by an X-ray diffraction study performed on a crystal obtained by diffusion of *n*-hexane into a dichloromethane solution of **15** (**Figure 4.2**).

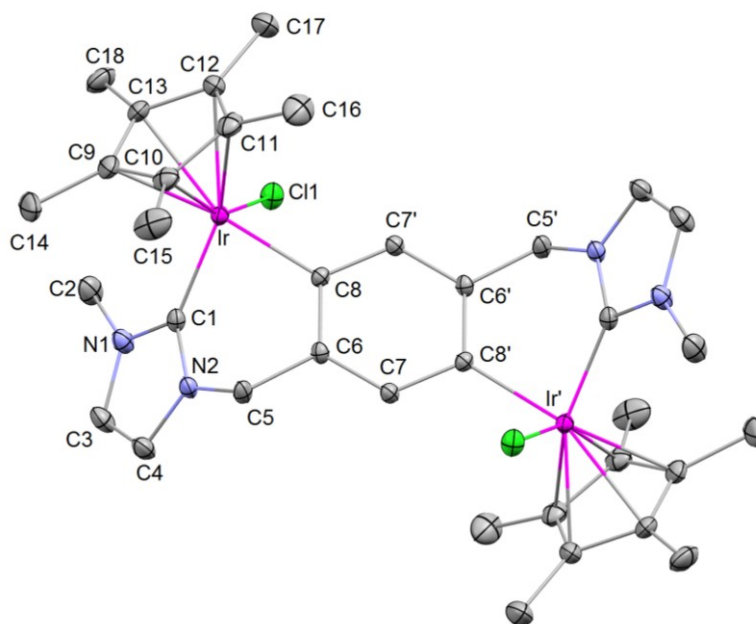


Figure 4.2: ORTEP diagram of complex **15**. Ellipsoids are drawn at their 30 % probability level. Hydrogen atoms and crystallization solvent (dichloromethane) have been omitted for clarity. Selected bond distances (Å) and angles (°): C1-Ir 1.998(3), C8-Ir 2.073(3), Cl1-Ir 2.4254(7), CT-Ir 1.903(3); C8-Ir-Cl1 89.03(8), C1-Ir-Cl1 92.69(9), CT-Ir-Cl1 120.57(10), CT-Ir-C1 128.40(12), CT-Ir-C8 129.53(12), C1-Ir-C8 84.65(11). Symmetry code ' : 1-x, -y, 1-z.

The structure is centrosymmetric, with the inversion center located in the middle of the phenylene ring. The coordination around the metal center is described as a three-legged piano stool, where the three legs are the chlorine atom and the carbon atoms of the imidazol-2-ylidene and of the metalated phenylene units. The centroid (CT) of the cyclopentadienyl ligand completes the coordination at the metal. The Ir-C1 and Ir-C8 bond distances are 1.998(3) and 2.073(3) Å respectively and are in good agreement with those found in a dinuclear Ir(III) complex containing a NHC donor and a *o*-metalated phenylene ligand (1.987(4) and 1.989(4), 2.089(3) and 2.091(3) Å respectively).^[120] The bite angle C1-Ir-C8 is 84.65(11)° falls in the range [83.2-87.2°] observed for C_{NHC}-Ir-C_{Ph} angles in Ir complexes containing a six membered chelating ring.^[51c,59,103b,121] The six membered chelating ring formed by Ir1, C1, N2, C5, C6 and C8 atoms, is in a boat conformation. The Ir-Cl and the Ir-CT bond distances (2.4254(7) and 1.903(3) Å respectively) fall in the typical range for similar chloride cyclopentadienyl iridium(III) compounds.

As the complex **15**, also complex **16** is dinuclear with the dicarbene ligand bridging the two metal centres. In the case of this latter complex, such structure is favoured by the saturation of the coordination sphere of the iridium(III) centre by the coordination of the nitrogen atoms of the pyridine wingtip substituents. The bridging coordination of the diNHC ligand is suggested by the ^1H NMR spectrum of **16**, which shows a singlet for the methylene protons of the dicarbene. The ^{31}P NMR spectrum shows the typical heptet for the PF_6^- counter-anion, confirming the cationic nature of the complex. Finally, the ESI-MS spectra (positive mode) present two peaks relative to the fragments $[\text{M-PF}_6]^+$ (1173 m/z) and $[\text{M-2PF}_6]^{2+}$ (514 m/z), thus accounting both the dicationic and dinuclear nature of the compound. Unfortunately, no suitable crystals for an X-ray measurement were obtained.

4.2 Transfer hydrogenation of ketones catalyzed by the dinuclear di-NHC complexes of iridium(III) **15 and **16****

This part of the work was performed in collaboration with the group of prof. Walter Baratta of the University of Udine.

The structures of the complexes **15** and **16** have some similarities to some mononuclear complexes of Ir(III) reported in literature and successfully employed during the last decade as catalysts for transfer hydrogenation reactions. In particular, the iridium(III) complexes, shown in **Figure 4.3** and bearing NHC ligands with a pendant group able to coordinate in hemilabile fashion to the metal centre, are very efficient.^[55,56,122]

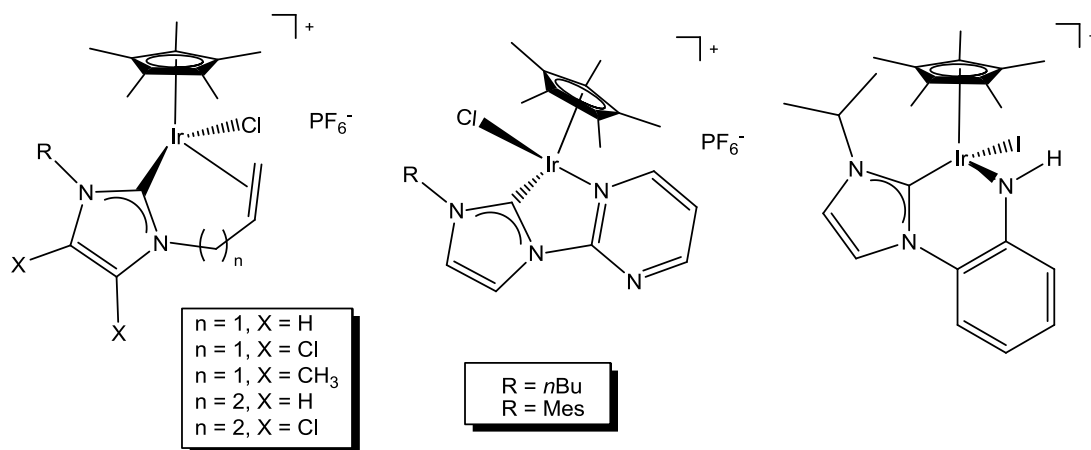
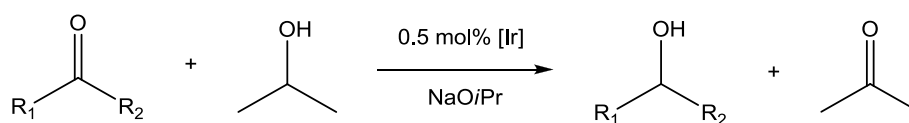


Figure 4.3: Iridium(III)-NHC complexes efficient as catalysts for transfer hydrogenation of ketones.

Such structural analogies suggested that also the two novel complexes, **15** and **16**, may be catalytically active for such reactions, so a study on the catalytic behaviour in transfer hydrogenation of ketones was carried out. As described in **Section 1.4.2**, the class of transfer hydrogenation reactions is comprehensive of a wide range of transformations, including the reduction of unsaturated functional groups of many substrates, especially C=O, N=N, N=O and C=C groups. Despite a number of transition metal complexes has been employed so far, the most active catalysts are Ru-, Rh- and Ir-based. Nowadays, the scope of the reaction is extended to a large number of substrates, both simple and highly functionalized, provided by the development of catalytic systems with high chemoselectivity; for instance, a selective reduction of the carbonyl group of a α,β -unsaturated ketone was reported. Moreover, the mechanistic insight provided the necessary knowledge in order to optimize the reaction conditions, like the employment of the appropriate hydrogen source and base. Focusing the attention on the hydrogen source, it is worth to underline why such category of reactions is so interesting: the reduction of the substrate is carried out under mild conditions, employing a sacrificial hydrogen-donor in place of molecular hydrogen, potentially dangerous and inconvenient in terms of practical handling. The employed hydrogen-donors are usually cheap and non-toxic compounds, as much as the by-products generated by the reaction, so the process may be considered economically and environmentally more sustainable.

In order to evaluate the catalytic activity of complex **16** and **15** in transfer hydrogenation reactions of ketones, and compare the results with those reported in literature for other Ir(III)-NHC based catalysts, we decided to carry out a screening of ketones with different structures using 2-propanol both as hydrogen-donor and solvent; the catalytic reactions were performed using 1 mol% of iridium, under basic conditions, in the presence of NaOiPr as base, at reflux conditions (**Scheme 4.3**). The obtained results are summarized in **Table 4.1**.

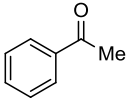
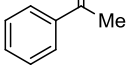
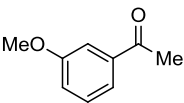
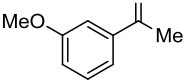
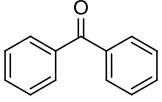
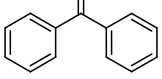
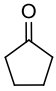

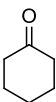
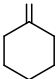
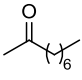
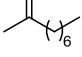
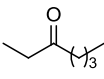
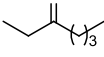
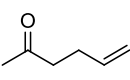
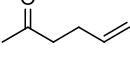


Scheme 4.3: Transfer hydrogenation of ketones catalyzed by complexes **15** and **16**.

Firstly, we decided to use acetophenone as model substrate and its reduction to 1-phenylethanol results to be catalyzed by both complexes, but only with complex **16** a good conversion was obtained (97 % after 4 hours, with a TOF of 38 h⁻¹), while with catalyst **15** the conversion was only 57 % in 14 hours, with a lower rate (TOF = 5.5 h⁻¹) (**Entries 1** and **2**). Under the same conditions, the catalyst loading was lowered to 0.2 mol%, but a very low conversion of acetophenone was obtained (< 10 % in 8 h); almost 0 % of conversion was obtained by further lowering the catalyst loading to 0.1 mol%.

Results and Discussion

Table 4.1: Catalytic transfer hydrogenations of ketones with complexes **15** and **16** (0.5 mol %) in the presence of NaOiPr (3 mol %).

| Entry | Ketone | Catalyst | Time (h) | Conversion (%) | TOF (h^{-1}) ^a |
|-----------|---|-----------|----------|----------------|-------------------------------|
| 1 |  | 15 | 14 | 54 | 6 |
| 2 |  | 16 | 4 | 97 | 38 |
| 3 |  | 15 | 5 | 86 | 50 |
| 4 |  | 16 | 4 | 99 | 30 |
| 5 |  | 15 | 16 | 99 | 13 |
| 6 |  | 16 | 12 | 95 | 16 |
| 7 |  | 15 | 8 | 99 | 9 |
| 8 |  | 16 | 3 | 98 | 50 |
| 9 |  | 15 | 4 | 99 | 61 |
| 10 |  | 16 | 0.67 | 100 | 170 |
| 11 |  | 15 | 12 | 22 | - |
| 12 |  | 16 | 12 | 99 | 25 |
| 13 |  | 15 | 8 | 5 | - |
| 14 |  | 16 | 12 | 98 | 13 |
| 15 |  | 15 | 10 | 86 | 17 |
| 16 |  | 16 | 6 | 96 | 40 |

^a The conversion and TOF (moles of ketone converted into alcohol per mole of catalyst per hour at 50 % conversion) were determined by GC analysis. Conditions: T = 82 °C, substrate 0.1 M in 2-propanol.

The scope of the reaction was broadened by a screening of alkyl aryl, diaryl, dialkyl and cyclic ketones as substrates, keeping the catalyst loading constant at 0.5 mol%. With 3-methoxyacetophenone, a complete conversion (99 %) in 4 hours was

achieved employing the complex **16**, with a TOF of 30 h^{-1} , whereas higher rate was observed with complex **15** (30 h^{-1}), but a lower final conversion was obtained (86 % after 5 hours) (**Entries 3 and 4**).

Using benzophenone as substrate a near complete conversion to benzhydrol was observed for both catalyst (95 % in 12 hours with **16**, 99 % in 16 hours with **15**), with comparable TOF values (16 h^{-1} for **16**, 13 h^{-1} for **15**), showing a lower activity employing this substrate with respect to the acetophenone substrates (**Entries 5 and 6**). The reduction of cyclopentanone into cyclopentanol was completed in 3 hours with complex **16** (98 %, TOF of 50 h^{-1}) and in 8 hours with **15** (99 %, TOF of 9 h^{-1}) (**Entries 7 and 8**). An even greater activity was observed for the conversion of cyclohexanone into cyclohexanol: a quantitative conversion (100 %) was obtained with **16** after 40 minutes (TOF of 170 h^{-1}), while a longer time is necessary with **15**, which achieved the complete conversion only after 4 hours (TOF of 61 h^{-1}) (**Entries 9 and 10**).

Good results were obtained with complex **16** also when employing aliphatic ketones: 2-nonanone and 3-heptanone were quantitatively converted to the corresponding alcohols (99 and 98 %, respectively) in 12 hours (**Entries 11 and 13**); with this two latter substrates, poor activity was observed for complex **15** (22 and 5 % of conversion after 12 and 8 hours, respectively; **Entries 12 and 14**). In order to further investigate the scope of the reaction, also an unsaturated ketone was employed as substrate: the chemoselective transformation of the carbonyl group of 5-hexen-2-one into 5-hexen-2-ol was complete with complex **16** in 6 hours (TOF of 40 h^{-1}), while the conversion with complex **15** reached 86 % in 10 hours (TOF = 17 h^{-1}) (**Entries 15 and 16**).

In absence of base complexes **15** and **16** are not catalytically active, suggesting that NaO*i*Pr is crucial for the formation of a Ir hydride species.^[123]

A possible mechanism of the transfer hydrogenation with these two complexes (**Figure 4.4**) involves the formation of the Ir isopropoxide species, by substitution of the chloride, which undergoes a β -hydrogen elimination, leading to the Ir hydride complex. Insertion of the ketone substrate into the Ir-H bond affords the Ir alkoxide,

which reacts with 2-propanol giving the alcohol product and the Ir isopropoxide that closes the cycle.^[55]

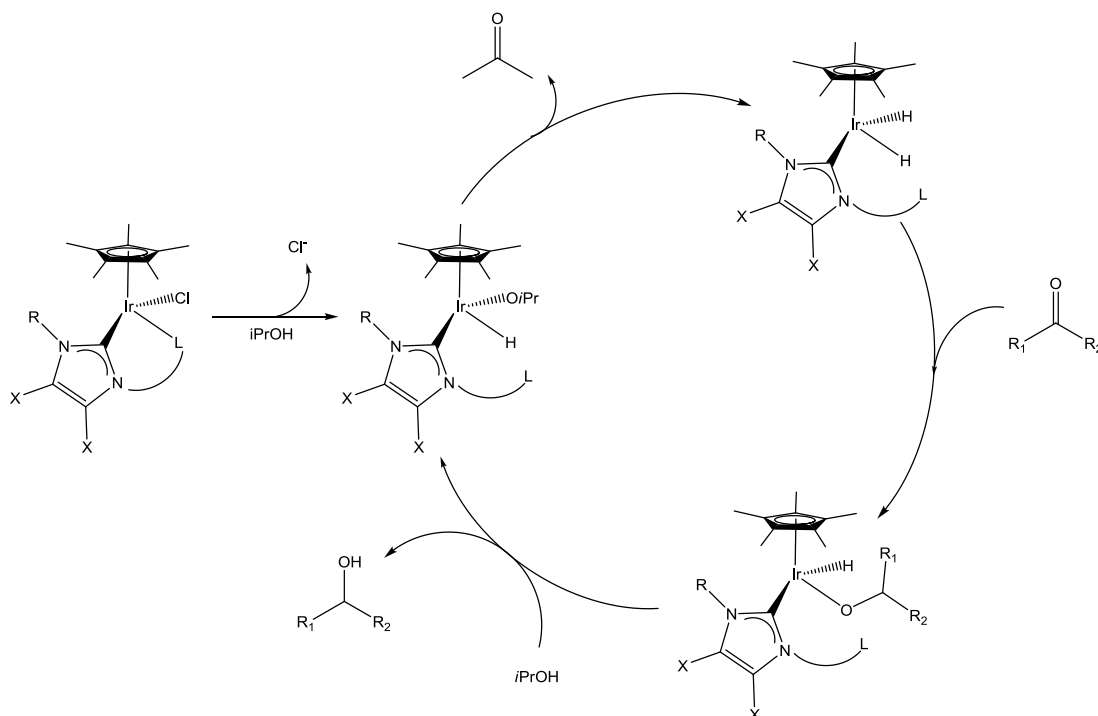


Figure 4.4: Proposed catalytic cycle for the transfer hydrogenation of ketones.

The higher activity of complex **16** with respect to complex **15** is likely due to the generation of a *cis* vacant site by displacement of the pyridine ligand, allowing an *inner sphere* mechanism.^[124] It is worth noting that an easy β -hydrogen elimination in 18-electron alkoxide Ir(III) complexes has been described by Blum and Milstein.^[125]

The superior catalytic activity of complex **16** than that observed for complex **15** may be further justified considering the different overall charge on the complexes: it is indeed well known that different charge may have great effects on the catalytic behaviour of a catalyst; complex **16** is dicationic, while **15** is neutral.

As mentioned previously in this chapter and in **Section 1.4.2**, a number of Ir(III)-NHC complexes were successfully employed as catalysts for such reactions. The results obtained employing **16** can be compared with those obtained by Crabtree and co-

worker with similar imidazol-2-ylidene based complexes bearing a pyridine or a pyrimidine pendant group, which coordinate in chelating fashion (**Figure 4.3**).^[56] With such complexes, the reduction reaction of acetophenone employing [Ir] 1 mol%, KOH (10 %) as base and 2-propanol as hydrogen-source, were obtained 98 and 86 % of conversion, respectively, in 3 hours (TOF of 33 and 29 h⁻¹). Such results can be considered very similar to those obtained with complex **16** (97 % of conversion in 4 hours, TOF of 38 h⁻¹).

The reported conversions of cyclohexanone with the same complexes (figura, richiamo ai numeri) are 90 and 94 %, respectively, in 6 hours, which means TOF values of 15 and 16 h⁻¹. With the same substrate complex **16** showed a quantitative conversion after only 40 minutes, indicating a superior activity (TOF of 170 h⁻¹).

Peris and co-workers reported a series of mononuclear Ir(III) catalysts bearing monocarbene ligands, active for the base-free transfer hydrogenation of ketones (**Figure 4.5**).^[55]

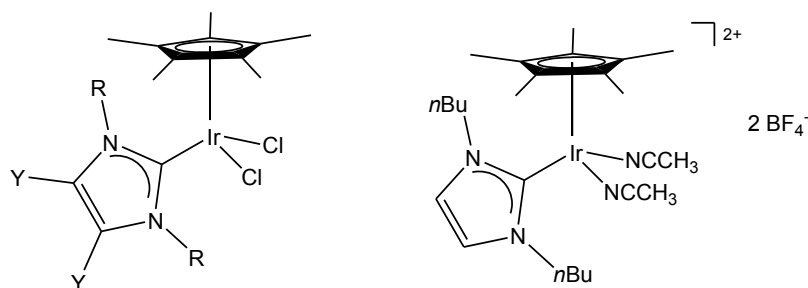


Figure 4.5: Iridium(III)-NHC complexes reported active as catalysts for base-free transfer hydrogenation reactions reported by Peris *et al.*

In their work they suggested that the strong electron-donating properties of the NHC ligand may favour the reaction with *i*PrOH, forming the complex [IrCp*(H)(O*i*Pr)(NHC)] which can be an intermediate of the catalytic cycle (see also **Figure 4.4**). In order to have some mechanistic insight of the reaction catalyzed by the complexes **15** and **16**, the pre-formation and the isolation of a similar intermediate was attempted. Complex **15** was treated with NaO*i*Pr in 2-propanol,

Results and Discussion

under conditions miming the catalytic reaction. After a variable period of stirring (1-2 hours), the darkened mixture were filtered and the product was analyzed via ^1H NMR spectroscopy, but unfortunately, no hydride signal was observed.

Chapter 5: RESULTS AND DISCUSSION

REACTIVITY AND COORDINATION PROPERTIES OF *NON-CLASSICAL* CARBENES

5.1 Studies on the synthesis and reactivity of expanded ring carbenes

As mentioned in **Chapter 1** and then demonstrated during this PhD studies (**Chapter 2**), the electron-donor ability of a N-heterocyclic carbene ligand is strongly influenced by the employed azole ring. The research on the properties and applications of NHC ligands has been mainly focused on five-membered N-heterocyclic-based carbenes (imidazole, benzimidazole, imidazoline,...). During the last years, the studies on these ligands have been extended also to the so-called “expanded ring” N-heterocyclic carbenes, which are based on six-, seven- and eight-membered saturated rings. The number of transition metal complexes bearing these ligands is quite limited, especially if compared to the five-membered analogues.

Actually, the first palladium complex bearing a pincer six-membered NHC was reported by Matsumura *et al.* in 1995,^[126] but the first six-membered saturated free carbene (1,3-diisopropyl-4,5,6-hexahydropyrimidin-2-ylidene) was reported only four years later by Alder *et al.*,^[127] who obtained such species by deprotonating the tetrafluoroborate salt precursor using sodium bis(trimethylsilyl)amide (NaHDMS) as base.

Several tetrahydropyridinium salts and the derived free carbenes have been reported by the groups of Buchmeiser, Herrmann and Cavell,^[128,129,130,131,132,133,134,135] who synthesized also the corresponding metal complexes (Ru(II), Rh(I), Ir(I), Ni(I,II), Pd(0, II), Pt(II), Cu(I), Ag(I) and Au(I)); successively, also complexes of rhodium(I), iridium(I), nickel(II), palladium(II), silver(I) with seven- and eight-membered NHC rings were obtained.^[130,132,133,136]

Some examples of known complexes are reported in **Figure 5.1**.

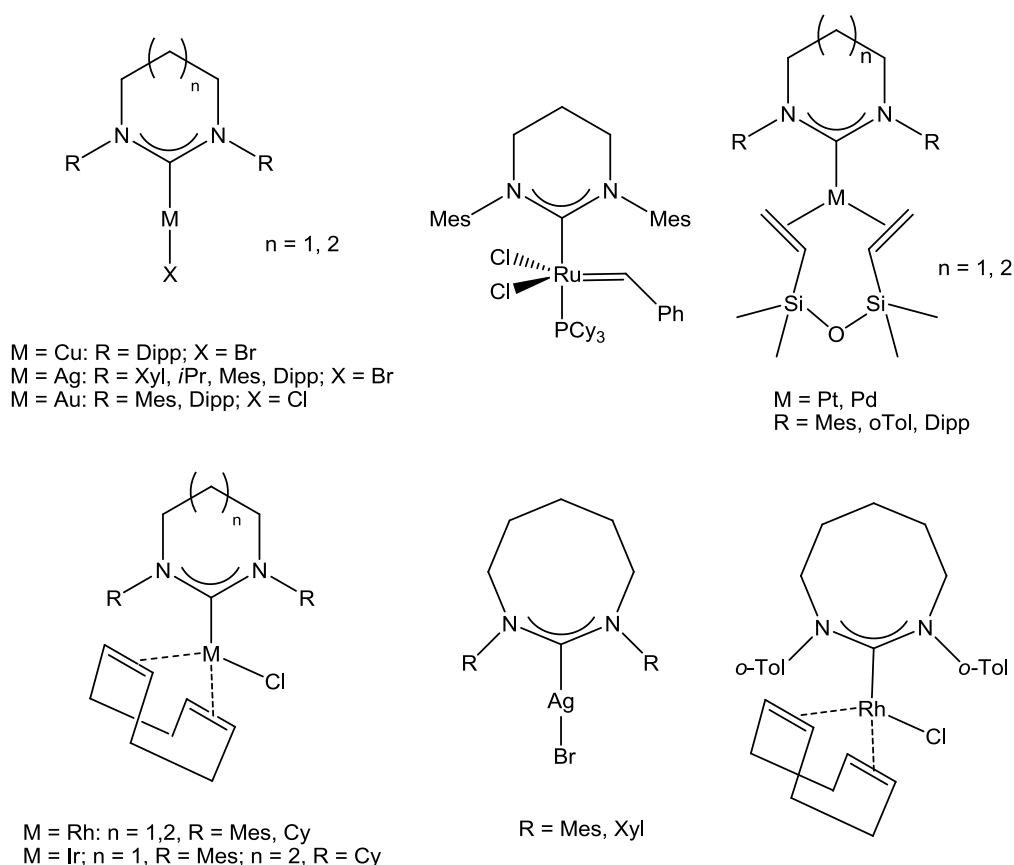


Figure 5.1: Metal complexes bearing saturated expanded ring NHCs reported in the literature.

The stereo-electronic properties of these ligands have been well studied:^[25] the expanded saturated ring NHCs are more basic than the five-membered analogues. The crystal structures, both of the free carbenes and the resulting complexes, have been useful to clarify the steric properties of these new carbenes; the N-C-N bond angle is larger than 120° and furthermore, in contrast to the imidazol-2-ylidene carbenes, the six-, seven- or eight-membered rings are not planar. These ligands adopt therefore a distorted structure in order to alleviate the constraints between the heterocyclic framework and the N-substituents, and as a result they are considered very encumbered ligands. As a general consideration, a ligand characterised by such steric hindrance is very interesting for possible catalytic applications, because it can both provide a sterical protection to the metal centre and favour, for steric reasons, the reductive elimination of the products during a catalytic cycle. Some of the cited complexes were indeed successfully employed as

catalyst for several organic transformations, like hydrogenation, transfer hydrogenation, hydrosilylation reactions, Heck-type C-C coupling and many other.

During the last year of this PhD project, in the frame of a collaboration with Prof. Connelis J. Elsevier (Van't Hoff Institute of Molecular Sciences - University of Amsterdam), the coordination ability of six-membered saturated NHC ligands (pyrimidine-based, as shown in **Figure 5.2**) toward iridium(III) centre was explored; it can be anticipated that these experiments were unsuccessful and no iridium(III) complexes have been isolated.

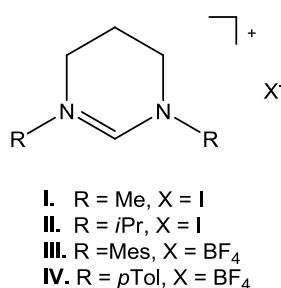


Figure 5.2: Ligand precursors employed in this part of the work.

The ligand precursors were readily synthesized under mild basic conditions, by reacting the corresponding *N,N'*-disubstituted diamidine with 1,3-diiodopropane in refluxing acetonitrile. In the case of the ligand precursors **III** and **IV**, a quantitative metathesis of the iodide ions with tetrafluoroborate ones was carried out, by treatment of the iodide salt with a slight excess of NaBF₄.

In order to synthesize novel iridium(III) complexes bearing the described ligands, several attempts were performed. A well-established two steps synthetic procedure was initially explored:

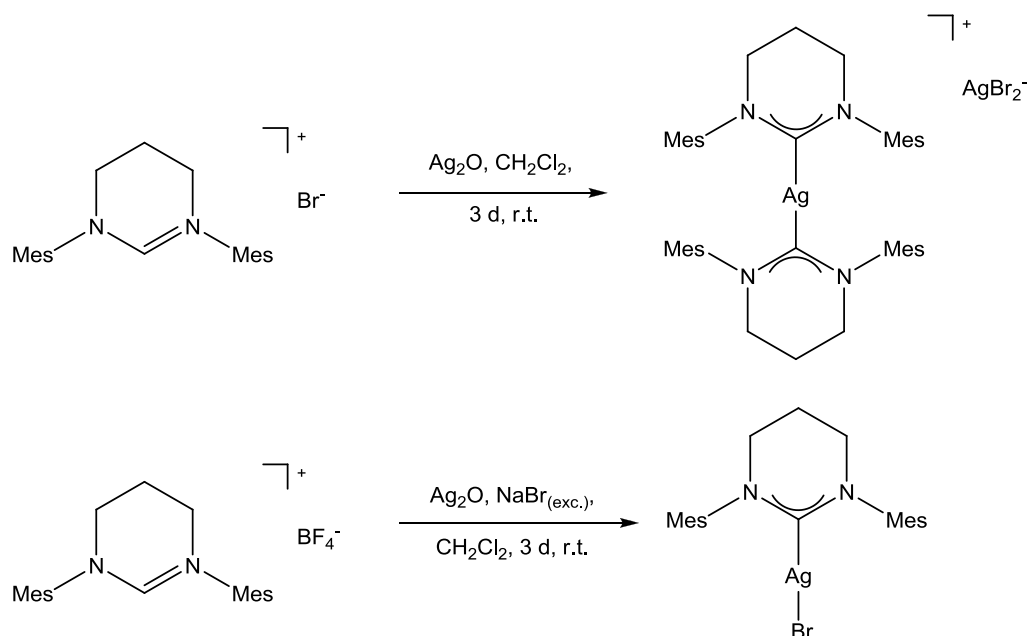
- i] pre-formation of the free carbene by treating the salt precursor with potassium bis(trimethylsilyl)amide (KHDMS, solid, stored in glove-box);
- ii] filtration through Celite® of the mixture obtained at point i), directly in an iridium(III) precursor solution.

Results and Discussion

Using salts **I** and **II**, the isolated solids were the unreacted starting materials. Since the free carbene deriving from the salt **II** was obtained by Buchmeiser *et al.* following a similar procedure,^[128] it is reasonable to believe that a re-protonation of the free carbene occurred within the frame of the second step of the synthesis.

The same procedure was carried out also employing the salts **III** and **IV**, both with ratio ligand/iridium 1:1 and 2:1. In all the experiments the addition of the free carbene solution to the iridium(III) precursor solution led to a progressive darkening of the reaction mixture (until dark brown); however, it was impossible to isolate and identify a unique species from the solid mixture.

Since the results obtained with the direct reaction between the pre-formed free carbene and the iridium(III) precursor were not satisfactory, the transmetalation route of the NHC moiety from the silver(I) complex was attempted. The synthesis of the silver(I) complexes bearing the ligand 1,3-dimesityl-4,5,6-hexahydropyrimidin-2-ylidene was reported both by the groups of Buchmeiser and Cavell, and the proposed procedures are summarized in the **Scheme 5.1**.^[128,130]



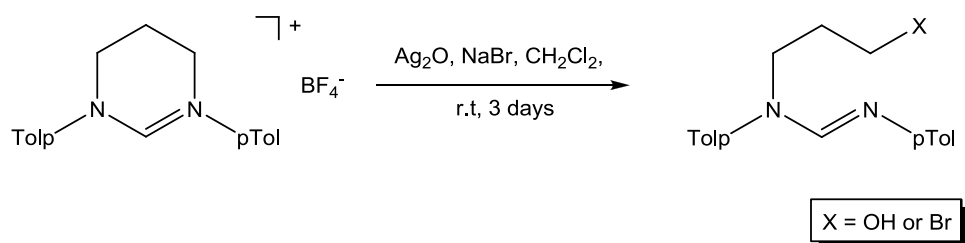
Scheme 5.1: Synthesis of silver(I) complexes bearing the 1,3-dimesityl-4,5,6-hexahydropyrimidin-2-ylidene ligand proposed by Buchmeiser *et al.* (top) and Cavell *et al.* (bottom).

The two synthetic procedures are very similar: in the procedure adopted by Buchmeiser *et al.*, the starting precursor is a bromide salt and the reaction leads to the formation of a cationic bis(NHC) silver(I) complex; instead, in the synthetic procedure proposed by Cavell *et al.* the product is a neutral mono-NHC silver(I) complex, the reaction is carried out in the presence of a slight excess of NaBr, starting from the tetrafluoroborate salt precursor of the NHC ligand.

Starting from the salt **III**, which bears tetrafluoroborate as counterion, we adopted the synthetic procedure proposed by Cavell and co-workers. The ^1H NMR spectrum of the isolated solid shows two set of signals, relative to the cationic complex $[\text{Ag}(\text{NHC})_2](\text{AgBr}_2)$ and the neutral one $[\text{AgBr}(\text{NHC})]$ in a 4:1.4 ratio respectively.

With such silver(I) complexes mixture, the transmetalation of the NHC moiety at room temperature was carried out, but unfortunately none of the attempts allow to obtain an Ir(III) complex: in all the experiments, the isolated solid was the starting Ag(I) material. On the other hand, by performing the same reaction at 50 °C, the quantitative re-protonation of the NHC ligand occurs. The whole of these results confirm the difficulties, already observed and reported in the literature, for the transfer of these ligands.^[25]

The same synthetic procedure described by Cavell *et al.* was performed also with salt **IV**, with the p-tolyl substituents, but, in this case, no silver complex has been isolated; a different product was instead obtained, resulting from the C-N bond cleavage (**Scheme 5.2**). The ^1H NMR spectrum of such product presents a high number of signals and this is ascribable to a species which has not retained the symmetric starting structure; furthermore, it is still present a signal at high ppm (8.35 ppm), relative to the C₂-proton and close to the same signal in the starting precursor.



Scheme 5.2: Reaction of salt **IV** with silver(I) oxide.

Concomitantly to the described work on mono-NHC ligands, also the properties of di-NHC ligands derived from analogues units were studied; the ligand precursors taken into account are reported in **Figure 5.3**.

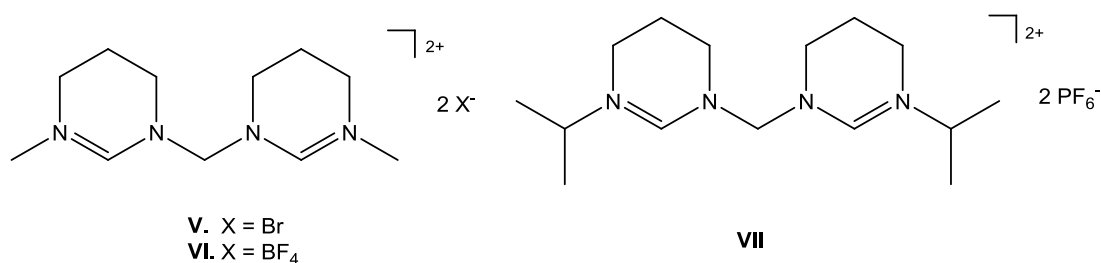


Figure 5.3: Expanded ring di-NHC ligand precursors

It is worth to note that no examples of isolated complexes bearing such di-NHC ligands have been reported so far, and to date similar ligand precursors were only employed as precursor to form *in situ* palladium(II) complexes as catalysts for Suzuki-Miyaura cross-coupling reaction.^[137]

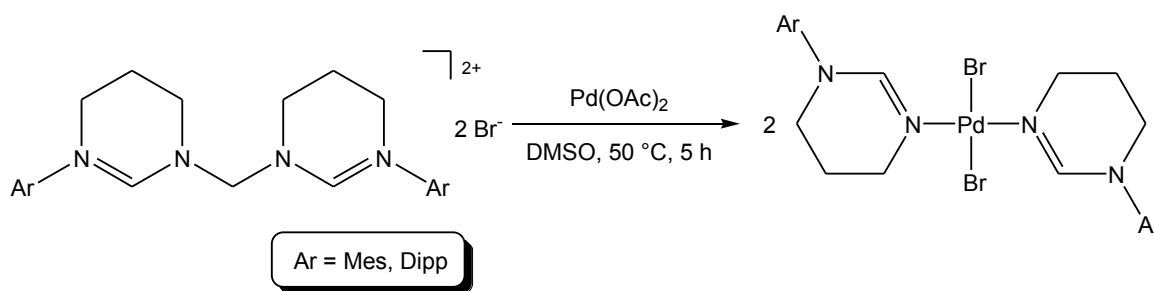
The ligand precursors can be readily synthesized by coupling reaction of two 1-alkyl-2,4,5,6-tetrahydropyrimidine with dibromomethane in DMF at room temperature. The resulting dibromide salts are highly hygroscopic and for this reason the salts **VI** and **VII** were synthesized by anion metathesis (Br⁻/BF₄⁻ for **VI** and Br⁻/PF₆⁻ for **VII**).

Several attempts have been carried out with the aim of obtaining the corresponding NHC silver(I) complexes, but in all cases the NMR spectra of the isolated solid were characterized by several signals, difficult to assign to a single and unique product.

Since the silver route was not applicable, the direct reaction between the pre-formed free carbene (formed by deprotonating the ligand precursor with a base)

and the Ir(III) precursor was carried out. Several different bases and reaction conditions were used (see **Table 7.1** in **Chapter 7**), but unfortunately the results obtained were unsatisfactory

The whole of these results suggest that this type of salts are not very stable under the adopted reaction conditions; for example, in some cases the signal of the CH₂ protons of the bridge was missing upon the reaction. The instability of the methylene bridge between the heterocyclic units has been demonstrated also by Mao *et al.*; they studied the reaction reported in **Scheme 5.3** and they obtained a complex in which two imine ligands were coordinated to the palladium(II) centre rather than a dicarbene Pd(II) complex.^[138]



Scheme 5.3: Reaction of palladium acetate with an expanded ring di-NHC precursor.

5.2 Studies on the synthesis and reactivity of asymmetric mixed di(N-heterocyclic) carbenes

Nowadays, there is an increasing interest towards non-classical N-heterocyclic carbene ligands and in particular 1,3,4-trisubstituted-1,2,3-triazol-5-ylidenes; these carbenes are often referred to as “mesoionic” carbenes (MICs) because of their persistent charge separation, which does not allow to write a neutral resonance structure for these species (**Figure 5.4**).^[23]

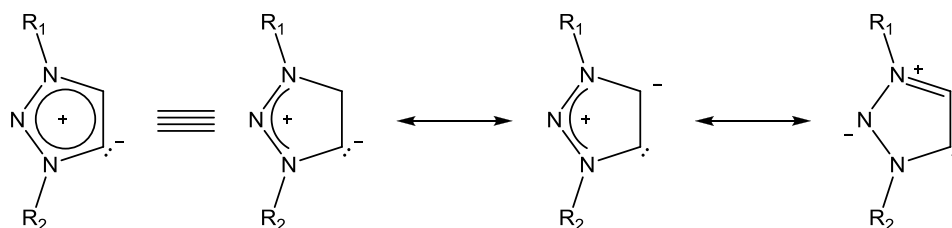


Figure 5.4: Resonance formula for a mesoionic carbene.

Actually, such charge separation is remarkably diminished by the delocalized aromatic system, and for this reason the coordination and electronic properties of MICs do not substantially differ from those of the more conventional 5-membered imidazol-2-ylidenes. In fact, they are singlet carbenes (due to the large singlet-triplet energy gap, which is around 230-250 KJ mol⁻¹), strong σ -donors and moderate π -acceptors. Mesoionic carbenes are stronger electron-donor ligands than imidazol-2-ylidenes, but weaker than the *abnormal* imidazol-4-ylidenes. The stereo-electronic properties of the mesoionic carbenes, as described in the case of the classical NHCs, can be finely tuned by changing the C₄- and the N₁,N₃-substituents. An advantage of such class of carbenes is represented by the minimized dimerization reaction to form the corresponding olefines, probably due to the electrostatic repulsion resulting from the anionic character of the carbene carbon.

The synthetic procedure for the obtainment of the ligand precursor is composed by two-steps.^[20,22,57,139] i] the copper(I)-catalyzed 1,3-cycloaddition of terminal alkynes with organic azide (the so-called CuAAC “click” reaction), forming the corresponding 1,4-disubstitued-1,2,3-triazole; ii] the regioselective quaternization of the N₃-position of the triazole ring with an aryl- or alkyl-substituent. As regard the synthesis of the metal complexes, the most widely used procedures are: i] the pre-formation of the free carbene by treating the salt precursor with a base (KHDMS, KOtBu), followed by the direct reaction with the metal precursor; ii] the transmetalation of the MIC moiety from the corresponding silver(I) complex.

Despite the chemistry of such category of ligands is very recent, a large number of MIC-metal complexes was reported so far, employing Ru, Rh, Ir, Pd, Cu, Ag, and Au,

and some of the obtained complexes have been successfully employed as catalysts in several catalytic reaction (C-C cross-coupling, transfer hydrogenation, water oxidation reaction,...).^[22]

Very recently, a new class of unsymmetrical dicarbene ligand precursors was published by Cowie *et al.*: the derived ligands are heteroditopic di-NHC in which the two carbene units, one is a classical imidazol-2-ylidene and the other a triazol-5-ylidene, are connected by an alkyl bridge;^[140] exploiting the different acidity of the two heterocyclic rings, it was also possible to obtain heterobimetallic Pd(II)/Rh(I) complexes (**Figure 5.5**).

Very recently, similar ligand precursors were successfully employed by Elsevier for the obtainment of novel mononuclear rhodium(I) and iridium(I) complexes, with the ligand coordinated to the metal in a chelating fashion (**Figure 5.5**).^[141]

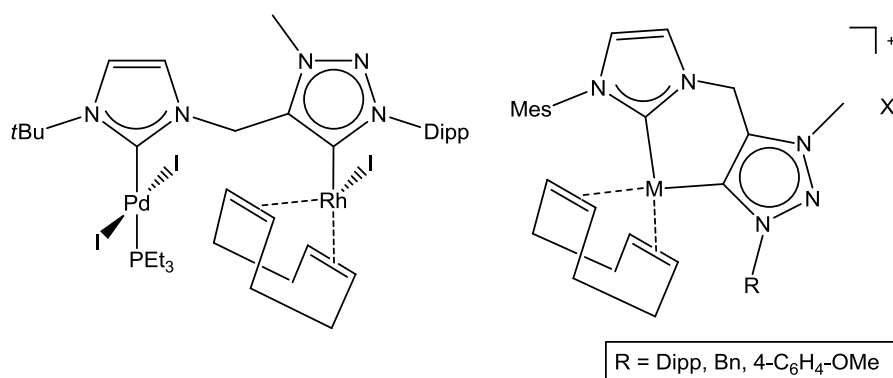
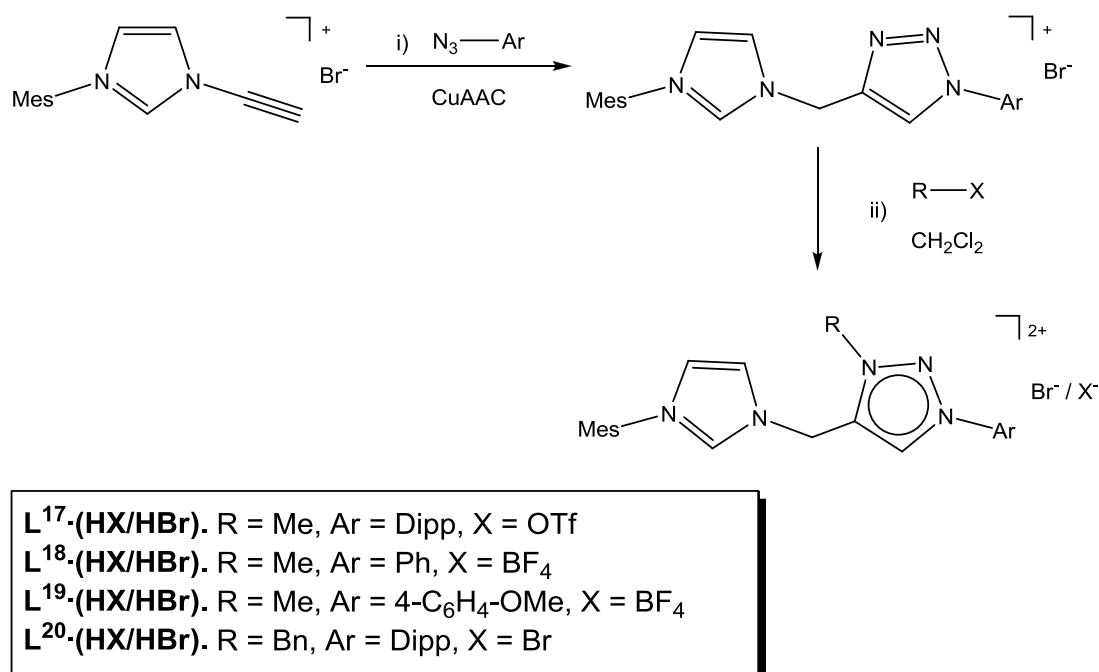


Figure 5.5: Metal complexes with unsymmetrical dicarbene ligand reported by Cowie (on the left) and Elsevier (on the right).

During the period spent at University of Amsterdam in Prof. Elsevier research group, the library of NHC-MIC ligands was extended; in particular, the ligand precursors **Lⁿ·(HX/HBr)** (n=17-20) were obtained with a two-step procedure (**Scheme 5.4**): i] CuAAC reaction starting from [(1-(prop-2-ynyl)-3-mesityl)imidazolium] bromide and the desired aryl-azide; ii] quaternization of the triazole ring by treatment with R-X.

Results and Discussion



Scheme 5.4: Synthesis of the NHC-MIC ligand precursors.

The copper(I)-catalyzed [3+2] cycloaddition reaction exhibits a good tolerance to the different aryl groups used, and the coupling products were obtained in high yields.

Methyl triflate or trimethyloxonium tetrafluoroborate were used to quaternize the nitrogen atom in 1 position, since it is reported that simple methyl iodide is not a sufficiently strong alkylating agent.^[141] The quaternization of N₁-triazole position with the benzyl group (precursor **L²⁰**) was performed by reaction with neat benzyl bromide at 110 °C for 24 hours. The obtained salts have mixed counteranions (Br⁻/OTf⁻ or Br⁻/BF₄⁻); by treating **L¹⁷·(HOTf/HBr)** with a slight excess of NH₄PF₆ (aqueous solution) for 1 hour under stirring, it was possible to isolate the corresponding bis(hexafluorophosphate) NHC-MIC salt precursor.

In order to evaluate the coordination properties toward the Ir(III) centre, two synthetic methods have been evaluated:

- The *in situ* reaction between the ligand and the metal precursor, in presence of a base (Cs₂CO₃);

- ii. The transmetalation of the NHC-MIC moiety from silver(I) to iridium(III).

It can be anticipated, that interesting results have been obtained, although they should be considered only preliminar and need to be further investigate in the future.

By reaction of the precursor $L^{17} \cdot (HOTf/HBr)$ with $[IrCl_2Cp^*]_2$ in the presence of an excess of Cs_2CO_3 (ca. 5 equivalents), in acetone at 30 °C for 48 h, it was possible to observe the disappearance of the signal attributable to the C₂-proton of the imidazole ring. This may be associated to the formation of a Ir(III) complex (**Figure 5.6**), in which only the imidazole-2-ylidene is coordinated to the iridium(III) centre, while the triazole ring remains protonated.

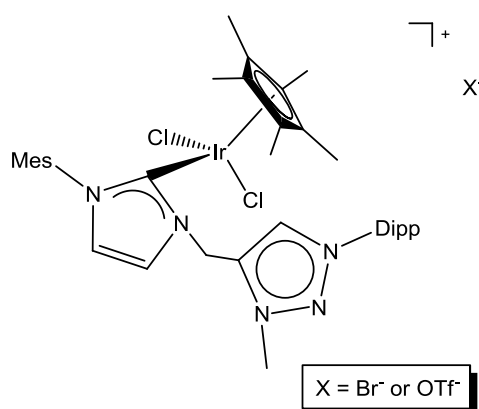
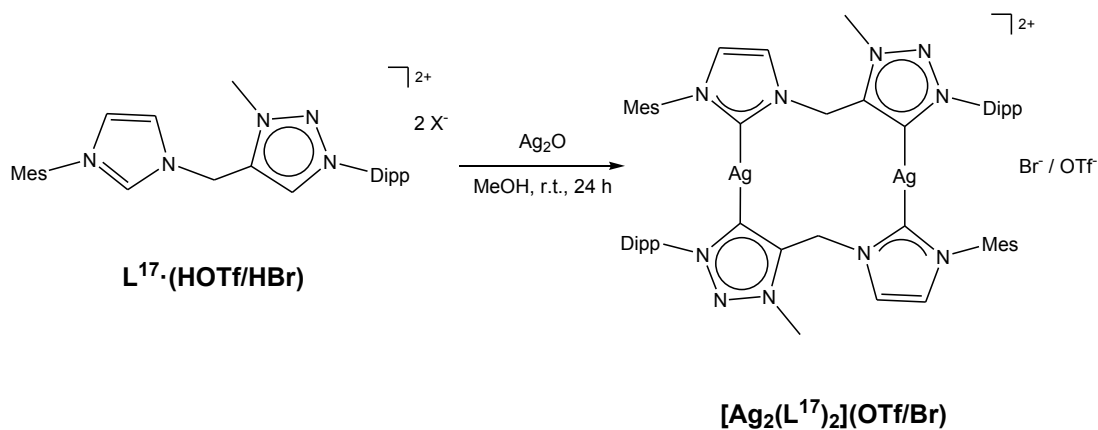


Figure 5.6: Possible reaction product, obtained in the reaction of the precursor $L^{17} \cdot (HOTf/HBr)$ with $[IrCl_2Cp^*]_2$ in the presence of an excess of Cs_2CO_3 .

This result is not surprising, because of the higher acidity of the imidazole C₂-H proton with respect to the triazole one and, moreover, similar results were observed by Cowie *et al.* during the synthesis of palladium complexes.^[140]

Finally, also the transmetalation method has been explored. The reaction conditions for the synthesis of the NHC-MIC silver(I) complexes have been optimized with the salt $L^{17} \cdot (HOTf/HBr)$. The reaction of $L^{17} \cdot (HOTf/HBr)$ with Ag_2O in acetonitrile at 60 °C for 24 hours affords the desired product, although with a low purity. The pure

silver(I) complex $[\text{Ag}_2(\text{L}^{17})_2](\text{Br}/\text{OTf})$ was obtained under milder conditions, carrying out the reaction between the salt $\text{L}^{17}\cdot(\text{HOTf}/\text{HBr})$ and an excess of Ag_2O (ca. 6 equivalents) in methanol at room temperature for 24 hours (**Scheme 5.5**).

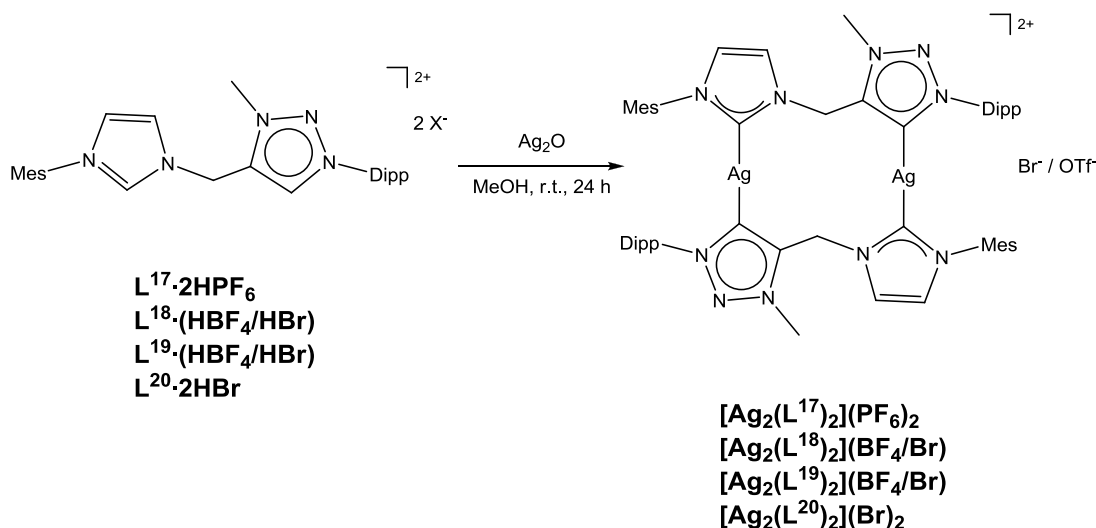


Scheme 5.5: Synthesis of the silver(I) complex $[\text{Ag}_2(\text{L}^{17})_2](\text{OTf}/\text{Br})$.

The formation of the silver(I) complex is confirmed, in the ^1H NMR of the isolated solid, by the lack of the signals at high ppm (9.65 and 9.35 ppm) ascribable to the protons in 2 position of the imidazole ring and in 5 position of the triazole ring. Moreover, the methylene bridge signal is an AB system, suggesting an increased rigidity due to the coordination of the ligand to two silver(I) centres; the same signal in the ligand precursor is in fact a singlet.

Under the described optimized conditions, also the silver(I) complexes bearing the mixed NHC-MIC dicarbene ligands L^{18} , L^{19} and L^{20} were obtained. In all cases, the lack of the signals at high ppm in the ^1H NMR spectra was considered diagnostic to confirm the formation of the corresponding silver(I) complexes.

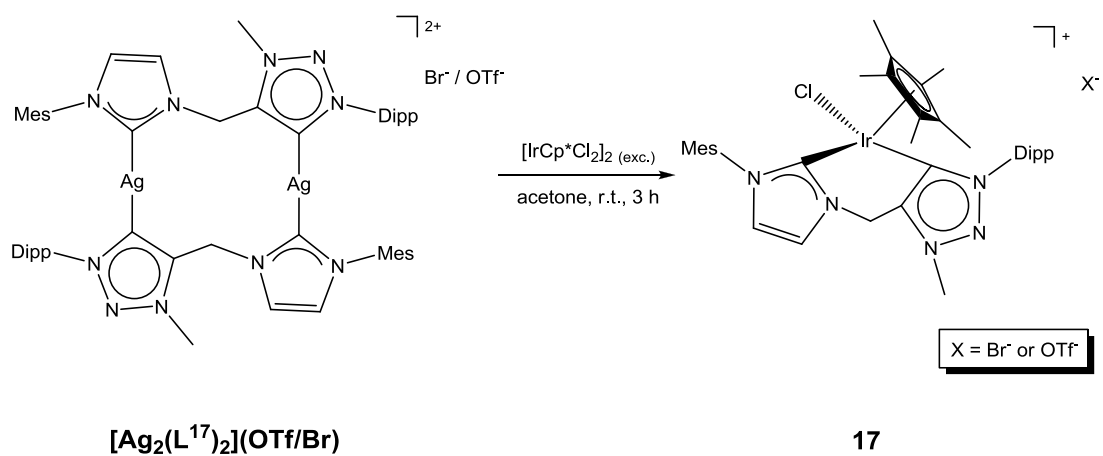
The dinuclear nature of the silver complexes has been assessed by the ESI-MS spectra of the complexes $[\text{Ag}_2(\text{L}^{17})_2](\text{PF}_6)_2$ and $[\text{Ag}_2(\text{L}^{18})_2](\text{BF}_4)(\text{Br})$; the main peak corresponds in both cases to the fragment $[\text{Ag}_2(\text{L})_2(\text{X})]^+$ (1243 m/z and $\text{X} = \text{PF}_6$ for L^{17} , 1017 m/z and $\text{X} = \text{BF}_4$ for L^{18}).



Scheme 5.6: Synthesis of the silver(I) complexes bearing the NHC-MIC ligands L^n ($n = 17 - 20$).

Unfortunately, the synthesized silver(I) complexes are unstable; in fact, they are very sensitive to air, moisture and light, and they decompose in few days even stored under inert atmosphere and exclusion of light.

The transmetalation of the NHC-MIC ligand from the silver(I) complexes to the iridium(III) precursor has been investigated via NMR-scale reaction. Preliminary results suggest that the transmetalation can be carried out successfully in acetone at room temperature within three hours. In fact, the 1H NMR spectrum of the reaction between the silver(I) complex $[Ag_2(L^{17})_2](OTf/Br)$ and the iridium(III) precursor $[IrCl_2Cp^*]_2$, presents a single set of signals similar to the one ascribable to the starting silver(I) complex, although slightly upfielded. Particularly diagnostic for the formation of the iridium(III) complex **17** is the AB system relative to the protons of the methylene bridge, which becomes larger, thus suggesting a more rigid structure of the ligand. This may be ascribable to a possible chelating coordination of the NHC-MIC ligand.

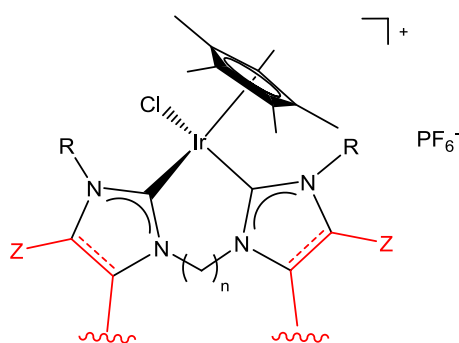


Scheme 5.7: Transmetalation from the silver(I) complex $[Ag_2(L^{17})_2](OTf/Br)$ and the iridium(III) precursor $[IrCl_2Cp^*]_2$.

Chapter 6: CONCLUSIONS

In the present research activity, the coordination properties of di-(N-heterocyclic) carbene ligands have been explored and it has been further demonstrated their ability to bind transition metal centres, in this particular project iridium(III), and their capacity to stabilize active catalytic species.

A library of diimidazolium salts has been employed as accessible precursor for di-(N-heterocyclic carbene) ligands, whose steric and electronic properties can be finely tuned by a proper choice of the ring substituents and the bridge between the carbene moieties. In frame of the project, a synthetic procedure for the synthesis of mononuclear iridium(III) complexes bearing a chelating di-NHC ligand has been optimized, and it follows the so-called “silver-route”, i.e. the transmetalation of the ligand from the corresponding dinuclear silver(I) complex. Following this procedure, several dinuclear silver(I) complexes bearing the di-NHC ligand in bridged fashion between two silver(I) centres, have been obtained. Successively, the step of transmetalation of the dicarbene moiety from the silver(I) to iridium(III) centre, using $[\text{IrCl}_2\text{Cp}^*]_2$ as metal precursor, affords generally the corresponding novel mononuclear Ir(III) complexes bearing a chelating di-NHC ligand. The synthesized complexes have been fully characterized in solution, by employing the classical investigative methods, as NMR spectroscopy and mass measurements; in most of the cases, the characterization was accomplished by the obtaining of the X-ray crystal structure.



Conclusions

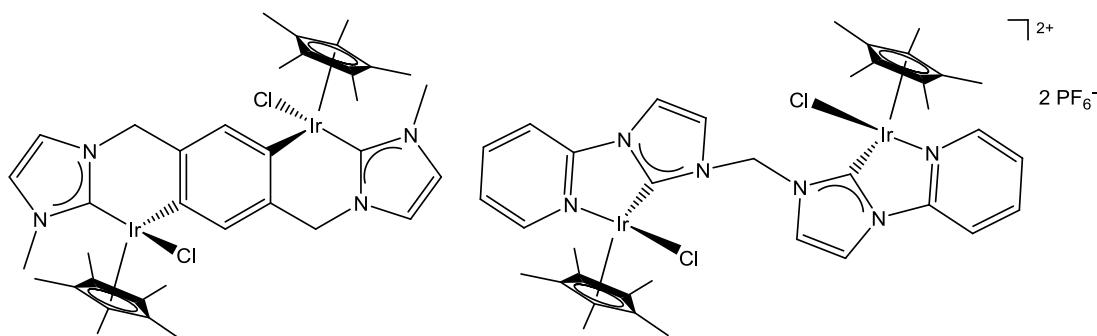
The influence of the ligand structure on the final stereo-electronic properties of the resulting complexes has been addressed, in particular via electrochemical measurements (cyclic voltammetry) and analysis of the carbene carbon chemical shift in the ^{13}C NMR spectra of the complexes. The larger effect on the electron density of the iridium(III) centre is provided by the changing of the N-heterocyclic ring, while the variation of the wingtip substituents seems to not affect significantly the electronic properties of the complex.

As a consequence of this similar electronic properties, the obtained complexes do not show a significant difference in the catalytic efficiency in the water oxidation reaction. The small observed differences could be ascribed mainly to steric effects. All the tested complexes are in fact active in presence of Ce(IV) (or in some cases NaIO_4) as sacrificial oxidant, and either the short- and the long-time activity may be considered satisfactory. Moreover, analyzing the linear correlation between the initial rate of evolving oxygen vs. the catalyst concentration it was possible to demonstrate a first order kinetic in the catalyst; this suggests that the active species has a molecular nature and that no iridium oxide nanoparticles are formed during the catalytic test.

In order to have some insight on the catalyst's fate under turnover conditions, several aspects have been taken into account, combining the catalytic tests with other experiments (for instance, following the catalytic reaction *via* GC-MS or UV-vis): formation of CO_2 in traces occurs concomitantly to oxygen evolution, probably deriving by the partial oxidative decomposition of the Cp^* ligand.

Complex **2** was also active as catalyst in the photo-driven water oxidation, coupled with a photosensitizer ($[\text{Ru}(\text{bpy})_3]^{2+}$) and a sacrificial acceptor of electrons ($\text{S}_2\text{O}_8^{2-}$). The activity of complex **2** was compared with that of IrCl_3 , which is a well-known IrO_x nanoparticles precursor, thus indirectly demonstrating the different nature of the active species. Moreover, through EPR measurements, the formation of an Ir(IV) species was detected, further confirming the molecular nature of the catalyst.

An other part of the work has concerned the synthesis of two dinuclear iridium(III) complexes with the di(N-heterocyclic carbene) ligands bridging two IrCp* fragments and reported in the following figure. The crystal structure of complex **15** was obtained, establishing the ortho-metalation of the phenylene ring of the bridging group.



These last two complexes have been tested in transfer hydrogenation of ketones, showing a good activity for a wide scope of substrates. Such results may be considered promising for the employment of such class of complexes in the transfer hydrogenation of more challenging ketones and other unsaturated substrates or in other catalytic processes, for instance the Oppenauer-type oxidation of primary and secondary alcohols.

Finally, the reactivity and the coordination properties of non-classical carbene units have been evaluated. No satisfactory results have been obtained with saturated six-membered ring NHC precursors, probably because of the instability of the precursors and of strictly controlled required reaction conditions. Better results have been instead achieved in the synthesis and coordination properties of novel mixed NHC-MIC dicarbene ligands; the corresponding dinuclear dicarbene silver(I) complexes have been synthesized and preliminary results endorse the possibility to carry out the transmetalation reaction to give the corresponding Ir(III) complex. This latter results should be considered preliminary, but it appears promising since the employed ligands combine the properties of two different carbene units, and the

Conclusions

resulting Ir(III) complexes should present an asymmetrical structure, so they may be applied as catalysts in asymmetric organic transformation.

Chapter 7: EXPERIMENTAL SECTION

7.1 Materials and methods

All manipulations were carried out using standard Schlenk techniques under an atmosphere of argon or dinitrogen. The reagents were purchased by Aldrich as high-purity products and generally used as received; all solvents were used as received as technical grade solvents.

Elemental analysis were carried out by the microanalytical laboratory in the Department of Chemical Sciences (University of Padova) with a Fisons EA 1108 CHNS-O apparatus.

NMR Spectroscopy: NMR spectra were recorded on a Bruker Avance 300 MHz or a Varian Mercury 300 MHz (300.1 MHz for ^1H , 75.5 MHz for ^{13}C and 125.5 MHz for ^{31}P) spectrometers. The chemical shifts (δ) are reported in units of ppm relative to the residual solvent signals and the coupling constants are reported in Hertz (Hz). Multiplicity of the signals are reported with the following abbreviations: s (singlet), d (doublet), t (triplet), q (quartet), quint (quintet), m (multiplet) and br (broad signal).

Mass spectrometry: ESI-MS were recorded with an Agilent LC/MSD Trap SL spectrometer at a capillary potential of 1500 V or using a LCQ-Duo (Thermo-Finnigan) operating in positive ion mode. Instrumental parameters for the LCQ-Duo: capillary voltage 10 V, spray voltage 4.5 kV; capillary temperature 200 °C; mass scan range from 150 to 2000 amu; N_2 was used as sheath gas; the He pressure inside the trap was kept constant. The pressure directly read by an ion gauge (in the absence of the N_2 stream) was 1.33×10^{-5} Torr. Sample solutions were prepared by dissolving the compounds in acetonitrile and directly infused into the ESI source by a syringe pump at 8 $\mu\text{L}/\text{min}$ flow rate. **MALDI-TOF MS** analyses were performed with an AB-SCIEX 4800 TOF-TOF spectrometer.

Electrochemistry: Cyclic voltammetry experiments were performed by using a BAS EC-epsilon potentiostat. A standard three-electrode electrochemical cell was used. Potentials were referenced to an Ag/AgCl/3 M NaCl, reference electrode. A glassy

Experimental Section

carbon electrode (3 mm diameter, geometric surface area: 7 mm²) from BAS and a Pt wire were used, respectively, as working and auxiliary electrode.

EPR Spectroscopy: X-band continuous-wave EPR spectra were recorded with a Bruker ELEXSYS E580 spectrometer equipped with an ER4102ST cavity operating at 9.38 GHz. Cryogenic temperatures were achieved by using a liquid helium flow cryostat (Oxford Instruments ESR-900) driven by a temperature controller (Oxford Instruments ITC503). The experimental conditions were the following: $T = 10$ K, non-saturating microwave power: 2 mW, modulation amplitude: 10 G, conversion time: 81.92 ms and time constant: 163.84 ms. Simulations of the CW EPR spectra, to obtain the g -tensor principal components, were performed by using the Easyspin^[142] routine in Matlab®; g values were estimated by calibration using a sample of strong pitch.

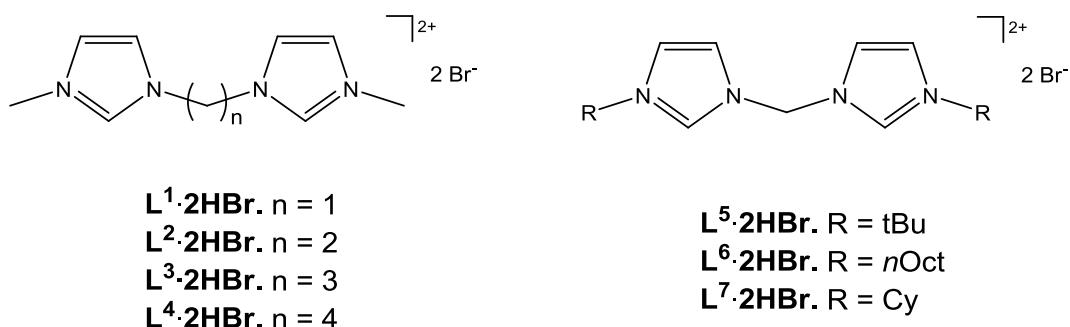
Fluorimetric analyses were performed with a Perkin–Elmer LS50B instrument with 1 cm quartz cell.

Dynamic light scattering was performed with a Malvern Zetasizer Nano-S instrument.

7.2 Synthesis of the dimeric iridium(III) precursor [IrCl₂Cp*]₂

The iridium(III) precursor was prepared according to a literature procedure^[143]: IrCl₃·nH₂O (1.5 mmol) and 1,2,3,4,5-pentamethylcyclopentadiene were placed in a two-necked round bottom flask. Under inert atmosphere, CH₃OH (30 mL) was added and the mixture was refluxed for 48 hours, and then allowed to cool at room temperature. A first crop of product (orange solid) was collected by filtration. The filtrate solution was concentrated under reduced pressure and diethyl ether was added, leading to the precipitation of a second crop of product, collected by filtration. The two fractions of product were washed with diethyl ether and dried in vacuum. Yield 85 %.

¹H NMR (CD₃CN, 25 °C, ppm): $\delta = 1.60$ (s, 15H, CH₃).

7.3 Synthesis of the diimidazolium salts $L^1 \cdot 2HBr$ – $L^7 \cdot 2HBr$ 

The diimidazolium salts 1,1'-dimethyl-3,3'-methylenediimidazolium dibromide ($L^1 \cdot 2HBr$),^[144] 1,1'-dimethyl-3,3'-ethylenediimidazolium dibromide ($L^2 \cdot 2HBr$),^[145] 1,1'-dimethyl-3,3'-propylenediimidazolium dibromide ($L^3 \cdot 2HBr$),^[146] 1,1'-dimethyl-3,3'-butylenediimidazolium dibromide ($L^4 \cdot 2HBr$)^[146] and 1,1'-dicyclohexyl-3,3'-methylenediimidazolium dibromide ($L^7 \cdot 2HBr$)^[147] were prepared according to literature procedures. In the following section, only their 1H NMR spectra are reported.

1,1'-dimethyl-3,3'-methylenediimidazolium dibromide ($L^1 \cdot 2HBr$)

1H NMR (D_2O , 25 °C, ppm): $\delta = 3.88$ (s, 6H, CH_3), 6.62 (s, 2H, CH_2), 7.51 (d, $^3J = 1.5$ Hz, 2H, CH), 7.68 (d, $^3J = 1.5$ Hz, 2H, CH), signal of NCHN hydrogen not detected.

1,1'-dimethyl-3,3'-ethylenediimidazolium dibromide ($L^2 \cdot 2HBr$)

1H NMR ($dmsO-d_6$, 25 °C, ppm): $\delta = 3.83$ (s, 6H, CH_3), 4.74 (s, 4H, CH_2), 7.73 (br s, 4H, CH), 9.25 (s, 2H, NCHN).

1,1'-dimethyl-3,3'-propylenediimidazolium dibromide ($L^3 \cdot 2HBr$)

1H NMR (D_2O , 25 °C, ppm): $\delta = 2.34$ (m, 2H, CH_2), 3.73 (s, 6H, CH_3), 4.16 (t, 4H, $^3J = 9.9$ Hz, NCH_2), 7.30 (s, 2H, CH), 7.35 (s, 2H, CH), 8.62 (br, 2H, NCHN).

1,1'-dimethyl-3,3'-butylenediimidazolium dibromide (L⁴·2HBr)

¹H NMR (D₂O, 25 °C, ppm): δ = 1.94 (m, 4H, CH₂), 3.91 (s, 6H, CH₃), 4.28 (t, ³J = 7.3 Hz, 4H, NCH₂), 7.47 (s, 2H, CH), 7.50 (s, 2H, CH), 8.58 (s, 2H, NCHN).

1,1'-dicyclohexyl-3,3'-methylenediimidazolium dibromide (L⁷·2HBr)

¹H NMR (dmso-*d*₆, 25 °C, ppm): δ = 1.00 – 2.13 (m, 20H, CH₂), 4.37 (m, 2H, CH), 6.73 (s, 2H, CH₂), 8.03 (s, 2H, CH), 8.16 (s, 2H, CH), 9.77 (s, 2H, NCHN).

7.3.1 Synthesis of the diimidazolium salt 1,1'-di-*tert*-butyl-3,3'-methylenediimidazolium dibromide L⁵·2HBr

N-*tert*-butyl imidazole (4 mmol)^[101] and dibromomethane (2 mmol) were placed in a two-necked round bottom flask and heated to 100 °C for 24 hours in 1,4-dioxane. The mixture was then cooled to room temperature and filtered. The product (white solid) was washed with small portion of diethyl ether and dried at low pressure. The spectroscopic characterization data exactly matched those previously published.^[101]

¹H NMR (dmso-*d*₆, 25 °C, ppm): δ = 1.61 (s, 18H, CH₃), 6.65 (s, 2H, CH₂), 8.17 (br s, 4H, 2CH), 9.78 (s, 2H, NCHN).

7.3.2 Synthesis of the diimidazolium salt 1,1'-di-*n*-octyl-3,3'-methylenediimidazolium dibromide L⁶·2HBr

N-octyl imidazole was prepared following a literature procedure.^[148] 1-bromooctane (5.18 mL, 30 mmol) and THF (15 mL) were added to a solution of N-1*H*-imidazole (2.40, 10 mmol) in 2.9 mL aqueous NaOH (50%). The mixture was refluxed for 3 days, then cooled to room temperature. Solvent was removed in vacuum and the residue was dissolved in CH₂Cl₂, then washed with H₂O (3 x 15 mL). The organic layer was collected and dried over Na₂SO₄. The drying agent was filtered off, and the filtrate was concentrated in vacuum. The ¹H NMR spectrum of the product (yellow oil) corresponds to the one reported in literature.

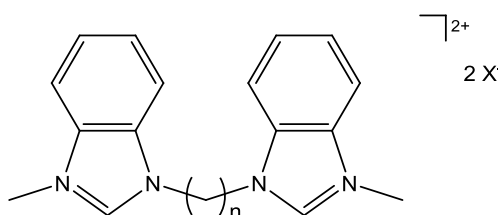
^1H NMR (CDCl_3 , 25 °C, ppm): δ = 0.88 (t, 3J = 7.0 Hz, 3H, CH_3), 1.28 (m, 10H, CH_2), 1.76 (m, 2H, CH_2), 3.91 (t, 3J = 7.0 Hz, 2H, NCH_2), 6.90 (s, 1H, CH), 7.04 (s, 1H, CH), 7.45 (s, 1H, NCHN).

N-octyl imidazole (1.0 g, 5.5 mmol) and dibromomethane (0.2 mL, 2.8 mmol) were placed in a two-necked round bottom flask and heated to 110 °C for 24 hours in toluene. The mixture was then cooled to room temperature and the solvent was removed in vacuum, giving a white solid. Yield 15 %.

^1H NMR (CD_3CN , 25 °C, ppm): δ = 0.88 (s, 6H, CH_3), 1.28 (s, 20H, CH_2), 2.37 (s, 8H, CH_2), 4.17 (s, 4H, CH_2), 7.14 (s, 2H, CH), 7.45 (s, 2H, CH), 8.56 (s, 2H, CH_2), 10.52 (s, 2H, NCHN).

$^{13}\text{C}\{^1\text{H}\}$ NMR (CD_3CN , 25 °C, ppm): δ = 13.8 (CH_3), 20.0-33.0 (6CH_2), 50.7 (NCH_2), 57.4 (NCH_2N), 123.1 (CH), 123.3 (CH), 138.2 (NCHN).

7.4 Synthesis of the dibenzimidazolium salts $\text{L}^8 \cdot 2\text{HPF}_6$ and $\text{L}^9 \cdot 2\text{HBr}$



$\text{L}^8 \cdot 2\text{HX}$. $n = 1$, $\text{X} = \text{PF}_6$

$\text{L}^9 \cdot 2\text{HX}$. $n = 2$, $\text{X} = \text{Br}$

7.4.1 Synthesis of the dibenzimidazolium salt 1,1'-dimethyl-3,3'-methylenedibenzimidazolium bis(hexafluorophosphate) $\text{L}^8 \cdot 2\text{HPF}_6$

The diimidazolium salt 1,1'-dimethyl-3,3'-methylenedibenzimidazolium dibromide ($\text{L}^8 \cdot 2\text{HBr}$) was prepared according to literature procedures.^[149] Following it is reported only its ^1H NMR spectrum.

^1H NMR ($\text{dms}\text{-}d_6$, 25 °C, ppm): δ = 4.15 (s, 6H, CH_3), 7.50 (s, 2H, CH_2), 7.75 – 7.79 (m, 4H, Ar-H), 8.09 (d, 3J = 9.0 Hz, 2H, Ar-H), 8.40 (d, 3J = 9.0 Hz, 2H, Ar-H), 10.31 (s, 2H, NCHN).

Experimental Section

To a solution of **L⁸·2HBr** (0.87 g, 2 mmol) in deionised water (10 mL), an aqueous solution of NH_4PF_6 (0.52 g, 4.2 mmol) was added. After 30 minutes of stirring at room temperature, the product (white solid) was filtered off and dried in vacuum. Overall yield 75 %.

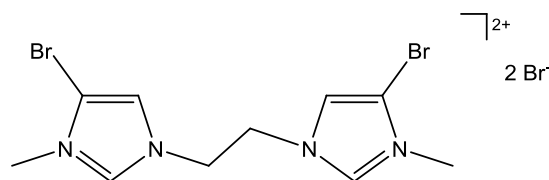
^1H NMR ($\text{dms}\text{-}d_6$, 25 °C, ppm): δ = 4.13 (s, 6H, CH_3), 7.39 (s, 2H, CH_2), 7.76 – 7.81 (m, 4H, Ar-H), 8.75 (d, 3J = 9.0 Hz, 2H, Ar-H), 8.30 (d, 3J = 9.0 Hz, 2H, Ar-H), 10.11 (s, 2H, NCHN).

7.4.2 Synthesis of the dibenzimidazolium salt **1,1'-dimethyl-3,3'-ethylenedibenzimidazolium dibromide L⁹·2HBr**

N-methyl benzimidazole (2.10 g, 16 mmol) and 1,2-dibromoethane (1.5 g, 8 mmol) were placed in a two-necked round bottom flask and heated to 120°C for 24 hours in 1,4-dioxane (20 mL). The mixture was then cooled to room temperature and filtered. The product (white solid) was washed with small portion of diethyl ether and dried at low pressure. Yield 81 %.

^1H NMR ($\text{dms}\text{-}d_6$, 25 °C, ppm): δ = 4.05 (s, 6H, CH_3), 5.11 (s, 4H, CH_2), 7.63 – 7.70 (m, 4H, Ar-H), 7.91 (d, 3J = 8.1 Hz, 2H, Ar-H), 8.03 (d, 3J = 8.1 Hz, 2H, Ar-H), 9.72 (s, 2H, NCHN).

7.5 Synthesis of the diimidazolium salt **1,1'-dimethyl-3,3'-ethylene-5,5'-dibromodiimidazolium dibromide L¹⁰·2HBr**



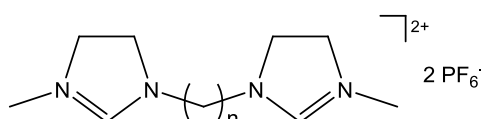
L¹⁰·2HBr

5-bromo-1-methyl-imidazole (0.64 g, 4 mmol) and 1,2-dibromoethane (0.38 g, 2 mmol) were placed in a two-necked round bottom flask and heated to 100°C for 24 hours in 1,4-dioxane (20 mL). The mixture was then cooled to room temperature

and filtered. The product (white solid) was washed with small portions of diethyl ether and dried at low pressure. Yield 73 %.

^1H NMR ($\text{dms}\text{-}d_6$, 25 °C, ppm): δ = 3.78 (s, 6H, CH_3), 4.68 (s, 4H, CH_2), 7.98 (s, 2H, CH), 9.23 (s, 2H, NCHN).

7.6 Synthesis of the diimidazolinium salts $\text{L}^{11}\cdot 2\text{HPF}_6$ and $\text{L}^{12}\cdot 2\text{HPF}_6$



7.6.1 Synthesis of the diimidazolinium salt 1,1'-dimethyl-3,3'-methylenediimidazolinium bis(hexafluorophosphate) $\text{L}^{11}\cdot 2\text{HPF}_6$

N-methyl imidizoline was prepared following a literature procedure.^[150] Following it is reported only its ^1H NMR spectrum.

^1H NMR (CDCl_3 , 25 °C, ppm): δ = 2.83 (s, 3H, CH_3), 3.15 (m, 2H, CH_2), 3.79 (m, 2H, CH_2), 6.75 (s, 2H, NCHN).

N-methyl imidazoline (1.00 g, 12 mmol) and dibromomethane (1.04 g, 6 mmol) were placed in a two-necked round bottom flask and heated to 100 °C for 24 hours in 1,4-dioxane (30 mL). The mixture was then cooled to room temperature and the solvent removed in vacuum. The product (brownish suspension) was dissolved in methanol (20 mL) and a solution of NH_4PF_6 (4.10 g, 25 mmol) in methanol (15 mL) was added. After 30 minutes of stirring a solution of diethyl ether/THF 3.5:1 was added and the product (brown solid) was filtered off; the residual solvent was removed from the product in vacuum. Overall yield 37 %.

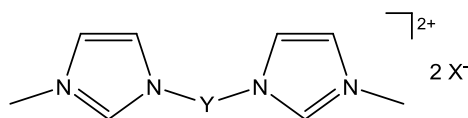
^1H NMR (CDCl_3 , 25 °C, ppm): δ = 3.17 (s, 6H, CH_3), 3.89 (m, 8H, CH_2), 4.97 (s, 2H, CH_2), 7.95 (s, 2H, NCHN).

7.6.2 Synthesis of the diimidazolium salt 1,1'-dimethyl-3,3'-ethylenediimidazolium bis(hexafluorophosphate) $L^{12} \cdot 2\text{HPF}_6$

N-methyl imidazoline (0.53 g, 6.3 mmol) and 1,2-dibromoethane (0.52 g, 3 mmol) were placed in a two-necked round bottom flask and heated to 100 °C for 24 hours in 1,4-dioxane (25 mL). The mixture was then cooled to room temperature and the solvent removed in vacuum. The product (brownish solid) was dissolved in methanol (15 mL) and a solution of NH_4PF_6 (2.12 g, 13 mmol) in methanol (10 mL) was added. After 30 minutes of stirring the mixture was filtered and the product (white solid) dried in vacuum. Overall yield 35 %.

^1H NMR (CD_3CN , 25 °C, ppm): $\delta = 3.11$ (s, 6H, CH_3), 3.87 (m, 12H, CH_2), 7.79 (s, 2H, NCHN).

7.7 Synthesis of the diimidazolium salts $L^{13} \cdot 2\text{HBr}$ - $L^{15} \cdot 2\text{HBr}$



$L^{13} \cdot 2\text{HPF}_6$. Y = *o*-xylylene
 $L^{14} \cdot 2\text{HBr}$. Y = *m*-xylylene
 $L^{15} \cdot 2\text{HBr}$. Y = *p*-xylylene

The diimidazolium salts 1,1'-dimethyl-3,3'-(*o*-xylylene)diimidazolium dibromide ($L^{13} \cdot 2\text{HBr}$),^[151] 1,1'-dimethyl-3,3'-(*m*-xylylene)diimidazolium dibromide ($L^{14} \cdot 2\text{HBr}$)^[151] and 1,1'-dimethyl-3,3'-(*p*-xylylene)diimidazolium dibromide ($L^{15} \cdot 2\text{HBr}$)^[152,46c] were prepared according to literature procedures. In the following section, only their ^1H NMR spectra are reported.

1,1'-dimethyl-3,3'-(*o*-xylylene)diimidazolium dibromide $L^{13} \cdot 2\text{HBr}$

^1H NMR ($\text{dms-}d_6$, 25 °C, ppm): $\delta = 3.83$ (s, 6H, CH_3), 5.62 (s, 4H, CH_2), 7.29 (m, 2H, Ar-*H*), 7.45 (m, 2H, Ar-*H*), 7.71 (s, 2H, CH), 7.74 (s, 2H, CH), 9.19 (s, 2H, NCHN).

1,1'-dimethyl-3,3'-(*m*-xylylene)diimidazolium dibromide L¹⁴·2HBr

¹H NMR (dms-*d*₆, 25 °C, ppm): δ = 3.90 (s, 6H, CH₃), 5.49 (s, 4H, CH₂), 7.45 – 7.86 (m, 8H, 2CH + Ar-H), 9.39 (s, 2H, NCHN).

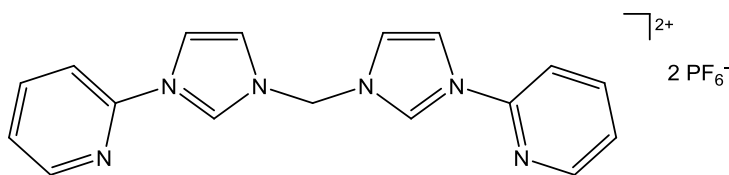
1,1'-dimethyl-3,3'-(*p*-xylylene)diimidazolium dibromide L¹⁵·2HBr

¹H NMR (dms-*d*₆, 25 °C, ppm): δ = 3.86 (s, 6H, CH₃), 5.49 (s, 4H, CH₂), 7.71 (m, 4H, Ar-H), 7.85 (m, 4H, Ar-H), 9.42 (s, 2H, NCHN).

7.7.1 Synthesis of the diimidazolium salt 1,1'-dimethyl-3,3'-(*o*-xylylene)diimidazolium bis(hexafluorophosphate) L¹³·2HPF₆

To an aqueous solution of L¹³·2HBr (0.87 g, 2 mmol in 10 mL) a solution of NH₄PF₆ (0.68 g, 4.2 mmol) in deionised water (5 mL) was added. After 30 minutes of stirring, the product (white solid) was filtered off and dried in vacuum. Yield <99 %.

¹H NMR (dms-*d*₆, 25 °C, ppm): δ = 3.81 (s, 6H, CH₃), 5.51 (s, 4H, CH₂), 7.27 (s, 2H, Ar-H), 7.45 (m, 2H, Ar-H), 7.63 (s, 2H, CH), 7.71 (s, 2H, CH), 9.02 (s, 2H, NCHN).

7.8 Synthesis of the diimidazolium salt 1,1'-di(2-pyridine)-3,3'-methylene diimidazolium bis(hexafluorophosphate) L¹⁶·2HPF₆**L¹⁶·2HPF₆**

2-(Imidazolyl)pyridine was prepared according to a literature procedure.^[100] 2-bromopyridine (0.34 g, 2.2 mmol), N-1*H*-imidazole (0.14 g, 2.0 mmol), copper iodide (0.04 g, 0.2 mmol), L-proline (0.05 g, 0.4 mmol) and K₂CO₃ (0.55 g, 4.0 mmol) were placed in a two-necked round bottom flask. Under inert atmosphere DMSO (3 mL) was added and the resulting mixture was heated at 60°C for 45 hours. After cooling

Experimental Section

at room temperature, the mixture was then washed with deionised water (2 x 10 mL). The collected organic phase was then washed with ethyl acetate (2 x 10 mL). The resulting organic phase was treated with brine and dried with Na₂SO₄; the drying agent was then filtered off and the filtrate solution was concentrated at reduced pressure. The resulting oil was purified in silica chromatographic column using ethyl acetate/petroleum ether 1:8 as mobile phase.

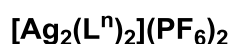
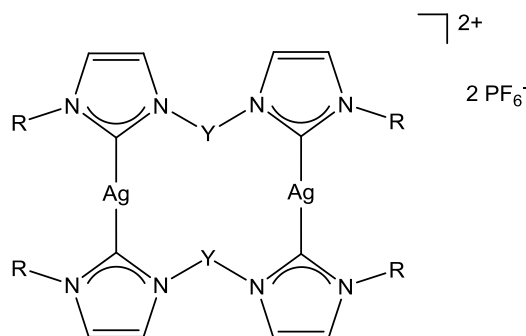
¹H NMR (CDCl₃, 25 °C, ppm): δ = 7.20 (m, 2H, Ar-H), 7.33 (m, 1H, Ar-H), 7.63 (m, 1H, Ar-H), 7.78 (m, 1H, Ar-H), 8.34 (m, 1H, Ar-H), 8.43 (m, 1H, Ar-H).

The diimidazolium salt **L¹⁶·2HPF₆** was prepared according to a literature procedure: a solution of 2-(Imidazolyl)pyridine (0.43 g, 3 mmol) in CH₂Br₂ (7.4 g, 3 mL, 42 mmol) was placed in a two-necked round bottom flask and refluxed for 24 hours. After cooling, the resulting white solid was filtered off and dissolved in H₂O (10 mL). NH₄PF₆ (0.99 g, 6.1 mmol) was added and the product (white solid) was collected by filtration.

¹H NMR (dmsO-*d*₆, 25 °C, ppm): δ = 6.83 (s, 2H, CH₂), 7.70 (m, 2H, Ar-H), 8.05 (d, 2H, Ar-H), 8.26 (m, 4H, CH + Ar-H), 8.64 (s, 2H, CH), 8.71 (d, 2H, Ar-H), 10.37 (s, 2H, NCHN).

7.9 General procedure for the synthesis of the silver(I) complexes [Ag₂(L¹)₂](PF₆)₂ - [Ag₂(L⁴)₂](PF₆)₂, [Ag₂(L⁶)₂](PF₆)₂, [Ag₂(L⁷)₂](PF₆)₂, [Ag₂(L⁹)₂](PF₆)₂, [Ag₂(L¹⁰)₂](PF₆)₂, [Ag₂(L¹⁴)₂](PF₆)₂, [Ag₂(L¹⁵)₂](PF₆)₂

The diimidazolium salt (1 mmol) and Ag₂O (2.5 mmol) were placed in a two-necked round bottom flask. Under inert atmosphere, deionised water (50 mL) was added and the mixture was stirred for 24 hours under light exclusion. Subsequently, the reaction mixture was filtered via cannula through Celite and the filtrate was treated with NH₄PF₆ (2.1 mmol). The resulting precipitate was filtered off and dried under reduced pressure under light exclusion.



$$n = 1 - 4, 6, 7, 14, 15$$

Bis(1,1'-dimethyl-3,3'-methylenediimidazol-2,2'-diylidene)disilver(I)

bis(hexafluorophosphate) $[\text{Ag}_2(\text{L}^1)_2](\text{PF}_6)_2$ ^[28]

White solid. Yield 69 %. ¹H NMR (dms o - d_6 , 25 °C, ppm): δ = 3.83 (s, 12H, CH₃), 6.39 (br s, 4H, CH₂), 7.24 (s, 4H, CH), 7.48 (s, 4H, CH).

Bis(1,1'-dimethyl-3,3'-ethylenediimidazol-2,2'-diylidene)disilver(I)

bis(hexafluorophosphate) $[\text{Ag}_2(\text{L}^2)_2](\text{PF}_6)_2$ ^[28]

White solid. Yield 49 %. ¹H NMR (dms o - d_6 , 25 °C, ppm): δ = 3.76 (s, 12H, CH₃), 4.67 (s, 8H, CH₂), 7.34 (s, 4H, CH), 7.56 (s, 4H, CH).

Bis(1,1'-dimethyl-3,3'-propylenediimidazol-2,2'-diylidene)disilver(I)

bis(hexafluorophosphate) $[\text{Ag}_2(\text{L}^3)_2](\text{PF}_6)_2$ ^[28]

White solid. Yield 45 %. ¹H NMR (dms o - d_6 , 25 °C, ppm): δ = 2.50 (m, 4H, CH₂) 3.49 (s, 12H, CH₃), 4.07 (m, 8H, NCH₂), 7.57 (s, 4H, CH), 7.68 (s, 4H, CH).

Bis(1,1'-dimethyl-3,3'-butylenediimidazol-2,2'-diylidene)disilver(I)

bis(hexafluorophosphate) $[\text{Ag}_2(\text{L}^4)_2](\text{PF}_6)_2$

Grey solid. Yield 53 %. ¹H NMR (dms o - d_6 , 25 °C, ppm): δ = 1.78 (s, 8H, CH₂) 3.77 (s, 12H, CH₃), 4.14 (s, 8H, NCH₂), 7.44 – 7.46 (m, 8H, CH). ESI-MS (positive ions) m/z : 797 $[\text{Ag}_2(\text{L}^4)_2(\text{PF}_6)]^+$, 325 $[\text{Ag}_2(\text{L}^4)_2]^{2+}$.

Bis(1,1'-dioctyl-3,3'-methylenediimidazol-2,2'-diylidene)disilver(I)

bis(hexafluorophosphate) [Ag₂(L⁶)₂](PF₆)₂

White solid. Yield 34 %. (CD₃CN, 25 °C, ppm): δ = 0.82 (m, 12H, CH₃), 1.20 – 1.24 (m, 40H, CH₂), 1.77 (m, 8H, CH₂), 4.08 (m, 8H, NCH₂), 6.37 (br, 8H, CH₂), 7.29 (s, 4H, CH), 7.48 (s, 4H, CH).

¹³C{¹H} NMR (CD₃CN, 25 °C, ppm): δ = 14.3 (CH₃), 23.2, 26.9, 29.7, 29.8, 32.1, 32.4 (6CH₂), 53.0 (NCH₂), 65.1 (NCH₂N), 122.4 (CH), 123.8 (CH), Ag-C not detected.

Bis(1,1'-dicyclohexyl-3,3'-methylenediimidazol-2,2'-diylidene)disilver(I)

bis(hexafluorophosphate) [Ag₂(L⁷)₂](PF₆)₂^[28]

White solid. Yield 41 %. ¹H NMR (dmsO-*d*₆, 25 °C, ppm): δ = 0.90 – 2.10 (m, 40H, CH₂) 4.25 (s, 4H, CH), 6.89 – 6.37 (AB system, 4H, CH₂), 7.72 (s, 4H, CH), 7.84 (s, 4H, CH).

Bis(1,1'-dimethyl-3,3'-(*m*-xylylene)diimidazol-2,2'-diylidene)disilver(I)

bis(hexafluorophosphate) [Ag₂(L¹⁴)₂](PF₆)₂

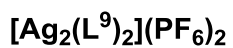
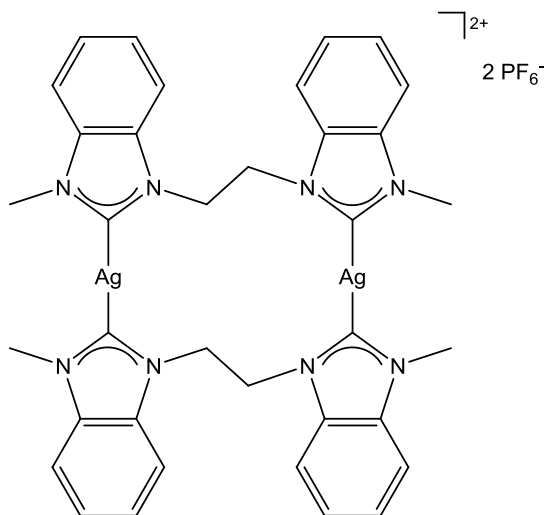
White solid. Yield 43 %. ¹H NMR (dmsO-*d*₆, 25 °C, ppm): δ = 3.64 (s, 12H, CH₃), 5.19 (s, 8H, CH₂), 7.00 – 7.43 (m, 8H, Ar-H), 7.46 (bs, 2H, C-H), 7.51 (bs, 2H, C-H).

Bis(1,1'-dimethyl-3,3'-(*p*-xylylene)diimidazol-2,2'-diylidene)disilver(I)

bis(hexafluorophosphate) [Ag₂(L¹⁵)₂](PF₆)₂

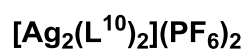
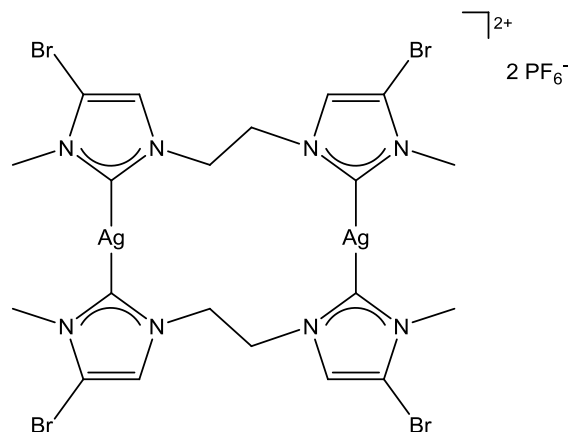
White solid. Yield 56 %. ¹H NMR (CD₃CN, 25 °C, ppm): δ = 3.84 (s, 12H, CH₃), 5.16 (s, 8H, CH₂), 7.07 (s, 8H, Ar-H + CH), 7.19 (s, 8H, Ar-H + CH).

**Bis(1,1'-dimethyl-3,3'-ethylenedibenzimidazol-2,2'-diylidene)disilver(I)
bis(hexafluorophosphate) [Ag₂(L⁹)₂](PF₆)₂**



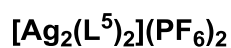
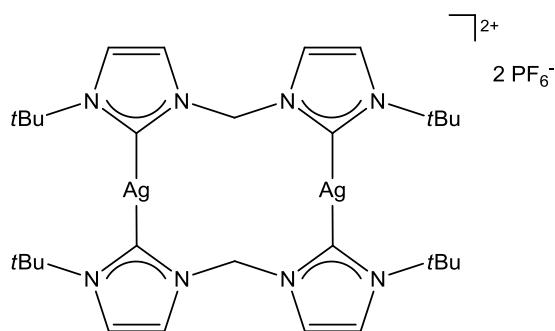
White solid. ¹H NMR (dms_o-d₆, 25 °C, ppm): δ = 3.93 (s, 12H, CH₃), 5.23 (s, 8H, CH₂), 7.31 (m, 4H, CH), 7.42 (m, 4H, CH), 7.57 (m, 4H, CH), 7.69 (m, 4H, CH). ¹³C{¹H} NMR (dms_o-d₆, 25 °C, ppm): δ = 35.2 (CH₃), 47.1 (CH₂), 112.0 (Ar-CH), 113.1 (Ar-CH), 125.3 (Ar-CH), 135.0 (Ar-C), 188.4 (Ar-C), 191.0 (NCN). ESI-MS (positive ions) *m/z*: 940 [Ag₂(L⁹)₂(PF₆)]⁺, 398 [Ag₂(L⁹)₂]²⁺.

Bis(1,1'-dimethyl-3,3'-ethylene-5,5'-dibromoimidazol-2,2'-diylidene)disilver(I) bis(hexafluorophosphate) $[\text{Ag}_2(\text{L}^{10})_2](\text{PF}_6)_2$



White solid. ^1H NMR ($\text{dms}\text{-}d_6$, 25 °C, ppm): δ = 3.77 (s, 12H, CH_3), 4.64 (s, 8H, CH_2), 7.63 (s, 4H, CH). ESI-MS (positive ions) m/z : 1057 $[\text{Ag}_2(\text{L}^{10})_2(\text{PF}_6)]^+$. Anal. Calcd for $\text{C}_{20}\text{H}_{24}\text{Ag}_2\text{Br}_4\text{F}_{12}\text{N}_8\text{P}_2$: C, 20.07; H, 2.02; N, 9.37 %. Found: C, 19.65; H, 1.59; N, 8.62 %.

7.10 Synthesis of the silver(I) complex bis(1,1'-*tert*-butyl-3,3'-methylene-2,2'-diylidene)disilver(I) bis(hexafluorophosphate) $[\text{Ag}_2(\text{L}^5)_2](\text{PF}_6)_2$



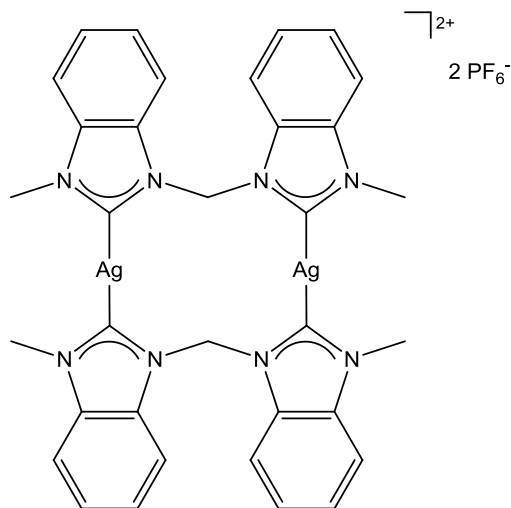
The diimidazolium salt $L^5 \cdot 2HBr$ (0.422 g, 1 mmol) and Ag_2O (0.93 g, 4 mmol) were placed in a two-necked round bottom flask. Under inert atmosphere, deionised water (20 mL) was added and the mixture was stirred for 30 minutes at $0^\circ C$ under light exclusion. Subsequently, the reaction mixture was filtered via cannula through Celite and the filtrate was treated with KPF_6 (0.39 g, 2.1 mmol). The resulting precipitate was filtered off and dried under reduced pressure under light exclusion. White solid. Yield 89 %. 1H NMR ($dmsO-d_6$, $25^\circ C$, ppm): $\delta = 1.63$ (s, 36H, CH_3), 6.44 – 6.99 (AB system, 4H, CH_2), 7.79 (br s, 8H, CH).

7.11 General procedure for the synthesis of the silver(I) complexes $[Ag_2(L^8)_2](PF_6)_2$, $[Ag_2(L^{12})_2](PF_6)_2$, $[Ag_2(L^{13})_2](PF_6)_2$ and $[Ag_3(L^{16})_2(CH_3CN)_2](PF_6)_3 \cdot 2H_2O \cdot 0.5HPF_6$

The following procedure was firstly reported by Wang *et al.* for the synthesis of the silver(I) complexes bearing the dicarbene ligands L^{16} .^[100]

The diimidazolium salt (1 mmol) and Ag_2O (4 mmol) were placed in a two-necked round bottom flask. Under inert atmosphere, CH_3CN (20 mL) was added and the mixture was stirred for 24 hours at $60^\circ C$ under light exclusion. Subsequently, the reaction mixture was filtered via cannula through Celite and the filtrate was concentrated under reduced pressure (3 mL). Diethyl ether (15 mL) was added and the resulting precipitate was filtered off and dried under reduced pressure in light exclusion.

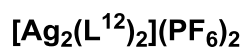
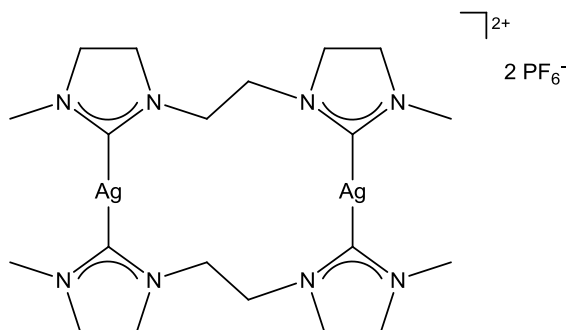
**Bis(1,1'-dimethyl-3,3'-methylenedibenzimidazol-2,2'-diylidene)disilver(I)
bis(hexafluorophosphate) $[\text{Ag}_2(\text{L}^8)](\text{PF}_6)_2$**



$[\text{Ag}_2(\text{L}^8)](\text{PF}_6)_2$

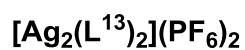
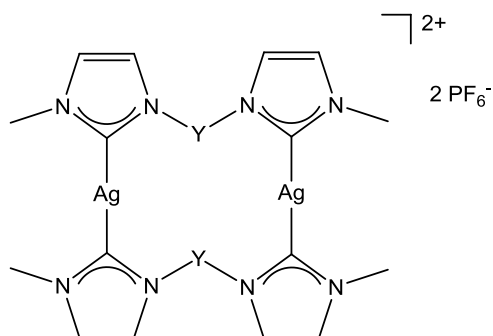
White solid. ^1H NMR (dms- d_6 , 25 °C, ppm): δ = 4.10 (s, 12H, CH_3), 7.40 (bs, 4H, CH_2), 7.57 – 7.62 (m, 8H, Ar- H), 7.87 (m, 4H, Ar- H), 8.11 (m, 4H, Ar- CH). $^{13}\text{C}\{^1\text{H}\}$ NMR (dms- d_6 , 25 °C, ppm): δ = 36.0 (CH_3), 59.2 (CH_2), 112.0 (Ar- CH), 113.2 (Ar- CH), 123.2 (Ar- CH), 125.3 (Ar- CH), 135.6 (C), carbene carbon not detected. ESI-MS (positive ions) m/z : 912 $[\text{Ag}_2(\text{L}^8)(\text{PF}_6)]^+$.

**Bis(1,1'-dimethyl-3,3'-ethylenediimidazolin-2,2'-diylidene)disilver(I)
bis(hexafluorophosphate) [Ag₂(L¹²)₂](PF₆)₂**



Off-white solid. ¹H NMR (dmso-*d*₆, 25 °C, ppm): δ = 3.13 (s, 12H, CH₃), 3.65 (bs, 16H, CH₂), 3.73 (bs, 8H, CH₂).

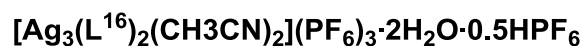
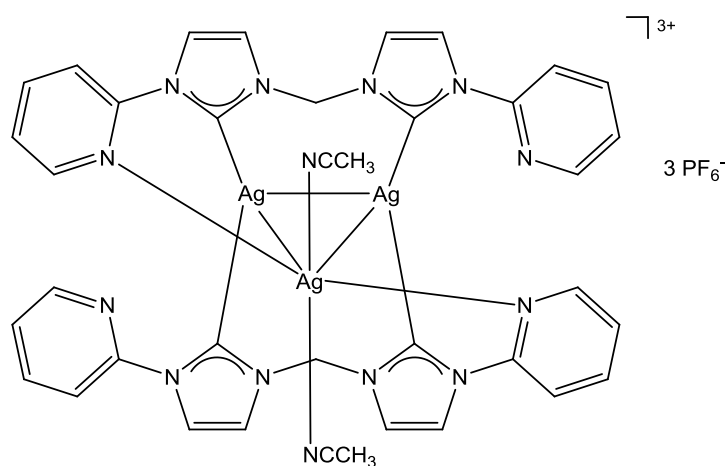
**Bis(1,1'-dimethyl-3,3'-(*o*-xylylene)diimidazol-2,2'-diylidene)disilver(I)
bis(hexafluorophosphate) [Ag₂(L¹³)₂](PF₆)₂**



Y = *o*-xylylene

Experimental Section

White solid. ^1H NMR (CD_3CN , 25 °C, ppm): δ = 3.67 (s, 12H, CH_3), 5.35 (s, 8H, CH_2), 6.74 (s, 4H, CH), 7.01 (s, 4H, CH), 7.41 (m, 4H, Ar-H), 7.51 (m, 4H, Ar-H).

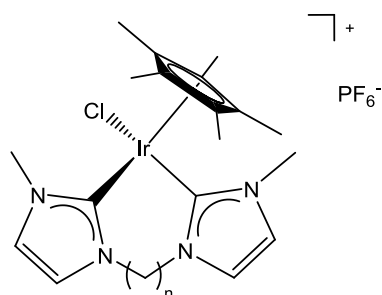


This silver complex has been already published in the literature^[100] and the obtained spectroscopic data perfectly matched those already reported.

White solid. Yield 81 %. ^1H NMR ($\text{dms}\text{-}d_6$, 25 °C, ppm): δ = 2.07 (s, 6H, CH_3CN), 6.88 (br, 4H, CH_2), 7.34 (m, 4H, Ar-H), 7.87 (m, 8H, Ar-H + CH), 7.97 (m, 4H, Ar-H), 8.14 (bs, 4H, CH), 8.27 (m, 4H, ar-H).

7.12 Synthesis of the iridium(III) complexes of general formula $[\text{IrClCp}^*(\text{L}^n)](\text{PF}_6)$

A solution of $[\text{IrCl}_2\text{Cp}^*]_2$ (0.1 mmol) in acetonitrile (15 mL) was added to a solution of the corresponding silver(I) complex (0.1 mmol) in acetonitrile (15 mL); the resulting suspension was stirred at room temperature under the exclusion of light for 5 h. The mixture was then filtered through Celite and the filtrate concentrated under reduced pressure. Addition of diethyl ether (10 mL) afforded the product, which was filtered off and dried in vacuum.



1. $n = 1$
2. $n = 2$
3. $n = 3$

[IrClCp*(L¹)](PF₆) (1)

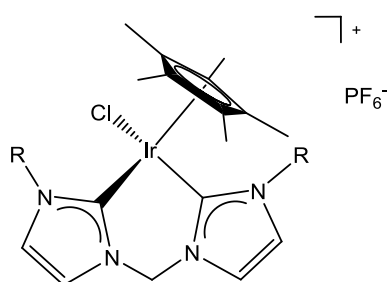
Yellow solid. Yield 70 %. ¹H NMR (CD₃CN, 25 °C, ppm): $\delta = 1.78$ (s, 15H, Cp*-CH₃), 3.80 (s, 6H, NCH₃), 5.46 – 5.99 (AB system, 2H, CH₂), 7.23 (s, 2H, CH), 7.31 (s, 2H, CH). ¹³C{¹H} NMR (CD₃CN, 25 °C, ppm): $\delta = 14.9$ (Cp*-CH₃), 37.9 (NCH₃), 63.3 (CH₂), 93.7 (Cp*-C), 122.1 (CH), 124.1 (CH), 151.4 (NCN). ESI-MS (positive ions) m/z : 539 [IrClCp*(L¹)]⁺. Anal. Calcd for C₁₉H₂₇ClIrN₄P: C, 33.33; H, 3.98; N, 8.19 %. Found: C, 33.49; H, 3.96; N, 8.04 %.

[IrClCp*(L²)](PF₆) (2)

Yellow solid. Yield 73 %. ¹H NMR (CD₃CN, 25 °C, ppm): $\delta = 1.62$ (s, 15H, Cp*-CH₃), 3.82 (s, 6H, NCH₃), 4.35 – 4.57 (AA'BB' system, 4H, CH₂), 7.14 (s, 2H, CH), 7.19 (s, 2H, CH). ¹H NMR (CDCl₃, 25 °C, ppm): $\delta = 1.66$ (s, 15H, Cp*-CH₃), 3.87 (s, 6H, NCH₃), 4.45 – 4.75 (AA'BB' system, 4H, CH₂), 7.03 (s, 2H, CH), 7.12 (s, 2H, CH). ¹³C{¹H} NMR (CD₃CN, 25 °C, ppm): $\delta = 9.3$ (Cp*-CH₃), 39.3 (NCH₃), 49.9 (CH₂), 93.9 (Cp*-C), 124.4 (CH), 125.7 (CH), 146.8 (NCN). ³¹P{¹H} NMR (CD₃CN, 25 °C, ppm): $\delta = -144.1$ (hept, PF₆). ESI-MS (positive ions) m/z : 553 [IrClCp*(L²)]⁺. MALDI-MS (positive ions, CHCl₃, α -CHCA): [IrClCp*(L²)]⁺ calculated for C₂₀H₂₉ClIrN₄ 553.17, found 553.20; [IrCp*(L²)]⁺ calculated for C₂₀H₂₉IrN₄ 518.20, found 518.20. Anal. Calcd for C₂₁H₂₉ClIrN₄P: C, 34.41; H, 4.19; N, 8.02 %. Found: C, 34.28; H, 4.10; N, 7.37 %.

[IrClCp*(L³)](PF₆) (3)

Yellow solid. The isolated solid presents two set of signals, one broad and one sharp. The sharp signals are assigned to complex **3**: ¹H NMR (CD₃CN, 25 °C, ppm): δ = 1.50 (s, 15H, Cp*-CH₃), 3.67 (s, 6H, NCH₃), 6.93 (s, 2H, CH), 7.02 (s, 2H, CH), the signals of the propylene bridge are not easily identified because they are overlapped to other signals and to the residual solvent signals. The identifiable broad signals are: ¹H NMR (CD₃CN, 25 °C, ppm): δ = 1.64 (bs, Cp*), 7.10-7.50 (bs, CH). ESI-MS (positive ions) *m/z*: 567 [Cp*IrCl(L³)]⁺. Anal. Calcd for C₂₁H₃₁ClF₆IrN₄P (pure complex **3**): C, 35.39; H, 4.39; N, 7.86 %. Found: C, 33.46; H, 4.38; N, 6.87 %. The EA of this solid does not fit exactly the proposed formulation but, as emerged by the ¹H NMR spectrum, the solid is a mixture of two species.



5. R = *t*Bu
 6. R = *n*Oct
 7. R = Cy

[IrClCp*(L⁵)](PF₆) (5)

Yellow solid. ¹H NMR (CD₃CN, 25 °C, ppm): δ = 1.53 (s, 15H, Cp*-CH₃), 1.53 (s, 18H, CH₃), 5.86 – 5.45 (AB system, 2H, CH₂), 7.43 (s, 2H, CH), 7.48 (s, 2H, CH). ¹³C{¹H} NMR (CD₃CN, 25 °C, ppm): δ = 10.2 (Cp*-CH₃), 32.0 (CH₃), 62.9 (CH₂), 64.8 (C(CH₃)₃), 94.7 (Cp*-C), 122.4 (CH), 123.6 (CH), 145.6 (NCN). ESI-MS (positive ions) *m/z*: 623 [IrClCp*(L⁵)]⁺. The isolated solid contains appreciable quantity of the precursor [IrCl₂Cp*₂]₂ (*ca.* 25 %) as indicated by the elemental analysis and by the signal relative to the Cp* group of the precursor in the ¹H NMR spectrum. Anal. Calcd for

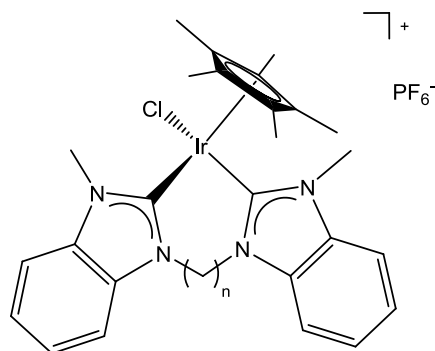
$C_{25}H_{39}ClF_6IrN_4P$ (pure complex **5**): C, 39.05; H, 5.12; N, 7.29 % and for **5**/ $[IrCl_2Cp^*_2]_2$ in ratio 75/25: C, 36.85; H, 4.78; N, 5.46 %. Found: C, 37.13; H, 4.89; N, 4.83 %.

$[IrClCp^*(L^6)](PF_6)$ (6**)**

Yellow solid. Yield 94 %. 1H NMR (CD_3CN , 25 °C, ppm): δ = 0.89 (m, 6H, CH_3), 1.29 (m, 24H, CH_2), 1.74 (s, 15H, Cp^*-CH_3), 3.89 and 4.19 (2m, 4H, NCH_2), 5.48 – 5.97 (AB system, 2H, CH_2), 7.30 (s, 2H, CH), 7.34 (s, 2H, CH). $^{13}C\{^1H\}$ NMR (CD_3CN , 25 °C, ppm): δ = 9.4 (Cp^*-CH_3), 14.3 (CH_3), 23.3, 27.3, 29.7, 31.9, 32.4 (6 CH_2), 50.7 (CH_2), 62.9 (CH_2), 94.0 (Cp^*-C), 122.1 (CH), 122.6 (CH), 151.5 (NCN). ESI-MS1 (positive ions) m/z : 735 $[IrClCp^*(L^6)]^+$. Anal. Calcd for $C_{33}H_{55}ClF_6IrN_4P$: C, 44.98; H, 6.36; N, 6.30 %. Found: C, 44.47; H, 6.50; N, 6.17 %.

$[IrClCp^*(L^7)](PF_6)$ (7**)**

Yellow solid. 1H NMR (CD_3CN , 25 °C, ppm): δ = 1.35 (m, 4H, CH_2), 1.48 (m, 4H, CH_2), 1.31 (m, 4H, CH_2), 1.76 (s, 15H, Cp^*-CH_3), 4.24 (m, 2H, CH), 5.41 – 5.94 (AB system, 2H, CH_2), 7.30 (s, 2H, CH), 7.36 (s, 2H, CH). $^{13}C\{^1H\}$ NMR (CD_3CN , 25 °C, ppm): δ = 9.0 and 9.9 (Cp^*-CH_3), 25.8, 26.1, 26.6, 34.5, 37.0 (5 CH_2), 60.4 (CH_2), 87.7 (CH Cy), 94.0 (Cp^*-C), 120.3 (CH), 122.9 (CH), 151.0 (NCN). ESI-MS (positive ions) m/z : 675 $[IrClCp^*(L^7)]^+$. The isolated solid contains appreciable quantity of the precursor $[IrCl_2Cp^*_2]_2$ (*ca.* 35 %) as indicated by the elemental analysis and by the signal relative to the Cp^* group of the precursor in the 1H NMR spectrum. Anal. Calcd for $C_{29}H_{43}ClF_6IrN_4P$ (pure complex **7**): C, 42.43; H, 5.28; N, 6.83 % and for **7**/ $[IrCl_2Cp^*_2]_2$ in ratio 65/35: C, 38.16; H, 4.73; N, 4.44 %. Found: C, 37.65; H, 4.70; N, 4.24 %.



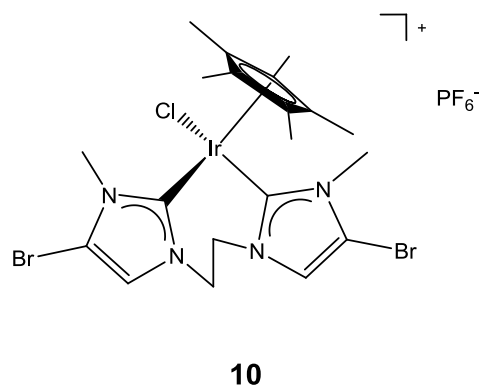
- 8.** $n = 1$
9. $n = 2$

[IrClCp*(L⁸)](PF₆) (8)

Yellow solid. Yield 50 %. ¹H NMR (CD₃CN, 25 °C, ppm): δ = 1.89 (s, 15H, Cp*-CH₃), 4.07 (s, 6H, NCH₃), 5.80 – 6.84 (AB system, 2H, CH₂), 7.48 (m, 4H, Ar-CH), 7.64 (d, 2H, Ar-CH), 7.94 (d, 2H, Ar-CH). ¹³C{¹H} NMR (CD₃CN, 25 °C, ppm): δ = 14.9 (Cp*-CH₃), 34.0 (NCH₃), 94.8 (Cp*-C), 110.0 (CH), 111.1 (CH), 123.9 (CH), 124.0 (CH), 133.2 (C), 135.1 (C), 163.0 (NCN), bridging CH₂ not detected. ESI-MS (positive ions) *m/z*: 639 [Cp*IrCl(L⁸)]⁺. The isolated solid contains appreciable quantity of the precursor [IrCl₂Cp*₂]₂ (ca. 10 %) as indicated by the elemental analysis and by the signal relative to the Cp* group of the precursor in the ¹H NMR spectrum. Anal. Calcd for C₂₇H₃₁ClF₆IrN₄P (pure complex **8**): C, 41.32; H, 3.98; N, 7.14 % and for **8**/[IrCl₂Cp*₂]₂ in ratio 90/10: C, 40.23; H, 3.96; N, 6.42 %. Found: C, 40.98; H, 3.28; N, 5.55 %.

[IrClCp*(L⁹)](PF₆) (9)

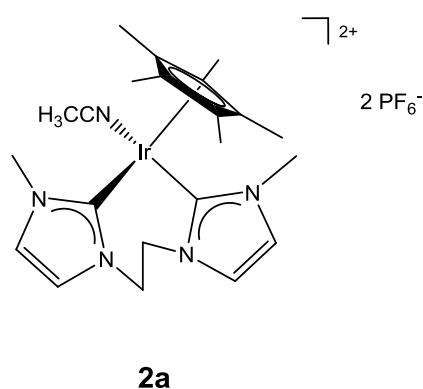
Yellow solid. Yield 70 %. ¹H NMR (CD₃CN, 25 °C, ppm): δ = 1.72 (s, 15H, Cp*-CH₃), 4.05 (s, 6H, NCH₃), 4.86 – 4.96 (AA'BB' system, 4H, CH₂), 7.42 (m, 4H, Ar-CH), 7.59 (m, 4H, Ar-CH). ¹³C{¹H} NMR (CD₃CN, 25 °C, ppm): δ = 14.8 (Cp*-CH₃), 36.3 (NCH₃), 45.7 (CH₂), 95.3 (Cp*-C), 111.3 (CH), 111.8 (CH), 124.7 (CH), 124.9 (CH), 135.4 (C), 136.5 (C), 160.7 (NCN). ESI-MS (positive ions) *m/z*: 653 [Cp*IrCl(L⁹)]⁺. Anal. Calcd for C₂₈H₃₃ClF₆IrN₄P: C, 42.10; H, 4.17; N, 7.02 %. Found: C, 43.01; H, 3.66; N, 6.57 %.



[IrClCp*(L¹⁰)](PF₆) (**10**)

Yellow solid. Yield 83 %. ¹H NMR (CD₃CN, 25 °C, ppm): δ = 1.62 (s, 15H, Cp*-CH₃), 3.80 (s, 6H, NCH₃), 4.30 – 4.59 (AA'BB' system, 4H, CH₂), 7.29 (s, 2H, CH). ¹³C{¹H} NMR (CD₃CN, 25 °C, ppm): δ = 8.0 (Cp*-CH₃), 37.5 (NCH₃), 48.9 (CH₂), 94.5 (Cp*-C), 108.1 (CH), 123.5 (C), 149.4 (NCN). ESI-MS (positive ions) *m/z*: 711 [Cp*IrCl(L¹⁰)]⁺. Anal. Calcd for C₂₀H₂₇Br₂ClF₆IrN₄P: C, 28.10; H, 3.19; N, 6.56 %. Found: C, 28.52; H, 3.46; N, 6.57 %.

7.13 Synthesis of the iridium(III) complexes [IrCp*(L²)(CH₃CN)](PF₆)₂ (**2a**)



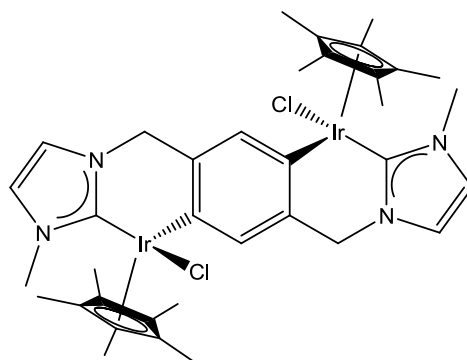
To a solution (20 mL) of **2** in acetonitrile (0.07 g, 0.1 mmol), AgPF₆ (0.03 g, 0.12 mmol) was added under inert atmosphere. After 5 hours of stirring at room temperature under inert atmosphere and exclusion of light, the mixture was filtered through Celite and the filtrate solution was concentrated under reduced pressure. Addition of diethyl ether (10 mL) afforded the product, which was filtered off and

Experimental Section

dried in vacuum. Yield 95 %. ^1H NMR (CD_3CN , 25 °C, ppm): δ = 1.72 (s, 15H, $\text{Cp}^*\text{-CH}_3$), 1.96 (CH_3CN), 3.69 (s, 6H, NCH_3), 4.37 – 4.51 (AA'BB' system, 4H, CH_2), 7.24 (s, 2H, CH), 7.32 (s, 2H, CH). $^{13}\text{C}\{^1\text{H}\}$ NMR (CD_3CN , 25 °C, ppm): δ = 9.2 ($\text{Cp}^*\text{-CH}_3$), 39.1 (NCH_3), 49.7 (CH_2), 96.4 ($\text{Cp}^*\text{-C}$), 125.5 (CH), 126.2 (CH), 141.3 (NCN). ESI-MS (positive ions) m/z : 259 [$\text{IrCp}^*(\text{L}^2)$] $^{2+}$. Anal. Calcd for $\text{C}_{22}\text{H}_{32}\text{ClF}_{12}\text{IrN}_5\text{P}_2$: C, 31.13; H, 3.80; N, 8.25 %. Found: C, 28.41; H, 3.31; N, 6.83 %.

7.14 Synthesis of the dinuclear iridium(III) complexes [$\text{Ir}_2\text{Cl}_2\text{Cp}^*_2(\text{L}^{15})$] - [$\text{Ir}_2\text{Cl}_2\text{Cp}^*_2(\text{L}^{16})$](PF_6) $_2$

A solution of [IrCl_2Cp^*] $_2$ (0.2 mmol) in acetonitrile (15 mL) was added to a solution of the corresponding silver(I) complex (0.1 mmol) in acetonitrile (15 mL); the resulting suspension was stirred at room temperature under the exclusion of light for 5 h. The mixture was then filtered through Celite and the filtrate concentrated under reduced pressure. Addition of diethyl ether (10 mL) afforded the product, which was filtered off and dried in vacuum.

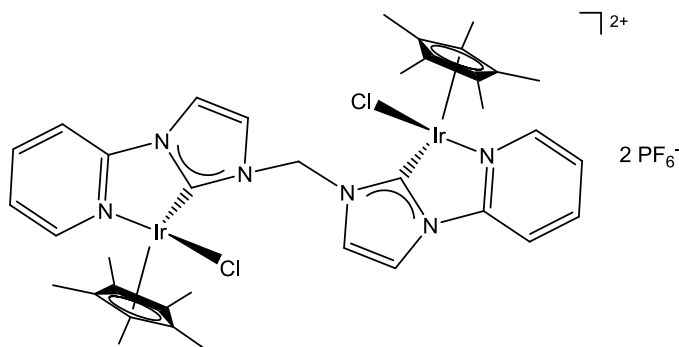


15

[$\text{Ir}_2\text{Cl}_2\text{Cp}^*_2(\text{L}^{15})$] (15)

Yellow solid. Yield 64 %. ^1H NMR (CDCl_3 , 25 °C, ppm): δ = 1.62 (s, 15H, $\text{Cp}^*\text{-CH}_3$), 3.80 (s, 6H, NCH_3), 4.60 – 4.80 (AB system, 4H, CH_2), 6.91 (d, 2H, CH), 6.95 (d, 2H, CH), 7.10 (s, 2H, CH). $^{13}\text{C}\{^1\text{H}\}$ NMR (CDCl_3 , 25 °C, ppm): δ = 8.9 ($\text{Cp}^*\text{-CH}_3$), 38.5 (NCH_3), 57.2 (CH_2), 90.1 ($\text{Cp}^*\text{-C}$), 120.0 (CH), 120.6 (CH), 121.4 (CH), 133.3 (C), 138.1

(C), 149.4 (NCN). MALDI (CHCl_3 ; sinapinic acid in 75 % MeCN, 0.1 % TFA): m/z 955.9 $[\text{M}-\text{Cl}]^+$. Anal. Calcd for $\text{C}_{36}\text{H}_{44}\text{Cl}_2\text{Ir}_2\text{N}_4$: C, 42.71; H, 4.48; N, 5.67 %. Found: C, 42.74; H, 4.50; N, 5.49 %.



16

$[\text{Ir}_2\text{Cl}_2\text{Cp}^*_2(\text{L}^{16})](\text{PF}_6)_2$ (16)

Yellow solid. Yield 58 %. ^1H NMR (300 MHz, CD_3CN): δ = 1.85 (s, 30H, CH_3 Cp*), 6.57 (s, 2H, CH_2), 7.60 (t, 2H, J = 6 Hz, H_{pyr}), 7.92-8.00 (m, 6H, H_{im} and H_{pyr}), 8.21 (t, 2H, J = 6 Hz, H_{pyr}), 8.69 (d, 2H, J = 6 Hz, H_{pyr}). ^1H NMR (300 MHz, $\text{DMSO}-d_6$): δ 1.87 (s, 30H, CH_3 Cp*), 6.54 (s, 2H, CH_2), 7.67 (t, 2H, J = 6 Hz, H_{pyr}), 7.87 (d, 2H, H_{im}), 8.30-8.35 (m, 4H, H_{pyr}), 8.58 (d, 2H, H_{im}), 8.83 (d, 2H, J = 6 Hz, H_{pyr}). ^1H NMR (300 MHz, D_2O): δ = 1.71 (s, 30H, CH_3 Cp*), 6.58 (s, 2H, CH_2), 7.49 (t, 2H, J = 6 Hz, H_{pyr}), 7.60 (d, 2H, H_{im}), 7.85 (m, 2H, H_{pyr}), 7.93 (d, 2H, H_{im}), 8.08 (t, 2H, J = 6 Hz, H_{pyr}), 8.63 (d, 2H, J = 6 Hz, H_{pyr}). ^{13}C NMR (75 MHz, CD_3CN): δ = 9.0 (CH_3 Cp*), 64.0 (CH_2), 94.8 (C Cp*), 112.5 (C_{im}), 120.0 (C_{im}), 123.5 (C_{pyr}), 125.1 (C_{pyr}), 142.9 (C_{pyr}), 152.0 (C_{pyr}), 152.9 (C_{pyr}), 172.0 (C-Ir). ^{31}P NMR (121 MHz, CD_3CN): δ = -144.1 (heptet, PF_6). ESI-MS (CH_3CN): m/z 1173 $[\text{M}-\text{PF}_6]^+$, 514 $[\text{M}-2\text{PF}_6]^{2+}$. Anal. Calcd for $\text{C}_{37}\text{H}_{44}\text{Cl}_2\text{F}_{12}\text{Ir}_2\text{N}_6\text{P}_2$: C, 33.78; H, 3.36; N, 6.37 %. Found: C, 33.57; H, 3.69; N, 5.96 %.

7.15 Water oxidation

7.15.1 Water oxidation reaction with Ce(IV) as sacrificial oxidant: procedure using the pressure/voltage transducer

The catalytic oxidation of water was performed in 40 mL glass EPA vial with pressure/voltage transducer mounted into the reaction headspace. The evolution of O₂ was monitored by using a home-made interface designed in LabView.

In a typical experiment, a freshly prepared solution of (NH₄)₂[Ce(NO₃)₆] (0.38 M) in Milli-Q water was allowed to equilibrate at 25 °C with stirring for 10 minutes. Data collection over 3 minutes showed equilibration of the system, and when a steady baseline was achieved, an aliquot of a 10 mM solution of the catalyst in CH₃CN was injected into the reactor. Oxygen evolution started immediately and was monitored until a plateau was observed. The amount of dissolved oxygen was assumed to be negligible.

7.15.2 Water oxidation reaction with NaIO₄ as sacrificial oxidant: procedure using the pressure/voltage transducer

The catalytic oxidation of water was performed in 40 mL glass EPA vial with pressure/voltage transducer mounted into the reaction headspace. The evolution of O₂ was monitored by using a home-made interface designed in LabView.

In a typical experiment, a freshly prepared solution of NaIO₄ (50 mM) in Milli-Q water was allowed to equilibrate at 25 °C with stirring for 10 minutes. Data collection over 3 minutes showed equilibration of the system, and when a steady baseline was achieved, an aliquot of a 10 mM solution of the catalyst in CH₃CN was injected into the reactor. Oxygen evolution started immediately and was monitored until a plateau was observed. The amount of dissolved oxygen was assumed to be negligible.

7.15.3 Water oxidation reaction with Ce(IV) as sacrificial oxidant: procedure using the GC-MS

Experiments to analyse the time-frame of O₂ and CO₂ evolution were performed in a reactor in which a continuous flow of nitrogen at 10 mL/min was passed through the headspace, and by analysing by GC the composition of the gas mixture as it exits the reactor. Quantification of the CO₂ was performed by previous calibration of its response factor with respect to nitrogen/oxygen mixtures by sampling commercial available gas mixtures containing 249.8 and 498.5 ppm of CO₂ in air; the response factor at the TCD detector of CO₂ versus N₂/O₂ was 1.13.

In a typical experiment, a freshly prepared solution of (NH₄)₂[Ce(NO₃)₆] (0.38 M) in Milli-Q water was allowed to equilibrate at 25 °C with stirring, while a flow of nitrogen was passing through the headspace in order to eliminate the O₂ contained in it. After 20 minutes of equilibration, a first run long (blank run) starts; before the beginning of the second run, an aliquot of a 10 mM solution of the catalyst in CH₃CN was fastly injected into the reactor. Data were collected every 387 seconds (the time of one run) until the plateau was reached.

The identity of the evolved gas was confirmed by GC analysis with an Agilent 7890A instrument equipped with HP-PLOTQ and HPMOLSIEVE columns and thermal conductivity (TCD) and mass selective (MSD) detectors.

7.15.4 Water oxidation reaction with NaIO₄ as sacrificial oxidant: procedure using the GC-MS

For the gas analysis evolved using NaIO₄ as sacrificial oxidant, the same apparatus described in **Section 7.15.3** was used; in a typical experiment, a freshly prepared solution of NaIO₄ (50 mM) in Milli-Q water was allowed to equilibrate at 25 °C with stirring, while a flow of nitrogen was passing through the headspace in order to eliminate the O₂ contained in it. The kinetic was then run and followed as described in **Section 7.15.3**.

CO₂ production employing NaIO₄ as the oxidant could be underestimated due to the presence of the hydrogen carbonate ion (HCO₃⁻) in solution at neutral pH.

7.15.5 Light driven oxidation of water

In a typical experiment, a 50 mm Na_HCO₃/Na₂SiF₆ aqueous buffer (15 mL, pH 5.2) containing [Ru(bpy)₃]Cl₂·6H₂O (1mm), Na₂S₂O₈ (5 mm) and the catalyst (25–100 μm) was introduced into a glass reactor (internal diameter 18 mm, total internal volume of 24 mL), deoxygenated with nitrogen and allowed to equilibrate at 25 °C under the exclusion of light. The solution was then irradiated with a series of six monochromatic LEDs emitting at 450 nm (LED450–06 from Roithner Lasertechnik GmbH). Oxygen evolution started immediately after irradiation and was monitored with a FOXY-R-AF probe inserted into the reaction headspace and interfaced with Neofox Real-Time software for data collection. The quantum efficiencies (QEs) were determined by **Equation 7.1**.

$$\text{QE} = \frac{\text{molecules of O}_2 / \text{time}}{\text{absorbed photons} / \text{time}} \times 2 \times 100$$

Equation 7.1

The number of molecules of O₂ per unit of time was calculated from the maximum rate of oxygen production reported in **Table 3.5**. Given the high optical density of the solution and the negligible loss of photons by reflection events, the number of absorbed photons was assumed to be equivalent to the number of incident photons. The number of incident photons on the reactor was obtained by measuring the power emitted from the series of six LEDs (42 mW, 7 mW per single LED), corresponding to 9.5 x 10¹⁶ photons s⁻¹ (1.58 x 10⁻⁷ einstein s⁻¹) at 450 nm. The power of the light was measured by using a Newport 1835-C Multi-Function Optical Power Meter equipped with a model 818-UV calibrated silicon detector. The multiplying factor 2 in the equation above stems from evidence that in photoactivated cycles in which persulfate anion is used as the sacrificial electron acceptor, two photons are required to produce one molecule of oxygen.^[66,70]

7.15.6 Dynamic light-scattering experiments:

In a typical experiment, after the catalytic test an aliquote of the reaction mixture was introduced in a cuvette and a DLS experiment was carried out. In all cases, the absence of nanoparticles was observed.

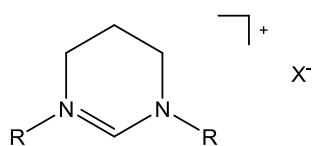
7.15.7 UV-Vis experiments

In a typical experiment, an aliquote of a 10 mM solution of **2** in acetonitrile was added to 2 mL of water. A first spectrum was registered, then an aliquote of a solution of sacrificial oxidant was added. The bubbling started immediately and the data were collected over 2 hours recording the spectra every 2 minutes.

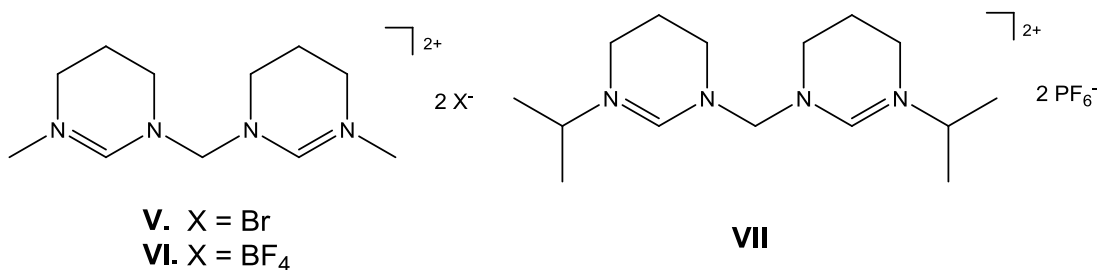
7.16 Transfer hydrogenation of ketones

In a typical experiment, the iridium complex (2.5 μmol) was introduced into an oven-dried Schlenk and the ketone (0.5 mmol) and 2-propanol were added under argon (total volume 4.85 ml). The yellow mixture was refluxed (90 °C bath temperature) under argon for 5 minutes and 150 μL of a solution of NaOiPr (0.1 M; 0.015 mmol) in 2-propanol were added. The reaction started and the mixture changed its color. With complex $[\text{Ir}_2\text{Cl}_2(\text{Cp}^*)_2(\text{L}^{15})]$ the solution turned gradually into deep red, whereas with $[\text{Ir}_2\text{Cl}_2(\text{Cp}^*)_2(\text{L}^{16})](\text{PF}_6)_2$ it became deep yellow. The reaction was sampled by removing an aliquot of the reaction mixture and diethyl ether was added (1/1 in volume). The solution was filtered over a short silica pad and the conversion was determined by GC analysis (ketone 0.1 M, Ir 0.5 mol %, NaOiPr 3 mol %).

7.17 Synthesis of the salts I-VII



- I.** R = Me, X = I
- II.** R = *i*Pr, X = I
- III.** R = Mes, X = BF₄
- IV.** R = *p*-Tol, X = BF₄



The salts **IV**, **VI** and **VII** were already available in the laboratory and were used without any further purification.

7.17.1 Synthesis of I

1-methyl-1,4,5,6-tetrahydropyrimidine (0.98 g, 10 mmol) and methyl iodide (1.42 g, 10 mmol) were placed in a two-necked round-bottom flask. Under inert atmosphere, toluene (15 mL) was added and the resulting mixture was refluxed for 24 hours. The resulting product (red solid) was filtered off and washed with diethyl ether (3 x 5 mL), then dried under reduced pressure.

Yield 92 %. ¹H NMR (acetone-d₆, 25 °C, ppm): δ = 2.21 (quin, ³J = 6 Hz, 2H, CH₂), 3.33 (s, 6H, CH₃), 3.50 (t, 4 H, ³J = 6 Hz, CH₂), 8.75 (s, 1H, NCHN).

7.17.2 Synthesis of II ^[130]

The corresponding amidine (1 eq.), 1,3-diiodopropane (1.1 eq.) and K₂CO₃ (0.5 eq.) were placed in a two-necked round-bottom flask. Acetonitrile was added and the resulting mixture was refluxed for 16 hours. After then, the solvent was removed under reduced pressure; CH₂Cl₂ was added to the residue and the insoluble species were removed by filtration. Diethyl ether (20 mL) was added, affording the product as yellow-white solid.

¹H NMR (CDCl₃, 25 °C, ppm): δ = 1.32 (d, ³J = 6 Hz, 12H, CH₃), 2.09 (quint, ³J = 6 Hz, 2H, CH₂), 3.35 (t, ³J = 6 Hz, 4H, CH₂), 4.04 (hept, ³J = 6 Hz, 2H, CH₂), 8.18 (s, 1H, NCHN)

7.17.3 Synthesis of III

The corresponding amidine (1 eq.), 1,3-diiodopropane (1.1 eq.) and K₂CO₃ (0.5 eq.) were placed in a two-necked round-bottom flask. Acetonitrile was added and the resulting mixture was refluxed for 16 hours. After then, the solvent was removed under reduced pressure; CH₂Cl₂ was added to the residue and the insoluble species were removed by filtration. Diethyl ether (20 mL) was added, affording the product as yellow-white solid. The solid obtained in this way (0.9 g, 2 mmol) was dissolved in 5 mL of acetone and an aqueous solution of NaBF₄ (0.27 g, 2.5 mmol, in 5 mL of H₂O) was added. After 30 minutes of stirring, the volume of the solution was reduced under vacuum, then the residue was washed with CH₂Cl₂ (3 x 10 mL). The collected organic layer was treated with MgSO₄. The drying agent was removed by filtration and the solvent was removed from the filtrate solution under vacuum. Yield 95 %. ¹H NMR (CDCl₃, 25 °C, ppm): δ = 2.28 (s, 6H, CH₃), 2.31 (s, 12H, CH₃), 2.57 (m, 2H, CH₂), 3.93 (t, ³J = 6 Hz, 4H, CH₂), 6.96 (s, 4H, Ar-H), 7.48 (s, 1H, NCHN).

7.17.4 Synthesis of V

1-methyl-1,4,5,6-tetrahydropyrimidine (0.98 g, 10 mmol) and methylene dibromide (0.87 g, 5 mmol) were placed in a two-necked round-bottom flask. Under inert atmosphere, DMF (10 mL) was added and the resulting mixture was kept under

Experimental Section

stirring at room temperature for 6 hours. Diethyl ether (15 mL) was added, affording the precipitation of the product (white-yellow hygroscopic solid), which was filtered off and washed with diethyl ether (5 x 5mL).

Yield 75 %. ^1H NMR (CDCl_3 , 25 °C, ppm): δ = 2.01 (m, 4H, CH_2), 3.21 (s, 6H, CH_3), 3.38 (t, 3J = 3 Hz, CH_2), 5.06 (s, 2H, CH_2), 8.76 (s, 2H, NCHN).

7.18 Reactions with the expanded rings salts I-VII

Table 7.1

| Salt | Reaction conditions | Observations: |
|------|--|---|
| I | 4 eq. Ag_2O , CH_2Cl_2 , r.t., 3 d | unreacted salt precursor and decomposition products |
| I | i) 2.2 eq. KHDMS, THF, r.t., 30'; ii) $[\text{IrCl}_2\text{Cp}^*]_2$, THF, r.t., 3 h | crowded ^1H NMR spectrum |
| II | i) 2.2 eq. KHDMS, THF, r.t., 30'; ii) $[\text{IrCl}_2\text{Cp}^*]_2$, THF, r.t., 3 h | crowded ^1H NMR spectrum |
| II | i) 2.2 eq. KHDMS, CH_3CN , r.t., 30'; ii) $[\text{IrCl}_2\text{Cp}^*]_2$, CH_3CN , r.t., 3 h | unreacted salt precursor and decomposition products mixture of |
| III | 4 eq. Ag_2O , 5 eq. NaBr, CH_2Cl_2 , r.t., 3 d | $[\text{Ag}(\text{NHC})_2](\text{AgBr}_2)$ + $[\text{AgBr}(\text{NHC})]$ (unsuccessful transmetalation Ag(I)/Ir(III) of ligand) |
| III | i) 2.2 eq. KHDMS, THF, r.t., 30'; ii) 0.5 eq. $[\text{IrCl}_2\text{Cp}^*]_2$, THF, r.t., 3 h | crowded ^1H NMR spectrum |
| III | i) 2.2 eq. KHDMS, THF, r.t., 30'; ii) 1 eq. $[\text{IrCl}_2\text{Cp}^*]_2$, THF, r.t., 3 h | crowded ^1H NMR spectrum |
| III | i) 2.2 eq. KHDMS, THF, r.t., 30'; ii) 0.5 eq. $[\text{IrCl}_2\text{Cp}^*]_2$, CH_3CN , r.t., 3 h | crowded ^1H NMR spectrum |
| IV | 4 eq. Ag_2O , 5 eq. NaBr, CH_2Cl_2 , r.t., 3 d | C-N cleavage in the ligand precursor |

| | | |
|-----|--|--|
| IV | i] 2.2 eq. KHDMS, THF, r.t., 30'; ii] 0.5 eq. [IrCl ₂ Cp*] ₂ , CH ₃ CN, r.t., 3 h | crowded ¹ H NMR spectrum |
| V | 2.5 eq. Ag ₂ O, H ₂ O, r.t., 24 h | unreacted salt precursor |
| VI | 4 eq. Ag ₂ O, CH ₃ CN, 60 °C, 24 h | crowded ¹ H NMR spectrum |
| VI | 4 eq. Ag ₂ O, CH ₂ Cl ₂ , r.t., 3 d | unreacted salt precursor |
| VI | 4 eq. Ag ₂ O, 5 eq. NaBr, CH ₂ Cl ₂ , r.t., 3 d | unreacted salt precursor |
| VI | i] 3.5 eq. Ag ₂ O, CH ₃ CN, r.t., 3 d; ii] [IrCl ₂ Cp*] ₂ , CH ₂ Cl ₂ , r.t., 2 d | unreacted starting material |
| VI | 2.2 eq. KHDMS, [IrCl ₂ Cp*] ₂ , THF, -78 °C, 3 h | crowded ¹ H NMR spectrum |
| VI | i] 2.2 eq. KHDMS, CH ₃ CN, r.t., 30'; ii] [IrCl ₂ Cp*] ₂ , CH ₃ CN, r.t., 3 h | unreacted salt precursor and decomposition products |
| VI | i] 2.2 eq. KHDMS, THF, r.t., 30'; ii] [IrCl ₂ Cp*] ₂ , CH ₃ CN, r.t., 3 h | unreacted salt precursor and decomposition products |
| VI | i] 2.2 eq. KHDMS, THF, r.t., 30'; ii] [IrCl ₂ Cp*] ₂ , THF, 70 °C, 3 h | unreacted salt precursor and decomposition products |
| VI | 2.5 eq. NaOAc, [IrCl ₂ Cp*] ₂ , DMF, 120 °C, 2 h; | unreacted salt precursor |
| VII | 4 eq. Ag ₂ O, CH ₃ CN, 60 °C, 24 h | crowded ¹ H NMR spectrum |
| VII | 4 eq. Ag ₂ O, CH ₂ Cl ₂ , r.t., 3 d | unreacted salt precursor |
| VII | 2.2 eq. KHDMS, [IrCl ₂ Cp*] ₂ , THF, -78 °C, 3 h | crowded ¹ H NMR spectrum |
| VII | i] 2.2 eq. KHDMS, THF, r.t., 30'; ii] [IrCl ₂ Cp*] ₂ , THF, r.t., 3 h | unreacted salt precursor and decomposition products |
| VII | i] 3 eq. NaH, [IrCl ₂ Cp*] ₂ , MeOH, r.t., 1 h; ii] 50 °C, 2 h | unreacted salt precursor |
| VII | i] 2.5 eq. KO ^t Bu, [IrCl ₂ Cp*] ₂ , MeOH, r.t., overnight | crowded ¹ H NMR spectrum |

7.19 Synthesis of azides

The azides were synthesized according to a literature procedure reported by Moses *et al.*^[153]

Phenyl-azide:

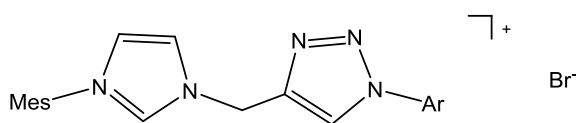
Aniline (0.3 g, 3.2 mmol) was placed in a two-necked round-bottom flask and 6 mL of CH₃CN were added. The mixture was cooled under stirring to 0 °C, then *t*BuONO was added (570 μL, 4.8 mmol), then trimethylsilyl azide was added (510 μL, 3.84 mmol). The resulting mixture was kept under stirring for 1 hour at room temperature. The reaction mixture was then concentrated under vacuum and the crude product (grey solid) was purified by silica gel chromatography (hexane) to give the product (yellow oil). Yield: 84 %. The ¹H NMR exactly matches to the one reported in literature.

¹H NMR (CDCl₃, 25 °C, ppm): δ = 6.96 (dd, ³*J* = 7.6 and 0.7 Hz, 2H, CH), 7.06 (td, ³*J* = 7.6 and 0.7 Hz, 1H, CH), 7.27 (t, ³*J* = 7.6 Hz, 2H, CH).

p-methoxyphenyl-azide:

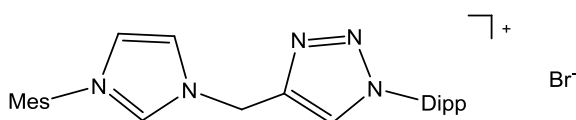
p-anisidine (0.4 g, 3.2 mmol) was placed in a two-necked round-bottom flask and 6 mL of CH₃CN were added. The mixture was cooled under stirring to 0 °C, then *t*BuONO was added (570 μL, 4.8 mmol), then trimethylsilyl azide was added (510 μL, 3.84 mmol). The resulting mixture was kept under stirring for 2 hours at room temperature. The reaction mixture was then concentrated under vacuum and the crude product (grey solid) was purified by silica gel chromatography (hexane/ethyl acetate 8:2) to give the product (pale yellow oil). Yield: 76 %. The ¹H NMR exactly matches to the one reported in literature.

¹H NMR (CDCl₃, 25 °C, ppm): δ = 3.70 (s, 3H, CH₃), 6.81 (d, ³*J* = 8.8 Hz, 2H, CH), 6.88 (d, ³*J* = 8.8 Hz, 2H, CH).

7.20 General procedure for the synthesis of the coupled imidazole-triazole^[154]

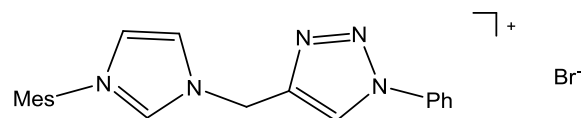
Ar = Dipp, Ph, 4-C₆H₄-OMe

CuSO₄·5H₂O (0.05 g, 0.2 mmol), sodium ascorbate (2.5 mmol, as 25 mL of 0.1 M of CH₃CN solution) were placed in a two-necked round-bottom flask and the mixture was kept under stirring for 20 minutes at 60 °C. After then, [(1-(prop-2-ynyl)-3-mesityl)imidazolium] bromide (0.6 g, 2 mmol) was added and the mixture was kept under stirring for 1 hour; the corresponding azide (2 mmol) was added (as solution in a small volume of CH₃CN) and the mixture was kept at 60 °C under stirring for 2 days. The mixture was then allow to cool at room temperature and filtered; the volume of the filtrate solution was reduced under reduced pressure and the residue was dissolved in CH₂Cl₂ (50 mL) and washed with water (3 x 30 mL). The collected organic layer was treated with MgSO₄. The drying agent was filtered off and the solvent was removed from the filtrate solution under vacuum.

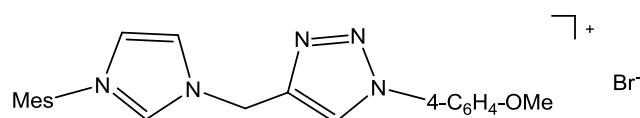


Yellow solid. Yield 86 %. ¹H NMR (dms_o-d₆, 25 °C, ppm): δ = 1.04 (d, ³J = 6.9 Hz, 6H, *i*Pr-CH₃), 1.06 (d, ³J = 6.9 Hz, 6H, *i*Pr-CH₃), 1.99 (s, 6H, Mes-CH₃), 2.04 (dq, ³J = 6.9 Hz, ³J = 6.9 Hz, 2H, *i*Pr-CH), 2.32 (s, 3H, Mes-CH₃), 5.78 (s, 2H, CH₂), 7.15 (s, 2H, Mes-CH), 7.40 (d, ³J = 7.5 Hz, 2H, Dipp-CH), 7.58 (d, ³J = 7.5 Hz, 1H, Dipp-CH), 7.98 (s, 1H, CH), 8.14 (s, 1H, CH), 8.62 (s, 1H, trz-H), 9.63 (s, 1H, NCHN).

Experimental Section

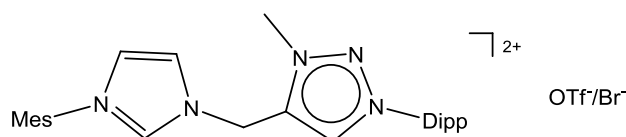


Grey solid. Yield 72 %. ^1H NMR (acetone- d_6 , 25 °C, ppm): δ = 2.10 (s, 6H, CH_3), 2.35 (s, 3H, CH_3), 6.05 (s, 2H, CH_2), 7.13 (bs, 2H, CH), 7.63 (m, 3H, CH), 7.93 (s, 3H, CH), 8.25 (m, 1H, CH), 9.78 (s, 1H, trz-H), 9.92 (s, 1H, NCHN).



Brown solid. Yield 95 %. ^1H NMR (CDCl_3 , 25 °C, ppm): δ = 2.02 (s, 6H, CH_3), 2.31 (s, 3H, CH_3), 3.84 (s, 3H, O- CH_3), 6.18 (s, 2H, CH_2), 6.96 (s, 2H, Ar-H), 6.98 (d, 3J = 9 Hz, 2H, Ar-H), 7.12 (s, 1H, CH), 7.68 (d, 3J = 9 Hz, 2H, Ar-H), 8.09 (s, 1H, CH), 9.02 (s, 1H, trz-H), 10.33 (s, 1H, NCHN).

7.21 Synthesis of [3-(2,6-diisopropylphenyl)-1-methyl-5-((3-mesitylimidazolium) methyl)-1,2,3-triazolium] trifluoromethanesulfonate/bromide $\text{L}^{17} \cdot (\text{HOTf}/\text{HBr})$ ^[141]

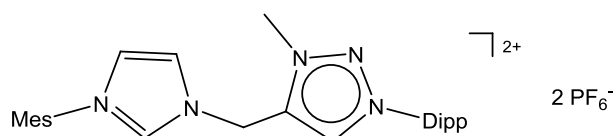


$\text{L}^{17} \cdot (\text{HOTf}/\text{HBr})$

In a two-necked round-bottomed flask, a solution of triazolylimidazolium bromide (0.15 g, 0.3 mmol) in CH_2Cl_2 (5 mL) was cooled to -78 °C, then methyl triflate (0.14 g, 0.8 mmol) was added dropwise. The mixture was allowed to warm to room temperature and kept under stirring for 16 hours. Addition of diethyl ether (10 mL) afforded the product (white solid), which was filtered off, washed with diethyl ether (3 x 5 mL) and dried in vacuum.

Yield 80 %. ^1H NMR (CD_3CN , 25 °C, ppm): δ = 1.16 – 1.20 (m, 12H, *iPr-CH*₃), 2.06 (s, 6H, Ar-*CH*₃), 2.32 (m, 2H, *iPr-CH*), 2.39 (s, 3H, Mes-*CH*₃), 4.47 (s, 3H, N*CH*₃), 5.95 (s, 2H, *CH*₂), 7.16 (s, 2H, Mes-*H*), 7.51 (d, 3J = 5.7 Hz, 2H, Dipp-*H*), 7.63 (s, 1H, *CH*), 7.73 (t, 3J = 5.7 Hz, 1H, Dipp-*H*), 7.93 (s, 1H, *CH*), 8.74 (s, 1H, trz-*H*), 9.09 (s, 1H, N*CHN*).

7.22 Synthesis of [3-(2,6-diisopropylphenyl)-1-methyl-5-((3-mesitylimidazolium) methyl)-1,2,3-triazolium] bis(hexafluorophosphate) $\text{L}^{17} \cdot 2\text{HPF}_6$

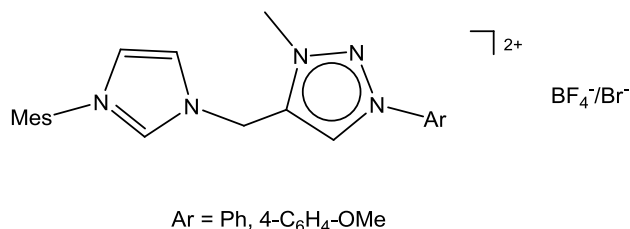


$\text{L}^{17} \cdot 2\text{HPF}_6$

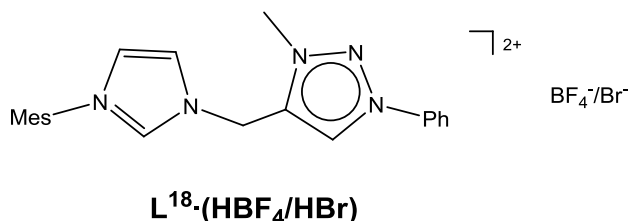
A solution of NH_4PF_6 in CH_3OH (0.04 g, 0.22 mmol, in 2 mL) was added to a solution of $\text{L}^{17} \cdot (\text{HOTf}/\text{HBr})$ (0.13 g, 0.2 mmol) in CH_3OH (10 mL). After 30 minutes of stirring the volume of the solution was reduced under reduced pressure; diethyl ether (25 mL) was added and the resulting precipitate was filtered off, washed with diethyl ether (2 x 5 mL) and dried under reduced pressure.

White solid. Yield >99 %. ^1H NMR (acetone- d_6 , 25 °C, ppm): δ = 1.08 – 1.10 (m, 12H, *iPr-CH*₃), 1.99 (s, 6H, Ar-*CH*₃), 2.29 (m, 2H, *iPr-CH*), 2.91 (s, 3H, Mes-*CH*₃), 4.70 (s, 3H, N*CH*₃), 6.39 (s, 2H, *CH*₂), 7.08 (s, 2H, Mes-*H*), 7.20 (br s, 2H, Dipp-*H*), 7.38 (br s, 1H, *CH*), 7.46 (br s, 1H, *CH*), 7.49 (br s, 1H, Dipp-*H*), 7.55 (s, 1H, *CH*), 8.74 (s, 1H, trz-*H*), 9.09 (s, 1H, N*CHN*).

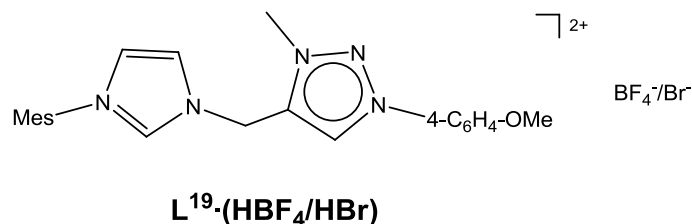
7.23 General procedure for the synthesis of the ligand precursors $L^{18} \cdot (HBF_4/HBr)$ and $L^{19} \cdot (HBF_4/HBr)$



The triazolylimidazolium bromide (0.5 mmol) and the Meerwein's salt (Me₃O·BF₄, 1.5 mmol) were placed in a two-necked round-bottomed flask and dissolved in CH₂Cl₂; the reaction mixture was kept under stirring at room temperature for 48 hours. The precipitated product (grey-white solid) was then filtered off by filtration and washed with CH₂Cl₂ (2 x 5 mL) and diethyl ether (2 x 5 mL).

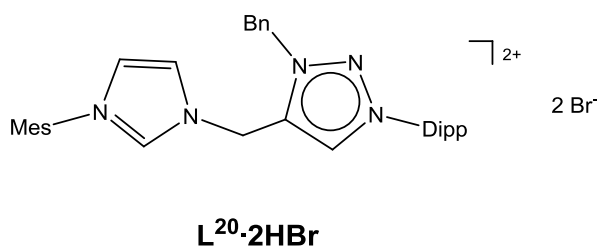


Grey-green solid. Yield 41 %. ¹H NMR (acetone-d₆, 25 °C, ppm): δ = 2.12 (s, 6H, CH₃), 2.35 (s, 3H, CH₃), 4.73 (s, 3H, CH₃), 6.37 (s, 2H, CH₂), 7.13 (bs, 2H, CH), 7.79 (m, 3H, CH), 8.00 (m, 3H, CH), 8.32 (s, 1H, CH), 9.48 (s, 1H, trz-H), 9.55 (s, 1H, NCHN). ESI-MS (positive ions) *m/z*: 446 [L¹⁸(BF₄)]⁺.



White solid. Yield 57 %. ¹H NMR (dms_o-d₆, 25 °, ppm): δ = 2.06 (s, 6H, Mes-CH₃), 2.33 (s, 3H, Mes-CH₃), 3.89 (s, 3H, O-CH₃), 4.45 (s, 3H, N-CH₃), 6.01 (s, 2H, CH₂), 7.17 (s, 2H, Mes-CH), 7.31 (d, ³J_{HH} = 8.6 Hz, 2H, Ar-CH), 7.93 (d, ³J_{HH} = 8.6 Hz, 2H, Ar-CH), 8.07 (s, 1H, CH), 8.16 (s, 1H, CH), 9.50 (s, 1H, tz-H), 9.58 (s, 1H, NCHN).

7.24 Synthesis of [3-(2,6-diisopropylphenyl)-1-benzyl-5-((3-mesitylimidazolium)methyl)-1,2,3-triazolium] bis(hexafluorophosphate) L²⁰·2HBr



Triazolylimidazolium bromide (0.3 g, 0.6 mmol) was placed in a two-necked round-bottomed flask and benzyl bromide (2.5 mL) was added under inert atmosphere, and the mixture was refluxed under stirring for 3 days. The reaction mixture was then allowed to cool at room temperature, and the product (white solid) was filtered off and washed with diethyl ether (3 x 5 mL).

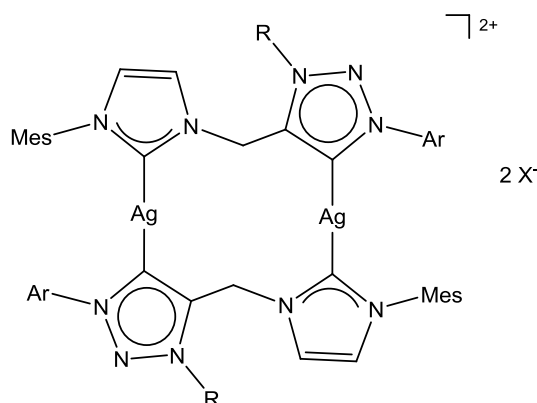
¹H NMR (acetone-d₆, 25 °C, ppm): δ = 1.00 – 1.22 (m, 12H, *i*Pr-CH₃), 2.14 (s, 6H, Ar-CH₃), 2.34 (s, 3H, Ar-CH₃), 2.53 (m, 2H, *i*Pr-CH), 4.65 (s, 2H, CH₂), 6.70 (s, 2H, CH₂), 6.80-7.80 (m, 12H, Ar-H), 9.27 (s, 1H, trz-H), 10.04 (s, 1H, NCHN).

7.25 Attempt to coordinate ligand L¹⁷ to iridium, via deprotonation with Cs₂CO₃

L¹⁷·2HPF₆ (10 mg, 0.07 mmol), [IrCl₂Cp*]₂ (5 mg) and Cs₂CO₃ (10 equiv.) were placed in a vial, CD₃CN was added (2 mL) and kept under stirring at room temperature for

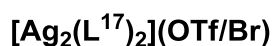
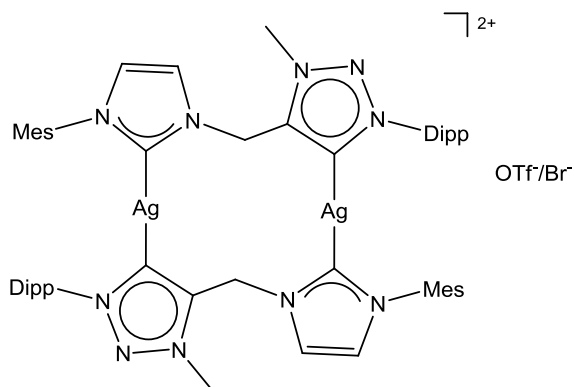
24 hours. After then, the temperature was raised to 30 °C and the mixture was kept under stirring for 24 hours. The ^1H NMR spectrum of the reaction mixture is quite complicated, however one can notice: i) the disappearance of the signal at higher ppm, relative to the imidazolium NCHN proton; ii) the presence of an AB system, at 5.60 and 6.20 ppm, ascribable to the CH_2 bridging group. These data suggest the deprotonation of the imidazolium ring and formation of an iridium complex, with only the imidazol-2-ylidene coordinated, while the triazole remains protonated and free.

7.26 General procedure for the synthesis of silver(I) NHC-MIC complexes
 $[\text{Ag}_2(\text{L}^{17})_2](\text{OTf}/\text{Br})$, $[\text{Ag}_2(\text{L}^{17})_2](\text{PF}_6)_2$, $[\text{Ag}_2(\text{L}^{18})_2](\text{BF}_4/\text{Br})$, $[\text{Ag}_2(\text{L}^{19})_2](\text{BF}_4/\text{Br})$,
 $[\text{Ag}_2(\text{L}^{20})_2](\text{Br})_2$.

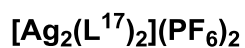
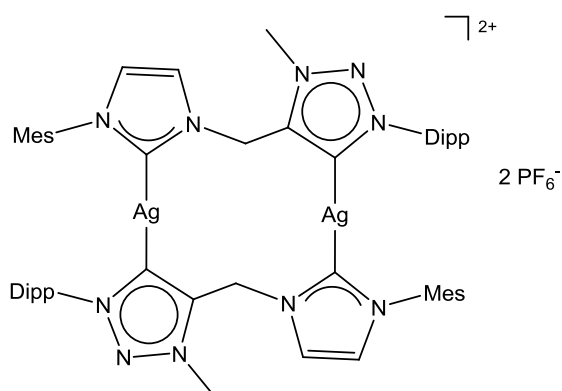


Ar = Dipp, 4- C_6H_4 -OMe, Ph
 R = Me, Bn
 X = OTf, BF_4 , Br

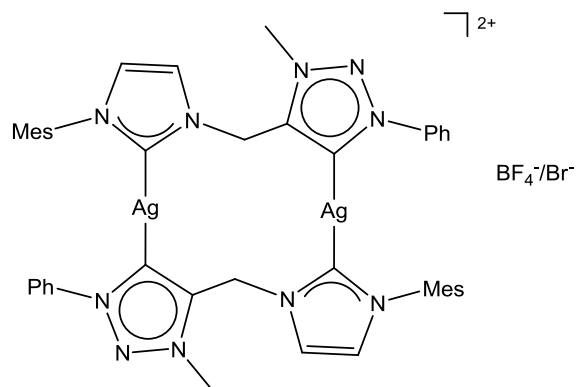
The ligand precursor (0.1 mmol) and the Ag_2O (0.6 mmol) were placed in a two-necked round-bottom flask. Under inert atmosphere, CH_3OH (10 mL) was added and the mixture was stirred for 24 hours at room temperature under light exclusion. Subsequently, the reaction mixture was filtered via cannula through Celite and the solvent was removed under vacuum.



Pale grey solid. Yield 93 %. ^1H NMR (methanol- d_4 , 25 °C, ppm): δ = 0.42, 1.02, 1.12 and 1.22 (m, 12H, *i*Pr- CH_3), 1.24, 1.45 and 2.32 (3s, 9H, Ar- CH_3), 1.75 and 2.50 (m, 2H, *i*Pr- CH), 4.51 (s, 3H, CH_3), 5.67 and 6.06 (AB system, 2H, CH_2), 6.80 - 7.70 (m, 7H, Ar- H).

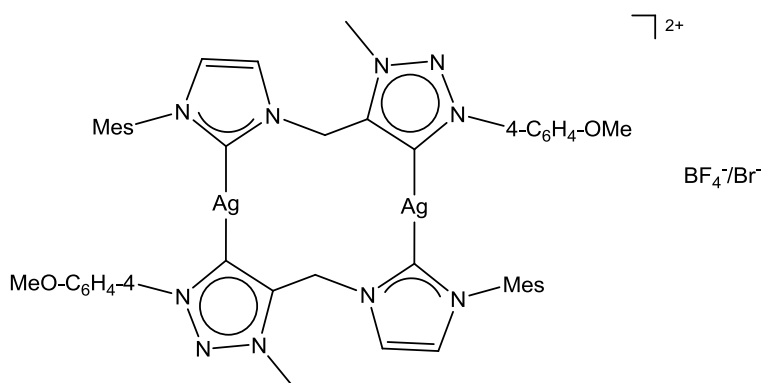


Pale grey solid. ^1H NMR (methanol- d_4 , 25 °C, ppm): δ = 0.42, 1.02, 1.12 and 1.22 (m, 12H, *i*Pr- CH_3), 1.24, 1.45 and 2.32 (3s, 9H, Ar- CH_3), 1.75 and 2.50 (m, 2H, *i*Pr- CH), 4.51 (s, 3H, CH_3), 5.67 and 6.06 (AB system, 2H, CH_2), 6.80 - 7.70 (m, 7H, Ar- H).



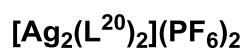
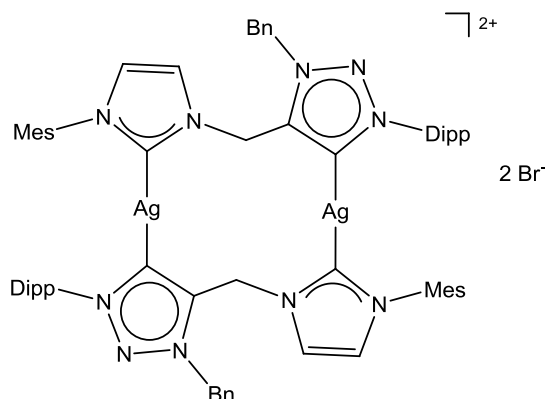
[Ag₂(L¹⁸)₂](BF₄/Br)

Pale grey solid. ¹H NMR (methanol-d₄, 25 °C, ppm): δ = 1.52 (bs, 6H, CH₃), 2.34 (s, 3H, CH₃), 4.62 (s, 3H, CH₃), 5.86 (s, 2H, CH₂), 6.91 (bs, 2H, CH), 7.23 (m, 1H, CH), 7.53 - 7.79 (m, 6H, CH). ESI-MS (positive ions) *m/z*: 1017 [Ag₂(L¹⁸)₂BF₄]⁺.



[Ag₂(L¹⁹)₂](BF₄/Br)

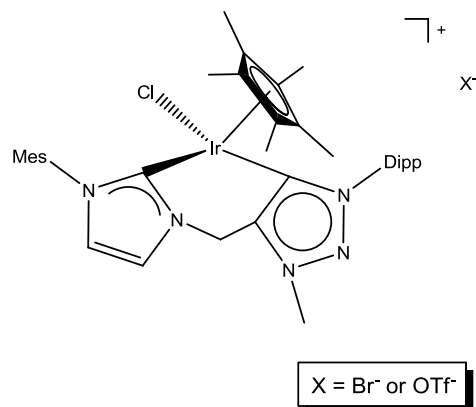
¹H NMR (methanol-d₄, 25 °, ppm): δ = 1.54 (bs, 6H, Mes-CH₃), 2.34 (s, 3H, Mes-CH₃), 3.92 (s, 3H, O-CH₃), 4.62 (s, 3H, N-CH₃), 5.84 (s, 2H, CH₂), 6.87 – 7.86 (m, 8H, Ar-H).



^1H NMR (methanol- d_4 , 25 °C, ppm): δ = 0.42, 1.02, 1.12 and 1.22 (m, 12H, *i*Pr- CH_3), 1.24, 1.45 and 2.32 (3s, 9H, Ar- CH_3), 1.65 and 2.31 (2m, 2H, *i*Pr- CH), 6.77 (s, 2H, CH_2), 6.80-7.80 (m, 12H, Ar- H), bridging CH_2 not detected probably because it is overlapped with the residual solvent signal.

7.27 Attempt to coordinate ligand L^{17} to iridium, via transmetalation from the corresponding silver complex

$[\text{Ag}_2(\text{L}^{17})_2](\text{OTf}/\text{Br})$ (10 mg, 8 μmol) was dissolved in acetone- d_6 and $[\text{IrCl}_2\text{Cp}^*]_2$ (7 mg, 8.5 μmol) was added. In the ^1H NMR spectrum of the reaction mixture it is possible to observe the disappearance of the set of signals relative to the silver complex, within 3 hours. Furthermore, one can appreciate the new AB system at 5.20 and 6.04 ppm, relative to the CH_2 bridging group. Due to the small scale reaction, it was not possible to completely characterize the product, however the reported results suggest the formation of the iridium complex **17**. The larger AB system should in fact be a direct consequence of an increased rigidity, due to the chelating coordination of the NHC-MIC ligand.



17

7.28 X-ray crystal structure determination

Crystal data for complexes **1-3**, **7-10** and **15** were collected on a Bruker APEX II single-crystal diffractometer, working with Mo-K α graphite monochromatic radiator ($\lambda = 0.71073 \text{ \AA}$) and equipped with an area detector.^[155] The structures were solved by direct methods with SHELXS-97 and refined against F² with SHELXL-97,^[156] using anisotropic thermal parameters for all non-hydrogen atoms. The hydrogen atoms were placed in the ideal geometrical positions. Details for the X-ray data collection are reported in **Tables 7.2** and **7.3**.

Table 7.2: Details for the X-ray data collection.

| Complex | 1 | 2 | 3 | 7 |
|---------------------------------------|---|---|---|---|
| Formula | C ₁₉ H ₃₁ ClF ₆ IrN ₄ P | C ₂₀ H ₂₉ ClF ₆ IrN ₄ P | C ₂₁ H ₃₁ ClF ₆ IrN ₄ P | C ₂₉ H ₄₃ ClF ₆ IrN ₄ P |
| Formula weight | 688.10 | 698.09 | 712.12 | 820.29 |
| Crystal system | Orthorhombic | Orthorhombic | Monoclinic | Triclinic |
| Space group | Pnma | Pbca | P2 _{1/n} | P-1 |
| a/Å | 13.294(2) | 17.2395(13) | 11.073(7) | 14.203(3) |
| b/Å | 12.716(2) | 13.7369(11) | 8.495(6) | 14.614(3) |
| c/Å | 13.932(2) | 20.4888(15) | 26.905(18) | 17.395(3) |
| α/° | 90.00 | 90.00 | 90.00 | 98.454(3) |
| β/° | 90.00 | 90.00 | 99.774(11) | 108.515(3) |
| γ/° | 90.00 | 90.00 | 90.00 | 95.100(3) |
| Volume, Å ³ | 2355.1(7) | 4852.1(6) | 2494(3) | 3350.9(10) |
| T (K) | 296(2) | 203(2) | 293(2) | 293(2) |
| Z | 4 | 8 | 4 | 4 |
| D _{calc} /g cm ⁻³ | 1.941 | 1.911 | 1.896 | 1.626 |
| F(000) | 1344 | 2720 | 1392 | 1632 |
| μ(Mo-Kα)/mm ⁻¹ | 5.913 | 5.724 | 5.587 | 4.170 |
| Reflections collected | 33558 | 60574 | 8791 | 54268 |
| Unique reflections | 3771 | 7148 | 4779 | 20417 |
| Observed reflections [I > 2σ(I)] | 3515 [R _{int} = 0.0377] | 4438 [R _{int} = 0.1003] | 2676 [R _{int} = 0.0855] | 10190 [R _{int} = 0.0777] |
| R [I > 2σ(I)] | R1 = 0.0315, wR2 = 0.0853 | R1 = 0.0382 wR2 = 0.0717 | R1 = 0.1026 wR2 = 0.2249 | R1 = 0.0549 wR2 = 0.1146 |
| R [all data] | R1 = 0.0332, wR2 = 0.0867 | R1 = 0.0815 wR2 = 0.0857 | R1 = 0.1766 wR2 = 0.2715 | R1 = 0.1292 wR2 = 0.1442 |

Experimental Section

Table 7.3: Details for the X-ray data collection.

| Complex | 8 | 9 | 10 | 15 |
|---------------------------------------|---|---|---|--|
| Formula | C ₂₇ H ₃₁ ClF ₆ IrN ₄ P | C ₂₈ H ₃₃ ClF ₆ IrN ₄ P | C ₂₀ H ₂₇ Br ₂ ClF ₆ IrN ₄ P | C ₃₈ H ₅₀ Cl ₆ Ir ₂ N ₄ P |
| Formula weight | 784.18 | 798.20 | 855.90 | 1159.92 |
| Crystal system | Orthorombic | Monoclinic | Monoclinic | Monoclinic |
| Space group | <i>Pnma</i> | <i>P2_{1/n}</i> | <i>P2_{1/n}</i> | <i>P2_{1/c}</i> |
| a/Å | 11.282(2) | 14.439(3) | 13.798(3) | 11.2125(6) |
| b/Å | 13.508(3) | 12.898(3) | 12.135(2) | 14.7547(8) |
| c/Å | 19.020(4) | 15.652(3) | 15.460(3) | 13.6141(7) |
| α/° | 90.00 | 90.00 | 90.00 | 90.00 |
| β/° | 90.00 | 92.895(3) | 91.923(3) | 111.2420(10) |
| γ/° | 90.00 | 90.00 | 90.00 | 90.00 |
| Volume, Å ³ | 2898.5(9) | 2911.2(11) | 2587.2(8) | 2099.25(19) |
| T (K) | 293(2) | 293(2) | 293(2) | 203(2) |
| Z | 4 | 4 | 4 | 2 |
| D _{calc} /g cm ⁻³ | 1.797 | 1.821 | 2.197 | 1.835 |
| F(000) | 1536 | 1568 | 1632 | 1124 |
| μ(Mo-Kα)/mm ⁻¹ | 4.817 | 4.798 | 8.476 | 6.747 |
| Reflections collected | 45431 | 44448 | 41255 | 32802 |
| Unique reflections | 4697 | 8807 | 7868 | 6173 |
| Observed reflections [I > 2σ(I)] | 4030 [R _{int} = 0.0594] | 6324 [R _{int} = 0.0443] | 5527 [R _{int} = 0.0664] | 5080 [R _{int} = 0.0468] |
| R [I > 2σ(I)] | R1 = 0.0314, wR2 = 0.0821 | R1 = 0.0276 wR2 = 0.0518 | R1 = 0.0380, wR2 = 0.0780 | R1 = 0.0245, wR2 = 0.0520 |
| R [all data] | R1 = 0.0381, wR2 = 0.0876 | R1 = 0.0570 wR2 = 0.0616 | R1 = 0.0672, wR2 = 0.0905 | R1 = 0.0349, wR2 = 0.0557 |

$$R1 = \Sigma |F_o - F_c| / \Sigma (F_o); wR2 = [\Sigma [w(F_o^2 - F_c^2)^2] / \Sigma [w(F_o^2)^2]]^{1/2}.$$

Publications

“N-heterocyclic dicarbene iridium(III) catalysts enabling water oxidation under visible light irradiation”

Andrea Volpe, Andrea Sartorel, Cristina Tubaro, Laura Meneghini, Marilena Di Valentin, Claudia Graiff, Marcella Bonchio

Eur. J. Inorg. Chem. **2014**, 665-675.

Communications to congresses

A. Volpe, C. Tubaro, A. Sartorel, M. Bonchio, M. Basato, C. Graiff

Chelating N-heterocyclic carbene iridium(III) complexes: catalytic activity in water oxidation

X Co.G.I.C.O – X Congresso del Gruppo Interdivisionale di Chimica Organometallica, P40, Padova (Italy), 5-8 June 2012.

C. Tubaro, A. Volpe, A. Sartorel, M. Basato, M. Bonchio, C. Graiff

N-heterocyclic carbene ruthenium(II) and iridium(III) complexes: synthesis and catalytic activity in water oxidation

XXV ICOMC – International Conference on Organometallic Chemistry, PA.146, Lisbon (Portugal), 2-7 September 2012.

A. Volpe, C. Tubaro, A. Sartorel, M. Bonchio, M. Di Valentin, L. Meneghini, C. Graiff

diNHC-Ir(III) complexes: synthesis and catalytic activity in water oxidation

20th EuCheMS Conference on Organometallic Chemistry, P154A, St Andrews (Scotland) 30 June-4 July 2013.

A. Volpe, C. Tubaro, A. Sartorel, L. Meneghini, M. Di Valentin, C. Graiff, M. Bonchio

Novel dicarbene iridium(III) catalysts for water oxidation reaction

9th I.S.O.C. – International School of Organometallic Chemistry, Poster 17, Camerino (Italy), 30 August - 3 September 2013.

A. Volpe, C. Tubaro, A. Sartorel, M. Bonchio, M. Di Valentin, L. Meneghini, C. Graiff
Novel dicarbene iridium(III) complexes: synthesis and catalytic activity in water oxidation

XLI Congresso Nazionale della Divisione di Chimica Inorganica della Società Chimica Italiana, OC21, Parma (Italy), 3-6 September 2013.

Chapter 8: REFERENCES

- [1] (a) K. Öfele, *J. Organomet. Chem.* **1968**, *12*, 42. (b) H.-W. Wanzlick, H.-J. Schönherr, *Angew. Chem. Int. Ed. Engl.* **1968**, *7*, 141.
- [2] (a) D. J. Cardin, B. Cetinkaya, M. F. Lappert, L. Manojlovic'-Muir, K.W. Muir, *Chem. Commun.* **1971**, 400. (b) M. F. Lappert, *J. Organomet. Chem.* **1975**, *100*, 139. (c) M. F. Lappert, *J. Organomet. Chem.* **1988**, *358*, 185. (d) M. F. Lappert, *J. Organomet. Chem.* **2005**, *690*, 5467.
- [3] (a) A. J. Arduengo III, R. L. Harlow, M. Kline, *J. Am. Chem. Soc.* **1991**, *113*, 361. (b) D. A. Dixon, A. J. Arduengo III, *J. Phys. Chem.* **1991**, *95*, 4180. (c) A. J. Arduengo III, H. V. R. Dias, R. L. Harlow, *J. Chem. Am. Soc.* **1992**, *114*, 5530.
- [4] (a) S. P. Nolan, *N-Heterocyclic Carbenes, Effective Tools for Organometallic Synthesis* **2014**, Weinheim: Wiley-VCH. (b) S. Diez-Gonzalez, *N-Heterocyclic Carbenes: From Laboratory Curiosities to Efficient Synthetic Tools* **2010**, Cambridge: RSC Catalysis Series, RSC. (c) C. S. J. Cazin, *N-Heterocyclic Carbenes in Transition Metal Catalysis and Organocatalysis*, in *Catalysis by Metal Complexes*. **2010**, vol. 32, Heidelberg: Springer. (d) O. Kühl *Functionalised N-heterocyclic carbene complexes* **2010**, John Wiley and Sons. (e) F. Glorius, *N-Heterocyclic Carbenes in Transition Metal Catalysis*, in *Topics in Organometallic Chemistry*, **2007**, vol. 21, Heidelberg: Springer.
- [5] See for example: (a) M. Scholl, T. M. Trnka, J. P. Morgan, R. H. Grubbs, *Tetrahedron Lett.* **1999**, *40*, 2247. (b) M. S. Sanford, M. Ulman, R. H. Grubbs, *J. Am. Chem. Soc.* **2001**, *123*, 749.
- [6] D. Bourissou, O. Guerret, F. P. Gabbaï, G. Bertrand, *Chem. Rev.* **2000**, *100*, 39.
- [7] W. A. Herrmann, *Angew. Chem. Int. Ed.* **2002**, *41*, 1290.
- [8] W. A. Herrmann, T. Weskamp, V. P. W. Böhm, *Adv. Organomet. Chem.* **2001**, *48*, 1.
- [9] (a) S. Fantasia, J. L. Petersen, H. Jacobsen, L. Cavallo, S. P. Nolan, *Organometallics* **2007**, *26*, 5880. (b) X. Hu, I. Castro-Rodriguez, K. Olsen, K.

References

- Meyer, *Organometallics* **2004**, *23*, 755. (c) D. Nemcsok, K. Wichmann, G. Frenking, *Organometallics* **2004**, *23*, 3640.
- [10] I. Huang, H.-J. Schanz, E. D. Stevens, S. P. Nolan, *Organometallics* **1999**, *18*, 2370.
- [11] (a) M. T. Lee, C. H. Hu, *Organometallics* **2004**, *23*, 976. (b) R. Dorta, E. D. Stevens, C. D. Hoff, S. P. Nolan, *J. Am. Chem. Soc.* **2003**, *125*, 10490.
- [12] L. Jafarpour, S. P. Nolan, *Adv. Organomet. Chem.* **2001**, *46*, 181.
- [13] F. E. Hahn, M. C. Jahnke, *Angew. Chem. Int. Ed.* **2008**, *47*, 3122.
- [14] W. A. Herrmann, C. Köcher, *Angew. Chem. Int. Ed. Engl.* **1997**, *36*, 2162.
- [15] S. Diez-Gonzalez, S. P. Nolan, *Coord. Chem. Rev.* **2007**, *251*, 874.
- [16] D. J. Debon, S. P. Nolan, *Chem. Soc. Rev.* **2013**, *42*, 6723.
- [17] C. A. Tolman, *Chem. Rev.* **1977**, *77*, 313.
- [18] (a) L. Cavallo, A. Correa, C. Costabile, H. Jacobsen, *J. Organomet. Chem.* **2005**, *690*, 5407. (b) A. C. Hillier, W. J. Sommer, B. S. Yong, J. L. Petersen, L. Cavallo, S. P. Nolan, *Organometallics* **2003**, *22*, 4322. (c) A. Poater, B. Cosenza, A. Correa, S. Giudice, F. Ragone, V. Scarano, L. Cavallo, *Eur. J. Inorg. Chem.* **2009**, 1759.
- [19] D. G. Gusev, *Organometallics* **2009**, *28*, 6458.
- [20] R. H. Crabtree, *Coord. Chem. Rev.* **2013**, *257*, 755.
- [21] (a) M. Albrecht, *Adv Organomet Chem.* **2014**, *62*, 111. (b) M. Albrecht, *Chem. Commun.* **2008**, 3601.
- [22] K. F. Donnelly, A. Petronilho, M. Albrecht, *Chem. Commun.* **2013**, *49*, 1145.
- [23] B. Schulze, U. S. Schubert, *Chem. Soc. Rev.* **2014**, *43*, 2522.
- [24] G. Guisado-Barrios, J. Bouffard, B. Donnadieu, G. Bertrand, *Angew. Chem. Int. Ed.* **2010**, *49*, 4759.
- [25] (a) J. Li, W. Shen, X. Li, *Current Organic Chemistry* **2012**, *16*, 2879. (b) L. Yang, D. Wei, W. Mai, P. Mao, *Chin. J. Org. Chem.* **2013**, *33*, 943.
- [26] (a) A. A. Danopoulos, N. Tsoureas, S. A. Macgregor, C. Smith, *Organometallics* **2007**, *26*, 253. (b) A. P. Marchenko, H. N. Koidan, A. N. Hurieva, O. V. Gutov, A. N. Kostyuk, C. Tubaro, S. Lollo, A. Lanza, F. Nestola, A. Biffis, *Organometallics*

- 2013**, 32, 718. (c) Y. Unger, D. Meyer, O. Molt, C. Schildknecht, I. Münster, G. Wagenblast, T. Strassner, *Angew. Chem. Int. Ed.* **2010**, 49, 10214.
- [27] (a) M. Poyatos, J. A. Mata, E. Peris, *Chem. Rev.* **2009**, 109, 3677. (b) R. Corberán, E. Mas-Marzá, E. Peris, *Eur. J. Inorg. Chem.* **2009**, 1700.
- [28] (a) C. Tubaro, A. Biffis, R. Gava, E. Scattolin, A. Volpe, M. Basato, M. Mar Díaz-Requejo, P. J. Perez, *Eur. J. Org. Chem.* **2012**, 1367. (b) M. Baron, C. Tubaro, M. Basato, A. Biffis, M. M. Natile, C. Graiff, *Organometallics* **2011**, 30, 4607. (c) M. Baron, C. Tubaro, A. Biffis, M. Basato, C. Graiff, A. Poater, L. Cavallo, N. Armaroli, G. Accorsi, *Inorg Chem.* **2012**, 51, 1778.
- [29] (a) A. Rit, T. Pape, F. E. Hahn, *Organometallics* **2011**, 30, 6393. (b) R. Maity, A. Rit, C. Schulte to Brinke, J. Kösters, F. E. Hahn, *Organometallics* **2013**, 32, 6174.
- [30] (a) J. A. Mata, F. E. Hahn, E. Peris, *Chem Sci.* **2014**, 5, 1723. (b) H. Li, T. J. Marks, *PNAS* **2006**, 103, 15295. (c) J. M. Serrano-Becerra, A. F. G. Maier, S. González-Gallardo, E. Moos, C. Kaub, M. Gaffga, G. Niedner-Schatteburg, P. W. Roesky, F. Breher, J. Paradies, *Eur. J. Org. Chem.* **2014**, 4515. (d) M. R. Salata, T. J. Marks, *Macromolecules* **2009**, 42, 1920.
- [31] (a) S. Gründemann, M. Albrecht, J. A. Loch, J. W. Faller, R. H. Crabtree, *Organometallics* **2001**, 20, 5485. (b) M. Poyatos, J. A. Mata, E. Falomir, R. H. Crabtree, E. Peris, *Organometallics* **2003**, 22, 1110. (c) E. Peris, R. H. Crabtree, *Coord. Chem. Rev.* **2004**, 248, 2239. (d) W. Wei, Y. Qin, M. Luo, P. Xia, M. S. Wong, *Organometallics* **2008**, 27, 2268.
- [32] (a) X. Hu, I. Castro-Rodriguez, K. Meyer, *J. Am. Chem. Soc.* **2003**, 125, 12237. (b) X. Hu, K. Meyer, *J. Organomet. Chem.* **2005**, 690, 5474.
- [33] (a) R. McKie, J. A. Murphy, S. R. Park, M. D. Spicer, S. Zhou, *Angew. Chem. Int. Ed.* **2007**, 46, 6525. (b) F. E. Hahn, V. Langenhahn, T. Lügger, T. Pape, D. Le Van, *Angew. Chem. Int. Ed.* **2005**, 44, 3759. (c) H. M. Bass, S. A. Cramer, J. L. Price, D. M. Jenkins, *Organometallics* **2010**, 29, 3235. (d) S. A. Cramer, D. M. Jenkins, *J. Am. Chem. Soc.* **2011**, 133, 19342. (e) Z. Lu, S. A. Cramer, D. M. Jenkins, *Chem. Sci.* **2012**, 3, 3081. (f) H. M. Bass, S. A. Cramer, A. S. McCullough, K. J. Bernstein, C. R. Murdock, D. M. Jenkins, *Organometallics* **2013**, 32, 2160.

- [34] B. Çetinkaya, P. B. Hitchcock, M. F. Lappert, D. B. Shaw, K. Spyropoulos, N. J. W. Warhurst, *J. Organomet. Chem.* **1993**, *459*, 311.
- [35] I. Özdemir, B. Yiğit, B. Çetinkaya, D. Ülkü, M. N. Tahir, C. Arici, *J. Organomet. Chem.* **2001**, *633*, 27.
- [36] (a) C. Y. Liu, D. Y. Chen, G. H. Lee, S. M. Peng, S. T. Liu, *Organometallics* **1996**, *15*, 1055 and references cited therein. (b) A. S. K. Hashmi, C. Lothschütz, Constantin Böhling, F. Rominger, *Organometallics* **2011**, *30*, 2411. (c) A. S. K. Hashmi, C. Lothschütz, C. Böhling, T. Hengst, C. Hubbert, F. Rominger, *Adv. Synth. Catal.* **2010**, *352*, 3001.
- [37] I. J. B. Lin, C. S. Vasam, *Coord. Chem. Rev.* **2007**, *251*, 642.
- [38] H. M. J. Wang, I. J. B. Lin, *Organometallics* **1998**, *17*, 972.
- [39] J. C. Garrison, W. J. Youngs, *Chem. Rev.* **2005**, *105*, 3978.
- [40] W. A. Herrmann, M. Elison, J. Fischer, C. Köcher, G. R. J. Artus, *Angew. Chem. Int. Ed. Engl.* **1995**, *34*, 2371.
- [41] S. Diez-Gonzalez, N. Marion, S. P. Nolan, *Chem. Rev.* **2009**, *109*, 3612.
- [42] L. Mercks, M. Albrecht, *Chem. Soc. Rev.* **2010**, *39*, 1903.
- [43] (a) L. Oehninger, R. Rubbiani, I. Ott, *Dalton Trans.* **2013**, *42*, 3269. (b) M.-L. Teyssot, A.-S. Jarrouse, M. Manin, A. Chevy, S. Roche, C. Beaudoin, L. Morel, D. Boyer, R. Mahiov, A. Gautier, *Dalton Trans.* **2009**, 6894. For the palladium(II) complex in Figure 1.12 see: S. Ray, R. Mohan, J. K. Singh, M. K. Samantaray, M. M. Shaikh, D. Panda, P. Ghosh, *J. Am. Chem. Soc.* **2007**, *129*, 15042. For the copper(I) complex in Figure 1.12 see: M.-L. Teyssot, A.-S. Jarrouse, A. Chevy, A. De Haze, C. Beaudoin, M. Manin, S. P. Nolan, S. Diez-Gonzalez, L. Morel, A. Gautier, *Chem. Eur. J.* **2009**, *15*, 2203.
- [44] S. B. Aher, P. N. Muskawar, K. Thenmozhi, P. R. Bhagat, *Eur. J. Med. Chem.* **2014**, *81*, 408.
- [45] C. Hu, X. Li, W. Wei, R. Zhang, L. Deng, *Curr. Med. Chem.* **2014**, *21*, 1220.
- [46] (a) A. Kascatan-Nebioglu, M. J. Panzner, C. A. Tessier, C. L. Cannon, W. J. Youngs, *Coord. Chem. Rev.* **2007**, *251*, 884. For the silver(I) complex with xanthine-NHC in Figure 1.12 see: (b) A. R. Knapp, M. J. Panzner, D. A. Medvetz,

- B. D. Wright, C. A. Tessier, W. J. Youngs, *Inorg. Chim. Acta* **2010**, *364*, 125. For the silver(I)-NHC oligomer in Figure 1.12 see: (c) A. Melaiye, R. S. Simons, A. Milsted, F. Pingitore, C. Westemiotis, C. A. Tessier, W. J. Youngs, *J. Med. Chem.* **2004**, *47*, 973.
- [47] (a) R. T. W. Huang, W. C. Wang, R. Y. Yang, J. T. Lu, I. J. B. Lin, *Dalton Trans.* **2009**, 7121. (b) C. K. Lee, J. C. C. Chen, K. M. Lee, C. W. Liu, I. J. B. Lin, *Chem. Mater.* **1999**, *11*, 1237. (c) T. Tu, X. Bao, W. Assenmacher, H. Peterlik, J. Daniels, K. H. Dötz, *Chem. Eur. J.* **2009**, *15*, 1853.
- [48] For a general review see: (a) R. Visbal, M. C. Gimeno, *Chem. Soc. Rev.* **2014**, *43*, 3551. For the specific examples reported see: (b) Y. Unger, A. Zeller, S. Ahrens, T. Strassner, *Chem. Commun.* **2008**, 3263. (c) Y. Unger, A. Zeller, A. Taige, T. Strassner, *Dalton Trans.* **2009**, 4786.
- [49] X.-Q. Xiao, Y.-J. Lin, G.-X. Lin, *Dalton Trans.* **2008**, 2615.
- [50] A. Petronilho, M. Rahman, G. A. Woods, H. Al-Sayyed, H. Müller-Bunz, G. M. D. MacElroy, S. Bernhard, M. Albrecht, *Dalton Trans.* **2012**, *41*, 13074.
- [51] (a) F. Hanasaka, K. Fujita, R. Yamaguchi, *Organometallics* **2005**, *24*, 3422. (b) J. H. Barnard, C. Wang, N. G. Berry, J. Xiao, *Chem. Sci.* **2013**, *4*, 1234. (c) R. Corberán, V. Lillo, J. A. Mata, E. Fernandez, E. Peris, *Organometallics* **2007**, *26*, 4350.
- [52] (a) W. B. Cross, C. G. Daly, Y. Boutadla, K. Singh, *Dalton Trans.* **2011**, *40*, 9722.
- [53] R. Corberán, M. Sanaú, E. Peris, *Organometallics* **2007**, *26*, 1954.
- [54] A. Pontes da Costa, M. Viciano, M. Sanaú, S. Merino, J. Tejada, E. Peris, B. Royo, *Organometallics* **2008**, *27*, 1305.
- [55] R. Corberán, E. Peris, *Organometallics* **2008**, *27*, 1954.
- [56] D. Gnanamgari, E. L. O. Sauer, N. D. Schley, C. Butler, C. D. Incarvito, R. H. Crabtree, *Organometallics* **2009**, *28*, 321.
- [57] S. Hohloch, L. Suntrop, B. Sarkar, *Organometallics* **2013**, *32*, 7376.
- [58] (a) F. Hanasaka, K. Fujita, R. Yamaguchi, *Organometallics* **2004**, *23*, 1400. (b) F. Hanasaka, K. Fujita, R. Yamaguchi, *Organometallics* **2006**, *25*, 4643.
- [59] R. Corberán, M. Sanaú, E. Peris, *J. Am. Chem. Soc.* **2006**, *128*, 3974.

References

- [60] T. Sajoto, P. I. Djurovich, A. Tamayo, M. Yousufuddin, R. Bau, M. E. Thompson, R. J. Olms, S. R. Forrest, *Inorg. Chem.* **2005**, *44*, 7792.
- [61] R. J. Holmes, S. R. Forrest, T. Sajoto, A. Tamayo, P. I. Djurovich, M. E. Thompson, J. Brooks, Y.-J. Tung, B. W. D'Andrade, M. S. Weaver, R. C. Kwong, J. J. Brown, *Appl. Phys. Lett.* **2005**, *87*, 243507.
- [62] (a) C.-H. Yang, J. Beltran, V. Lemaur, J. Cornil, D. Hartmann, W. Sarfert, R. Frohlich, C. Bizzarri, L. De Cola, *Inorg. Chem.* **2010**, *49*, 9891. (b) N. Darmawan, C.-H. Yang, M. Mauro, M. Raynal, S. Heun, J. Pan, H. Buchholz, P. Braunstein, L. De Cola, *Inorg. Chem.* **2013**, *52*, 10756.
- [63] (a) N. S. Lewis, D. G. Nocera, *Proc. Natl. Acad. Sci. U.S.A.* **2006**, *103*, 15729. (b) N. Armaroli, V. Balzani, *ChemSusChem* **2011**, *4*, 21. (c) T. J. Meyer, *Nature* **2008**, *451*, 778.
- [64] M. D. Kärkäs, O. Verho, E. V. Johnston, B. Åkermark, *Chem. Rev.* **2014**, DOI:10.1021/cr400572f.
- [65] B. Limburg, E. Bouwman, S. Bonnet, *Coord. Chem. Rev.* **2012**, *256*, 1451.
- [66] F. Puntoriero, A. Sartorel, M. Orlandi, G. La Ganga, S. Serroni, M. Bonchio, F. Scandola, S. Campagna, *Coord. Chem. Rev.* **2011**, *255*, 2594.
- [67] M. D. Kärkäs, E. V. Johnston, O. Verho, B. Åkermark, *Acc. Chem. Res.* **2014**, *47*, 100.
- [68] (a) J. Barber, *Chem. Soc. Rev.* **2009**, *38*, 185. (b) B. Loll, J. Kern, W. Saenger, A. Zouni, J. Biesiadka, *Nature* **2005**, *438*, 1040.
- [69] Y. Umena, K. Kawakami, J. R. Shen, N. Kamiya, *Nature* **2011**, *473*, 55.
- [70] A. Sartorel, M. Bonchio, S. Campagna, F. Scandola, *Chem. Soc. Rev.* **2013**, *42*, 2262.
- [71] C. W. Cady, R. H. Crabtree, G. W. Brudvig, *Coord. Chem. Rev.* **2008**, *252*, 444.
- [72] X. Sala, I. Romero, M. Rodriguez, L. Escriche, A. Llobet, *Angew. Chem. Int. Ed.* **2009**, *48*, 2842.
- [73] S. W. Gersten, G. J. Samuels, T. J. Meyer, *J. Am. Chem. Soc.* **1982**, *104*, 4030.
- [74] A. R. Parent, R. H. Crabtree, G. W. Brudvig, *Chem. Soc. Rev.* **2013**, *42*, 2247.

-
- [75] N. D. McDaniel, F. J. Coughlin, L. L. Tinker, S. Bernhard, *J. Am. Chem. Soc.* **2008**, *130*, 210.
- [76] C. Sens, I. Romero, M. Rodriguez, A. Llobet, T. Parella, J. Benet-Buchholz, *J. Am. Chem. Soc.* **2004**, *126*, 7798.
- [77] (a) R. Zong, P. Thummel, *J. Am. Chem. Soc.* **2005**, *127*, 12802. (b) R. Zong, D. Wang, R. Hammit, R. P. Thummel, *J. Org. Chem.* **2006**, *71*, 167. (c) Z. Deng, H.-W. Tseng, R. Zong, D. Wang, R. Thummel, *Inorg. Chem.* **2008**, *47*, 1835.
- [78] (a) A. Sartorel, M. Carraro, G. Scorrano, R. De Zorzi, S. Geremia, N. D. McDaniel, S. Bernhard, M. Bonchio, *J. Am. Chem. Soc.* **2008**, *130*, 5006. (b) Y. V. Geletii, B. Botar, P. Kögerler, D. A. Hillesheim, D. G. Musaev, C. L. Hill, *Angew. Chem. Int. Ed.* **2008**, *47*, 3896. (c) A. Sartorel, P. Mirò, E. Salvadori, S. Romain, M. Carraro, G. Scorrano, M. Di Valentin, A. Llobet, C. Bo, M. Bonchio, *J. Am. Chem. Soc.* **2009**, *131*, 16051.
- [79] E. A. Karlsson, B.-L. Lee, T. Åkermark, E. V. Johnston, M. D. Kärkäs, J. Sun, Ö. Hansson, J.-E. Bäckvall, B. Åkermark, *Angew. Chem. Int. Ed.* **2011**, *50*, 11715.
- [80] W. C. Ellis, N. D. McDaniel, S. Bernhard, T. J. Collins, *J. Am. Chem. Soc.* **2010**, *132*, 10990.
- [81] (a) J. Kiwi, M. Grätzel, *J. Am. Chem. Soc.* **1979**, *101*, 7214. (b) W. J. Youngblood, S.-H. A. Lee, Y. Kobayashi, E. A. Hernandez-Pagan, P. G. Hoertz, T. A. Moore, A. L. Moore, D. Gust, T. E. Mallouk, *J. Am. Chem. Soc.* **2009**, *131*, 926. (c) N. Sivasankar, W. W. Weare, H. Frei, *J. Am. Chem. Soc.* **2011**, *133*, 12976.
- [82] J. F. Hull, D. Balcells, J. D. Blakemore, C. D. Incarvito, O. Eisenstein, G. W. Brudvig, R. H. Crabtree, *J. Am. Chem. Soc.* **2009**, *131*, 8730.
- [83] J. D. Blakemore, N. D. Schley, D. Balcells, J. F. Hull, G. W. Olack, C. D. Incarvito, O. Eisenstein, G. W. Brudvig, R. H. Crabtree, *J. Am. Chem. Soc.* **2010**, *132*, 16017.
- [84] N. D. Schley, J. D. Blakemore, N. K. Subbaiyan, C. D. Incarvito, F. D'Souza, R. H. Crabtree, G. W. Brudvig, *J. Am. Chem. Soc.* **2011**, *133*, 10473.
- [85] D. B. Grotjahn, D. B. Brown, J. K. Martin, D. C. Marelus, M. C. Abadjian, H. N. Tran, G. Kalyuzhny, K. S. Vecchio, Z. G. Specht, S. A. Cortes-Llamas, V. Miranda-

References

- Soto, C. van Niekerk, C. E. Moore, A. L. Rheingold, *J. Am. Chem. Soc.* **2011**, *133*, 19024.
- [86] J. D. Blakemore, N. D. Schley, G. W. Olack, C. D. Incarvito, G. W. Brudvig, R. H. Crabtree, *Chem. Sci.* **2011**, *2*, 94.
- [87] U. Hintermair, S. M. Hashmi, M. Elimelech, R. H. Crabtree, *J. Am. Chem. Soc.* **2012**, *134*, 9785.
- [88] J. D. Blakemore, M. W. Mara, M. N. Kushner-Lenhoff, N. S. Schley, S. J. Konezny, I. Rivalta, C. F. A. Negre, R. C. Snoeberger, O. Kokhan, J. Huang, A. Stickrath, L. A. Tran, M. L. Parr, L. X. Chen, D. M. Tiede, V. S. Batista, R. H. Crabtree, G. W. Brudvig, *Inorg. Chem.* **2013**, *52*, 1860.
- [89] A. Savini, G. Bellachioma, G. Ciancaleoni, C. Zuccaccia, D. Zucaccia, A. Macchioni, *Chem. Commun.* **2010**, *46*, 9218.
- [90] A. Savini, P. Belanzoni, G. Bellachioma, C. Zuccaccia, D. Zucaccia, A. Macchioni, *Green Chem.* **2011**, *13*, 3360.
- [91] C. Zuccaccia, G. Bellachioma, S. Bolaño, L. Rocchigiani, A. Savini, A. Macchioni, *Eur. J. Inorg. Chem.* **2012**, 1462.
- [92] A. Bucci, A. Savini, L. Rocchigiani, C. Zuccaccia, S. Rizzato, A. Albinati, A. Llobet, A. Macchioni, *Organometallics* **2012**, *31*, 8071.
- [93] C. Zuccaccia, G. Bellachioma, O. Bortolini, A. Bucci, A. Savini, A. Macchioni, *Chem. Eur. J.* **2014**, *20*, 3446.
- [94] A. Savini, A. Bucci, G. Bellachioma, S. Giancola, F. Palomba, L. Rocchigiani, A. Rossi, M. Suriani, C. Zuccaccia, A. Macchioni, *J. Organomet. Chem.* **2014**, *771*, 24.
- [95] A. Savini, A. Bucci, G. Bellachioma, L. Rocchigiani, C. Zuccaccia, A. Llobet, A. Macchioni, *Eur. J. Inorg. Chem.* **2014**, 690.
- [96] D. Hong, M. Murakami, Y. Yamada, S. Fukuzumi, *Energy. Environ. Sci.* **2012**, *5*, 5708.
- [97] (a) C. Wang, Z. Xie, K. E. deKrafft, W. Lin, *J. Am. Chem. Soc.* **2011**, *133*, 13445.
(b) C. Wang, G.-L. Wang, W. Lin, *J. Am. Chem. Soc.* **2012**, *134*, 19895.
- [98] K. Hirai, A. Nutton, P. M. Maitlis, *J. Mol. Catal.* **1981**, *10*, 203.

- [99] S. Sabiah, C.-S. Lee, W.-S. Hwang, I. J. B. Lin, *Organometallics* **2010**, *29*, 290.
- [100] Z. Xi, X. Zhang, W. Chen, S. Fu, D. Wang, *Organometallics* **2007**, *26*, 6636.
- [101] C. H. Leung, A. R. Chianese, B. R. Garrett, C. S. Letko, R. H. Crabtree, *Inorg. Synth.* **2010**, *35*, 84.
- [102] J. A. Mata, A. R. Chianese, J. R. Miecznikowski, M. Poyatos, E. Peris, J. W. Faller, R. H. Crabtree, *Organometallics* **2004**, *23*, 1253.
- [103] (a) S. Sanz, A. Azua, E. Peris, *Dalton Trans.* **2010**, *39*, 6339. (b) R. Corberán, M. Sanaú, E. Peris, *Organometallics* **2006**, *25*, 4002.
- [104] G. Su, X.-K. Huo, G.-X. Jin, *J. Organomet. Chem.* **2011**, *696*, 533.
- [105] C. Tubaro, M. Baron, M. Costante, M. Basato, A. Biffis, A. Gennaro, A. A. Isse, C. Graiff, G. Accorsi, *Dalton Trans.* **2013**, *42*, 10952.
- [106] M. Vogt, V. Pons, D. M. Heinekey, *Organometallics* **2005**, *24*, 1832.
- [107] (a) X.-Q. Xiao, G.-X. Jin, *J. Organomet. Chem.* **2008**, *693*, 3363. (b) W.-G. Jia, Y.-F. Han, G.-X. Jin, *Organometallics* **2008**, *27*, 6035. (c) M. Albrecht, J. R. Miecznikowski, A. Samuel, J. W. Faller, R. H. Crabtree, *Organometallics* **2002**, *21*, 3596.
- [108] G. Buscemi, M. Basato, A. Biffis, A. Gennaro, A. A. Isse, M. M. Natile, C. Tubaro, *J. Organomet. Chem.* **2010**, *695*, 2359.
- [109] H. V. Huynh, Y. Han, R. Jothibas, J. A. Yang, *Organometallics* **2009**, *28*, 5395.
- [110] M. M. Rahman, H.-Y. Liu, K. Eriks, A. Prock, W. P. Giering, *Organometallics* **1989**, *8*, 1.
- [111] A. B. P. Lever, *Inorg. Chem.* **1990**, *29*, 1271.
- [112] D. G. H. Hetterscheid, J. N. H. Reek, *Chem. Commun.* **2011**, *47*, 2712.
- [113] T. P. Brewster, J. D. Blakemore, N. D. Schley, C. D. Incarvito, N. Hazari, G. W. Brudvig, R. H. Crabtree, *Organometallics* **2011**, *30*, 965.
- [114] R. Lalrempuia, N. D. McDaniel, H. Müller-Bunz, S. Bernhard, M. Albrecht, *Angew. Chem. Int. Ed.* **2010**, *49*, 9765.
- [115] A. Petronilho, A. Llobet, M. Albrecht, *Inorg. Chem.* **2014**, DOI:10.1021/ic501894u.

References

- [116] A. R. Parent, T. P. Brewster, W. De Wolf, R. H. Crabtree, G. W. Brudvig, *Inorg. Chem.* **2012**, *51*, 6147.
- [117] A. J. Ingram, A. B. Wolk, C. Flender, J. Zhang, C. J. Johnson, U. Hintermair, R. H. Crabtree, M. A. Johnson, R. N. Zare, *Inorg. Chem.* **2014**, *53*, 423.
- [118] (a) A. Macchioni, I. Corbucci, A. Petronilho, H. Müller-Bunz, L. Rocchigiani, M. Albrecht, Atti del Co.G.I.C.O.-XI Congresso del Gruppo Interdivisionale di Chimica Organometallica, Milano, 24-27 Giugno 2014, OC05. (b) I. Corbucci, A. Petronilho, H. Müller-Bunz, L. Rocchigiani, M. Albrecht, A. Macchioni, Atti del XXV Congresso Nazionale della Società Chimica Italiana, Rende, 7-12 Settembre 2014, INO-O40.
- [119] M. V. Baker, D. H. Brown, R. A. Haque, B. W. Skelton, A. H. White, *J. Incl. Phenom. Macrocycl. Chem.* **2009**, *65*, 97.
- [120] (a) R. Maity, A. Rit, C. Schulte to Brinke, C. G. Daniliuc, F. E. Hahn, *Chem. Commun.* **2013**, *49*, 1011.
- [121] (a) R. Zhong, Y.-N. Wang, X.-Q. Guo, Z.-X. Chen, X.-F. Hou, *Chem.-Eur. J.* **2011**, *17*, 11041. (b) C.-F. Chang, Y.-M. Cheng, Y. Chi, Y.-C. Chiu, C.-C. Lin, G.-H. Lee, P.-T. Chou, C.-C. Chen, C.-H. Chang, C.-C. Wu, *Angew. Chem. Int. Ed.* **2008**, *47*, 4542. (c) A. P. da Costa, M. Sanau, E. Peris, B. Royo, *Dalton Trans.* **2009**, 6960.
- [122] R. Corberán, M. Sanaú, E. Peris, *Organometallics* **2007**, *26*, 3492.
- [123] (a) S. E. Clapham, A. Hadzovic, R. H. Morris, *Coord. Chem. Rev.* **2004**, *248*, 2201. (b) P. Espinet, A. C. Albéniz In *Fundamentals of Molecular Catalysis, Current Methods in Inorganic Chemistry*, Vol. 3; Kurosawa, H., Yamamoto, A., Eds.; Elsevier: Amsterdam, **2003**, Chapter 6. (c) *Recent Advances in Hydride Chemistry*; Peruzzini, M., Poli, R., Eds.; Elsevier: Amsterdam, **2001**.
- [124] (a) J. S. M. Samec, J. E. Bäckvall, P. G. Andersson, P. Brandt, *Chem. Soc. Rev.* **2006**, *35*, 237. (b) M. C. Warner, J.-E. Bäckvall, *Acc. Chem. Res.* **2013**, *46*, 2545.
- [125] O. Blum, D. Milstein, *J. Organomet. Chem.* **2000**, *593*, 479.
- [126] N. Matsumura, J. Kawano, N. Fukunishi, H. Inoue, *J. Am. Chem. Soc.* **1995**, *117*, 3623.

- [127] R. W. Alder, E. M. Blake, C. Bortolotti, S. Bufali, C. P. Butts, E. Linehan, J. M. Oliva, G. A. Orpen, M. J. Quayle, *Chem. Commun.* **1999**, 241,
- [128] M. Mayr, K. Wurst, K. H. Ongania, M. R. Buchmeiser, *Chem. Eur. J.* **2004**, *10*, 1256.
- [129] W. A. Herrmann, S. K. Schneider, K. Öfele, M. Sakamoto, E. Herdtweck, *J. Organomet. Chem.* **2004**, *689*, 2441.
- [130] (a) M. Iglesias, D. J. Beetstra, J. C. Knight, L. L. Ooi, A. Stasch, S. Coles, L. Male, M. B. Hursthouse, K. J. Cavell, A. Dervisi, I. A. Fallis, *Organometallics* **2008**, *27*, 3279. (b) A. Binobaid, M. Iglesias, D. J. Beetstra, B. Kariuki, A. Dervisi, I. A. Fallis, K. L. Cavell, *Dalton Trans.* **2009**, 7099.
- [131] J. J. Dunsford, K. L. Cavell, B. M. Kariuki, *J. Organomet. Chem.* **2011**, *696*, 188.
- [132] (a) A. Binobaid, M. Iglesias, D. J. Beetstra, B. Kariuki, A. Dervisi, I. A. Fallis, K. J. Cavell, *Eur. J. Inorg. Chem.* **2010**, 5426. (b) A. Binobaid, M. Iglesias, D. J. Beetstra, B. Kariuki, A. Dervisi, I. A. Fallis, K. J. Cavell, *Dalton Trans.* **2009**, 7099.
- [133] E. L. Kolychev, I. A. Portnyagin, V. V. Shuntikov, V. N. Khrustalev, M. S. Nechaev, *J. Organomet. Chem.* **2009**, *694*, 2454.
- [134] C. J. E. Davies, M. J. Page, C. E. Ellul, M. F. Mahon, M. K. Whittlesey, *Chem. Commun.* **2010**, *46*, 5151.
- [135] G. A. Blake, J. P. Moerdyk, C. W. Bielawski, *Organometallics* **2012**, *31*, 3373,
- [136] (a) J. J. Dunsford, K. L. Cavell, B. M. Kariuki, *Organometallics*, **2012**, *31*, 4118. (b) W. Y. Lu, K. L. Cavell, J. S. Wixey, B. Kariuki, *Organometallics* **2011**, *30*, 5649. (c) M. Iglesias, D. J. Beetstra, A. Stasch, P. N. Horton, M. B. Hursthouse, S. J. Coles, K. J. Cavell, A. Dervisi, I. A. Fallis, *Organometallics* **2007**, *26*, 4800.
- [137] B. Ahci, I. Özdemir, N. Gürbüz, E. Çetinkaya, B. Çetinkaya, *Heterocycles* **2005**, *65*, 1439.
- [138] P. Mao, L. Yang, Y. Xiao, J. Yuan, X. Liu, M. Song, *J. Organomet. Chem.* **2012**, *705*, 39.
- [139] R. Maity, S. Hohloch, C.-Y. Su, M. van der Meer, B. Sarkar, *Chem. Eur. J.* **2014**, *20*, 9952.

References

- [140] M. T. Zamora, M. J. Ferguson, R. McDonald, M. Cowie, *Organometallics* **2012**, *31*, 5463.
- [141] S. N. Sluijter, C. J. Elsevier, *Organometallics* **2014**, *33*, 6389.
- [142] S. Stoll, A. Schweiger, *J. Magn. Reson.* **2006**, *178*, 42.
- [143] A. Nutton, P. M. Bailey, P. M. Maitlis, *J. Chem. Soc., Dalton Trans.* **1981**, 1997.
- [144] K. D. Wells, M. J. Ferguson, R. McDonald, M. Cowie, *Organometallics* **2008**, *27*, 691.
- [145] W. A. Herrmann, C. Köcher, L. J. Gooßen, G. R. J. Artus, *Chem. Eur. J.* **1996**, *2*, 1627.
- [146] F. M. Nachtigall, Y. E. Corilo, C. C. Cassol, G. Ebeling, N. H. Morgon, J. Dupont, M. N. Eberlin, *Angew. Chem. Int. Ed.* **2008**, *47*, 151.
- [147] K. Okuyama, J. Sugiyama, R. Nagahata, M. Asai, M. Ueda, K. Takeuchi, *J. Mol. Catal. A: Chem.* **2003**, *203*, 21.
- [148] M. Lee, U. H. Choi, S. Wi, C. Slebodnick, R. H. Colby, H. W. Gibson, *J. Mater. Chem* **2011**, *21*, 12280.
- [149] (a) S. K. U. Riederer, P. Giegler, M. P. Ögerl, E. Herdtweck, B. Bechlars, W. A. Herrmann, E. E. Kühn, *Organometallics* **2010**, *29*, 5681. (b) T. Scherg, S. K. Schneider, G. D. Frey, J. Schwarz, E. Herdtweck, W. A. Herrmann, *Synlett* **2006**, 2894.
- [150] M. Bessel, F. Rominger, B. F. Straub, *Synthesis* **2010**, *9*, 1459.
- [151] A. M. Magill, D. S. McGuinness, J. K. Cavell, G. J. P. Britovsek, V. C. Gibson, A. J. P. White, D. J. Williams, A. H. White, B. W. Skelton, *J. Organomet. Chem.* **2001**, *546*, 617.
- [152] C. E. Willans, K. M. Anderson, M. J. Paterson, P. C. Junk, L. J. Barbour, J. W. Steed, *Eur. J. Inorg. Chem.* **2009**, 2835.
- [153] K. Barrall, A. D. Moorhause, J. E. Moses, *Org. Lett.* **2007**, *9*, 1809.
- [154] S. Warsink, R. M. Drost, M. Lutz, A. L. Spek, C. J. Elsevier, *Organometallics* **2010**, *29*, 3109.
- [155] SMART Software Users Guide, Version 5.1; Bruker Analytical X-ray Systems: Madison, WI, 1999. SAINT Software Users Guide, Version 6.0; Bruker Analytical

X-ray Systems: Madison,WI, 1999. Sheldrick, G. M. SADABS; Bruker Analytical X-ray Systems: Madison,WI, 1999. APEX II Software User Guide; Bruker AXS Inc., Madison, WI, 2008. SAINT, Version 7.06a; Bruker AXS Inc.: Madison, WI, 2008. SADABS, Version 2.01; Bruker AXS Inc.: Madison, WI, **2008**.

[156] Sheldrick, G. M. SHELX-97, Programs for Crystal Structure Analysis, Release 97-2; University of Göttingen: Göttingen, Germany, **1997**.